Diego I. Murguía

Global Area Disturbed and Pressures on Biodiversity by Large-Scale Metal Mining

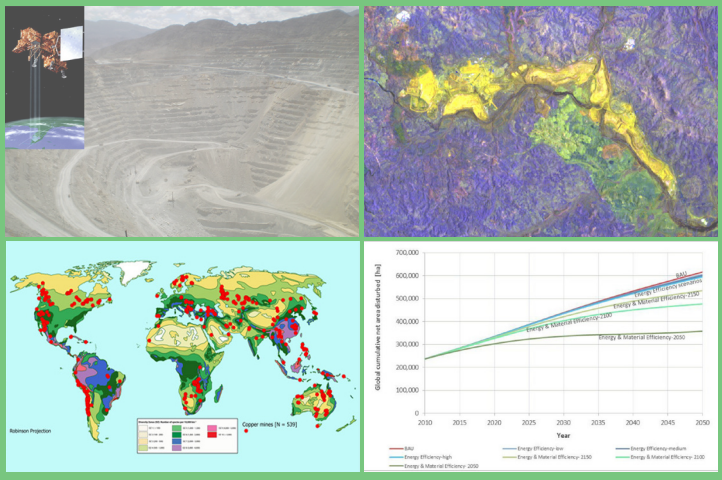

kassel university press

Diego I. Murguía

Global Area Disturbed and Pressures on Biodiversity by Large-Scale Metal Mining

kassel university press

This work has been accepted by the Faculty of Civil and Environmental Engineering of the University of Kassel as a thesis for acquiring the academic degree of Doktor der Ingenieurwissenschaften (Dr.-Ing.).

Supervisor:	Prof. Dr. Stefan Bringezu, Wuppertal Institut für Klima, Umwelt, Energie und CESR, Universität Kassel
Co-Supervisor:	PD Dr. Rüdiger Schaldach, CESR, Universität Kassel

Defense day: 16th. July 2015

Bibliographic information published by Deutsche Nationalbibliothek
The Deutsche Nationalbibliothek lists this publication in the Deutsche Nationalbibliografie; detailed bibliographic data is available in the Internet at http://dnb.dnb.de.

Zugl.: Kassel, Univ., Diss. 2015
ISBN 978-3-7376-0040-8 (print)
ISBN 978-3-7376-0041-0 (e-book)
URN: http://nbn-resolving.de/urn:nbn:de:0002-400418

Cover illustration: (top left) open pit at Bajo de la Alumbrera mine in Argentina in 2010 with a superimposed drawing of a Landsat satellite; (top right) false color composite, Red/Green/Blue Band combination 5,7,1 of a Landsat 7 ETM+ satellite image of the Yandi iron ore mine in Australia at the end of 2012, yellow colors represent the net area disturbed by the mine; (bottom left) global map of plant diversity zones overlaid with large-scale copper mines; and (bottom right) scenarios of global cumulative net area disturbed by iron ore mining until 2050.

Cover designer: Ilknur Kocer, Kassel

www.upress.uni-kassel.de/

Printed in Germany

We cannot solve problems by using the same kind of thinking we used when we created them.

Albert Einstein

The fallacy that economic determinists have tied around our collective neck and which we now need to cast off is that economics determines all land use. This is simply not true.

Aldo Leopold, A Sand County Almanac (1949)

Study how a society uses its land, and you can come to pretty reliable conclusions as to what its future will be.

E.F. Schumacher, Small is Beautiful:
A study of economics as if people mattered (1973)

Summary

Measuring current land use and projecting possible future scenarios of the global area disturbed by large-scale metal mining activities is at the core of this dissertation. The rising global demand for metals in a context of declining ore grades is driving the increased opening of new mines, and expansion of existing mines, disturbing substantial land areas. This is particularly striking in surface operations (or open pit mines) mining copper, gold and silver which need to extract and process higher quantities of ore and waste rock than underground mines to obtain the same amount of metal. Henceforth, the land required, and the socio-environmental pressures caused at local levels, have increased alongside falling ore grades and increasing bulk earth moving.

In this study the global area disturbed by mining of iron, bauxite, copper, gold, and silver is investigated for the first time. Area disturbances refer to the area influenced by the activities of the mine related to the extraction and beneficiation of ore. Such area must be visible and measurable using optical satellite imagery. The study encompasses large-scale mines and their direct impacts, while excludes artisanal and small-scale mines and mines without precise geographic coordinates. The findings provide the orders of magnitude to better understand the land use impact caused by the large-scale metal mining industry compared to extensive land uses. The results can be used as a frame to develop policies and incentives to reduce the amount of area directly disturbed by mines.

The dissertation comprises four parts. The first consists of the calculation of the specific land requirements, i.e. the area newly disturbed caused by the material extraction at the mine site over the same period. To calculate the indicator the first step involved the random selection of a sample of mines from a global inventory encompassing 13 bauxite open pit mines, 27 iron ore open pit mines and 66 mines producing copper, gold and silver (45 open pit and 21 underground). Measurements are conducted covering a defined period of the mine´s lifespan in order to calculate the cumulative ore extracted and the cumulative net area disturbed in that period. *Net* area differs from the *gross* area disturbed in that the former includes only the land surface in use for mining – excluding areas

potentially reclaimed or affected by subsidence (i.e. areas not clearly discernible to be affected by a mine as observed in satellite images). Cumulative net area disturbances are measured on Landsat satellite images using object based image analysis and visual image interpretation aided by ancillary material. In the case of polymetallic mines cumulative variables are allocated using average metal prices. The relationship between the cumulative variables is investigated using a power function and nonlinear regression analysis. Weighted disturbance rates per metal are computed for each sample resulting in the annual amount of newly disturbed land (hectares) per million metric ton (Mt) of ore extracted. The rates for bauxite, gold, silver, copper, and iron, respectively, are: 7.98 ha/Mt, 6.70 ha/Mt, 5.53 ha/Mt, 4.5 ha/Mt, and 4.25 ha/Mt. These results became the first land metric to understand the dynamics of how the mining sector has been affecting land.

Secondly, the cumulative net area disturbed per mine in 2011 is determined in five random samples (one sample per metal) covering 116 mines in total. The area disturbed by all mines per sample is multiplied by a three year average factor. Such factor results from dividing the world mine production (of ore or metal) by the sample production (of ore or metal) during the years 2010-2012. The global cumulative net area disturbed caused by large-scale metal mining activities (2011) is estimated at 1.2 million hectares, almost half the area of Belgium. It excludes the area disturbed by abandoned or orphaned mines.

Thirdly, forward-looking scenarios of how the global cumulative net area disturbed might behave until 2050 are created. Departing from the global status quo in 2011, projections of annual world ore extraction (adopted from existing models) are multiplied by the specific land requirements. This delivers three to six future pathways (scenarios and scenario corridors) per metal showing projected business-as-usual scenarios contrasted with others emphasizing material efficiency measures. For copper, gold and silver, a scenario corridor catering for an uncertainty range (around a business-as-usual scenario) was introduced. The pathways presented highlight the importance of implementing aggressive increases in energy and material efficiency so as to reduce global environmental pressures.

Finally, the last researched topic addresses current and potential future spatial distribution of pressures on global biodiversity caused by metal mines, using the map developed by Barthlott and colleagues (Barthlott et al. 2007). This map utilizes the abundance of vascular plants species as a proxy for global terrestrial biodiversity richness (excluding Antarctica) and differentiates between ten diversity zones: three low, three intermediate, and four high diversity zones. A global inventory of 2,860 metal mines and 2,055 known deposits (sourced from the SNL Metals & Mining database) was overlaid with this map. A graphical and statistical analysis was carried out testing the null hypothesis asserting that the amount of mines and deposits per diversity zone was random. The analysis involved comparing the frequency distribution of the world´s terrestrial area (excluding Antarctica) per diversity zone (the expected random or null model) with the observed distribution of mines and deposits per diversity zone.

In all cases the statistical analysis showed that mines and deposits are not randomly distributed; they are spatially concentrated in some zones. The analysis revealed that 23% of mines and 20% of ore deposits are located in areas of high plant diversity and that 50% of all deposits are located in three low and one intermediate plant diversity zone. From the graphical analysis it becomes noticeable that in the cases of bauxite and silver mining there is a clear concentration of mines and deposits in some areas of high biodiversity whereas for iron, copper and gold, the concentration in higher biodiversity areas exists but it is not as salient. Moreover mines and deposits of the latter are predominantly concentrated in intermediate diversity zones. A common characteristic to all metals is that they all have a large reserve base in areas of lower biodiversity.

The analyses in this thesis have been delimited in the selection of the mines´ sample by the availability of public technical information, a necessary aid for the visual interpretation and classification of mines and their boundaries with adjacent land covers. Information was not found, at least in English, for mines operating in China and Russia; in contrast, Australia provided numerous public reports which, coupled with the fact that climate allows for a large number of cloud-free satellite images, explains the selection of many Australian mines, particularly in the iron ore sample. Another delimitation of the method employed is inherent to the visual

image interpretation as it is subject to the criterion of the trained interpreter which adds some degree of subjectivity; this latter aspect was dealt with by using high resolution imagery as contextual ancillary information and technical reports in order to reduce it to a minimum.

It can be concluded that the global cumulative net area directly disturbed by large-scale mining of the five metals studied, calculated at 1.2 million hectares (for the year 2011), is rather small if compared to more extensive global land uses like cropland or forestry (approximately 1,670 and 3,890 million hectares respectively). The number would certainly increase if more minerals (e.g. coal) were investigated and indirect impacts considered. Nevertheless, despite the relatively small number, at a local level and in the long-run, the direct transformations and socio-environmental impacts caused by large-scale mining of non-renewable metallic ores are, or may be, significant.

The scenarios have shown that final demand for most metals is expected to keep on rising following a growing world population, increasing urbanization and industrialization trends. However, for bauxite and iron, models forecast a per-capita in-use stock saturation at different points in time with a subsequent increasing availability of metals in the form of scrap. They project that global primary mining is expected to keep its role as a main source of metal supply to the world market at least until the decades of 2025-2040 as in-use stocks keep on growing, particularly led by the developing world. Models coincide that, with the exception of bauxite, the primary mining of iron, copper, gold and silver may peak within that period and then incur in a subsequent gradual decline while at the same time the market will observe a surge in the supply of recycled metals (scrap) in order to cater for an overall increasing global demand for metals. Therefore, primary mining is expected to enhance its pressures on land and biodiversity for the next decades, doubling or tripling the current global level by 2050.

The expected growing pressures of land use change by mining might be mitigated by the simultaneous deployment of material efficiency and land rehabilitation strategies. On the one hand, the demand for metals can be decreased by enhanced material efficiency (obtaining the same level of technical service while

using less metal) in manufacturing, final production and consumption, and by lowering the amount of buildings, infrastructures and final goods which determine the level of in-use stock which in turn affect the demand for both primary and secondary metals. On the other hand, projections on future cumulative global net area disturbed could be reduced if more investments were destined towards land reclamation and rehabilitation, namely, lowering the specific land requirements calculated in this study.

Last but not least, it can be concluded that the global extent of mining-induced biodiversity loss might be reduced if biodiversity-richness had more weight as a key criterion in the decision-making process of where to explore or open new mines. Viewed from a global scale and a global sustainable resource management perspective, results of this study allow concluding that for iron ore, copper, gold and silver, numerous deposits exist in regions with a low biodiversity, which indicates the option of promoting a shift in the mining investments towards these areas while at the same time reducing the pressure on biodiversity-rich tropical areas. This may prove more difficult for bauxite and silver due to the high geographic concentration of mines and deposits in tropical areas. However, it may be more viable for iron, copper and gold avoiding mining in those high biodiversity ecosystems already suffering strong pressure from other pressing land use and land cover change activities.

Acknowledgements & Dedication

First of all, I would like to thank my *Doktorvater*, Prof. Dr. Stefan Bringezu since he has been the designer and driver of all these less researched topics. Always flexible and supportive, he has provided helpful guidance and we have engaged in a learning process during the Ph.D. time. He has always motivated me and supported my professional needs, also considering my personal situation, for all that, warm thanks! Likewise, I thank all colleagues at the Wuppertal Institute for financing my years of research; I hope results through publications become a valuable return for this wonderful institution to keep inspiring pioneer work in transition research.

Second, I want to express my deep gratitude to the colleagues at the ZFL in Bonn. From the start, Mort Canty, Sven Nussbaum, Frank Thonfeld, Olena Dubovyk, Ellen Götz and other members were most welcoming, shared their knowledge, experience and time with me and made me part of the group even though I was a sort of difficult-to-categorize Ph.D. student from Wuppertal. My heartfelt thanks to Carsten Oldenburg (ZFL) for debugging my scripts in IDL and to Guido Lüchters (ZEF) for providing unvaluable guidance and timely support for statistical analyses.

Third, I expresss my thanks to the whole Research Group 3 “Material Flows and Resource Management” of the Wuppertal Institute and especially to José Acosta, Arkaitz Usubiaga, Helmut Schütz, Mathieu Saurat, Raimund Bleischwitz, Michael Ritthoff and Henning Wilts for all thoughtful comments, suggestions and technical help. Heatfelt thanks to Dominic Wittmer for translating the thesis´ summary to German and to Katie Meinhold for proofreading my English summary. Special and warm thanks to Janina Ubachs who gave me essential help in the classification of images. Kind thanks to Thomas Orbach and the “Vereinigung der Freunde” of the Wuppertal Institute for supporting my commuting expenses to Bonn during 2013.

Fourth, thanks a lot to Rüdiger Schaldach for acting as my second supervisor and second link to the CESR, reading and commenting the thesis´ drafts. Sincere thanks also to the USGS (and indirectly to the U.S. tax contributors) for their freely accessible Landsat archive, a *sine qua non* condition for this study. Also my gratitude is expressed to Jeffrey Massek for sharing the Ledaps software. Much

gratitude is also due to Magnus Ericsson, Irene Geuken and to SNL Metals & Mining for granting access to their mining database. Sincere thanks also to Dr. Stefan Pauliuk, Dr. Gang Liu, Colton E. Bangs and Prof. Daniel B. Müller from NTNU in Norway, Dr. Stephen Northey from CSIRO in Australia and Prof. Dr. Harald Sverdrup from Lund University for generously sharing their modeled data. Also thanks to the Nees Institute for Biodiversity of Plants at the University of Bonn.

Other big thanks to the Taringa! and Wikipedia online communities for providing fast and specific support. I also feel thankful to the library team at the Wuppertal Institute (Jana Züge and Nadja Schiemann) for always precisely supporting my needs; also my thanks to Jara Rossenbach from the BBK I library at the RWTH Aachen for scanning materials and sparing my the trip.

Last but not least, I acknowledge and profoundly thank my family, my girlfriend Alexia and my neighbor Giuseppa for steadfast support in daily and psychological aspects, and all my friends in Germany and abroad for making the whole Ph.D. process meaningful despite ups and downs.

This work is dedicated to all those who never surrender in the pursuit of social and environmental justice.

And to all who daily decide not to follow the easy road but that of creativity, solidarity, and the collective well-being instead of the privileges of a few.

Diego Murguía, Wuppertal, November 2015

CONTENTS

List of Tables

List of Figures

Acronyms, Terms and Measurement Units

Units

Bha	Billion hectares (10^9 hectares)
Bn	Billion (10^9)
ha	Hectare (one hectare = 2.47 acres)
g	Gram
g/t	Grams per metric ton
Gt	Gigaton (10^9 metric tons)
kg	Kilogram (10^3 grams)
kha	Thousand hectares
km	Kilometer (1 km = 0.62 miles)
kt	Kiloton (1,000 metric tons)
m	Meter
M	Million
Mha	Million hectares
Mkm^2	Million square kilometers
Mt	Megaton (10^6 tons)
t	Metric ton (10^6 grams)
t/a	Metric tons per annum
oz	Troy ounce (1 oz = 31.1034768 grams)
a	Year (January to December) or annum
USD or US$	United States Dollars
µm	Micrometer

Common Chemical Symbols Used

Ag	Silver
Al	Aluminium (used also to refer to bauxite)
Au	Gold
Cr	Chromium
Cu	Copper
Dia	Diamonds
Fe	Iron
Mo	Molybdenum
Mn	Manganese
Ni	Nickel
Pb	Lead
Sn	Tin
Zn	Zinc

Used Acronyms, Abbreviations and Terms

AMD	Acid mine drainage, synonym for ARD.
ARD	Acid rock drainage. Drainage that occurs as a result of natural oxidation of sulphide minerals contained in rock that is exposed to air and water; it is not

	confined to mining activities and can occur wherever sulphide-bearing rock is exposed to air and water.
ASM	Artisanal and small-scale mining
BAU	Business-as-usual
BGS	British Geological Survey
Beneficiation	Also called ore enrichment, it refers to the process of treating ore so that the resulting product is richer or more concentrated with mineral, reaching a saleable quality. The process is performed at the mine site and is the previous step to refining or smelting.
Beneficiation waste	It refers to the materials (ground rock and process effluents) generated in a mine processing plant during the beneficiation process. It equals the term tailings and can be dry stack tailings or wet ones disposed in tailings ponds.
BOF	Basic oxygen furnace, a method of primary steelmaking by blowing oxygen through molten pig iron.
Bullion	It refers to gold, silver or other precious metals bar or ingots produced by an accredited refinery which guarantees a certain level of purity and makes it a tradable in commodity markets like the LBMA.
CBD	Convention on Biological Diversity
CCS	Carbon capture and storage
CCU	Carbon capture and utilization
Claim	Refers to a mining interest giving its holder the right to prospect, explore for and exploit minerals within a defined area. It is also called mining concession
Complex ore	Ore that contains several metals of economic interest, for example an ore containing zinc, copper, lead, gold and silver.
CP	Coupled production mine (also called polymetallic or multi-metal mine); mine producing more than one target metal, namely, co-products like gold and silver or zinc and lead.
Cut-off grade	It refers to the minimum metal grade at which a ton of rock can be processed on an economic basis (at a profit). Above the cut-off grade the rock is considered ore and below is waste or gangue; in the process of mining this determines where the material mined flows to. The cut-off grade changes over time according to market conditions (market price of the metal) and cost considerations.
Deposit	Refers to geological deposits, namely, an accumulation of mineral ores
Doré bar	An unrefined (therefore impure) alloy of gold with variable quantities of silver and smaller quantities of base metals produced at a mine site. Gold content (or purity level) varies, but usually consists of 85% gold on average. Doré bars are sent to refineries where bars are purified to a high level (typically 99.9%, almost pure metal), obtain the good delivery standard and become financially tradable gold bullion.
DSO	Direct shipping ore grade (for iron ore mines)
DZ	Diversity zone, belongs to those ones defined by Barthlott et al. (2007)
EAF	Electric arc furnace
EC	European Commission
EO	Earth Observation
EU	European Union
EW-MFA	Economy-wide material flow analysis
EEA	European Environment Agency
EOL-RR	End of life recycling rate. It refers to functional recycling (the portion of end-of-life recycling in which the metal in a discarded product is separated to

	obtain recyclates that are returned to raw material production processes) and includes recycling as a pure metal (e.g. copper) and as an alloy (e.g. brass).
ETM+	Refers to the Enhanced Thematic Mapper Plus multispectral sensor mounted onboard the Landsat 7 satellite.
Extraction waste	Refers to the hard rock removed in a mine site while digging to access the ore; extraction waste usually ends up placed in waste dumps. See also waste rock below.
Flotation	A common physic-chemical process in the concentration of minerals. When the various mineral particles have been ground sufficiently to allow separation from one to another and the gangue material, they are pumped in suspension to flotation cells. With the addition of certain chemicals and the passage of air through the suspension, the different mineral particles can be made to attach themselves selectively to the air bubbles to form a froth which is then skimmed from the remaining bulk of suspension. Water is then filtered from the bubble-rich liquid and the resulting material is an ore concentrate. Once all valuable metal-bearing minerals have been floated off, a water-rich slurry remains as a waste product called tailings which is dumped into large ponds called impoundments, ponds or tailings dams.
Gangue	From an economic point of view, the worthless or uneconomic minerals associated with valuable minerals in an ore deposit.
GDP	Gross domestic product
GHG	Greenhouse gas, often measured in Co_2 eq.
GIS	Geographic Information System
Grade	The concentration of metal in ore expressed as troy ounces or grams per metric ton for precious metals and as a percentage for most other metals.
Heap leaching	A process whereby gold is extracted by “heaping” broken ore on sloping impermeable pads and repeatedly spraying the heaps with a weak cyanide solution which dissolves the gold content.
Heap leach spent ore	Rock remaining after recovery of metals and some soluble constituents through heap leaching and heap rinsing of ores (the low-cost method being used extensively for extracting valuables from lower grade ores).
IAI	International Aluminium Institute
ICMM	International Council on Mining & Metals
ICTs	Information and communication technologies
IEA	International Energy Agency
IPCC	International Panel on Climate Change
IRP	International Resource Panel
IUCN	International Union for Conservation of Nature
JORC	The Australasian Code for Reporting on Exploration Results, Mineral Resources and Ore Reserves.
L5	Satellite Landsat 5
L7	Satellite Landsat 7
L8	Satellite Landsat 8
LBMA	London Bullion Market Association
LCA	Life cycle assessment. Used to assess the potential environmental impacts associated with a product, process or activity during its entire life-cycle.
LCI	Life cycle inventory
LSM	Large-scale mines (industrial-scale mines)
LULC	Land use and land cover

LULCC	Land use and land cover change
Metal concentrate	Also known as dressed ore or mined concentrate. A product of metal mining operations, actually, the concentrated form of a mineral after processing. A concentrate is enriched ore (as a result of beneficiation) which transports several minerals at different concentrations and is normally sold to a smelter where further processing takes places before shipping to a refinery.
MIA	Mine industrial area. Includes the processing plant (mill, crusher, concentrator), conveyors, access roads, accommodation village (if placed close to the plant), run-of-mine stockpile pads and other infrastructure next to the processing plant (excludes open pits, dumps, heap leach pads, ponds).
Mill	A plant where ore is ground fine and undergoes physical or chemical treatment to extract the valuable metals.
Mineral resource	According to the JORC Code, a 'Mineral Resource' is a concentration or occurrence of material of intrinsic economic interest in or on the Earth's crust in such form, quality and quantity that there are reasonable prospects for eventual economic extraction.
NASA	U.S. National Aeronautics and Space Administration
NDVI	Normalized Difference Vegetation Index. It is a simple graphical indicator used to quickly identify vegetated areas and their condition on satellite images.
NCP	No coupled production mine (mine producing only one target metal); also called monometallic mine.
NDSO	Non direct shipping ore grade mine (for iron ore mines exclusively). It refers to iron ore mines for which the ore grade is too low for direct shipping and requires beneficiation.
NGO	Non-governmental organization
NIR	Near infrared, it refers to the Band 4 of the TM/ETM sensors (wavelength 0.76-0.90μm) and Band 5 of the OLI sensor (0.85-0.88μm) of the electromagnetic spectrum. Also called visible near infrared (VNIR).
OBIA	Object-based image analysis
OLI	Refers to the Operational Land Imager instrument on board the Landsat 8 satellite.
OLS	Ordinary least-squares
OP	Open pit (mine)
Opening year	Refers to the first year of commercial production of a mine.
OPUG	Open pit and underground (mine)
Ore	A mixture of minerals and gangue from which at least one of the minerals can be extracted at a profit. Normally expressed in million metric tons [Mt].
Ore reserve	According to the JORC Code, it is the economically mineable part of a Measured and or Indicated Mineral Resource. It includes diluting materials and allowances for losses, which may occur when the material is mined and is defined by studies at Pre-Feasibility or Feasibility level as appropriate that include application of Modifying Factors. Such studies demonstrate that, at the time of reporting, extraction could reasonably be justified.
Overburden	The soil and rock above the mineral deposit that must be removed in order to expose and mine the mineral resource (ore).
Payable metal content	The percentage of the metal content of the concentrate (or doré) for which the smelters/refineries agree to pay (after final assaying) when purchasing the mine final product.
PGM	Platinum group metals

Placer	A placer deposit is an accumulation of valuable minerals formed by gravity separation during sedimentary processes, i.e. alluvial sands and gravel in a stream bed of floodplain containing metals such as gold, tin, or diamonds.
Primary raw minerals	Refers to minerals (in the form of ore) removed directly from the crust of the Earth. It is equivalent to the terms “fresh-mined”, “newly-mined”, or “virgin” minerals.
Reclamation or Rehabilitation	Refers to the process by which lands disturbed as a result of mining activity are reclaimed back to some degree of its former state or pre-mining condition or a similar one. It includes the removal of buildings, equipment, machinery and other physical remnants of mining, closure of tailing ponds, leach pads and other mine features, and contouring, covering and re-vegetation of waste rock piles and other disturbed areas. An ecological restoration process and a post-closure environmental monitoring program should ensue.
RGB	Red, green and blue, three necessary channels to create color.
ROM	Run of mine or run-of-mine. It refers to the material mined considered ore (above the cut-off grade) as it emerges from the open pits or underground operations, before being crushed. It does not include waste or gangue. Synonyms in MFA studies for run of mine include gross ore or crude ore. Often expressed in million metric tons [Mt].
SDG	Sustainable Development Goals
SEC	U.S. Securities and Exchange Commission
Secondary raw materials	Refers to minerals embedded in waste streams of industrialized products which can be recovered and recycled; they includes pre- and post-consumer scrap for metals, minerals, paper, glass and plastic waste.
SLC	Scan line corrector, an instrument onboard the Landsat 7 satellite.
Smelter	A plant in which metal raw materials, metal concentrates or secondary raw materials are processed to separate metals from impurities by means of high-temperature reactions.
Smelting	Smelting is the term used to describe the separation of metal from an ore using heat. In other words, it refers to the partial recovery of metal in molten form from processed ore. The latter will have been treated and concentrated at a mill, but smelting is required to actually recover the metal content and convert it to a form that is ready for refining.
Strip ratio	The ratio of tons of overburden and waste material to tons of ore in an open pit mine. Also called waste-to-ore ratio.
SVMs	Support-vector machines, supervised learning models that analyze data and recognize patterns, used for supervised classification of satellite imagery.
SX-EW	Solvent extraction-electrowinning, a metallurgical technique applied to copper ores in which metal is dissolved from the rock by organic solvents and recovered from solution by electrolysis.
Tailings (or beneficiation waste)	Refers to the materials left over after the process of separating the valuable fraction from the worthless fraction (gangue) of an ore. If dewatered, tailings can be dry-stack disposed, otherwise they are disposed of as slurry in tailings storage facilities called tailings dams, ponds or impoundments.
TM	Thematic Mapper. Refers to the main multispectral scanning radiometer (sensor) carried on board the Landsat 4 and 5 satellites.
TSF	Tailings storage facility, also called tailings management facility (TMF)
UG	Underground (mine)
UNEP	United Nations Environment Programme
UNFCCC	United Nations Framework Convention on Climate Change

Used extraction	Refers to the part of the material mined at a mine site which contains a sufficient concentration of metal to be economically processed, namely, ore. Common terms for used extraction are: run of mine, gross ore or crude ore.
Unused extraction	It refers to the materials removed to get access to the ore and includes the interburden, the overburden and the extraction waste.
U.S. or USA	United States of America
USGS	United States Geological Survey
VHRI	Very high resolution imagery
VNIR	Visible near infrared. See above NIR.
Waste rock (or extraction waste)	Barren or uneconomic mineralized rock that has been mined together with the ore, but it is not of sufficient value to warrant treatment and is not further processed (it is deposited in waste rock stockpiles). The economic and dynamic limit separating ore from waste rock is defined by the cut-off grade. Waste rock is produced during the extraction phase and might become ore if economic conditions, including technology status, change.
Waste dump	A, usually permanent, pile of waste, also called gangue or valueless rock. If economic conditions change over time, waste rock can be reevaluated and become ore.
WBGU	German Advisory Council on Global Change
WRS2	World Reference System-2, a global notation used in cataloging Landsat data belonging to Landsat 4, 5, 7 and 8 (previous Landsat satellites used the WRS1).

CHAPTER ONE

This first chapter serves as an introduction into the topic of the land use by the large-scale metal mining sector, its importance and the existing research gap at the global level. First, the hypotheses and the research questions are described. Second, a brief methodological overview with the steps followed in each chapter is given followed by the outline of the thesis. Then follows a concise description of the most important concepts employed throughout the text and of the main socio-environmental pressures and conflicts associated with large-scale metal mining. Finally the scope and boundaries of the research are presented along with a short global overview of the key trends in world mine production for each of the five metals under investigation.

1 Introduction

1.1 Background and current state of science

Land is increasingly becoming the center of attraction in scholarly and policy making-influencing debates. Viewed as a finite resource and embedded in high-level international scientific and inter-governmental discussions about earth system science, human-induced global environmental change and pathways to accomplishing the Sustainable Development Goals (SDG) (UN Open Working Group 2014), access to land and its nexus to other resources (Andrews-Speed et al. 2014, 2012) are topics increasingly gaining attention at global and local scales. Likewise, land degradation and land-use and land-cover change progressively are gaining space in political and research agendas (Dolman et al. 2003; Feddema et al. 2005; Fischer-Kowalski and Haberl 2007; Foley et al. 2005; Gutman et al. 2004; Lambin and Geist 2006; Lambin and Meyfroidt 2011; Rockström et al. 2009; Seto and Reenberg 2014; Verburg et al. 2011; Steffen et al. 2015).

Even though land use has generally been considered a local environmental issue, it is now becoming a force of global importance (Foley et al. 2005). This can be explained as the teleconnections (interactions over distances) between the global market demand, local or regional production in croplands, pastures, plantations or

urban areas and the effects on climate change, biodiversity loss and other global socio-environmental problems are more investigated and become apparent (Haberl et al. 2009; Liu et al. 2013a; Seto et al. 2012; Tukker et al. 2014).

Mining involves one of the greatest transformations of the landscape through human activity (Douglas and Lawson 2002) and acts, particularly with metals and in reserves-rich regions, as a major driver of anthropogenic land use and land cover change at the local level (Sonter et al. 2014b). Metal mining operations use the land for extractive purposes temporarily but often create long-term land and soil degradation (Haigh 1992; Miao and Marrs 2000; Poenaru et al. 2011). The global demand for mined minerals is foreseen to keep growing (PwC 2012; UN-DESA 2010; OECD 2015) and, given that recycling flows are not forecasted to surpass primary mining of metallic raw materials in the short term (Milford et al. 2013; Pauliuk et al. 2013; Sverdrup et al. 2014a, 2014b, 2012), pressures on the environment and biodiversity by mining are expected to increase and gain more relevance, at least in the next two decades.

In the past land system science research has traditionally been dominated by extensive land uses like forestry, agriculture and urban sprawl (Sonter et al. 2013), with fewer attention directed to the role of mining as a land-transforming agent. The focus is gradually changing since more attention is now being driven to the local direct and indirect impacts created by mining. Among these, long-term pollution and competition for access to resources like water or land can be counted (Andrews-Speed et al. 2012; Bringezu and Bleischwitz 2009; Smith et al. 2010). These impacts and pressures associated with mining are responsible for triggering socio-environmental land-related conflicts (Bebbington 2014; Hilson 2002).

Past previous research of land area disturbances associated with mining has been conducted by mining engineering disciplines which generated indicators relating land surface take with mining. One of the main research goals was the attempt to quantify the relationship between the material mined at a mine site and its specifc land requirements; this was done for instance for bauxite mines considering specific land requirements during the entire mine´s life cycle (Sliwka 2001), by

using a model based on volume data or estimates for ore and waste and fixed design parameters for the mine infrastructure in copper mines (Martens et al. 2002; Ruhrberg 2002) or by using density and quality of the ore for bauxite ones (Sliwka et al. 2001). All investigations conducted share the characteristic of assuming and including in the calculations a certain time required for site reclamation (Sliwka 2001; Spitzley and Tolle 2004)[1]. As the literature in the field of ecological restoration evidences, this latter aspect may be estimated for specific sites but it becomes very difficult for a global generalization as the success of an ecological restoration or a reclamation process depends on the contextual factors (Meli et al. 2014) (ecosystem type, natural climate, topography, rainfall conditions). Moreover, it also depends on the kind of transformation and rehabilitation actions performed by each mining project (experimental design, restoration age, amount of toxic materials present in the soil, human contingencies, etc), all of which determine the success and the velocity of the process.

While previous investigations were limited by a lack of data at a reasonable cost, nowadays investigations measuring actual on-the-ground performances (and their mine-induced surface disturbaces not asumming any disturbance rates) are possible due to the existence of remotely sensed data belonging to real mines made available by the opening of the USGS Landsat archive of satellite images. Such source provides free access to global coverage of medium spatial resolution imagery from 1972 until these days. The analysis of such imagery for measuring the land dynamics of metal mines has only been applied to single cases of local or, at most, regional scale but no attempts have yet been made to investigate measurements derived from many mines globally distributed.

With regards to the global area currently disturbed by large-scale metal mining, previous research has not been targeted at calculating the land disturbances by mines; existing research has only broadly estimated that mining might be

[1] Given the variety of possibilities in restoration times, the selection of the adequate time is site-specific. In some cases restoration of mine sites to near original conditions is possible whereas in other land degradation might be permanent and complete restoration becomes impossible or long-term. Whereas most LCA studies assume a certain amount of years for restoration, other models, like the Model IMAGE 3.0 assume no recovery of natural vegetation in areas mined (Stehfest and Planbureau voor de Leefomgeving 2014).

occupying considerably less than 1% of the world´s terrestrial land surface (Bridge 2004) or that mining and quarrying have transformed around 40 Mha (until 2007) (Hooke and Martín-Duque 2012). Yet, besides such coarse estimations, a research gap of the actual amount of land disturbed by mining remains. If future projections are considered, in the variety of models and scenarios which project future global land use trends (Hurtt et al. 2011; OECD 2012; Ozkaynak et al. 2012; Rose et al. 2012; Stehfest and Planbureau voor de Leefomgeving 2014), the future area disturbed by metal mining, to date and to my knowledge, has not been investigated. Also in scenarios specifically targeted towards metal mining, quantitative future projections of the global area disturbed by mining are absent (World Economic Forum 2010).

Besides occupying the land surface, one of the direct effects created by mining is the contribution to the alteration of ecosystems´ ecological character and the exercise of additional pressures on the global biodiversity richness. Past recent research has often focused on local-level studies of the relationship between mining and biodiversity (Bowles and Prickett 2001; Cooke and Johnson 2002; Hernández and Pastor 2008; Sonter et al. 2014a; Zhang et al. 2010) with numerous studies documenting the negative impacts on areas of high biodiversity (Banks 2002; Cardiff et al. 2012; Van Zyl et al. 2002a, 2002b). Global studies approaching the pressures of metal mining on biodiversity have only been directed to protected areas (Durán et al. 2013; Kobayashi et al. 2014; Koziell and Omosa 2003; Miranda et al. 2003) but no investigations exist on pressures outside of them from a global perspective. Likewise, no research has yet been conducted exploring the implications of a global biodiversity management strategy aiming to evaluate the availability of mineral reserves and resources in areas of low biodiversity and the potential to shift new mines and exploration efforts towards such areas, lowering the pressure on high biodiversity ones.

This Ph.D. research seeks to fill in the knowledge gaps associated with large-scale metal mining, specific land requirements and direct pressures on global biodiversity by investigating current and future land use for the global extraction of **iron ore, bauxite, copper, gold** and **silver**. The study draws on an original methodology combining advances in the remote sensing field and material flow

analysis, thereby establishing correlations between material extractions at mine sites and area disturbances. Likewise, based on these results and on work by colleagues, exploratory scenarios and scenario corridors until 2050 are constructed which provide approximations to pressures on land caused by mining and allow observing potential reductions of global land disturbances subject to the deployment of energy and material efficiency measures.

1.2 Hypotheses and Research Questions

Metal mining activities occupy and transform the land surface creating a disturbance during the ore mining and milling phase until the mine closes and, theoretically, rehabilitation takes place. However, how much land is often disturbed in a typical industrial operation? Is it related to the amount of material mined? In this study the first hypothesis asserts that:

the cumulative material extracted at a mine site determines the cumulative net area disturbed by the mine.

Based on this hypothesis, the **first research questions inquire: how many hectares become newly disturbed by large-scale metal mines per million metric ton of ore extracted? In other words, what is their specific land requirement?** And how does it vary for each of the metals under study?

The second topic of the research is about the global area currently disturbed by metal mining. Assuming there is a direct relationship between material mined and land surface affected, the research questions ask: how much material (ore) is currently being globally extracted (per metal)? And how much land is currently disturbed by its extraction?

The third research problem is about the future development of the global area disturbed by metal mining. Given the expected trends of continued and increasing global demand for primary metals, the research questions ask: how might the current global area disturbed by metal mining likely behave in the next decades? What do forward-looking scenarios look like? Which mitigation measures could be applied in order to reduce the global area disturbed by mining to a minimum?

The fourth topic investigated is about the pressure on biodiversity exerted by metal mining as a driver of land use and land cover changes. The second (null) hypothesis of this thesis affirms that:

the frequency distribution of mines and deposits across diversity zones equals the frequency distribution of diversity zones in the world´s terrestrial surface area (excluding Antarctica). In other words, the observed frequency distribution of mines and deposits across diversity zones matches a natural, random (by chance) pattern.

Consequently, the target questions ask: how are metal mines and geological ore deposits spatially distributed across the world? And how are they distributed across biodiversity zones? What is the share of each diversity zone within the world´s terrestrial surface area (excluding Antarctica)? Are frequency distributions equal?

1.3 Methodology overview

In order to answer the specific land requirements question, five samples of large-scale metal mines were selected, each of them belonging to the five metals under scrutiny. For copper, gold and silver, mines´ samples include polymetallic operations which were classified according to the main metal produced in each mine. Samples and data on cumulative material mined were retrieved from the SNL Metals & Mining database[2] (SNL Metals & Mining 2015) and the area disturbances were measured using multiple Landsat satellite images (USGS 2015). The specific land requirements of each metal were derived from weighted disturbance rates calculated by applying least squares nonlinear regression analysis regresing the cumulative net area disturbed onto the cumulative material mined.

[2] The SNL Metals & Mining database (www.snl.com/Sectors/MetalsMining) is the result of the combination of the former IntierraRMG and SNL Metals Economics Group databases. The database is one of the world´s most extensive commercial data sets with information on current and historical yearly production and other variables on a (legal industrial) mine-per-mine basis for 30 minerals as well as information on deposits, their status, etc. Given that research work on this thesis was begun before the merging of the Raw Materials Group (RMG) with Intierra first and then with SNL (January 2014), the dataset was extracted only from the RMG database according to different updates along the year. Although the reference along the study is SNL Metals & Mining, updates are included as they were done by the RMG group.

Figure 1: Methodological overview. Steps followed in each chapter.

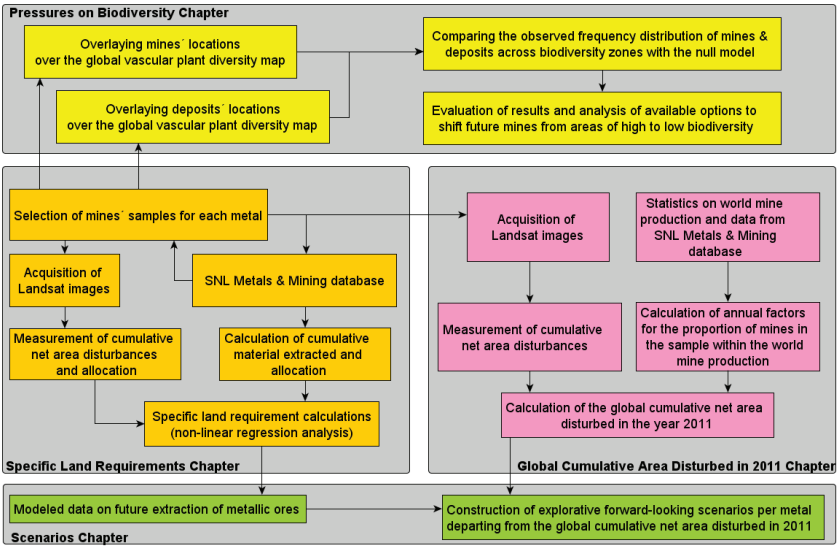

The global area currently disturbed was computed by, first, calculating the cumulative net area disturbed in 2011 for each metal; this was done for each sample by measuring net area disturbances in Landsat satellite images and, for copper, gold and silver by allocating area disturbances according to economic value relations (average metal prices). Second, an annual (proportion) factor for the period 2010-2012 was calculated dividing the world mine production by the sample production (of ore or metal content). Such proportion factor was multiplied with the cumulative net area disturbed (for 2011) of all mines in each sample to obtain the global status quo in 2011 for each sample. Finally all samples were added together to achieve a global estimate.

With regards to the scenarios, the global status quo in 2011 (or area disturbed calculated for the year 2011) was used as the basis and scenarios and scenario corridors were constructed using modeled data of future annual primary ore extraction per metal obtained from existing models. The specific land requirements were multiplied by the annual projections of ore extracted. This delivers the annual amount of hectares newly disturbed globally, which were added annually until

2050. As a result three to six future pathways per metal were built showing possible business-as-usual scenarios contrasted with others emphasizing energy and material efficiency measures. For copper, gold and silver, one business-as-usual scenario was built based on data modelled by colleagues (Northey et al. 2014; Sverdrup et al. 2014a, 2012), and a scenario corridor catering for an uncertainty range was added.

Concerning the pressures on biodiversity, the method consisted in comparing the frequency distribution of the observed data (actual global spatial distribution of mines and deposits across biodiversity zones as defined by Barthlott et al. 2007) with a null model. According to Barthlott et al., the species diversity is represented by species richness of higher vascular plants graphically displayed in a global map with ten diversity zones (from low to high plant species diversity). Such map was overlaid with records of mines and deposits extracted from the SNL Metals & Mining database. The frequency distribution of the observed data (per diversity zone) was compared with a "null model" (random or natural pattern) which was constructed by calculating the share of the area occupied by each diversity zone in the world terrestrial surface (in percentages, excluding Antarctica). The null hypothesis, arguing that the frequency distribution between the observed and the null model was equal, was tested statistically using a Pearson´s chi square goodness-of-fit test and Fisher´s exact test of independence with Monte Carlo simulation and visually using bar charts and maps.

1.4 Structure of the thesis

This thesis is structured around four main research questions which orientate the Chapters.

First, the specific land requirements for each metal were investigated; the second step consisted in calculating the global cumulative area disturbed by metal mines in 2011 which served as the basis for the scenarios. The third step consisted in combining the calculations on specific land requirements with existing projections of metal primary supply to explore pathways of growth of the cumulative area globally disturbed. The last section of each Chapter belongs to the global pressures on biodiversity.

Figure 2: Overview of the thesis structure.

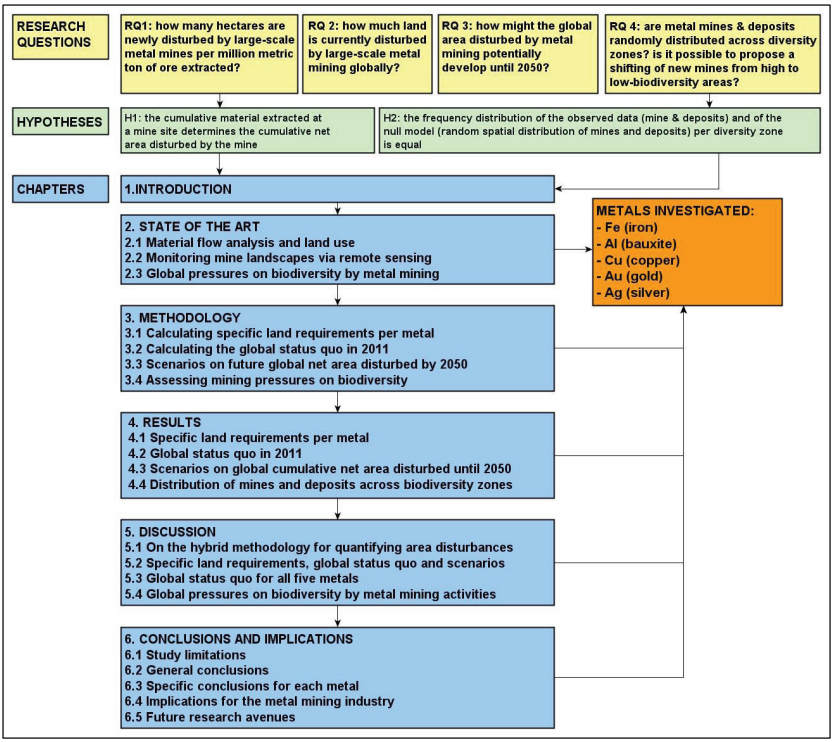

Chapter 1 provides an introduction to the topic of large-scale metal mining and its associated land use and socio-environmental impacts and pressures, summarizing existing research and knowledge gaps focused on area disturbances. It presents the main research questions and hypotheses, a methodology overview, terminology employed throughout the text, the scope and research boundaries. A brief introduction into basic aspects of mine production for each of the five metals under investigation is presented.

Chapter 2 provides the reader with a concise introduction into the topic of material flow analysis and land use with relation to mining issues. The Chapter then draws on the available remote sensing methods for the monitoring of large-scale mines.

It is ensued by a review of literature on land use impact indicators for mining, models to forecast primary mining trends, and the approach employed to operationalize the concept of biodiversity.

Chapter 3 is central to this dissertation as it describes the method and the sample of active mines and Landsat satellite images used per metal to answer the different research questions. The chapter describes the workflow developed and applied for the measurement of the cumulative net area disturbed on each of the mines sampled and the allocation (of cumulative ore and area disturbances) for polymetallic ones. The method used for constructing scenarios and scenario corridors is also described along with how pressures on biodiversity were evaluated across plant diversity zones.

Chapter 4 provides detailed results of specific land requirements calculations, the global status quo in 2011, results from the scenarios and scenario corridors, and the global analysis of mines and deposits and their pressures on biodiversity zones.

Chapter 5 discusses the hybrid methodology for measuring area disturbances and frames results of specific land requirements, the global status quo and the scenarios with existing literature. Finally approaches to operationalize the concept of biodiversity, the possibility of shifting new mining operations towards low biodiversity areas and implications for different actors are discussed.

Chapter 6 provides general and per-metal conclusions acknowledging limitations and a series of implications for the metal mining industry. **Chapter 7, 8** and **9** comprise the list of References, the Appendix and a short biography of the author.

1.5 Concepts and terminology

1.5.1 Open pit and underground mining methods

Mining begins with the discovery and determination of a mineral deposit being minable according to the current state of technology, the economic conditions of the global market and the jurisdiction where it is located. Once a deposit has been identified and deemed profitable to mine, an extraction method is selected according to the characteristics of the deposit; this depends on the geometry (size

and location) of the ore reserves[3] buried underground, the local topography and cost considerations included in the feasibility study. For instance, an open pit operation is preferred if the ore body is relatively close to the surface (<500 m), the overlaying soil (called overburden) is shallow or the surrounding environment is too unstable to tunnel beneath (Burt 2008). If the ore body is located deeper, an underground operation might be the preferred method. Regulations applied to mining or nearby land uses to the deposit location influence the method selection. Besides open pit and underground, other methods encompass placer mines, tailings mines and the combination of open pit and underground in the same site.

Of the methods available for surface mining, open pit is currently the preferred one for mining many metallic ores like copper or gold ones. For greenfield projects[4] taking place in previously undisturbed areas, e.g. zones within tropical rainforests, this method entails the site preparation (vegetation clearance, removal and storage of top and sub-soil), removing the overburden to expose the ore body and gradually create a large hole in the ground by drilling, blasting and forming of benches, referred to as open pit or borrow-pit, from which the ore is blasted and removed. A typical open pit is shown below in Figure 3; an explanation of each term forming an open pit and an underground mine is displayed in Figure 4.

To remove the mineral endowed rock, waste rock (extraction waste) must also be removed. During mining, ore and waste may be encountered on each bench and are selectively mined and transported by haul trucks to processing facilities or waste dumps adjacent to the pit.

In open pit operations, waste is often dumped outside the mined-out area since no room is available within the pit; waste can also be dumped back into the main pit but this practice is costly and unusual. In underground mining, the waste rock can be left underground and overburden is never removed (Rajaram et al. 2011).

---

[3] Ore reserves is also a dynamic concept, namely, the amount of reserves (and resources) calculated for a deposit changes over time since they can be materially affected by adverse changes in commodity and consumable prices, exchange rates, taxes or operating and labour costs.

[4] The opposite are brownfield projects which refer to areas where historic mining has been occurring and disturbances already exist, e.g. brownfield exploration refers to near-mine exploration, i.e. (satellite) deposits adjacent to operating mines which ensure low additional capital costs for the processing of the new found ore.

Figure 3: Pictures of an open pit (left) and an underground (right) gold mine.

Source: GHHLORS[5] and Great Basin Gold Ltd (2011).

The strip, stripping or waste-to-ore ratio determines the relationship between the waste rock and the ore to be removed[6].

Figure 4: Schemes of open pit (left) and underground (right) mining methods.

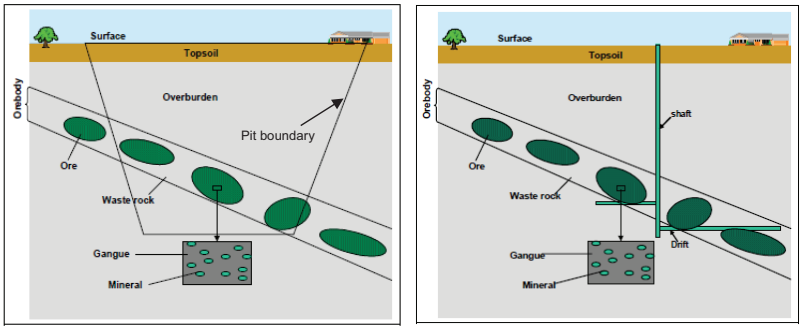

Source: European Commission (2009)

In both surface and underground operations, the difference between what is considered ore and waste rock is set by the cut-off grade which is defined as the lowest grade which can be mined profitably or as the minimum amount of valuable metal for the mineralization to be considered ore. In other words, it is a percentage

[5] Photo credits belong to Charlotte Gild, Richard Hastik, Fabian Heimann, Maria Lemper, Christian Obermayr, Theresa Ringwald and Korbinian Schmidtner; their initials constitute the acronym GHHLORS.

[6] When adopting this definition, the ratio is expressed as metric ton of waste per metric ton of ore mined (e.g. 2:1, two tons of waste per each ton of ore mined). However, it must be noted that in layered fossil fuel deposits the ratio is stated as m^3 of waste per ton of raw material, for instance, in the U.S. in open pit coal mines the term cubic yard to short ton of coal is used frequently (Wellmer et al. 2008).

determined by many factors and continuously re-calculated through continuous assaying and cost considerations. For any metal the cut-off grade depends on economic factors, for instance, iron is a relatively cheap metal so ores with less than 25% iron content are not worth mining. On the other hand, tin is extracted profitably from ores which contain as little as about 0.5% Sn. The exhaustion of rich or high-grade ore leads to a progressive lowering of cut-off grades so large-volume low-grade ores become economically extractable; this has been the historic trend.

Once the ore has been blasted and removed from the pit or from the drifts, this ore, called usually run of mine (ROM) or used extraction in EW-MFA terminology, is loaded onto haul trucks and transported to the mill for beneficiation. The final product leaving the mine site is often a concentrate containing payable metals, doré bars in the case of gold and silver mines and sinter feed or pellets in the case of iron ore mines, which are then shipped to the next step in the value chain (a smelter or refinery, as depicted in Figure 5).

Figure 5: Simplified scheme of material flows at a generic metal surface mine.

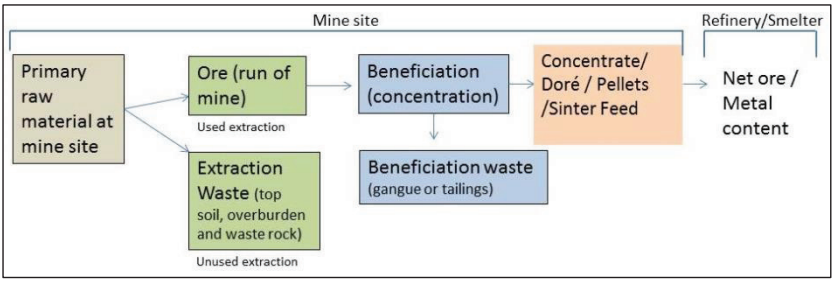

Source: self-elaboration based on Eurostat (2011)

In underground mines, minimal amounts of topsoil or overburden are removed to gain access to the ore deposit. Access to this ore deposit is gained by tunnels or shafts and its extraction is performed through a series of vertical shafts, ramps and horizontal drifts (Figure 4). Extraction is more selective than in open pit mining,

and the ratio of waste rock to ore generated is much lower given that ore grades[7] are usually higher; i.e. open pit mines produce eight to ten times as much waste rubble as underground mines (Earthworks and Oxfam America 2004). Besides, the waste rock generated is used in many cases as mine backfill to provide roof and wall support underground. Waste rock that is not used for construction or as backfill is disposed of on the surface.

In both open pit and underground operations, beneficiation takes place depending on the quality of the ore removed, measured by the metal content. During beneficiation the metal content of the ore needs to be increased and the gangue, native rock and minerals of lesser value within the ore, need to be separated out. Physical methods such as screening, crushing, grinding are used along with magnetic separation and other chemical methods in order to increase the grade of the final product and produce the gangue which ends up as beneficiation waste in tailings ponds or as dry stacks. Reclamation might start early at the mine site by stabilizing and vegetating waste dumps or other landforms.

1.5.2 Land use and land cover

As Comber (2008) argues the concepts of 'land use' and 'land cover' are not synonymous. While land cover refers to the vegetation and artificial constructions covering the land, land use concepts target the human activities on the land. Both are clearly connected since changes in land use can and do change the land cover and vice versa. However, the connection may be complex since a given land use (e.g. grazing) may be associated with several different types of land cover (e.g. grassland and forestland), and a land cover (e.g. forestland) may have several different land uses (e.g. timber production, recreation, wildlife conservation) (Loveland and DeFries 2004). Furthermore, land cover tends to be static over short periods of time whereas there may be multiple land uses at any given place. In the case of mining this is more straightforward as mining activities take place only in a mining landscape. Therefore, when performing measurements of the land cover disturbed by a mine, this study will be referring to them as the

[7] Grade is defined as the percentage of the desired metal contained in the ore. For example, a copper ore with a grade of 1% would contain 10 kg of copper for each 1,000 kg (metric ton) of ore.

cumulative net area disturbed or the amount of land occupied to carry out the mining activities. It includes all active areas used once commercial production of the mine has started; it does not include nearby explored areas.

1.6 Socio-environmental pressures and conflicts

Large-scale metal mining operations, and in some cases artisanal ones too, e.g. illegal operations such as Madre de Dios in Peru (Asner et al. 2013), cause substantial modifications in the ecosystems, societies, economic settings and landscapes where they operate. Such activities create numerous positive and negative socio-economic and environmental impacts which have different intensities, time-scales of occurrence, potentiality of occurrence and reversibility.

Direct pressures

Once a deposit has been classified as profitable by a feasibility study, local authorities may grant a permit to a mining company to start with the development of the mine workings within a mining claim (or concession area). Unlike forestry, a mine site does not directly occupy the entire concession area and its net area disturbances may encompass only a few km^2 of a very big area.

Direct pressures on livelihoods and ecosystems take place with different intensities during the whole life cycle of a mining project (exploration, mining development, extraction, beneficiation, shipping of product, land rehabilitation and decommissioning). The most land-intensive pressures and impacts take place during the construction and operation phases (Villas Bôas and Barreto 1996) as the land is cleared of vegetation (de-bushing), the topsoil is removed and stockpiled, and the land is used for the construction of the mine workings and facilities (camps, waste dumps, tailings ponds, heap leach pads), the removal and placement of overburden and waste, etc. Furthermore, direct pressures can extend well beyond the concession area (Miranda et al. 2003); for instance, the mine waste dumped in the Jaba River in Papua New Guinea resulted in fish loss in 480 km^2 (Boge 1998).

During decommissioning positive aspects include the land reclamation but also adverse impacts may occur; one of the worst is the generation of acid mine

drainage (AMD) which involves the formation and movement of highly acidic water rich in heavy metals which forms through the chemical reaction of surface water and shallow subsurface water with rocks that contain sulfur-bearing metals, resulting in sulfuric acid. For instance, this is currently a most serious problem in the gold mining region of Witwatersrand in South Africa, particularly in underground mines (Tutu et al. 2008). The main problem with AMD is its long-term permanence and the costs of remediating these sites; according to the U.S. Bureau of Reclamation in the U.S. there are close to 1,230 hazardous sites of which 142 are supersites because of their size and environmental devastation. Of those, almost all (133) are open pit mines with a remediation cost of over USD 50 million in each case (Gutman 2013). Nevertheless, other kinds of pollution originating from fractures in tailings ponds or bad tailings disposals practices (e.g. riverine tailings disposal) may also take place (e.g. Craig Vogt Inc 2012).

In the social realm, the issue of the paradox of plenty, also called the resource curse, is one of the hotspots of the debates; it posits that countries or regions very rich in non-renewables resource tend to show poor economic growth and worse development outcomes (i.e. higher poverty and inequality rates) than countries or regions less endowed with such resources. As Bebbington posits the thesis gained momentum in the early 1990s in an attempt to explain two decades of poor economic performance in mineral-rich countries (Bebbington 2011), and has been around much scholarly debate between those who subscribe and seek ways out of it (Bebbington et al. 2008; Bringezu and Bleischwitz 2013) and those who question it (e.g. Davis 1995; Davis and Tilton 2005).

Another main field of socio-environmental pressures revolves around competition for land. Land is a finite resource and has a competitive use as it serves for different purposes; given that not all services provided by the land can be maximized simultaneously, every land use decision involves trade-offs, often resulting in competing interests and conflicts about the desired use of land among stakeholders (Schueler et al. 2011). Large-scale mining and communities have been engaged in conflictive relationships for long (Bebbington 2011; Hilson 2002; Oxfam America 2014; USAID 2005); often big mines demanding significant amounts of area clash with surrounding communities, included indigenous people,

who depend directly upon the land and indirectly upon the services provided by it (Ali 2009). Other conflictive issues which are foreseen to become key drivers of social conflicts include competition for water (Bebbington and Williams 2008; Kemp et al. 2010) and with agriculture (Bringezu and Bleischwitz 2009; Harvey and Pilgrim 2011; Rathmann et al. 2010).

The negative environmental impacts and the competition for land have triggered numerous social conflicts around the world. The Environmental Justice Atlas of the EJOLT project[8] has a focus on mining-related conflicts and provides an updated global overview. By May 2015, globally 388 cases of environmental conflicts around mineral ore exploitation, mineral processing, tailings from mines and coal extraction and processing were reported.

Indirect pressures

Besides direct pressures, the literature and the political realm more and more recognize the complex and geographically distant interrelations of globalized supply and demand chains which frame mining projects. This idea that spatial heterogeneity is a more important factor governing land use change dynamics than land use spatial extent is rapidly gaining importance (Rounsevell et al. 2012; Smart et al. 2012).

Interactions between land uses is also illustrated with the emerging literature on 'indirect' land-use changes (Lapola et al. 2010), distant drivers of land change (Meyfroidt et al. 2013) and 'teleconnections' (Haberl et al. 2009; Liu et al. 2013a; Seto et al. 2012; Seto and Reenberg 2014) where a change in the demand and production of one resource in one geographical location affects the production opportunities for other resources elsewhere. The above discussion identifies an overlooked category of land uses, defined as 'intensive land uses'. These land uses occupy a relatively small spatial extent but can indirectly drive land use change dynamics through their operation (Sonter et al. 2013).

[8] http://ejatlas.org/ Website accessed: May 2015.

Positive indirect impacts include, for instance, creating unintentional deforestation buffers. Negative impacts include the provision of inputs for the processing of ores. In Brazil, the production of charcoal for steel production from short-rotation Eucalyptus monocultures with large land requirements is expected to grow in the future (Sonter et al. 2013). Likewise, and while mining may be directly protecting a small part of the rainforest through deforestation buffers around the mine site, it is indirectly exerting pressure through energy consumption which is increasingly being generated through new hydroelectric dams.

These examples only serve the purpose of enlightening the inherent complexities of indirect impacts and the difficulty of making a global outlook considering them. At most these can be understood at local or regional levels, but a global vision seems methodologically challenging. Therefore, this study only focuses on tackling the direct impacts related with land disturbances, with the hope it serves to those colleagues working on indirect ones.

1.7 Delimitations of scope

1.7.1 Selection of five key metals

In terms of mass flows, globally between 47 and 59 billion tons of materials are mined every year (Steinberger et al. 2010) of which sand and gravel (aggregates) account for the largest share: a conservative estimate for world consumption of aggregates exceeds 40 billion tons a year (UNEP-GEAS 2014). After these giants, the world production of mineral raw materials was led in 2011 by coal (in all forms) totaling over 7.7 billion tons, followed by petroleum (3.8 billion tons), iron (1.4 billion tons) and industrial minerals[9] (713 Mt) (Reichl et al. 2013); all other mineral fuels (oil sands, shales, uranium, natural gas) and also the rare earths (mined at a rate of 100,000 t/a) still play a minor role in terms of volumes extracted.

All massive solid material volumes are extracted worldwide in a very big number of mines and quarries. According to Ericsson (2012), assuming U.S. relationships in the number of mines and quarries, there would be some 25,000 mines in the world

[9] Includes asbestos, barite, bentonite, boron, diamonds (gem and industrial), diatomite, feldspar, fluorspar, graphite, gypsum, kaolin, magnesite, perlite, phosphates, potash, salt, sulfur, talc, vermiculite and zircon.

producing industrial minerals and almost 100,000 quarries producing aggregates for construction purposes. Quarries are excluded from this study as they do not produce metals.

Setting aside coal and oil, iron is by far the most massively extracted mineral, followed by bauxite (205 Mt/a), manganese (19 Mt/A), copper (16 Mt/a), zinc (12.8 Mt/a) and chromium (11.5 Mt/a); in 2011 there were no other metals produced in excess of 10 Mt/a globally (Figure 6).

Figure 6: Global extraction of selected minerals (Mt/a). 2011.

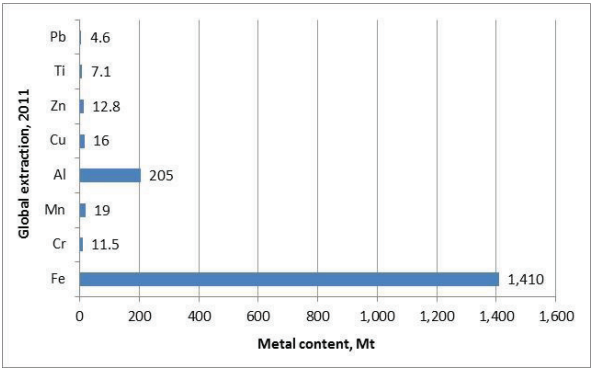

Source: self-elaboration based on Reichl et al., (2013)

In terms of global extraction of crude metallic ores (used extraction), iron and copper represent the highest amounts, followed by precious metals (Figure 7).

Figure 7: Global extraction of main metal ores. 2008.

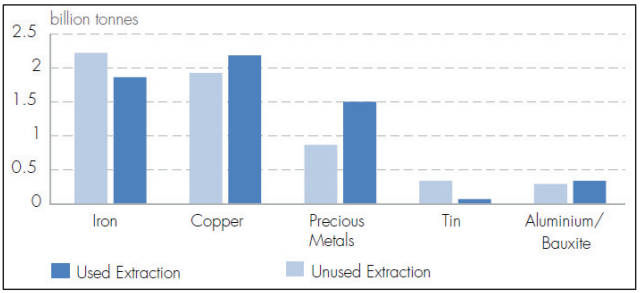

Source: Dittrich et al. (2012)

Iron, bauxite and copper were chosen not only due to the magnitude of global extraction but also because of their relevance to the industry; for instance, copper is considered as one of the most important metals for modern society, ranking after iron and aluminium in importance for infrastructure and technology (Sverdrup et al. 2014b).

Likewise if approached by the share in value as depicted in Figure 8, copper, iron and gold stand out as key metals.

Figure 8: Value of global production by metal. 2011.

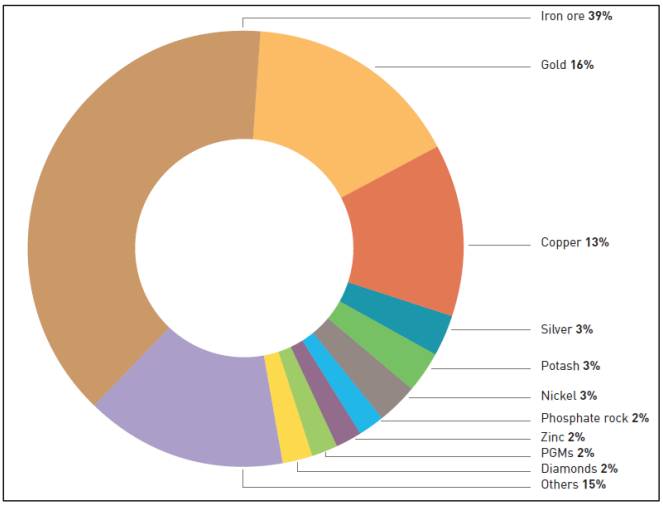

Source: Ericsson and Hodge (2012)

Gold and silver are not relevant in terms of direct mass flows but are relevant as precious metals to the industry and the investment sector. At the same time, their mining entails using conventional extraction and beneficiation methods which pose risks to the environment and communities; this type of mines have been and are expected to be at the center of socio-environmental conflicts for long. These reasons made their inclusion worthwhile. Thus the five metals selected for this study are: **iron, bauxite, copper, gold and silver**.

It is worth mentioning the increasing importance of phosphorus as a core component of conventional mineral fertilizers, essential for industrialized agriculture, a key sector for a socio-ecological transformation (Bleischwitz et al. 2012) as well as the increasing importance of lithium and critical raw materials like the platinum group metals and rare earths (Buchert et al. 2009; European Commission 2014b; MIT 2010). Nonetheless, despite their qualitative relevance, they have not been included due to their comparatively low extraction volumes.

1.7.2 Research scope

1.7.2.1 Specific land requirements calculations

Mines included in the sampling to calculate specific land requirements comprised only large-scale mines producing, having produced or to resume production of the five metals, with precise geographic location and being either open pit or underground; mines not fulfilling this criteria (e.g. artisanal mines, abandoned mines) were excluded (are placed outside the circle in Figure 9).

Direct impacts: The goal of this research is to determine the quantity of land *directly* disturbed by mining activities in relation to the quantity of material milled. Therefore, the system boundary is determined *by the areal extent of the mine site*. Indirect impacts on the land, i.e. land disturbances occurred in geographically distant places are excluded. Road building is one of the indirect impacts which have been approached by the land system science literature; often they create significant adverse impacts, particularly in primary forest areas; quantifiable direct damages measured in satellite images are relatively small but increased access to a previously hard-to-access area will encourage other agents of clearance into the area (Park 1992). Likewise, mining operations creates disturbances during exploration within the mining lease. Despite their importance, such impacts have been excluded.

Life cycle phase: Considering the metals´ life cycles, this study is focused only on the phase of extraction and beneficiation at the mine site which is the one with the largest land impacts (Villas Bôas and Barreto 1996). In the few cases in which next to the mine site a smelter or refinery is placed, it was not included in the net area disturbance calculation.

Figure 9: Research boundaries of mine selection for specific land requirements.

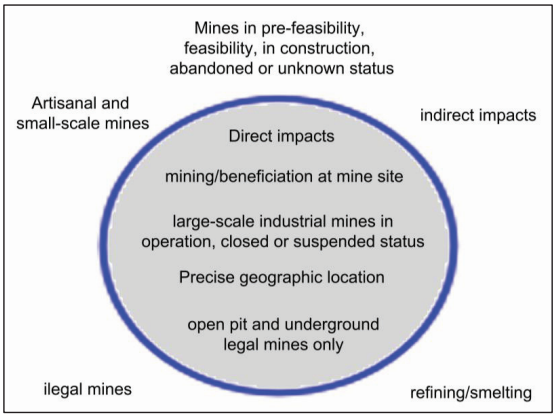

Large-scale industrial mines: the selection of mines to be worked with was determined by the mining entities available in the SNL Metals & Mining database. The latter does not include illegal mines. The cut-off criterion was determined by the list of mines and deposits available at a certain update; according to the former Raw Materials Group´s (RMG) manual: "normally a new deposit is included if published resource or reserve figures are available and if this figure is greater than 50 kt of ore" (Raw Materials Group 2004:55). Consequently, mines with resources or reserves lower than such limit were not considered large-scale and were not included. Another reason not to include ASM mines lies in that area disturbances´ calculations are performed using Landsat images with a pixel size of 30 meters in which only large-scale mines can be relatively well detected by visual interpretation[10].

Mine status: given that this study seeks to calculate disturbances arising from mine production of ore, only mines that have been operating (and for which material flows data are available) were considered. This means that only mines in the SNL Metals & Mining database with the status "operating", "closed" or

[10] In none of the five metals the ASM sector accounts for the lion´s share in metal production. The biggest share is for gold in which it represented (2011) between 12% and 25% of world annual production whereas in iron ore it was less than 4% (Sibaud and GAIA Foundation 2013) and for copper 0.5% (Ericsson and Hodge 2012).

"suspended" were examined, disregarding those mines under "construction", "abandoned" and still a project ("conceptual", "pre-feasibility" or "feasibility"). All records for which no status is given were also excluded.

Geographic coordinates: another requirement for mines to be considered eligible was the availability of exact coordinates to know their location and be able to separate their area disturbance from nearby mines or other land covers. The SNL Metals & Mining database provides coordinates for many mines but not for all; for those available, in some cases coordinates given were not totally exact and needed to be refined[11]; occasionally they were far from the correct one or the coordinates provided belonged to a mining complex comprising more than one mine, e.g. Vale´s iron ore mining complexes in Brazil. In all these cases corrections were necessary based on information publicly available. If possible, correct coordinates were obtained and the mine was included; otherwise it was left out.

Mine extraction type (or method): in order to simplify the research, this study is restricted to mines working as open pit or underground. The types open pit and underground (OPUG), tailings, offshore (including deep sea mining), placer or not given were excluded.

1.7.2.2 Boundaries for records´ selection for the analysis of global pressures on biodiversity

Research boundaries for the analysis of pressures on biodiversity for mines and deposits are all the same as above with the exception of the criteria "mine status" and "geographic coordinates". In this case SNL Metals & Mining entries considered "mines" included mines in "construction"; records counted as deposits included all entries under the status "project no spec", "feasibility", "pre-feasibility", "abandoned" or "project abandoned". Concerning geographic coordinates, they were not tested one by one in terms of accuracy; they were used as given since a 6-digit precision is sufficient for a global overlaying on the map of vascular plant

[11] This limitation is acknowledged by SNL Metals & Mining. The database provides geographic coordinates for each mine with a precision of six digits instead of seven which makes a difference when measurements are done mine-per-mine.

biodiversity zones as determined by Barthlott et al. (2007, 1996); further details on the process to select mines and deposits per metal can be consulted in the Appendix under the Section 8.6.1.

1.8 Brief introduction into mining of the five key metals

1.8.1.1 Iron (Fe)

Iron is the world´s preeminent metal: globally, it is the most widely used and recycled metal (Yellishetty et al. 2011) and steel making is one of the world´s largest industries (Nuss et al. 2014). The iron ore mining sector is closely related to the steel making industry as approximately 98% of the ore shipped is consumed in the production of cast iron and steel (Polinares 2012). Although underground mines are in operation, iron ore is predominantly mined worldwide in open pit operations (Polinares 2012) with ore grades ranging between 20% and 60% of metal content per metric ton of ore extracted. Once extracted, iron ores undergo a concentration process (except high-grade or direct shipping ore grade ones which are extracted, crushed, screened, blended and exported) to produce fines and lump ore; often fines are sintered and pelletized near the mine. The resulting iron ore products shipped from mines are lump ore, sinter feed and pellet feed with average grades of iron content around 65% which are exported out of the mine site to a smelter. These are generally incorporated into the steel making industry via the blast furnace-basic oxygen furnace (BF-BOF) steel production technique which is responsible for nearly 70% of all steel produced globally (World Steel Association 2012); this technique is the main source of primary steel. In contrast, the second steelmaking route is the electric arc furnace (EAF), which uses electricity to melt recycled steel and is considered a more resource efficient steel making option: whereas the production of a metric ton of crude steel using the BF-BOF process typically requires 1,400 kg of iron ore, 800 kg of coal, 300 kg of limestone and 120 kg of recycled steel, the production of a metric ton of crude steel using the recycled steel EAF process requires 800 kg of recycled steel, 16 kg of coal and 64 kg of limestone (World Steel Association 2012). Directly reduced iron by the usage of a reducing gas from natural gas or coal is another technique increasingly being used integrated with the EAF.

Currently world production of iron ore is dominated by supply from massive hematite deposits, for instance from Australia which produces ore from high-grade hematite and pisolithic geoethite-limonite deposits in the Hamersley Basin region. Global mine production of iron ore is in the range of 2,200 to 3,000 Mt/a being China, Australia and Brazil traditionally and currently the source countries hosting the mines and iron complexes which produce the highest quantities of iron concentrates in the world (Brown et al. 2014). In the case of iron and other metals, the role of China has become noteworthy in the last years as the country has become the dominant metals consumer in the world: between 2000 and 2010 it increased its production of iron ore by 233%, bauxite by 293%, zinc by 150% and copper by 124%, becoming the largest iron ore, zinc, gold and tin producer, second largest bauxite producer and third largest copper producer in the world (Lee et al. 2012).

Area disturbances at iron ore open pit mines include the open pits, waste dumps, the mine industrial area and infrastructure, including rail loops or rail loading areas, airstrips; in mines where beneficiation takes place tailing ponds are present.

The massive extraction of virgin ores from the earth´s crust constitutes the highest proportion of the global iron supply as the proportion of recycled steel is still relatively low: steel scrap to crude steel ratio was roughly 36% in 2013 (Bureau of International Recycling 2014) but is expected to grow after 2020. Forecasts predict that as large volumes of steel scrap become available, global primary production of iron may peak by 2025, and the subsequent rise of total steel demand might increasingly be met by EAF steel production, with the latter projected to surpass BOF steel production between 2050 and 2060 (Pauliuk et al. 2013).

However, in the next decades the cumulative area disturbances caused by primary iron ore production are expected to remain as enough iron ore reserves are available. World resources of crude iron ore are predominantly low-grade, e.g. in China, and estimated to exceed 800 billion tons containing more than 230 billion

tons of iron (USGS 2014b). Reserves are located mostly in Brazil, Australia, Russia and China (Figure 10)[12].

Figure 10: Iron ore reserves per country (Mt). 2014.

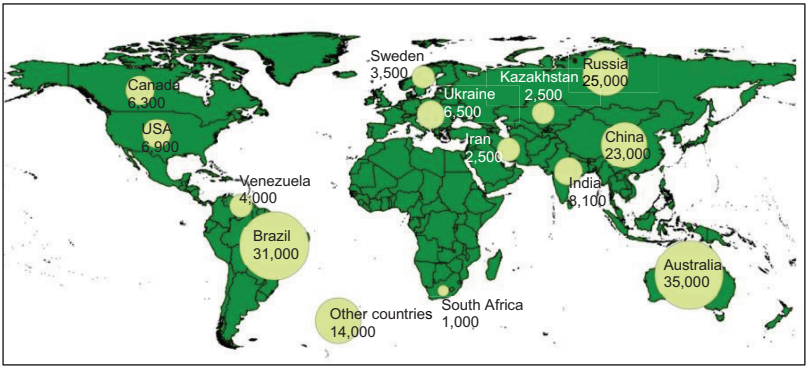

Source: self-elaboration based on USGS (2014b)

1.8.1.2 Bauxite (Al)

Globally and among the ferrous and non-ferrous raw metals mined, aluminium (bauxite) is second to iron ore production in quantity. Bauxite ore is the world´s primary source of aluminum: over 85% of the bauxite mined globally is converted to alumina (Al_2O_3) (Plunkert 2000) for the production of aluminium, used mostly for the transportation, building and construction, engineering and cable sectors. As shown in Figure 11 bauxite mining is concentrated in Australia, Brazil, Ghana, Guinea, India, Jamaica and parts of Russia and China, with some of largest bauxite mines operating in such countries (Table 1).

Bauxite ore mining is generally a relatively shallow, surface operation which removes a layer averaging two to five meter deep, located at about half a meter beneath the topsoil. Once the area to be mined has been determined, vegetation is removed and the (organic) topsoil (overburden) stripped.

[12] No data on reserves or resources in Antarctica are included. Commercial mining in such continent has been banned in 1998 for a period of 50 years under the Madrid Protocol.

Figure 11: Global production of bauxite ore and reserves. 2011.

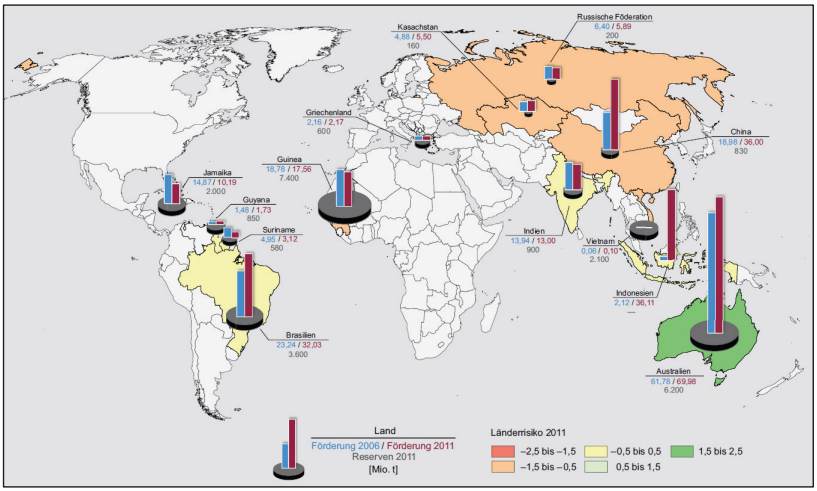

Source: BGR (2013)

The latter is generally stockpiled and used to regenerate land since the topsoil contains beneficial bacteria and organisms that assist newly planted trees (seedlings) to grow over previously mined areas. Bauxite develops over almost all types of geology but over one-third is formed on sedimentary rocks.

Table 1: Most important operating bauxite ore mines in the world.

Country	Mine name	Bauxite ore reserves (2011) [Mt]
Australia	Weipa	1,699
	Worsley	312
	Gove	170
Brazil	Trombetas	257.5
Indonesia	Munggu	54.0
	Tayan	52.4
China	Pingguo	86.4
Guinea	Sangaredi	53.1

Source: BGR (2013)

Lateritic bauxite comprises 85% of the total world tonnage of bauxite mined and globally most economic reserves of bauxite are located between 25° N and 20° S (Bárdossy and Aleva 1990). Since bauxite is a naturally occurring mineral, it has a number of impurities like iron, silica, titania, calcium and small quantities of phosphorous, sulfur, zinc, magnesium and various carbonates and silicate minerals. These impurities need to be removed as they increase costs of downstream products because of waste handling and disposal. Therefore most bauxite mines subject their run-of-mine (ROM) ore to a mineral dressing operation to remove iron and other impurities. This begins by crushing the ROM, and, depending on the quality required, the beneficiation phase comprises screening, scrubbing and washing, magnetic separation, drying and calcining. The beneficiated product is hauled by railway to the nearest port facility and shipped to a refinery where alumina is produced.

Bauxite is mined worldwide mostly in surface operations via strip mining and area disturbances include the area strip mined, the mine industrial area (MIA) where infrastructure is located and, in some cases, tailings ponds where thickened tailings resulting from washing (removing clay from bauxite) are stored; tailings remain permanently until wastewater is eliminated and native species can be planted. The main environmental problems associated with bauxite mining are related to the clearing of densely vegetated areas for mine facilities and pits areas, especially of primary tropical rainforests which are biodiversity hotspots (Myers et al. 2000; Myers 1996; Mittermeier et al. 2011), and cannot be quickly restored to a pre-mining state. Nevertheless, land restoration is a strong policy in the bauxite mining industry and it is claimed that the area of mined land rehabilitated every year globally is equivalent in size to the area newly mined (International Aluminium Institute 2009).

Currently the level of aluminium recycling is high; the recycled aluminium from scrap already constitutes over half of the global aluminium ingot production in 2009 (Liu et al. 2012). However, it is predominantly based on pre-consumer scrap, with a big potential lying in the post-consumer scrap. Compared with the production of primary aluminium, recycling of aluminium products needs 5% of the energy and emits 5% of the GHG gases (EAA, IAI, OEA 2009), thus, increasing

the recycling share of the global supply to the aluminium market is compatible with decarbonizing the production.

Still, in the next decades it is foreseen that primary mining of bauxite will be high as resources are abundant: world bauxite ore resources are estimated to be in the range of 55,000 to 75,000 Mt (USGS 2014c) while reserves are estimated to reach 29,000 Mt. This means that primary mining of bauxite ore could theoretically continue as usual for 112 years if the extraction level of 2012 (258 Mt) is maintained and the currently available technology (and metal yields) remain equal. Although reserve figures are poor proxies for future supply, they provide an indication that no lack of the virgin mineral is expected for the next 50 years.

It is foreseeable that environmental pressures will be at largest in the main center of reserves because they have the highest chances of being exploited as infrastructure is already developed. Reserves´ global distribution displays a spatial concentration mainly in Guinea and Australia, followed by reserves in Brazil, Vietnam, Jamaica and Indonesia, among other countries (Figure 12).

Figure 12: Bauxite ore reserves per country. 2014.

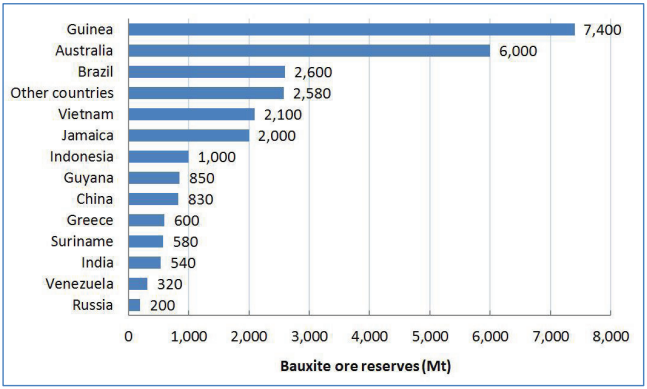

Source: self-elaboration based on USGS (2014c)

1.8.1.3 Copper (Cu)

Copper is a major industrial metal ranking third after iron and aluminum in terms of quantities consumed globally. Electrical uses of copper, including power

transmission and generation, building wiring, telecommunication and electrical and electronic products account for about 75% of total copper use (USGS 2014a). Since 1900 the world mine copper production has grown by around 3% per year (International Copper Study Group 2012) to reach over 16 Mt in 2011; Chile accounts for over one-third of the world copper mine production (concentrates supply) followed by China, Peru, the U.S. and other countries. This trend of rising global copper production has been paralleled by declining copper ore grades, the removal and processing of larger quantities of ore and waste, and larger depths at which new copper discoveries are located (Fisher and Schnittger 2012). The global demand for copper continues to grow with world refined usage having more than tripled in the last 50 years; China is the largest smelter (accounted for 32% of world copper smelter output in 2012), largest consumer of refined copper with an apparent usage of over 8.8 Mt (2012), and is expected to keep on leading the demand in the next decades (International Copper Study Group 2013).

Primary copper production starts with the extraction of copper-bearing ores, mainly in three ways: surface mining, underground mining and leaching; open pit mining is the dominant method and sulfide ores account for over 80% of copper mined worldwide (Giurco 2005). Once the ore has been mined, it is crushed and concentrated by flotation, a process through which minerals in an ore pulp are separated due to differing surface properties. In general the behavior of sulfide ore minerals is hydrophobic; they become attached to air bubbles which are stirred into the pulp, rise with them to the surface of the pulp and can be skimmed off. The copper content of a concentrate mainly depends on the mineralogy of the ore and the copper recovery rate[13] of the beneficiation process. It is normally between 20 and 30% copper; very rich concentrates contain up to over 50% copper (Lehne 1993). The obtained copper concentrate is further refined in a smelter through a roasting step and electro-refining whose output are copper cathodes assaying over 99.99% copper. Alternatively, in the hydrometallurgical route, copper is extracted from low grade oxide ores and from some sulfide ores through leaching

[13] Defined as the proportion of valuable material physically recovered in the processing of ore (Classen et al. 2007).

(solvent extraction) and electrowinning (SX-EW process), with an output similar to electro-refining methods.

Area disturbances at surface copper-producing mines are characterized by open pits, waste dumps, the mine industrial area, camp sites and tailings ponds where tailings from beneficiation are stored; in mines where gold is produced as a co-product, heap leach pads and tailings pond areas might also be included. In underground copper-producing mines, the surface area disturbances encompass the mine industrial area, possibly camp sites and airstrips, waste dumps and tailings ponds, and areas affected by subsidence.

Currently, it is estimated that the end-of-life recycling rate of copper is above 50%; for 2008, it was estimated that about "7.8 Mt of copper were recovered from all forms of scrap (post-consumer and new scrap) representing one-third of total worldwide copper consumption" (Five Winds, ICMM & IISD 2011:17). As observed in Figure 13 the primary copper smelter production currently accounts for nearly 80% of the global copper smelted.

Figure 13: World copper smelter production (thousand metric tons copper). 1980-2012.

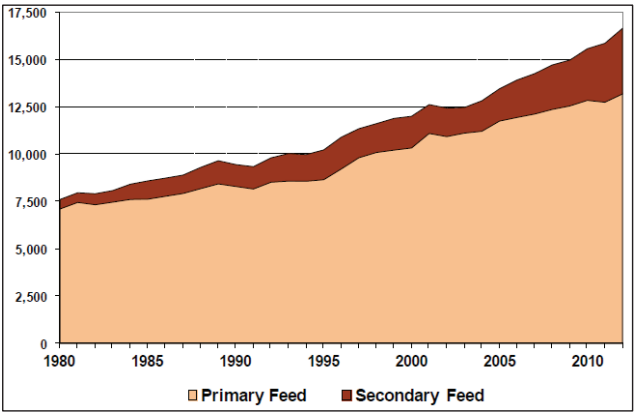

Source: International Copper Study Group (2013)

Concerning resources and reserves, world copper known resources are estimated by the USGS to reach 1,800 Mt of copper (USGS 2014d) whereas Northey et al.

(2014) have estimated an ultimate recoverable resource of 2,096 Mt of copper. USGS estimates reserves at 690 Mt (USGS 2014d), and assume a cut-off of 1%; if the cut-off was lowered to 0.4%, the ultimately recoverable reserves would reach around 2,900 Mt (Sverdrup et al. 2014b).

Considering the 2012 extraction level (16.8 Mt copper), current reserves would allow production to go on as usual for 41 years, although Sverdrup et al. (2014b) forecast a risk for copper shortage or limitation in the market within the next 30 years. Secondary copper reserves are still in use which provides a limitation to increase its supply in the short term. With regards to primary reserves, they are largely spatially concentrated in Chile, followed by Australia, Peru and the U.S. (Figure 14). By far the most important deposits are of the disseminated porphyry copper type, in which the dominant mineral is chalcopyrite.

Figure 14: Global copper reserves per country. 2014.

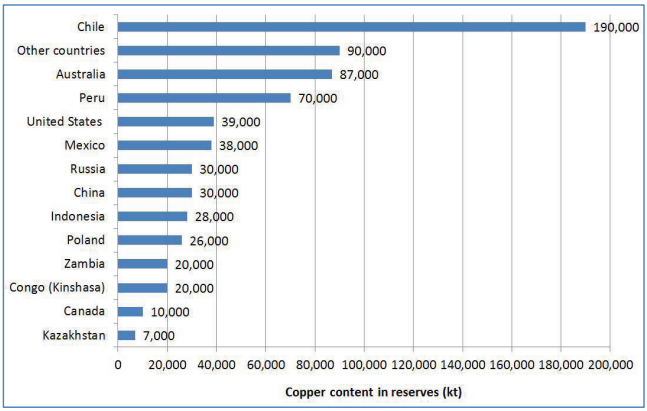

Source: self-elaboration based on USGS (2014d)

1.8.1.4 Gold (Au)

Gold is used around the world mostly for jewelry, followed by the investment sector (bars and coins), by the industrial-technology one, and more recently by central bank net purchases (World Gold Council 2014a). India, China and the U.S. are the largest consumers of gold and primary gold mine production takes place mainly in China (which remains at the forefront since 2007), the U.S., Australia,

the Russian Federation, Peru, South Africa, among others (PriceWaterhouseCooper 2013).

The global supply of mined gold has increased in recent years and is expected to reach a historical high in 2014 (World Gold Council 2014b). At the same time the share of the overall supply coming from scrap has also increased in the recent years and accounts for 36% of average annual total gold supply (World Gold Council 2011), of which around 22% comes from scrapped jewelry (the largest in-use above-ground stock of gold worldwide), most from the developing world (mainly India). Gold has an end-of-life recycling rate estimated at over 50% (UNEP 2011a).

With regards to extraction methods, for the vast majority of mines, gold was historically extracted using underground mining techniques until the advent of the 1980s gold bloom, when extraction changed towards large-scale, low-grade open pit mines (Mudd et al. 2012). In recent decades, underground mines are used where the deposit is deep or inaccessible via open pit, but the latter is preferred when the deposit is closer to the surface.

The world´s primary gold production (for 2013) took place around 52% in open pit mines and around 22% in underground mines; the rest in other types of mining (placer, tailings, dredging, etc). Hard-rock mining produces the world´s largest share of gold and generally consists of three major steps: extraction, beneficiation and processing. Extraction consists in removing the ore from benches or from the main shaft, its hauling or transport to the beneficiation plants where it can be treated via cyanidation, base-metal flotation, or gravity concentration (for placer deposits) (Mudd et al. 2012). Area disturbances in typical open pit or underground mines involve the pits, waste dumps, the mine industrial area, tailings storage facilities or heap leach pads.

World gold reserves are estimated at 54,000 t (USGS 2014e) and are mostly concentrated in Australia, South Africa, Russia, Chile, Indonesia and the United States (Figure 15).

Figure 15: Global gold reserves per country. 2014.

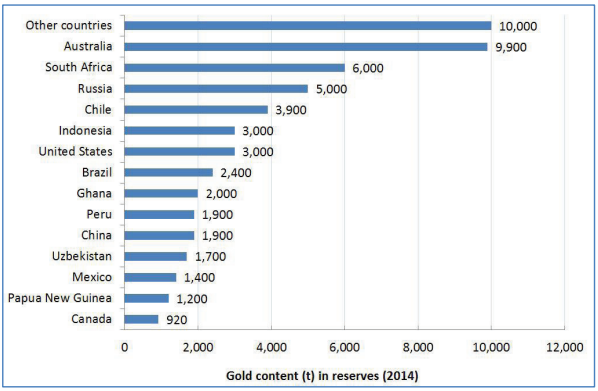

Source: self-elaboration based on USGS (2014e)

1.8.1.5 Silver (Ag)

Silver is recognized for its strength, malleability, reflectivity, thermal and electrical conductivity and is used in industrial and medical applications, including photography, jewelry, photovoltaic applications, and as an investment (coins, medals) (GFMS 2010). As depicted in Figure 16, the global silver supply has not shown a linear pathway during the last ten years; more recently, in 2012 global mine production reached 22,452 t and was led by Mexico, China, Peru, Australia and Bolivia under open pit and underground methods.

With regards to the share of silver supply catered by scrap in the period 2004-2013, it averaged around 30% (GFMS 2014); recycled silver (explained chiefly by recycling of jewelry, cutlery and personal items of use which are deemed the largest stock in society) is dependent on the market price. Similar to gold, few scientific trends can be found forecasting long-term silver production. According to Sverdrup et al. (2014a) global primary silver mining is forecast to keep on increasing until an expected peak by 2030-2035, to then slowly decline whereas the recycling will increase and may overtake primary mining silver rates already by 2040.

Figure 16: World silver supply (t/a). 2004-2013.

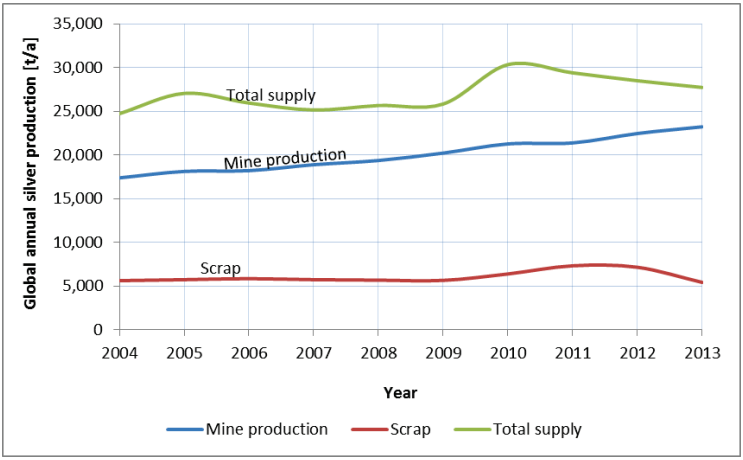

Source: self-elaboration based on GFMS (2014)

Mining of silver often naturally occurs in sulfide deposits along with copper, lead and zinc; hence, between 60% and 75% of virgin silver production is extracted as a by- or co-product of such metals in polymetallic mines. The silver contribution from copper, zinc and lead mining is independent of silver demand or silver price, depending on the dynamics of the carrier metal (Sverdrup et al. 2014a). At mine sites silver bearing ore is first crushed and grounded into a powder before froth flotation separates metal containing particles. Silver products often leave mine sites in the form of dore bars or in concentrates. Area disturbances at silver-producing mines sites are coupled with those at gold, copper, lead or zinc-producing mines and normally include pits and waste dumps (in open pit mines), or only waste dumps (in underground mines), and the mine industrial area, tailings ponds or heap leach pads.

Global silver reserves are estimated by the USGS at 520,000 t (USGS 2014f). Mexico is currently the biggest producer but has fewer resources than Australia, Peru, Poland or Chile (Figure 17). Silver reserves are associated with copper, zinc and lead ores in which silver averages a very low grade (content of native silver in

global reserves is estimated at 0.032% in copper ores, 0.050% in zinc ores and 0.008% in lead ores) (Sverdrup et al. 2014a).

Figure 17: Global silver reserves per country. 2014.

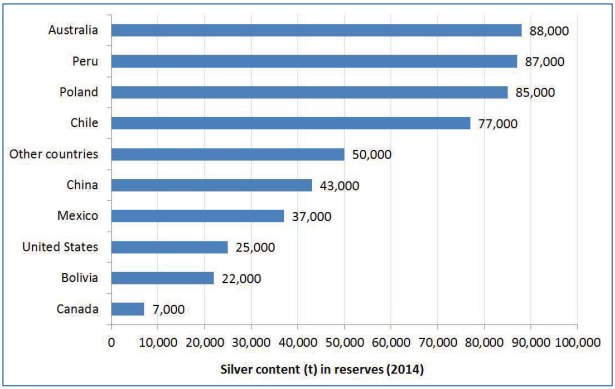

Source: self-elaboration based on USGS (2014f)

CHAPTER TWO

This second chapter summarizes the state of the art. First a brief overview of key concepts in material flow analysis is provided, followed by a review of literature addressing the topic of metal mining and the quantification of its land use. It is ensued by a review of existing literature on modelling future material flows with an emphasis on the five metals selected and a concise subsection on trends in metal mining. Second, the reader is introduced into the remote sensing field and available methods for processing satellite images in order to monitor mine-affected landscapes. Finally the last section reviews existing approaches to define biodiversity and the approach selected for this study.

2 State of the art

2.1 Material flow analysis and land use

Through the process of industrialization, modernization and globalization, the material basis of current societies has become increasingly complex, with producers and consumers understanding only part of the system and of the global supply and demand chains which characterize the global market (Bringezu et al. 2009). Gold buyers often only know the price of gold but tend to ignore the cost in terms of energy, water, emissions, deforestation or land degradation at the site where gold mining activities were performed or used for the transportation. Current pressing global environmental problems such as climate change or the increasing loss of biodiversity demonstrate the importance of understanding the interlinkages between the natural and the human system (Bringezu et al. 2009).

Research in the field of industrial ecology seeks to comprehend the structure and functioning of the socio-industrial metabolism (Figure 18), a concept treated as a metaphor to describe the interrelationship between the socioeconomic system and the bio-geosphere. The concept of (socio) industrial metabolism was first coined by Ayres and collaborators in a series of papers and books (Ayres 1993, 1989, 1994a, 1994b; Simonis and Ayres 1994), drawing its analogy from the biological meaning of metabolism and conveying the descriptive idea of the industrial system

as a living complex organism, ´feeding´ on natural resources, material and energy, ´digesting´ them into useful products, and ´excreting´ waste (Johansson 2002).

Figure 18: Scheme of the socio-industrial metabolism in exchange with the bio-geosphere.

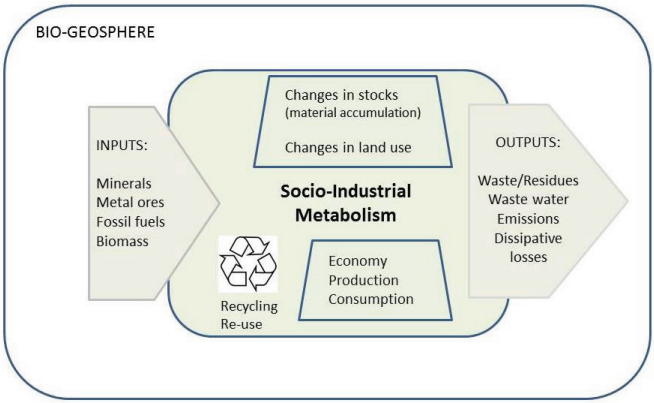

Source: adapted from Bringezu et al. (2009)

Industrial ecology, following the example of Nature, rejects the concept of waste (useless or worthless material) and argues that obsolete materials and products should be termed residues and should be reused or recycled (Graedel and Allenby 1995). The systems perspective is emphasized in industrial ecology with the goal of avoiding narrow, partial analysis that could overlook important variables; hence, the analysis of the socio-industrial metabolism tracks and measures, based on the mass balance principle, the material and energy flows on a variety of scales ranging from global, national, local to companies, products or substances (Lifset and Graedel 2002).

Material flow analysis refers to the analysis of the throughput of process chains comprising extraction or harvest, chemical transformation, manufacturing, consumption, recycling and disposal of materials and it is based in physical units quantifying the inputs and outputs of such processes (Bringezu and Moriguchi 2002). There exist a diversity of methodological approaches which are based on different goals, concepts, and targets questions; six of the most well-established

methods include: substance flow analysis, material system analysis, life-cycle analysis and assessment, business-level material flow analysis, input-out analysis, and economy-wide material flow analysis, the highest level of aggregation quantifying the physical exchange of national economies with the environment (Bringezu et al. 2009; Bringezu and Moriguchi 2002). Likewise, given the complexity of the socio-industrial metabolism, the large amounts of materials and the variety of environmental impacts and the interactions between them, there exists hardly a single indicator or method to assess the sustainability of the metabolism, and there exists a variety of indicators used to analyze various aspects of it; the choice depends on the target question (Bringezu et al., 2009).

2.1.1 Global land-use accounting and mining

The production and consumption of goods and services generates pressures not only related to material flows but also to land use. Land, a finite resource, is needed for cultivation and harvesting of biomass and for the extraction of mineral resources, infrastructure and deposition of wastes or residues, a fact that may lead to conflicts over competing uses of the land among socio-economic activities or with ecosystem services (Harvey and Pilgrim 2011; Rathmann et al. 2010; Smith et al. 2010). At a global scale some indicators have been developed to relate material flows and their land requirements. One of the most popular is the concept of Ecological Footprint which is a measure of how much area of biologically productive land and water an individual, population or activity requires to produce all the resources it consumes and to absorb the waste it generates (Global Footprint Network 2014). It represents society´s burden on the planet combining actual and a larger virtual land use dominated by the assumed terrestrial or maritime area required to absorb carbon dioxide emissions (Bringezu et al. 2012). Another is the global land-use accounting (GLUA) method developed to determine the global land use of a region or a country associated with the production and consumption of goods. Unlike the ecological footprint indicator which employs a normalized (or theoretical) measure (global hectares), the GLUA aims to provide a measure of actual land use (Bringezu et al. 2009) and is calculated using land for domestic production plus imports minus exports of all agricultural goods. Given that agricultural land dominates overall land use, its application has been so far

restricted to this domain, for agricultural goods and their associated land use (Bringezu et al. 2008; Bringezu and Schütz 1995; BUND and MISEREOR 1997; Schütz 2003; UNEP 2014).

2.1.1.1 Land use accounting for metal mining

One of the first modern attempts to map and quantify the extent of mining activities in the overall land use was conducted by the EU and the EEA in 1985 when the CORINE land cover project was initiated, in which the nomenclature included mining sites. Follow-up works include all EU-funded projects for developing tools for earth observation monitoring of mining sites. Results from the recently finished EO-Miners project show that all stakeholders surveyed in the workshops consider the "total land use" indicator (referring to the total area occupied by a mine) as a topic of high relevance (Teršič et al. 2013; Žibret et al. 2013).

Several authors have emphasized the need of a land use and land take indicator related to the mining industry (Azapagic 2004; Ewen and Öko-Institut 1998; Lindeijer 2000; Spitzley and Tolle 2004) and most of the research linking the material flows with the land use has traditionally been conducted in LCA studies. Surface area is now becoming a common metric in (corporate) performance reporting guidelines, either at the mine level or regional one, for instance by the Global Reporting Initiative. The last available version (G4 guidelines, Sector Disclosures) promote the reporting of the MM1 indicator: i) the total land disturbed and not yet rehabilitated; ii) total amount of land newly disturbed within the reporting period; iii) total amount of land newly rehabilitated within the reporting period to the agreed end use, and iv) total land disturbed and not yet rehabilitated (Global Reporting Initiative 2013).

The time dimension (temporary character of mining until reclamation is done) has been considered by various authors for equations to account for land use impacts (Eq. 1.) (Lindeijer 2000; Martens et al. 2002). Originating in the UNEP SETAC Working Group on Impact Assessment in 1996, the physical land use was divided into: land occupation impacts and land change (or land transformation, land conversion from one land cover to another) impacts; they can be summarized in Eq.1 and Eq. 2 (Lindeijer 2000):

$$land\ occupation\ impacts = area\ A\ *\ time\ t\ *\ Quality \quad \text{Eq. 1}$$

$$land\ change\ impacts = area\ A\ *\ Quality\ difference \quad \text{Eq. 2}$$

Land occupation includes the time dimension of the land disturbance and is normally expressed in [m^2.y] per functional unit of activity output [Mt ore] whereas land change or transformation refers to the net change in the type and quality of the land and is expressed in [m^2. Δ quality] per functional unit [Mt ore].

A general understanding of the land use impacts considering the time dimension can be observed in Figure 19. Applied to mining landscapes, the figure is interpreted arguing that at time t1 mining operations begin and the (environmental) quality of the land decreases from A to B. At time t2 the land use by mining is terminated and reclamation (recovery or renaturation) starts.

Figure 19: Dynamics of mining-induced land use impacts over time.

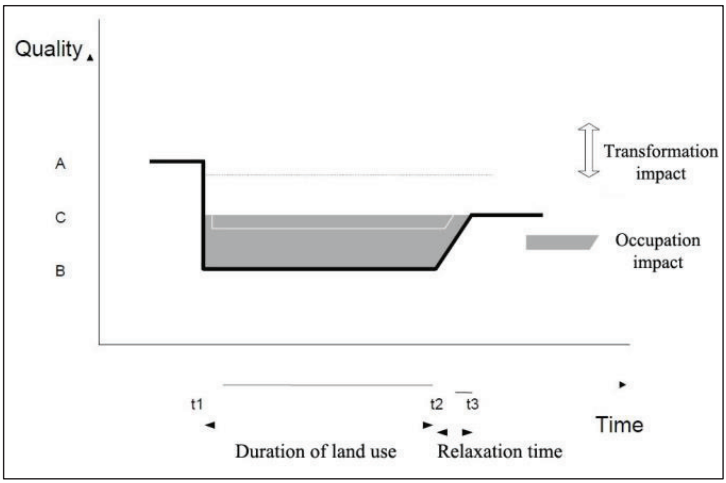

Source: adapted from van der Voet (2002)

At time t3 a new steady post-mining state has established itself which may differ in quality from the original pre-mining state; in this case the quality C is still lower than the original A and may remain so (sometimes even much worse than the A pre-mining level), but it can happen that the quality goes up again to A or even

better. Due to the multiple examples of metal mines which have created long-term post-closure negative environmental impacts (e.g. Curi and Mota de Lima 2002), more recent work by the SETAC LCI group has refined the former work, adding the category of permanent impacts. This category caters for situations in which the regeneration time, according to current knowledge, will exceed the modeling horizons of usual LCA studies, or even will exceed any finite number of years (Koellner et al. 2013).

Nevertheless, the usual practice in LCA studies and databases (e.g. the Ecoinvent database) comprises the assumption that land will be restored to pre-mining conditions according to generic estimates for the time needed for land to recover[14]. Once this is established the area disturbed by mines´ facilities is multiplied by units of time and divided by the amount of resource extracted; the resulting measurement unit is acres or ha-years per ton of resource extracted.

Following these distinctions, research was carried out at the RWTH Aachen by the Collaborative Research Center (CRC) 525. Research was performed by Sliwka (2001) and Sliwka et al. (2001) on the specific land requirements[15] and the land use[16] for bauxite mining:

- Specific land requirement is calculated by dividing the cumulative net area disturbed (the total area occupied by mining facilities[17]) by the total planned production over the entire mine life (including ore reserves); time is not accounted for. For the facilities which do not vary their land cover over time (roads, port facilities, mining camp) the total area occupied is divided by the total production; for facilities which get filled (waste dumps and tailings

[14] Renaturation time depends on local conditions and the severity of the mining method. For bauxite, Sliwka et al. (2001) establish that for sites where it can be supposed that no reclamation management system is applied, the duration between surface cleaning and natural succession of vegetation can be assumed with ten years. For all other sites the average duration of land use (time between surface cleaning and reclamation) is assumed to be about two years.

[15] *Spezisicher Flächenverbrauch, Flächenbedarf or Landinanspruchnahme* in German.

[16] *Flächeinanspruchnahme* or *Flächengebrauch* in German.

[17] Also called the "land disturbed to date" in Martens et al. (2002), and "*Gesamter Flächenberdarf seit Inbetriebnahme des Bergwerks [m^2]*" in Ruhrberg (2002).

ponds) a calculation is performed considering the depth and volume and density of the bauxite. Results were expressed in m^2/t.

- Land use calculations encompass the duration of the land disturbance. They are performed using the duration (in years) of the facilities; for fixed facilities the full life time is used, for tailings and waste dumps the years it takes until the reservoir is filled (one to three years). Sometimes it is calculated dividing the total land in use by mining for a certain year (cumulative area disturbed in that year) by the ore production for that same year. Results were expressed in (y*m^2)/t.

For copper, Martens et al. (2002) and Ruhrberg (2002) estimated the specific land requirement [m^2/t] of mines based on certain mathematical assumptions. They estimated the volume of an open pit by means of a (bank) volume estimate which relies on a frustum of a cone; for waste dumps and ponds they employed a similar method but added the compaction of the material after deposition. The results by the authors provide calculations for the world´s total land disturbed by copper mining up to the year 1998, the new land disturbed in such year, and specific land requirements. Specific land requirements include all land rehabilitated until the year research was performed and land undergoing rehabilitation.

For gold mining, Spitzley and Tolle (2004) compared surface area occupation for three gold mines, one bauxite and one copper mine, concluding that equivalency factors for gold are expected to be several orders of magnitude higher than for either bauxite or copper (all measured in acre-yr/ton). LCA databases, e.g. the Swiss Ecoinvent database (Classen et al. 2007), have incorporated their results into their inventories. In Germany, the Federal Ministry of Environment (UBA), the IFEU Institute and the Öko-Institut have developed the ProBas database[18] which provides public access to LCA data for energy, materials and products, transport, waste and other categories. Among these categories, data are provided for iron and steel, for precious metals (PGMs, silver and gold), and for non-ferrous metals (aluminium, bauxite, chromium, copper, copper ores, lithium).

[18] http://www.probas.umweltbundesamt.de/php/index.php (Website accessed: April 2014).

2.1.2 Modelling future material flows

Scenario types

Of the existing forward-looking approaches and methods to explore the future (environmental scanning, megatrend analysis, back casting, road mapping, system dynamics, etc.), scenarios are one of the most used in the field of mineral resources. Scenarios may be defined as a "consistent and plausible picture of a possible future´s alternative reality that informs the main issues of a policy debate" (EEA 2009:6); stated differently, scenarios are "systematically crafted stories about the future" (IEEP et al. 2009:15) which offer structured accounts of possible long-range futures. Scenarios are plausible views of the future based on "if,then" assertions (Alcamo et al. 2006); if the specific conditions are met, then future activities will occurr. Yet, scenarios are not necessarily the most likely, or plausible possible futures; rather than prediction, the goal of scenarios is to support informed and rational action by providing insight into the scope of the possible. They illuminate the links between issues, the relationship between global and regional development, and the role of human actions in shaping the future (Raskin et al. 2002). Again, their value lies not in their capacity to predict the future, but in their ability to provide insight into the present by helping to identify drivers of change, the implications of current trajectories, and options for actions (Raskin et al. 1998); in doing so, scenarios and their analysis can most usefully support decision-making by helping identify robust strategies (EEA 2009).

Scenarios can be classified in three types according to their target questions (Börjeson et al. 2006):

- **Baseline trend scenarios** (predictive scenarios): they assume that current trends will continue in the future and may include policy variants for different likely developments of sectors based on near-future decision alternatives. They address the question 'what will happen?' or 'what will most likely happen' (probable futures);
- **Normative scenarios** (or pathway scenarios): they describe a desirable future or set a specific goal for the future (e.g. halting biodiversity loss by

2020 or cutting CO_2 emissions to less than 50% of 2000 levels by 2050) and explore possible ways to reach that goal. They address the question 'how do we get there?';

- **Explorative scenarios** (forecasting, descriptive scenarios, possible futures): they are created to forecast the effect of specified measures (policies) on future development and conditions. They address the question 'where do we end up?'

According to the method employed, there are mainly two types of scenarios: **model-based quantitative** and **qualitative or narrative-based.** Where quantitative modelling offers structure, discipline and rigor, narratives offers texture, richness and insight (Raskin et al. 2002). Qualitative scenarios describe possible futures in the form of words or visual symbols rather than numbers and can take the form of images, diagrams or outlines, telling narratives called storylines (Alcamo 2001). A main advantage is that they can represent the view of several different stakeholders at the same time and that a well-written storyline can be an understandable way of communicating information. A drawback is that they do not satistfy a need for numerical information (Alcamo et al. 2006).

Quantitative scenarios are usually created by formalized computer models and provide numerical information in the form of tables, graphs and maps. Main disadvantages are in that that their exact appearance based on numbers gives the impression that more is known about the future than actually is and that they embed many implicit assumptions behind (Alcamo 2001). Main advantages comprise the transparency when assumptions, model equations, and coefficients are explicitly written and the fact that they have received a certain degree of scientific scrutiny as they are usually published in scientific journals (Alcamo et al. 2006).

Whereas global assessments, like the Millennium Ecosystem Assessment or the Global Environmental Outlook, mostly use narrative-based explorative scenarios (IEEP et al., 2009), existing scenarios projecting future primary mining of metals are, with some exception (e.g. World Economic Forum 2010), mostly quantitative, either based on system dynamics (Gerst 2009; Liu et al. 2012; Pauliuk et al. 2013;

Sverdrup et al. 2014a, 2012; van Vuuren et al. 1999), on extrapolated assumptions of market growth (IEA 2009; Schwarz et al. 2001) or economic indicators like, e.g. per-capita GDP (Halada et al. 2008; Kapur 2005; Luo and Soria 2008; Menzie et al. 2010).

Flow-driven and in-use stock-driven scenarios

Flow-driven scenarios are constructed extrapolating assumptions of economic growth using economic indicators like GDP, namely, they are based only on expected annual flows, e.g. metal supply or metal consumption or demand, and do not consider the dynamics of in-use stocks. Baseline trend scenarios are common among flow-driven scenarios. In the case of metal demand forecasts, these are commonly used in outlooks and projections from the industry (BHP Billiton 2012), international organizations (OECD 2008) or by scholars (Crompton 1999; Halada et al. 2008; Yellishetty et al. 2010). Although such scenarios may be useful for short-term predictions of demand (Sohn 2005), their main disadvantage is that they do not quantify the link between stocks and services (Brattebø et al. 2009). Such scenarios often neglect mass-balanced linkages and feedbacks owing to a lack of physical characterization of the entire metal cycle and they ignore temporal effects (e.g. lag times, saturation times) resulting from the evolution of built environmental stocks (Liu et al. 2012).

In other words, extrapolating metal consumption trends results in ignoring the dynamics of in-use stocks. The latter comprise the built environment (infrastructure and buildings) and artifacts (machinery and durable consumer goods); together with humans, livestock and other domestic animals, (anthropogenic) in-use stocks form the totality of stocks in the social metabolism (Fischer-Kowalski 2011). Additions to in-use stocks enter the mass balance of a process and therefore they have to be considered in mass-balance systems (Pauliuk and Müller 2014). If such in-use stocks are not fully taken into account, this impedes assessing the connection between consumption and the actual service provided or the estimation of future supply of post consumer scrap (Pauliuk et al. 2013); this makes flow-driven models for metals to a certain degree incomplete due to ignoring the potential of pre- and post-consumer scrap.

Static material flow studies including in-use stocks have been published for more than 20 years (Pauliuk and Müller 2014); yet, dynamic ones only more recently (Müller 2006; Du and Graedel 2011; van der Voet et al. 2002). Dynamic material flow models focusing on the estimation of current and future in-use stocks and their services (generically called **stock-driven** or in-use stock-based models) enable overcoming such limitations by including the structure and functioning (e.g. lifetime) of the anthropogenic flows of metals, including saturation levels, saturation times, and may include on-the-ground (litosphere) reserves (supply constraints). This makes stock-driven models, in general, more robust and reliable than flow-driven ones, especially for middle and long-term projections.

Existing models for the five major metals

The major engineering metals (iron, steel, copper, lead, zinc and aluminium) as well as silver and chromium have often been studied and their material cycles are the best well-understood. However, most of these studies modelling future flows have used static models with a time scale of one year offering only snapshots in time but no information about the dynamics of resource use and changes in stocks and flows over time (Müller et al. 2014). Of the existing dynamic MFA models, most are scaled for specific countries, with fewer models targeting metal cycles within a global system boundary. These are recent and have been aimed at understanding the pathways and magnitudes of stocks and flows of aluminium (Liu et al. 2012), steel (Milford et al. 2013; Pauliuk et al. 2013), copper (Glöser et al. 2013; Sverdrup et al. 2014b), gold (Sverdrup et al. 2012), and silver (Sverdrup et al. 2014a).

The normative study by Liu et al. (2012) is different from other existing models in that it develops a dynamic material flow analysis which enables an integrated analysis of the material-energy-emission nexus and considers system feedbacks (e.g. scrap availability and its influence on primary production of bauxite) and time lags (e.g. the accumulation and replacement of in-use stocks) based on the mass balance principle. The research was conducted to model the future global aluminium cycle and explores through various scenarios its associated emissions pathways and mitigation potentials under the question of: which mitigation

measures can the aluminium industry execute to achieve a 50% CO_2 emissions cut below 2000 levels by 2050?

With regards to steel, the investigation by Milford et al., (2013) is also normative and seeks to provide information on pathways to answer the same target question; it also provides recommendations and results based on an analysis of seven scenarios. Partner research by Pauliuk et al. (2013) on future final demand for steel is based on a dynamic stock model and seeks to provide answers to the questions: what trends in regional steel demand and scrap supply follow from a saturation of per capita stocks everywhere in the world? When and where may peaks in the steel demand occur? Authors provide results in terms of one baseline trend scenario of the model until 2100 of final demand by world region highlighting the role of China, the importance of the end-of-life scrap, and conclude that secondary production will exceed primary production, irrespective of the parameter values chosen.

The study by Glöser et al. (2013) developed the first dynamic material flow model for copper at the global level aiming to answer the question of how much copper is recycled compared to the amount of available copper scrap. However the model reconstructs the history of copper stocks and flows but does not provide future-oriented scenarios. No studies with scenario analysis of future projections of global copper anthropogenic flows have been found in the literature. Modeling of future global copper supply has only been covered in the works of Sverdrup et al. (2014b) and Northey et al. (2014) which present only one scenario but no alternative ones. The first authors developed a mass balance-based model to reconstruct the historical pathway of the global copper production (primary and secondary) and, based on system dynamics modeling, simulate the copper production providing one baseline trend scenario until 2380. In contrast, Northey et al. (2014) have used a global supply-focused model for estimating historic and future copper production (covering the period 1900-2100) based on estimates of the Ultimate Recoverable Resource for individual countries and deposit types. Results provide two baseline trend scenarios, one driven by static demand and another by dynamic demand, with similar results showing a dominance of porphyry copper resources during the entire period. Other existing studies on global copper

dynamics (Ayres et al. 2003; Gerst 2009; Kapur 2005) have been focused on the demand and have been criticized given that "the current reported copper resources appear insufficient to meet the demand scenarios presented" (Northey et al. 2014: 198). Northey and colleagues claim that peak mined copper production will not occur due to decreasing demand, but due to supply constraints.

With regards to modeling of future gold and silver flows, a baseline trend scenario has been developed under system dynamics by Sverdrup and colleagues (Sverdrup et al. 2014a, 2012). In the case of gold, Sverdrup and colleagues reconstructed the supply and price of gold in the past (1920-2010) and used the fitted data along with reserves of different ore grades to predict the future supply in the period 2010-2100. Based on system dynamics, the results are a baseline trend scenario of simulated gold production (primary and secondary) until 2100; likewise, the model predicts a shift from high-grade ores to low-grade deposits and that recycling will become the most important source of gold to the market. In the case of silver, the authors reconstructed the historical stocks of silver and, under a system dynamics approach, modeled the supply in the short and long-term covering the time span 1840-2340. Results show a baseline trend scenario of simulated silver production by primary and secondary mining. No other future-oriented studies have been found in the literature projecting the supply or demand of gold or silver via scenario modeling.

2.1.3 Material flows and trends in metal mining

2.1.3.1 The global extraction of metals is expected to keep growing

Among the principles of industrial ecology, the concept of efficiency is one of the most applied ones, especially to material and energy resources. In the last decades, alongside global economic growth, resource use efficiency has been increasing over time. Consequently, the global economy has been growing and has, simultaneously, been reducing the rate of resource use (input) per unit of economic activity (output). Between 1980 and 2008 the world economy increased the amount of economic value created per unit of consumed material by about 40%; in other words, the material intensity of the world economy decreased by about a third (Dittrich et al. 2012) (Figure 20).

Figure 20: Growth of global GDP and material consumption. 1980-2008.

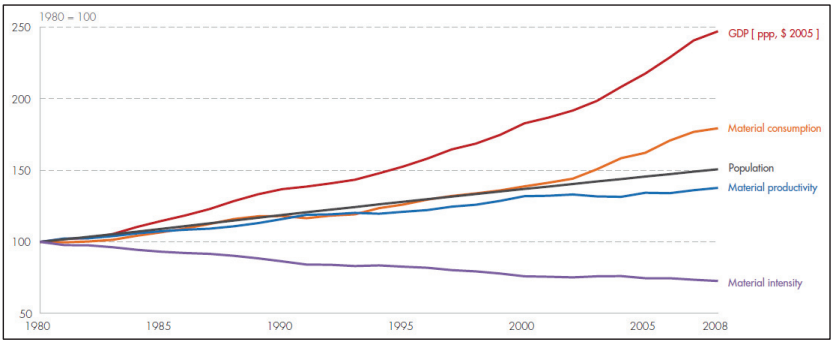

Source: Dittrich et al., (2012)

Therefore, the material productivity, also called the efficiency of production per unit of output (i.e. a ton of products), is higher; this trend, termed *dematerialization* (UNEP 2011b) or *relative resource decoupling*, has been the dominant trend across some countries over the afore-mentioned period.

However, despite such positive trend, the overall absolute amounts of resources extracted, consumed (material consumption) and the waste flows into the environment are still increasing (Lutter et al. 2011). Put differently, *absolute resource decoupling* is only occurring in some countries (e.g. Canada, Germany, Japan, the United Kingdom) and to a certain extent but is not a general overall trend. As a result, economic growth has not yet been dramatically decoupled from resource use and the global absolute demand for raw materials is expected to ascend: the global resource consumption by 2050 is expected to reach between 70 billion t/a and 140 billion t/a, far more than the current level (49 billion t/a) (UNEP 2011b).

Likewise, global trends of primary mining of metals, despite prices volatility, illustrate rising absolute resource consumption over time. In the past, it has been observed that during the 20th century the annual extraction of ores and industrial minerals grew by a factor of 27 (Krausmann et al. 2009) and during the period 1980-2008 the global consumption of metals increased by 87% (Dittrich et al. 2012). The mining of such metals, along with other raw materials, contributed to

provoking profound negative environmental impacts like resources over-exploitation, human-induced climate change, land-use changes, loss of biodiversity (UNEP 2011b). In the close future, despite short-term concerns and uncertainties (e.g. KPMG 2013), most existing studies agree, albeit quantitative differences and diverse scenarios, that demand will continue growing in the long-term due to several driving forces, among them: global population growth, the global industrial-military complex, rapid urbanization, electrification and industrialization in emerging economies like India and China, the global electronic industry, changes in mobility (e.g. increase in car ownership) and renewable energy generation technologies, among others (Keramidas et al. 2012). Accordingly, it is foreseen that the extraction of minerals will keep on growing significantly in the next decade and a half: a business-as-usual scenario shows that the global extraction of minerals is expected to double by 2030 (range of 267 to 300 Gt/a) in comparison to 2010 levels (range of 135 to 150 Gt/a) (Bringezu 2015). In general it is expected that global absolute reductions of metals use will probably not occur widely (Exner et al. 2013).

2.1.3.2 Declining ore grades, increasing waste flows

The key quantities to be addressed in establishing the material flows due to mining (and urbanization) are the annual masses of rock and earth surface materials extracted, including overburden and mineral processing residues at the mine site (Douglas and Lawson 2002).

A central key aspect is the ore grades as they determine the amount of material that needs to be processed in order to obtain a unit of the target metal. Over the last century a key trend upon which there is agreement by the industry and the scholars comprises declining ore grades, particularly for metallic ores bearing copper, zinc, lead and the precious metals. Enabled by technology breakthroughs (West 2011) and powered by cheap oil which allowed the economic processing of large-volume low-grade ore deposits (Sverdrup et al. 2014a), the annual average ore grades of copper, gold and silver have been declining (Crowson 2012; MinEx Consulting Pty Ltd 2011; Mudd 2007c, 2007b, 2004b) and tend now to level off at very low contents (or descend but at a rate slower than during the 20th century).

For instance, in the U.S. the copper ore mined at the beginning of the 20th century consisted of about 2.5% usable metal by weight; today that proportion has dropped to 0.51% (Earthworks and Oxfam America 2004). Forward-looking trends of these metals expect that, while iron ore and bauxite mining may remain stable, the precious metals, zinc, lead, nickel and particularly copper will be further affected by ore grades declining even more (Lee et al. 2012).

If the ore grade is smaller, then more ore needs to be processed to obtain the same amount of metal compared to higher-grade ores. A direct consequence of this is that open pit operations which mine low-grade deposits create much more waste than underground mines which mine higher-grade ore deposits. Therefore, alongside declining ore grades comes a trend of increasing waste flows (Mudd 2004b) which need to be stored at the mine site. Waste flows are two-fold: first appears the extraction waste mined out simultaneously while mining the ore and second comes the beneficiation waste which originates in the used extraction which is left behind once the material has been beneficiated[19]. The Table 2 shows that such beneficiation waste (or the share of ore that becomes waste after beneficiation) produces significant amounts of waste, particularly high in the case of gold and copper, which process low-grade ores.

Table 2: Share of ore becoming waste during beneficiation for selected metals. 1995.

Metal	Ore Mined (Mt)	Share of ore that becomes waste, not including overburden (%)
Iron	25,503	60
Copper	11,026	99
Gold	7,235	99.99
Lead	1,077	97.5
Aluminium	856	70

Source: Van Zyl et al., (2002)

[19] As a global average, the production of one ton of copper results in 110 tons of waste ore and 200 tons of overburden (Earthworks and Oxfam America 2004). If we compare open and underground mines, open pit operations create a significant stream of waste, e.g. open pits typically have a strip ratio of 2.5 (2.5:1) (Ericsson 2012); on the contrary, underground mines create a small amount, often not exceeding 10% of the total ore produced.

Given the increasing waste flows generated, the land occupied by mines for the deposition of waste is also expected to rise alongside declining ore grades for copper, gold and silver. Other direct consequences of declining ore grades involve dramatic increases on the energy, water and chemicals used as well as accompanying greenhouse and acid rain gas emissions from metal production processes (Norgate et al. 2007).

2.1.3.3 Slow trend towards open pit mining

Over recent decades and as a result of declining ore grades, there is a strong trend toward the increasing use of open pit mining (Mudd 2004a) given that underground mines are more costly to operate than open pit ones, making underground mining not feasible for extracting low-grade ores (Mikesell 2013). Of the total number of existing metal mines in the world some 52% are open-pit, 43% underground and 4% to 5% are placer or tailings (Ericsson 2012). Of the total tonnages handled some 85% come out of open pit operations (including placer operations) and 15% from underground mines (Ericsson 2012), with open pit mining being the dominant type of extraction, except in South Africa where gold mining has traditionally been done in underground mines. Due to lower ore grades and new technologies, it has been observed that during the first decade of the 21st century there has been a slow trend towards open pit production (Ericsson 2012) which indicates that this trend may continue in the coming years as metallic ore grades keep on declining.

2.2 Monitoring mine landscapes via remote sensing data

2.2.1 Pixel-based satellite image analysis of mining landscapes

Quantification of the land transformations caused up until now and in the foreseeable future by large-scale metal mining activities is a major research issue for a sustainable resource management. Over the past 20 years the use of satellite data and the sophistication of the methods for inferring land cover characteristics have significantly increased. Easier data access and lower data price than in the past are some of the reasons for such trend (Latifovic 2009). Currently pixel-based methods are the most commonly used type of classification

in remote sensing (Nussbaum and Menz 2008a) and, likewise, classification of pixels in satellite images into classes defined by the user is one of the most widely used remote sensing methods for investigating and monitoring the mining activities and related environments, especially for surface mining operations (Düzgün and Demirel 2011).

In the remote sensing field mine-affected landscapes having been investigated using medium spatial resolution satellite imagery such as Landsat data (Almeida-Filho and Shimabukuro 2002; Anderson et al. 1977; Hecheltjen et al. 2010; Myint et al. 2005; Townsend et al. 2009). However, and only more recently, high spatial resolution imagery is starting to be used when details need to be identified; for example, in the Canadian Ekati diamond mines Ikonos images were used to better distinguish technical features on the ground (access ramps to the terraces or benches) (Nowicki et al. 2003). Likewise, aircraft-based precision topographic mapping with laser scanning systems (LIDAR) can be applied in estimation of the volume of material removed from pits, monitor subsurface fires or identifying concealed mine-shafts (Lamb 2000). However, high spatial resolution data still remains expensive and is only available from the year 2000 when the IKONOS, the first commercial high spatial resolution satellite, was launched. In contrast, the Landsat program, a joint-initiative run by the NASA and the USGS, represents the world´s largest continuously acquired collection of space-based moderate-resolution data since 1972 (National Research Council (U.S.) 2011). On board of the Landsat satellites 1 to 8 the sensors MSS, TM, ETM+ and OLI provide imagery at medium spatial resolutions (15 meter to 100 meter pixel size) at a temporal resolution of 16 to 18 days. The acquisition of Landsat images has also been traditionally relatively expensive but in 2008, the USGS announced the full opening of the Landsat archive by providing all users with over 40 years of preprocessed, standard format scenes at no charge (USGS 2008a). The recent change to an open data policy has triggered notable advancements in technical capacity to analyze large data sets for long-term and large area and widespread use by a variety of users (Wulder et al. 2012); yet applications to monitoring mining-affected areas have been limited (Koruyan et al. 2012).

Most existing studies using multiple Landsat imagery are focused on developing algorithms to monitor extensive land-uses like forest dynamics (e.g. the LandTrendr or TimeSync) (Cohen et al. 2010; Kennedy et al. 2010) or changes in the vegetation (e.g. Vegetation Change Tracker) (Huang et al. 2010). These algorithms are designed to exploit the Landsat archive by taking advantage of high temporal densities of data and by applying it to forest change studies. Similar algorithms for quantifying mining surface dynamics do not exist and are challenging since they require the combination of imagery with mines locations and boundaries in order to precisely determine the limits between the mine and nearby land uses. Nonetheless there exist a small number of case studies which have used Landsat images for monitoring mines´ surface dynamics through pixel-based classification approaches.

Townsend et al. (2009) have mapped and determined the extent of surface mines and mines reclamation for eight large watersheds in the Central Appalachian region of West Virginia based on multi-temporal Landsat imagery, some spectral indices (NDVI, tasseled cap and wetness) and GIS mine permit data. Latifovic et al. (2005) have created land cover maps with Landsat imagery to quantify primary and secondary impacts of surface mining in the Athabasca Oil Sands region. Coal mining has received more attention: Chitade and Katyar (2010) have studied changes in land use and land cover in the Chandrapur district in India whereas others have tested machine learning methods (SVMs) for change detection in the context of lignite open pit mining using Landsat and ERS2-SAR scenes (Hecheltjen et al. 2010). Gold mining-related land cover changes have been studied in Western Ghana by Schueler et al. (2011) and Myint et al. (2005) used Aster and Landsat imagery to determine the effectiveness of remote sensing in the identification of iron oxide minerals. Feizi and Mansouri (2013) also used the same satellite data sources combined with geology maps to identify and compare iron potential zones.

In Europe, seeking to develop cost-effective monitoring methods for mine-influenced landscapes, the EU has financed some projects such as:

- **Mineo** (1998-2002): the project aimed at developing Earth Observation based methods and tools for assessing and updating environmental status (i.e. pollution) and impact in European mining areas. Data used was collected through airborne hyper spectral surveys, acquisition of conventional remote sensing archived data and simultaneous spectro radiometric field campaigns.

- **PECOMINES** (2003-2005): the objective of this project was to compile an inventory of toxic waste sites from mineral mining in Pre-Accession countries in relation to "sensitive" catchment areas. Other aims were to compare criteria for safety disposal of mining waste and for assessment and remediation of contaminated areas in candidate countries with regulations adopted by EU Member States and with the existing EU legislative framework in the area of waste. A methodology for regional mapping of wastes from the extractive industry was developed, that was applied and validated on time-series of Landsat-TM satellite data covering large parts of Romania and almost entire Slovakia (Vîjdea et al. 2004).

- **EO-Miners** (2010-2013, EC FP 7): the objectives of this project were to assess policy requirements at macro (public) and micro (mining companies) levels and define socio-economic, societal and sustainable development criteria and indicators to be possibly dealt using EO methods. In addition, another objective was to use existing EO knowledge and carry out new developments on demonstration sites to demonstrate the capabilities of EO-based methods and tools in monitoring, managing and contributing reducing the environmental and societal footprints of the extractive industry (Žibret et al. 2013). The data sources included conventional optical sensors (Landsat TM, Aster), very high resolution ones (Ikonos, Quickbird, Worldview_II, Spot 5) and radar, plus airborne combined with in-situ monitoring methods.

2.2.2 Object-based image analysis (OBIA)

In the last years the gradual lowering of costs for accessing very high spatial resolution (VHSR) images (e.g. IKONOS, GeoEye, QuickBird, Orbview,

Worldview) have triggered an increasing production of data generated at a broad range of spatial, spectral, radiometric and temporal resolutions which encouraged alternate image analysis techniques different to the traditional pixel-based classifications (Blaschke 2010). Led by applications in urban studies and landscape ecology, object-based image analysis (OBIA) has been increasingly receiving attention and is considered by some as a new paradigm (Blaschke et al. 2014). This technique applies a logic intended to mimic some aspects of the higher order logic employed by human interpreters (Campbell 2007) as it overcomes traditional multispectral pixel-based analysis by including elements of visual interpretation like forms, shapes, neighborhood, content and levels, among many other dimensions of the feature space. The focus of OBIA is to shift attention from the statistical analysis of single pixels towards the spatial patterns (or patches) they build, e.g. built-up urban areas or artificial objects with sharp, discrete boundaries (Blaschke and Strobl 2001).

Unlike pixel-based classification, object-based classification relies on first segmenting the image into homogeneous regions and assigning classes to each segment rather than a pixel. Segmentation groups pixels into homogeneous entities where the varying reflectance values are smoothed out creating segments that ideally correspond, or are often very close, to real-world objects (Memarian et al. 2013). Segmentation is followed by the creation and application of a semantic model constructed as a rule-based semantic network including declared and procedural knowledge; the first contains the concepts and relations whereas the second comprises the methods for calculating the concept attributes and for evaluating concepts and relations (Nussbaum and Menz 2008a). Based on this model, each segment is assigned to a number of classes defined by the user. Experience from current research reveals that object-based classifications are equally good or outperform pixel-based ones when comparing overall classification accuracy (Duro et al. 2012; Memarian et al. 2013), predominantly in complex situations like built environment (Myint et al. 2013, 2011), patterned landscapes and change detection (Blaschke and Strobl 2001) or land cover mapping (Dingle Robertson and King 2011). In some cases both approaches have been integrated (e.g. Dubovyk et al. 2013; Geneletti and Gorte 2003; Wang et al. 2004).

Current research shows that OBIA represents a significant trend in remote sensing and GIScience (Blaschke 2010). However, object-based image analysis for the measurement of large-scale industrial mines has rarely been conducted. This may be explained due to the fact that high resolution imagery is still expensive for academic research. Only one study was found in the literature using OBIA to classify artisanal alluvial, artisanal exploratory, and industrial mines related to diamond mining activities based on very high resolution satellite data (Ikonos images). Results showed precise maps and the adequacy of the classification method (Pagot et al. 2008). In addition, a recent thesis by Weitzel (2013) compared per-pixel supervised classification methods against OBIA for the detection of one gold mine in Landsat imagery; results show that classification by OBIA was as good as per-pixel methods, even with more accurate results for old pits and other mine facilities. Given the novelty of applying OBIA methods to moderate-resolution images like Landsat, no further scholarly references were found for surface mine monitoring.

2.2.3 Visual image interpretation

Image interpretation may be defined as “the extraction of qualitative and quantitative information in the form of a map, about the shape, location, structure, function, quality, condition, relationship of and between objects by using human knowledge or experience (Japan Association of Remote Sensing 1999). This technique constitutes an integrated analysis and classification of an image based on eight specific features or elements visible on the Earth´s surface: shape, size, tone, texture, pattern, shadow, association and site (topographic position) (Campbell 2007; Düzgün and Demirel 2011).

Visual interpretation was the backbone of remote sensing during many decades when aerial photographs were the only remotely sensed images available (Horning 2004) but since the digital era made satellite imagery available, computer-assisted methods are usually preferred to handle the large volume and quantitative nature of digital satellite data. One of the main reasons is that the higher computational power has made them more operational and they provide more cost-effective, objective, consistent and repeatable results in comparison to

manual methods (Kelly and Tuxen 2009). However, Landsat images can still be usefully analyzed with classical techniques of photointerpretation (Horning 2004; Short 1982; Horning et al. 2010). In some cases; for instance, it is recommended to use the ability of the human interpreter when the area under investigation is rather small and when there is a need to recognize and identify a specific phenomenon (Horning, 2004), for instance a mine area.

While effective and precise, visual interpretation can be expensive and time-intensive to achieve detailed classification results since these manual methods are not automated, i.e. require the manual delineation and on-screen classification. A drawback is that classifications by different interpreters or at different time periods can produce variable results that are not comparable across space or time. Despite these limitations, visual image interpretation for classification of land covers in Landsat images has been applied in the past for delineating landscape units (Mirajkar and Srinjvasan 1975), for monitoring environmental change (Gordon 1980; Howarth and Wickware 1981), mapping glaciers (Sidjak 1999), wildland vegetation (Beaubien 1986) or delineating hydromorphic units of groundwater studies on a regional scale (Roy 1978).

In the last years, the appearance of the object-based image analysis techniques has enabled new hybrid image classification methods since now manual delineation and classification must not be done at the pixel level, but objects created by segmentation can be used as the basis for on-screen digitizing and classification. Existing studies applying visual image interpretation for classification of OBIA-created segments on Landsat images comprise applications to: land use and land cover change (Abd El-Kawy et al. 2011), glacier mapping (Frank 2000), wetland mapping (Andresen et al. 2002; Jiping et al. 2012), monitoring soil sealing in urban environments (Kampouraki et al. 2008), quantitative assessments of parcels and biotopes (Lang et al. 2009) or for the detection of coca fields (Bauer and Kaiser 2006).

With regards to studies related to mining, existing literature comprises case studies using high spatial resolution images and conventional per-pixel classification methods or a mixture with object-based ones (Demirel et al. 2011;

Pagot et al. 2008); in the case of Landsat imagery for monitoring mines, existing studies have applied also pixel-based classifiers (Almeida-Filho and Shimabukuro 2002; Latifovic et al. 2005; Petropoulos et al. 2013; Schmidt and Glaesser 1998; Schueler et al. 2011) or a mixture with object-based ones (Hecheltjen et al. 2010). Yet, all in all, no studies were found using visual interpretation for monitoring of mines through Landsat images. This may be explained, first, by the labor-intensive activity of classifying mines on a one-by-one basis and, second, by the relative less interest in the land system discipline to the monitoring of mines in comparison to other more extensive land uses (Sonter et al. 2013) for which Landsat images are more suitable.

2.3 Global pressures on biodiversity by metal mining

It is now widely acknowledged that the global biological diversity, often defined as "the variability among living organisms from all sources including, inter alia, terrestrial, marine and other aquatic ecosystems and the ecological complexes of which they are part" (Convention on Biological Diversity 2014), is undergoing a state of crisis (Kupfer and Malanson 2004; Myers 1996; Bellard et al. 2012; Cardinale et al. 2012). The greatest threats to biological resources and biodiversity remain human-induced habitat loss and degradation, mostly by the conversion of natural habitats for agriculture or infrastructure development, overexploitation, invasive alien species and pollution (Armenteras and Finlayson 2012).

Even though metal mining activities do not figure among the top threats, they are relevant drivers at the local and regional scales as they cause direct and indirect pressures (Brummit and Bachman 2010). Among the first, land clearances may be particularly harmful by fragmenting the habitats and creating pollution problems like acid mine drainage or riverine tailings disposal. The location where the mining takes place is important as mining activities in the tropical rainforest, for example, "are likely to have more detrimental effects on the environment and the people dependent on it than activities carried out in remote, high altitude and sparsely vegetated and populated regions" (Bringezu et al. 2009:30). On the other hand, indirect negative impacts include unintended deforestation stemming from the opening of roads which may open the way for illegal poaching, logging or artisanal

and small-scale mining (Laurance et al. 2009, 2002; Park 1992; Sonter et al. 2014b) as well as offsite indirect environmental impacts (Sonter et al. 2014b) (e.g. pollution problems with impacts in people living downstream of mining activities) (Maurice-Bourgoin et al. 1999).

Given the anticipated increase in the global primary production of some metals at least during the next decade (Halada et al. 2008; Northey et al. 2014; Sverdrup et al. 2014a, 2014b), metal mining activities are expected to increase their pressure on ecosystems, a fact particularly relevant for biodiversity-rich areas given that for some metals nearly a third of the worldwide active mines and deposits are located within such areas (Miranda et al. 2003).

2.3.1 Global biodiversity mapping and plant species richness

Evaluating the global pressures on biodiversity requires the selection of a criterion to define biodiversity and a global map to operationalize it. Worldwide maps depicting the distribution of life on Earth and species-diversity have evolved over time following the expansion of databases, new mapping techniques, scientific knowledge (i.e. inventories, taxonomic systems, geospatial databases) (Gaston 1998). Mapping has been and continues to be applied to a diverse array of living organisms framed by numerous uncertainties and lack of consensus in the scientific knowledge as to how many living organisms inhabit the planet and how many are becoming extinct before their existence is discovered. Estimations of how many species may exist are as diverse as the methods employed to find answers, spanning between 3 and over 100 million (May 2010), with some recent estimates that 86% and 91% of existing species on Earth and in the ocean are still not catalogued (Mora et al. 2011). Nevertheless, these uncertainties are unevenly distributed and the knowledge of the diversity of vascular plants, in contrast to animal and insects group, is relatively comprehensive: of a total volume estimated at 400,000 species, 300,000 have been documented (Barthlott et al. 1996). Furthermore, the global spatial distribution of vascular plants is well-known due to many different regional floras. Other advantages of using this species group lies in that they play an important role as primary producers in most terrestrial ecosystems (Barthlott et al., 1996) and have great potential in determining the

diversity of other groups given that, in terrestrial ecosystems, they constitute the bulk of total biomass, provide the physical structure for other organisms (Santi et al. 2010), and are the basis of all terrestrial food webs (Kreft and Jetz 2007).

At a global scale, due mainly to data limitations, inventory-based approaches still seem to be the only possibility for the mapping of groups of organisms as large as the vascular plants species (Friis and Balslev 2005). Such approaches date back to the work of Alexander von Humboldt, followed in the past century by the pioneer work of Wulff (1935) but, nevertheless, the first modern mapped depiction of worldwide phytodiversity was published by Malyshev (1975) at a very coarse resolution of species numbers per 100,000 km^2. More recently, perhaps the most significant in terms of understanding broad patterns of biodiversity have been attempts to map the species richness of vascular plants worldwide by Barthlott and colleagues (Gaston 1998). Such global map was first published in 1995 at a spatial resolution of 10,000 km^2 and was improved in the subsequent decade by expanding the database and by using new GIS-based techniques (Barthlott et al., 2007). In its current status the database behind the map has expanded and contains more than 3,300 species richness figures referring to more than 1,800 suitable geographic regions. The richness estimates have been delineated into ten Diversity Zones distinguished by different colours creating a global plant diversity map (Figure 21) considered one of the best approaches for global mapping and monitoring of global terrestrial biodiversity (Barthlott et al. 2005).

2.3.2 Other major approaches to map global biodiversity

Other approaches than the one by Barthlott et al. (2007) to map the global biodiversity are given by various major institutional templates which have been designed by conservation organizations in order to guide their own efforts and attract attention by setting priorities in the sub-discipline of systematic conservation planning within conservation biology (Brooks 2010). Due to limited resources and the uneven distribution of human population and biodiversity in the planet, priority-setting for biodiversity conservation has become one of the most critical topics in conservation science, with schemes which have produced different results, some of them leading to ambiguity, especially due to the difficulty

of resolving tensions between site-specific and generic assessments (Freudenberger et al. 2013).

Over the last two decades, nine major schemes devised for global nature conservation priority-setting have been based on the criteria of vulnerability and irreplaceability (Figure 22). Of those, two have been described by Brooks et al. (2006) as reactive because they prioritize areas of high threat and high irreplaceability: the Biodiversity Hotspots (Myers et al. 2000; Mittermeier et al. 2005) and the Crisis Ecoregions (Hoekstra et al. 2004) (Figure 22).

On the other hand, three so-called proactive schemes prioritize more or less pristine ecosystems (areas of low threat but high irreplaceability): Frontier Forests (Bryant et al. 1997), High-biodiversity wilderness areas (Mittermeier et al. 2003) or the Last of the Wild (Sanderson et al. 2002). Other well-known biodiversity conservation priority templates do not incorporate vulnerability as a criterion (all prioritize high irreplaceability): Endemic Bird Areas (Stattersfield et al. 1998), Centers of Plant Diversity (WWF and IUCN 1997), Megadiversity countries (Mittermeier et al. 1997) and the Global 200 ecoregions (Olson et al. 2001; Olson and Dinerstein 2002, 1998) which also include marine priority ecoregions for conservation (Figure 22). Species are considered the major taxonomic unit for counting biodiversity (Mace et al. 2003); yet, none of the nine approaches relies on species richness (Brooks 2010).

Together with such approaches is a more recent type of conservation that prioritizes ecosystems and their goods and services (e.g. Naidoo et al. 2008; Sutton and Constanza 2002; Turner et al. 2007) alongside more recent papers which propose the concept of ecosystem thermodynamics as an appropriate model for understanding the complexities between biodiversity and ecosystem functioning (Norris et al. 2011). Others, from a more comprehensive perspective and explicitly considering climate change aspects, argue that priority-setting is not only determined by ecosystems providing the largest amount of services but also being more likely to have a high adaptive capacity towards unavoidable environmental change (Freudenberger et al. 2013).

Figure 21: Global biodiversity map per species number of vascular plants.

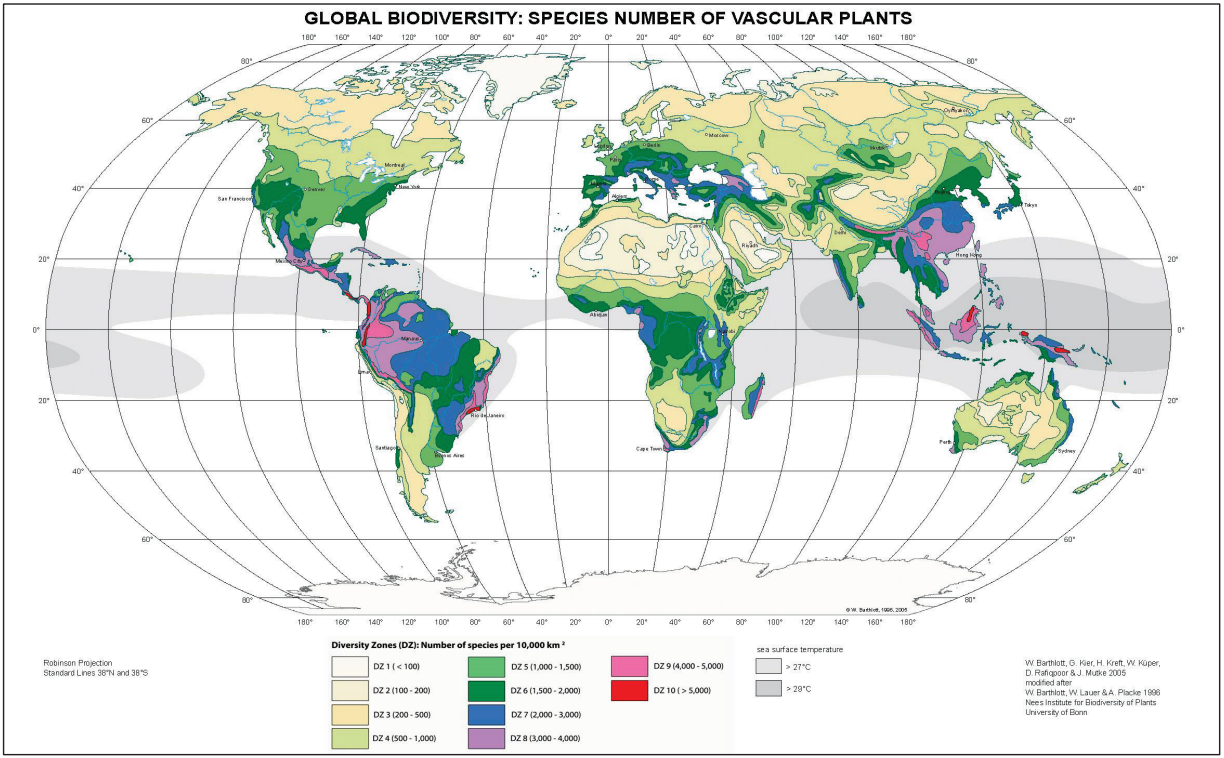

Source: Barthlott et al. (2007)

Figure 22: Maps of nine global biodiversity conservation priority templates.

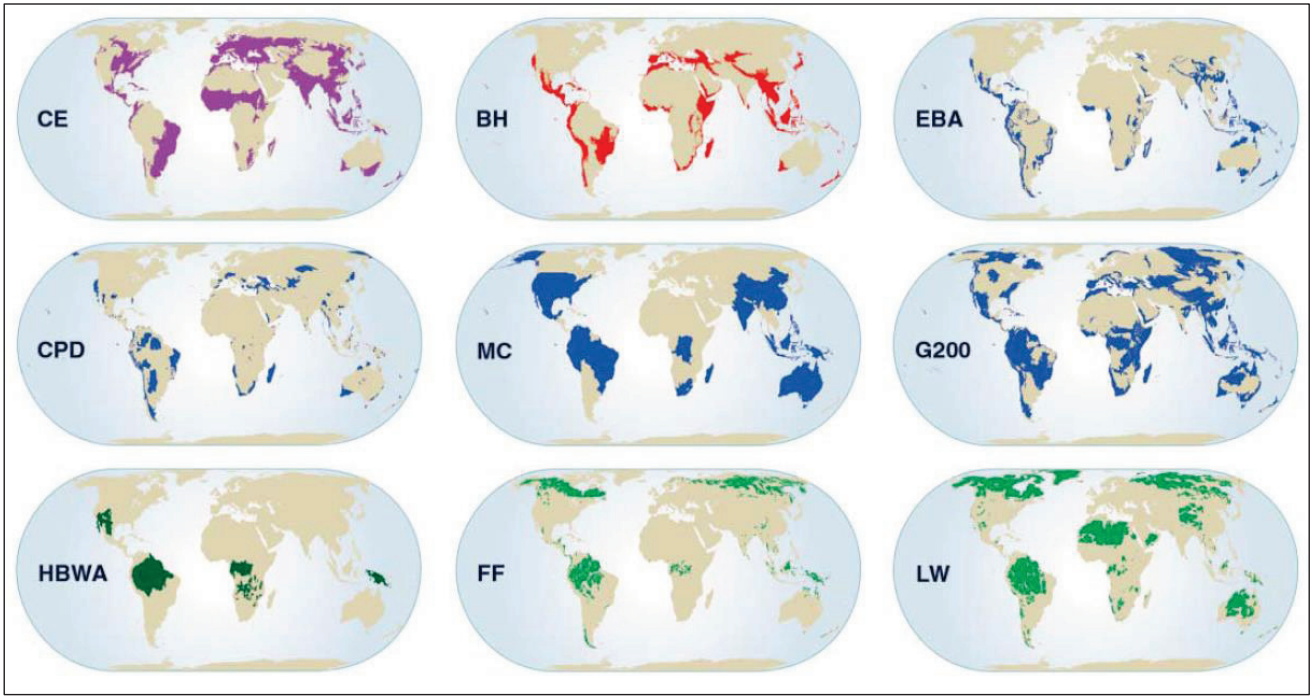

Source: Brooks et al. (2006). Crisis Ecoregions (CE), Biodiversity hotspots (BH), Endemic bird areas (EBA), Centers of Plant Diversity (CPD), Megadiversity countries (MC), Global 200 Ecoregions (G200), High-biodiversity wilderness area (HBWA), Frontier Forests (FF), and Last of the Wild (LW).

CHAPTER THREE

This methodological chapter is divided into four sections. The first addresses the calculation of the specific land requirements per metal and it is subdivided into four sub-sections. The first sub-section addresses the global inventory of metal mines and the procedure to select the samples used. The sub-section on cumulative ore produced describes the variables used to calculate cumulative values, how missing data was handled, and the allocation of the cumulative ore produced using economic value relations for polymetallic mines. The sub-section on cumulative net area disturbed describes the workflow applied to measure areas on Landsat images, including the allocation procedure. The final sub-section describes how the specific land requirements per metal were computed using a weighted disturbance rate per metal derived from a nonlinear regression analysis. The second section of the chapter describes how the global status quo for 2011 was calculated; the third section depicts the procedure for the construction of each scenario and scenario corridor and for ascertaining pressures by mining on the global map of biodiversity zones, including hypothesis testing procedures.

3 Methodology

3.1 Calculating specific land requirements per metal

3.1.1 Global inventory of metal mines and sample sizes

3.1.1.1 Global inventory of large-scale metal mines

An approximation to the global number of operating metal-producing mines in the world begins with the definition of what constitutes a mine, namely, how it is defined, according to productivity criteria (e.g. output per year) or resource-consumption (e.g. water, energy or land use per ton processed) and considerations as to whether mines are legal or illegal. Given the inexistence of global inventories for illegal or artisanal and small-scale mines, if only “industrial scale” legal operations are counted based on the SNL Metals & Mining database, there are some 2,700 metal-producing mines in the world, with a predominance of

open pit operations (Ericsson 2012). Such database provides data on a mine-per-mine basis with useful data on annual production of metal content, ore, geographic location and useful notes[20].

Metal-producing mines can be classified as coupled production (CP), i.e. polymetallic mines extracting metallic ores containing more than one (carrier) metal, or as no-coupled production (NCP), i.e. monometallic mines whose output is one metal. According to the SNL Metals & Mining database (update September 2012), of the global inventory of 2,738 metal-producing mines, around 38% are NCP and 61% are CP[21].

According to the Table 3, iron ore (Fe) and bauxite (Al) ore producing mines are dominated by NCP open pit operations; in both cases open pit (OP) operations represent more than 65% of the number of mines. This indicates that the lion´s share of the global production of these two metals takes place via monometallic open pit mines. In contrast, in the case of copper (Cu), gold (Au) and silver (Ag), production takes place to a large extent in polymetallic mines in which also other co-products (and by-products) are produced. For instance, copper can be produced as a co-product (second metal) in tin, nickel or PGM mines. Similar situations apply to gold and silver. In the cases of copper, gold and silver, the CP numbers shown in Table 3 must be handled with care given that mines are double accounted; namely, in many cases mines repeat themselves as they are polymetallic and have not been allocated to one metal. The idea of CP numbers of mines for copper, gold and silver is to provide a general overview of how production is distributed between NCP and CP.

---

[20] Other global studies linking mining with biodiversity or protected areas have used the commercially-available InfoMine database but have made the observation that most of the active mines and exploratory sites included in such database were located in North and South America, "reflecting gaps in the quality of global data" (Miranda et al., 2003:4). To overcome this limitation, a collaboration agreement was set up with the former Raw Materials Group and their former database (now merged into SNL Metals & Mining) was used.

[21] The compiled data out of which the numbers stem from refer to the SNL Metals & Mining database (former RMG, update September 2012) and includes data from the "Producers entry" for the following minerals: Mo, Ag, Al, Au, Cr, Cu, Dia, Fe, Mn, Ni, Pb, Sn and Zn. Data does not include mines in construction or abandoned, it only includes the status "operating –all forms", "closed –all forms", "suspended" and "suspended, restart plans". Counting only mines (excluding 626 records classified as "active" and "non-active" which indicate companies and not mines) for which production was more than zero, the total number of metal producing large-scale legal mines around the world was of 2,738 mines. Of those 1,046 were no coupled production, 1,670 coupled production and 22 could not be defined.

Table 3: Global number of NCP and CP operating mines. 1975, 1984-2011.

	NCP				CP				NCP+CP
Metal	OP	UG	Other[22]	Subtotal	OP	UG	Other	Subtotal	Total
Al	42	5	17	64	0	0	0	0	64
Fe	236	37	60	333	9	2	2	13	346
Cu	68	18	40	126	145	248	81	474	600
Au	302	277	257	836	238	295	113	646	1,482
Ag	3	4	17	24	237	322	115	674	698

Source: self-elaboration based on the SNL Metals & Mining database (update September 2012), Producers entry (1975, 1984-2011).

In the case of copper, Table 3 is indicating that its production in CP mines more than triples the number of NCP mines; a similar trend occurs for silver, a metal almost exclusively produced as a co-product of copper, gold or lead-zinc. In the case of gold, the distribution is more balanced, though the amount of NCP mines prevails in the global outlook.

In order to better evaluate metal production in CP mines, Table 4 provides a ranking of the frequency distribution of the metal groupings. In such table mines are not double accounted, they were grouped according to the five metals co-produced in each mine as reported in the SNL Metals & Mining database. As shown, mines producing gold-silver doré bars are the most frequent, followed by mines producing doré or copper concentrate.

The two main groupings in Table 4 (Au, Ag and Cu, Au, Ag) total 399 mines, namely, a 38.1% of all CP mines. With regards to the extraction types, open pit operations prevail for those two groupings, though the share of underground (UG) ones is also large.

Table 4: Global inventory of CP operating mines. 1975, 1984-2011.

Grouping	OP	UG	Other extraction methods (incl. not available)	Total
Au, Ag	138	115	48	301

[22] Includes records with no information available in the SNL Metals & Mining database.

Grouping	OP	UG	Other extraction methods (incl. not available)	Total
Cu, Au, Ag	43	37	18	98
Cu, Zn, Pb, Ag, Au	8	40	20	68
Pb, Zn, Ag	6	32	20	58
Pt, Pd, Rh, Au, Cu, Ni	2	43	9	54
Zn, Pb, Ag, Cu	22	17	10	49
Au, Cu, Zn, Ag	2	36	5	43
Cu, Au, Ag, Mo	12	23	3	38
Pb, Zn	1	23	6	30
Zn, Pb, Ag, Au	22	3	4	29
Cu, Au	5	18	1	24
Cu, Ag	1	21	2	24
Ni, Cu	12	9	2	23
Cu, Zn, Ag	15	0	2	17
Cu, Mo, Ag	6	7	3	16
Au, Cu, Pb, Ag	2	8	3	13
Ni, Cu, Pd, Pt, Au	1	5	6	12
Cu, Mo	10	1	0	11
Cu, Zn	8	1	1	10
Other groupings	34	54	40	128
Total	350	493	203	1,046

Source: self-elaboration based on the SNL Metals & Mining database (update September 2012) (1975, 1984-2011).

3.1.1.2 Sampling design and sample sizes

The sampling method applied to select mines´ samples was simple random sampling (without replacement) for iron ore and bauxite, and stratified random sampling (without replacement) for copper, gold and silver mines. The latter were stratified into two subclasses: OP and UG operations. For iron ore and bauxite a sub-classification was not necessary given the predominance of NCP OP operations as shown above in Table 3.

However, before random sampling could be performed, the groupings in the SNL Metals & Mining inventory were filtered according to a number of criteria delivering

mines for which all necessary data was available. The criteria applied to filter useful (eligible) from non-eligible observations encompassed:

1. The observation should be referring to a mine (not a mining company);
2. The mine is producing or has produced and its status equals “operating”, “suspended” or “closed”. Observations with status “under construction”, “proj, no spec”, “conceptual”, “pre- or feasibility”, “abandoned” or “not specified” were excluded;
3. There are data for mine production for the year 2011 (record was not empty or equals zero) indicating the mine was active;
4. Geographic coordinates were available in the SNL Metals & Mining database;
5. Geographic coordinates were precise enough to locate the mine or otherwise they could be located and verified in Google Earth (Google Earth V.7 2013), Mining Atlas (Mining Atlas 2015) or other technical source publicly available;
6. There was a clear visual differentiation of the mine boundaries with respect to other nearby or adjacent land covers and land uses[23];
7. There was sufficient information on historical annual production of ore for all producing years and technical reports to verify production and location information.

These criteria reduced substantially the number of eligible mines within the SNL Metals & Mining inventory. Then, the selection of sample sizes was also

[23] Typical examples of mines not fulfilling this criterion encompass mines located in mining districts where the areas disturbed by mines are spatially close to each other making it hard to establish which area belongs to which mine. Examples are the Harmony Doornkop gold mine (underground) in South Africa or iron ore mines in Brazil (Germano iron ore mine, Córrego de Feijao iron ore mine, Jangada iron ore mine, Itaminas and Paraopeba iron ore complex). Another example is given by the Rudna underground copper mine in Poland for which it becomes difficult to match with surface developments as other mines are also in the same area (Polkowice, Sieroszowice) and no technical reports could be found precisely associating surface disturbances with each mine.

conditioned by: i) the available time within the Ph.D. thesis work to implement the area measurement workflow to a reasonable amount of mines, and ii) the necessary number of terms in the regression equation to be employed[24]. It was assumed that a regression analysis with one term would best explain the association between variables. In order to calculate sample sizes, a simple rule of thumb commonly cited is that "there should be at least 10 or 15 observations in every term in a regression model" (Rothman, 2012:226). Consequently, assuming the usage of a regression model for computing specific land requirements, it was established that a minimum of ten observations should exist per sample. No maximum was defined. In the case of CP mines producing copper, gold and silver, it was decided to select two samples, one for OP and another for UG, out of the two most frequent groupings listed in Table 4. The total sample used for calculating specific land requirements totaled 106 mines. More detailed results are presented in Chapter four (Section 4.1.1).

3.1.2 Cumulative ore produced: calculation and allocation

3.1.2.1 Variables with historical data for ore and metal (concentrate) production

The dataset for calculating specific land requirements of the five selected metals consisted of five variables referring to the ore and metal content production per mine:

- "**Ore Produced (milled)**"[25]: refers to the annual amount of ore extracted and milled. Available from 1998 onwards. This is the main variable employed in this study;
- "**Main metal produced**": refers to the metal concentrate produced. In monometallic mines (iron, bauxite) it refers to the saleable concentrate. In polymetallic mines it refers to the main target metal extracted as defined by the SNL Metals & Mining database under "main metal". Available for the

[24] By testing pilot cases, it was determined that regression analysis would be the preferred method to evaluate the association between cumulative ore production and cumulative net area disturbances.

[25] Only in the case of iron ore the variable employed to approach the ore production was "Run-of-mine" (ROM); the reason is that the missing values rate in the SNL Metals & Mining database was considerably lower than the "Ore produced" variable. In all cases ROM and Ore Production figures were nearly equal.

year 1975 and from 1984 onwards; it was one of the variables used to allocate the cumulative ore production and the cumulative net area disturbances for polymetallic mines;

- "**Metal 2 Production**", "**Metal 3 Production**" and "**Metal 4 Production**": all refer to the metal concentrate produced as co-product in polymetallic mines. Available for the year 1975 and from 1984 onwards and also determined by the SNL database; also used for allocating cumulative ore and net area disturbances in polymetallic mines.

In addition to the afore-mentioned variables, the only additional variable in the SNL Metals & Mining dataset with historical data refers to "ore grade", provided from 1998 onwards; however, the completeness rate is very low to become a useful proxy variable to handle missing data.

3.1.2.2 Handling of missing data

By importing data from the SNL Metals & Mining database, the dataset in this study was organized as a cross sectional time series panel data using the software Microsoft Excel®. When importing the data from the database, attention was paid so that unknown data on production (missing values) was differentiated from production equal to zero (e.g. due to temporary suspension of activities).

For a total of 106 mines, the total number of observations (annual production per mine) for all five metals consisted of 2,149. The overall missing data rate for the main variable ("Ore Produced") reached a 25% and for the variable "Main metal produced" a 12%; for the remaining variables it spanned between 1% and 3%.

Before calculating and allocating the cumulative ore produced per mine, the missing data needs to be handled. The available strategies for handling missing data can be grouped into three options: deletion methods, non-stochastic imputation, and stochastic imputation methods (Schlomer et al. 2010). Deletion methods like list wise deletion (dropping subjects with missing data) provides the advantage of simplicity and comparability across analyses but it also reduces the sample size and statistical power, particularly in small samples, and may introduce severe bias if the assumption of data missing completely at random is violated

(Allison 2009); pairwise deletion has also the disadvantage that analyses cannot be compared because samples are different each time and if data are not missing completely at random it may yield biased estimates (Allison 2009).

Non-stochastic single imputation (any method to substitute missing values with estimates) is potentially more efficient than case deletion because no units are sacrificed, preventing a loss of power. It is considered that if the observed data contain useful information for predicting the missing values, “an imputation procedure can make use of this information and maintain high precision” (Schafer and Graham 2002:158). On the negative side, imputation can be difficult to implement well, particularly in multivariate datasets and may distort data distributions (Schafer and Graham, 2002).

Criticism of single imputation argues that this method causes analysis software to think the data have more observations than actually observed and exaggerates the confidence in the results by biasing standard errors and confidence intervals (Honaker and King 2010). An alternative to yield the least biased estimates are stochastic multiple imputation methods in which separate “completed” data sets are created where the observed data remain the same but the missing values are “filled in” with different imputations. The expected value for any missing value is the mean of the imputed values across these data sets; however, the uncertainty in the predictive model is represented by the variation across the multiple imputations for each missing value. This method removes the overconfidence that would result from a standard analysis of any one completed data set and gives accurate estimates of the uncertainty of any resulting inferences (Honaker and King 2010).

Given that specific land requirement calculations are computed separated for each metal, it was decided to handle the missing data metal-by-metal. Owing to the fact that the strategies afore-mentioned normally apply to big samples and to data missing at random, the selection of a strategy to deal with missing data was conditioned by the small size of the samples, the systematic character of the missing data, the need to estimate missing values for calculating cumulative ore production, and the limited amount of variables with historical data.

Iron (Fe)

Given the high missing data rate for both production variables (Table 5), the nature of the missing data was examined.

Table 5: Missing data rate for Fe.

Variable	Observations missing			Missing data rate
	Total	DSO	NDSO	
Ore Produced (milled)	234	43	191	32%
Main Metal Produced	249	43	206	34%

Source: self-elaboration based on SNL Metals & Mining database.

In the case of Ore Produced, it was found out that 97% of the missing data was due to the fact that it was production belonging to years before 1998; 8 out of the 16 DSO and 10 out of the 11 NDSO mines had begun operations before that year. Given that the SNL Metals & Mining database only collects data on Ore Production from 1998 onwards, it can be concluded that such a high percentage of missing data was a collection issue and data was systematically missing, i.e. was not missing at random. The imputation was performed separately for DSO and NDSO mines as follows.

DSO mines

In contrast to data on Ore Produced or run-of-mine (ROM) only available from 1998 onwards, the SNL Metals & Mining database provides data on mine production of concentrates (saleable iron shipped out of the mine, "Main Metal Produced" variable) for the year 1975 and from 1984 yearly onwards. This is of advantage in the case of DSO mines as the ore produced (and the run-of-mine) equals the production of concentrates shipped which allows filling in historical missing values on run-of-mine with historical data from production of concentrate and vice versa. In the cases were such fill-in procedure was not possible, the missing values for such mines were estimated "backwards in time" using a best fit curve for the available data (the years closest to the missing values in order to

keep the continuity in the time series); the best fit criterion was the highest coefficient of determination (R^2).

NDSO mines

For NDSO mines, the run-of-mine data were only available from 1998 onwards; hence for mines starting operations before 1998, data were estimated[26]. Estimations of missing values were performed first in the variable "Main Metal Produced" given that it was the most complete; missing values were estimated using a best fit curve back casting historical data from the known values; if a best fit curve could not be fitted to the data, a single value imputation method was applied based on the moving average of the two nearest production records. This was done in order to smooth out short term fluctuations in the production due to the opening of a new section in the mine. Using the imputed "Main Metal Produced" variable, the run-of-mine was estimated with a moving ratio (using the two nearest years) between the concentrate ("Main Metal Produced" variable) and the run-of-mine produced.

Bauxite (Al)

Annual ore production data was sourced from the SNL Metals & Mining database; the missing rate was of 10% for the only variable available ("Ore Production"). The imputation method applied entailed estimating "backwards in time" by using a best fit curve to the available data and extrapolating back in time. Only in the case of the Kindia mine a curve could not be fitted and the imputation was done using a moving average of the two nearest years with data on ore production within the mine´s time series.

Copper (Cu), gold (Au) and silver (Ag)

Similar to the case of iron ore mines, the missing data rate was high for the "Ore Produced" variable and low for the remaining ones (Table 6).

[26] Exceptions are the mines Sydvaranger, Frances Creek and Gole Gohar for which historic ore production could be found in technical reports.

Table 6: Missing data rate for Cu, Au and Ag mines.

Variable	Observations with missing values	Missing data rate
Ore Produced (milled)	271	29%
Main Metal Produced	17	1.8%
Metal 2 Production	56	6.1 %
Metal 3 Production	64	7.01%
Metal 4 Production	29	3.18%

Source: self-elaboration based on SNL Metals & Mining database.

An analysis of the missing data revealed that in the cases of copper, gold and silver, for Ore Production, a 94%, 72% and 84% of the missing values belonged to years of production prior to 1998, namely, data was systematically missing because those years were not collected by the SNL Metals & Mining database. No missing data was found for mines in the sample with silver as the main metal.

Imputation of the Ore Production variable

The imputation of the missing values was performed via single value imputation. This was done for years in which production was known to have occurred (indicated by two points in the database ("..")) but the value was unknown (missing); this was done preferably by establishing a rule of three between two known years of "Main Metal produced" (or "Main metal production") and a known "Ore Production" year as shown in Table 7 (value in red is imputed).

Table 7: Example of single value imputation using a rule of three.

Mine	Type	CP or NCP	Year	Ore produced (milled) (Mt)	Main metal production
Gualcamayo	OP	NCP	2011	7.578	4.941
Gualcamayo	OP	NCP	2012	7.742	4.582
Gualcamayo	OP	NCP	2013	6.32	3.743

The usage of this method was enabled by the high completeness rate of the "Main Metal production" variable. The advantage of using this imputation technique is that it uses the observed ratio between ore production and metal content and keeps continuity with the data provided by the database.

Imputation of the Main Metal Production and co-product variables

In the cases in which metal production data for Metal 2, 3 or 4 were missing for one year, it was filled in establishing a rule of three with the existing data for the Main Metal in the following year (see Table 8 where values in red were imputed).

Table 8: Example of single value imputation for co-products.

Mine	Type	CP or NCP?	Year	Ore produced (milled) (Mt)	Main metal production	Metal 2 production	Metal 3 production	Metal 4 production
Palito Gold m	UG	CP	2008	0.131	0.529	0.3	0	0
Palito Gold m	UG	CP	2009	0.042	0.17	0.096	0	0
Palito Gold m	UG	CP	2010	0.015	0.06	0.034	0	0

3.1.2.3 Allocation using economic value relations

Using the single-value imputed dataset, the cumulative (gross) ore production was computed for each mine by adding annual ore production and, in the cases of copper, gold and silver, the cumulative (gross) ore extracted was allocated using economic value relationships (average metal prices) following the Eurostat EW-MFA Guide 2013 (Eurostat 2013).

Value relations were determined using the long-term average metal prices from the USGS for the period 1990-2009[27] which have the advantage of neutralizing short term fluctuations and are more in accordance with economic decisions of opening or closing a mine which is also based on a rather long-term assessment. They were applied in each mine using the output value (in USD/t) of the metal produced in the period considered for the calculation of the new area disturbances. For instance, the Alamo Dorado Silver mine produced 1,174 t silver, 3.75 t gold and 931.4 t copper in the period 2007-2013 (mine started commercial production in 2007), which involved a cumulative output value of USD 270.4, USD 52.5 and USD 3.1 million USD respectively, namely, a 82.9% Ag, 16.1% Au and 0.97% Cu. By applying these percentages to the cumulative gross ore milled in the same period (11.3 Mt), the cumulative ore produced was allocated to each metal. Mine-per-mine allocation results are shown in the Section 8.4.1 of the Appendix.

[27] Such prices were for copper 3,382 USD/ton, for gold 14,008,593 USD/ton, for silver 230,197 USD/ton, for zinc 1,542 USD/ton, for lead 1,270 USD/ton, for molybdenum 21,426 USD/ton and 9,721 USD/ton for tin.

3.1.3 Cumulative net area disturbed: calculation and allocation

3.1.3.1 Using Landsat imagery and visual image interpretation

The research questions posed by this thesis require calculations of the cumulative area disturbances at mine sites for numerous mines at multiple locations. This requires the processing of several satellite images widely distributed across the world. In order to satisfy this information requirement and considering the need to freely obtain satellite images, two options exist among optical satellites: Landsat and Aster satellite images.

The spatial resolution of both satellites is similar, with the highest pixel-resolution of 15 m in both cases; however, unlike Landsat, Aster data has not been acquired at regular time intervals over the same location, with the result of a lower likelihood of obtaining imagery for a particular field for the correct time (GISAgMaps 2014). Although both types of images could have been combined, it was preferred, for continuity reasons and in order to have the highest chance of cloud-free available imagery, to make all measurements using the Landsat images available at the Landsat archive. Such images, especially those captured by more modern sensors (TM, ETM+ and OLI) provide a sufficient spatial resolution for a visual detection of mines and the area affected by them (e.g. Figure 23A), a fact ratified if compared to high spatial resolution images like those offered by Google Earth (Figure 23B).

Figure 23: Images of Marcona iron ore mine at different spatial resolutions.

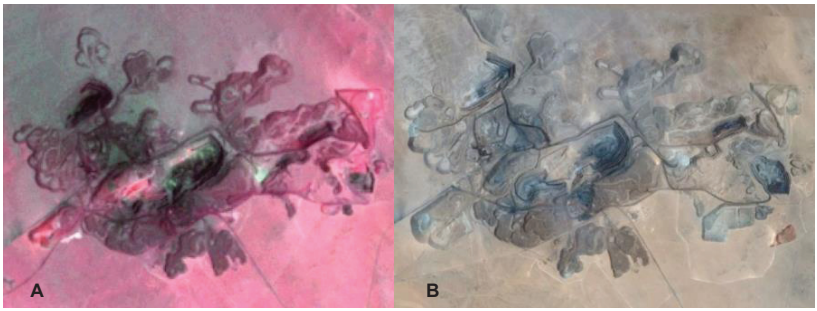

Source: self-elaboration based on a (A) L5 image (Acquired: 24/11/2010) and (B) a Google Earth capture.

Given that visual image interpretation is directly dependent on the spatial resolution (Düzgün and Demirel 2011), it was preferred to employ (if available) Landsat images captured by the TM and OLI sensors which have a satisfactory spatial resolution and, in contrast to images captured by the ETM+ sensor from 2003 onwards, are not affected by sensor malfunctioning.

Google Earth snapshots could not be employed to make measurements because they are so far only available in sufficient detail for some locations and because the acquisition date can not be known for certain in many cases nor can be chosen by the user. This makes it difficult to select images at the end of the year which can be matched with a full year of ore production by a mine. Furthermore, Google Earth does not grant access to the image itself (digital data with information per band) which impedes the application of machine algorithms working at pixel level and also hinders an effective visual interpretation as the software only provides a natural color image without the possibility of mixing bands to make use of several interpretation elements.

3.1.3.2 The cumulative net area disturbed term

The term *cumulative net area disturbed* is employed in this study in order to refer to the surface area which has been used for the purposes of mining ore during a certain period of a mine´s life. Such area can be visually differentiated from nearby land covers and can be ascertained to have been disturbed exclusively for the purposes of open pit or underground mining. Accordingly, it encompasses all infrastructure exclusively used by a mine.

The area calculated as cumulative *net* area disturbed is differentiated from the cumulative *gross* area disturbed with regards to areas potentially reclaimed and areas potentially affected by subsidence. This distinction is particularly striking in the case of case of bauxite mining because reclamation is a much more successful and common practice than in other types of large-scale metal mining. This can be explained given the shallow intervention on the soil that the method employs. Consequently, in some cases of bauxite mining, images allowed room for inferring or assuming that some parts of the land had been successfully reclaimed or rehabilitated, or had been cleared and would be mined soon; this

could be inferred given that the color and texture of the land were very similar to nearby land covers with vegetation. Given the lack of ground data this could not be validated.

The Figure 24 shows a traditional false color composite of the Gove bauxite mine (located in north-east Australia) in which bright yellow-green areas allow recognizing the temporary areas disturbed by mining (areas where bauxite ore is extracted and mine infrastructure determining the net area disturbed) in contrast to red tones which show the natural undisturbed and the regrowing vegetation (brighter red indicate more the growing vegetation). However, next to some bright yellow-green areas there are other areas which show a color transition to a brown-reddish color which are labeled as "areas potentially reclaimed or to be mined soon".

Therefore, in order to exclude those areas which could not be fully ascertained to have been disturbed by bauxite mining (or to be under rehabilitation), only the most clearly disturbed areas were measured and considered part of the cumulative net area disturbed.

Following this criterion, the Figure 25 shows highlighted in blue the area classified as cumulative *net* area disturbed (by October 2011) for the Gove bauxite mine, totaling 30,464 pixels (2,396.9 ha)[28]. As visible, it does not include the areas classified as "potentially reclaimed or soon to be mined" near to the blue color. Although this distinction between "gross" and "net" applies mostly for bauxite mining (for other types of mining no such subtle differences in tones could be observed), it was decided to highlight that only areas clearly distinguished as having been impacted by mining were included in the calculations.

In the case of underground mines, sometimes mines are affected by subsidence phenomena. This becomes difficult to visually interpret in Landsat images and hence it was excluded from the cumulative net area disturbance measurements.

---

[28] If compared with the List of images in the Appendix (Section 8.3), a difference of 344 ha can be observed with the final calculation. This is because in the subset shown here to calculate the cumulative net area disturbed there is a part of the mine missing; this part is the town where workers live located towards the North, off the image´s subset boundaries shown in Figure 25.

Figure 24: Gove bauxite mine. Color tones and selected land covers. 2011.

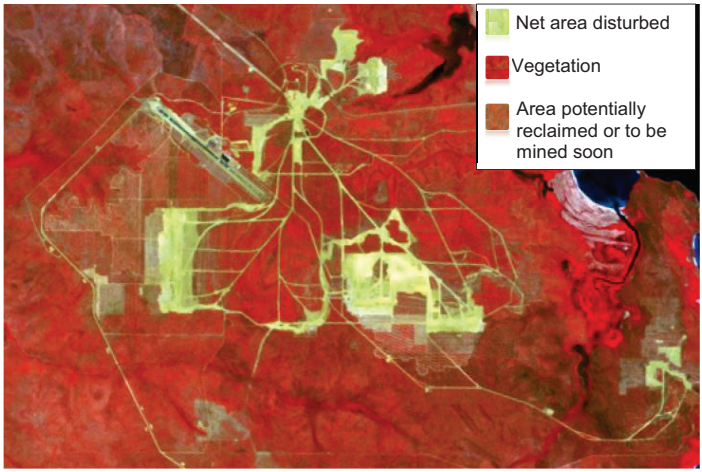

Source: L5 image (Acquisition date: 11/10/2011). Band combination (RGB): 432.

Figure 25: Gove bauxite mine. Cumulative net area disturbed. 2011.

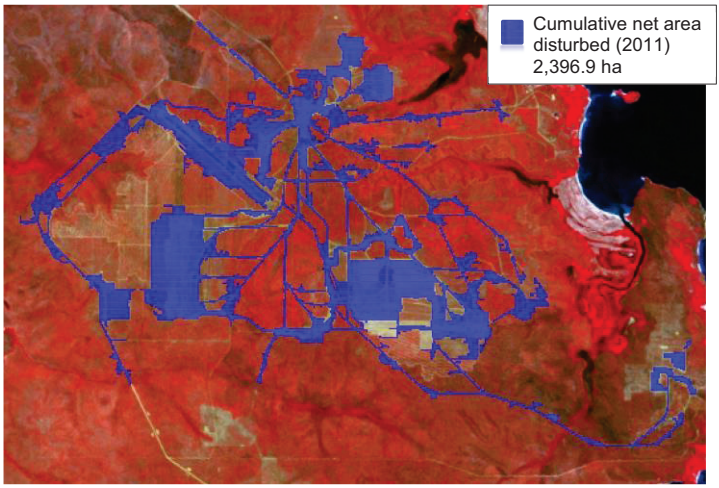

Source: L5 image (Acquisition date: 11/10/2011). Band combination (RGB): 432.

3.1.3.3 Using OBIA and visual image interpretation for classification

In order to develop a workflow to measure the cumulative net area disturbances caused by metal mining using Landsat images, several methods were tested. Pixel-based classification approaches were tested in subsets of Landsat images using training areas and supervised classification algorithms like support vector machines under the ENVI® environment (Exelis Visual Information Solutions 2009). Two classes ("mine" and "no-mine") to classify the image were established and results were not satisfactory due to misclassification of pixels. It was noticed that most existing algorithms are useful to classify several land covers within an image, but very few exist explicitly designed to extract a specific feature with high accuracy[29]. After testing several pixel-based methods, a feature extraction based on object-based image analysis was tested in the eCognition Definiens® software version 8.7 (Trimble 2011a).

Object-based image analysis (OBIA) under eCognition is usually performed, first, by conducting a segmentation of the image. Often with the aid of the multiresolution segmentation algorithm (MRS) (Trimble 2011b) customized by user-defined parameters, the image pixels from the image are grouped to form objects (segments); this creates a number of interrelated levels in which objects cover the full scene. The second usual step comprises semantic modeling. After segmentation and the creation of classes, the features and relations of the individual object classes are defined within a hierarchical network. For this, the features which best identify objects belonging to the same class must be extracted. Feature extraction is then a prerequisite for semantic modeling and rule set development is a tedious and time-consuming task because there are no comprehensive, statistical or really satisfactory tools generally applicable. The extraction takes place by several trial-and-error steps to filter out those features and threshold values that describe an object class well from the large number of possible features and values. A promising new tool for feature analysis is the

[29] One example of such algorithm that works very well is the Fmask one developed by Zhe Zhu and Curtis E. Woodock at Center for Remote Sensing of the Boston University. It works for automatically detecting clouds, clouds shadows and snow masking for Landsat 4, 5, 7 and 8 images. More details at: https://code.google.com/p/fmask/ (Website accessed: April 2014).

SEaTH (SEparability and THresholds)[30] (Nussbaum and Menz 2008b) which requires the selection of training objects (objects representative of each defined class) and calculates the thresholds which allow the maximum separability in the chosen features.

From the start, this OBIA approach seemed to work well since the applied multiresolution algorithm by the eCognition software provided satisfactory results to classify mining areas, establishing visually identifiable limits between the classes “mine” and “no-mine”. By following-up on this approach, attempts were pursued to develop a complex rule set to apply to a big number of pre-processed Landsat subsets for an automatic detection and separation of the “mine” class from the “no-mine” one. This was conceived to be run as a batch under the module eCognition Server® (Trimble 2013) by the Trimble company, however, despite several attempts, including the use of the SEaTH tool, it became clear that results were not satisfactory. After several runs, the tool provided useful separability thresholds based mostly on spectral values (e.g. redness index, ratio vegetation index for iron ore mines) but also other object features like distances to scene or edge contrast of neighbor pixels. However, classification based on these thresholds was never adequate; the usage of some thresholds in one image subset could not be readily transferred to others.

All in all, given the lack of satisfactory results, the option of performing a manual classification based on visual image interpretation aided on ancillary information was tested. After creating the basic rule set mentioned above, it was clear that the OBIA approach with manual classification based on visual image interpretation provided flexibility in searching for the right level (scale parameter) and resulted in mine areas measured in hectare with high accuracy and using short amounts of time.

3.1.3.4 Workflow applied

The workflow developed and applied to each satellite image is shown in Figure 26.

[30] The software to run SEaTH (SEATH_GUI) by Prashanth Reddy Marpu can be freely downloaded as an Envi plugin or as stand-alone from: http://www.treatymonitoring.de/index.html (Website visited: April 2014).

Data Acquisition and Pre-processing

Selection of periods and number of images per mine

The first step encompassed determining whether one or two Landsat images were required for each mine. For that, first a reference period (or period considered) was determined between two years based on the availability of reliable ore production data and the availability of cloud-free Landsat satellite images. 1984 was the eldest year given that older images did not have a spatial resolution good enough to visually detect mines. The chosen period and the number of images used per mine can be consulted in the Appendix in the Section 8.1. The idea behind selecting a period is that the land and material dynamics can be studied in it; by having two images, one can subtract the area measured in the most recent with the area of the eldest, obtaining the cumulative net area disturbed in the period. Such quantity can then be regressed against the cumulative ore extracted in the same period.

Figure 26: Workflow applied for calculating cumulative net area disturbances.

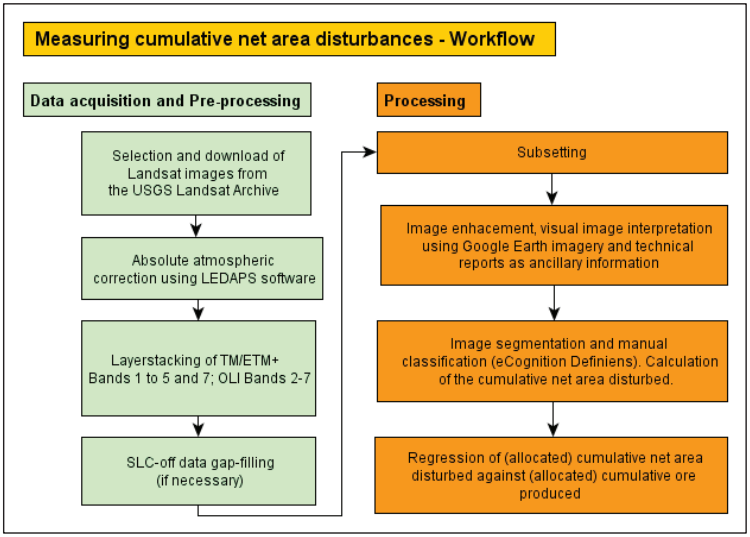

Source: self-elaboration

In order to determine the right period per mine, the necessity of one or two images was determined by the age of the mine; if the mine was historic (having begun operations before 1970), the chances of obtaining reliable annual ore mined (or metal produced) data for its full history were low and therefore the dynamic could only be determined for a period using two images[31]. For example, in the case of the historic Awaso bauxite ore mine (starting commercial production in 1941), it was determined that the period to be observed would be 1986-2002; ore data were available only from 1984 and the eldest Landsat satellite image with enough spatial resolution belonged to 1986. Hence, data were collected for cumulative ore mined between January 1986 and December 2002. One image acquired in January 1986 was used with another taken in December 2002; in this way the entire production period of 17 years was covered and both variables could be correlated. In the case of a modern mine (having begun operations after 1970), yearly ore or run-of-mine produced data were available, fully or partially, in the SNL Metals & Mining database; this means that estimations could be done to reconstruct the productive history of the mine and then only one image (a recent one) was used which accounts for the land dynamics.

Atmospheric correction and gap filling

All satellite images used in the study are Landsat and were downloaded free of charge from the Landsat archive with the aid of the USGS Earth Explorer website or from the Global Land Cover Facility website[32]. Each image was searched and selected using its corresponding path and row information from the grid of the WRS1 or WRS 2 based on the mine´s location according to the SNL Metals & Mining database coordinates, in some cases corrected using Google Earth (Google Earth V.7 2013; Google Earth Pro v. 7.1.4 2015) or Mining Atlas (Mining Atlas 2015). All images used were already corrected to a L1T (standard terrain correction) level.

[31] In some exceptions, cumulative ore production data could be found in technical reports or other sources and therefore the period considered spanned over years before 1970. This was the case for instance with the Chelopech gold/copper UG mine starting operations in 1954, with a period considered of 1954-2013, and for which only one image belonging to 2013 was used to measure the cumulative net area disturbed.

[32] http://earthexplorer.usgs.gov/; http://glcf.umd.edu/data/ Websites accessed: April 2014.

In the selection process, preference was given to Landsat TM images because they do not have problems of missing lines (SLC-off)[33]. Images pairs were selected seeking anniversary dates in the months of November or December, whenever possible and available. For example, in the cases in which no image was available in December of a year, and if one was available for November, the measurement in November was assumed as valid as if the measurement had been done in late December. In other cases, images acquired in January, for instance in January 2002, are considered representative of the area disturbed by the end of the year 2001. In some cases like iron ore or bauxite mines in the Brazilian Amazon area, images with a small-cloud cover were only available in June or July; in these cases, they were considered representative of the year they were acquired. The full list of images used per mine can be consulted in the Appendix under Section 8.3.

Once selected and downloaded, most images were radiometrically corrected for atmospheric effects using the Landsat Ecosystem Disturbance Adaptive Processing System (LEDAPS) algorithm originally developed by the NASA Goddard Space Flight Center and the University of Maryland[34]. This absolute correction procedure processes Landsat data from Landsat TM and ETM+ Level 1 digital numbers to surface reflectance based on the atmospheric conditions on the data and time of image acquisition. The corrections are based on the second simulation of a satellite signal in the solar spectrum radiative-transfer model used by the moderate resolution imaging spectroradiometer (MODIS) land science team (Schmidt et al. 2013). Briefly, the six modules of the algorithm follow three steps: i) convert digital numbers (DN) to top-of-atmosphere (TOA) reflectance; ii) detect cloud pixels based on the TOA reflectance; iii) correct to surface-reflectance from TOA reflectance and ancillary data sets. The product is a surface-reflectance

[33] On May 31, 2003, the Scan Line Corrector (SLC), which compensates for the forward motion of Landsat 7, failed. Without an operating SLC, the Enhanced Thematic Mapper Plus (ETM+) line of sight now traces a zig-zag pattern along the satellite ground track. As a result, imaged area is duplicated, with width that increases toward the scene edge. This only affects Landsat ETM+ images from 2003 onwards.

[34] A number of images used belong to the Landsat 8 satellite and, given that the quality was good enough, no atmospheric correction was performed.

image. Ledaps final products were layer- stacked using Bands 1-5 and Band 7 for TM and ETM+ images and Bands 2- 7 for L8 ones.

Most of the imagery downloaded for this study belongs to Landsat 5 (TM) imagery; however, in many cases Landsat 7 (ETM+) imagery was used due to lack of Landsat 5 or Landsat 8 coverage. Consequently, the usage of L7 images from 2003 onwards resulted in facing sensor-related noise caused by device malfunctions. During the pre-processing of Landsat images for this study the most frequently encountered error was the zig-zag pattern along the ETM+ ground track occurred in images taken from May 21 2003 onwards by the ETM+ sensor. Several methods for displaying and scientific use have been explored for image-processing and gap filling (Chen et al. 2011). The method used in this study for gap filling was the replacement of missing lines by interpolated values from proceeding and succeeding lines as performed by the Landsat gap fill tool developed for Envi 4.7® (Exelis Visual Information Solutions 2009). This resulted in some deformations of the gap filled images, especially when the mines were located on the borders of the scene (away from the central strip clear of the zig-zag pattern of the image where deformations due to the gap filling process are at minimum).

Processing

Subsetting and image classification

All Landsat pre-processed scenes cover an area of 185 km x 185 km. For each mine a subset was created using the Region of Interest tool by the software ENVI® (Exelis Visual Information Solutions 2009) covering the entire mine area and some extra kilometers. In order to extract information from the image data subsets, each of the latter were visually interpreted with the help of publicly available technical ancillary information which is necessary when lacking ground truth data. The latter comprises:

- Technical data publicly available (e.g. public environmental reports, environmental impact assessments, site inspection reports, Forms 20-F

to the SEC, corporate websites, reports and presentations, academic publications, particularly that by Mudd (2007c);

- High resolution imagery and landmarks available at Google Earth or Mining Atlas.

The availability of this ancillary information was crucial particularly for historic mines. Based on these technical reports and high resolution images, the Earth´s surface specific features related to mining (shape, size, tone, texture, pattern, shadow, association and site) (Düzgün and Demirel 2011) were visually inspected using band combinations of the subset reflecting different tones for each element of the mine. The mine elements potentially identifiable and recognizable on a Landsat satellite image are listed below in Table 9.

Table 9: Mine elements on the surface to determine the cumulative net area disturbed.

Reference on the surface	Open cut operations	Underground mines
Ore extraction area	Open pits	None
Area for facilities for mining, processing and final product out-of-mine transport	Industrial facilities or ancillary infrastructure: ROM pads, accommodation village, stockpile area, crusher, processing plant, conveyors, access and haul roads, train loadout and rail lines in and out of mine site, air strips, etc.	MIA measurable: accommodation village (camp), stockpile area, ROM pads, access roads, buildings on top of shafts and mine portals.
Area for beneficiation	Heap leach pads, processing plant	Heap leach pads, processing plant
Area for extraction wastes	Soil and overburden piles and waste rock dumps adjacent to the pits	Waste rock often left underground; sometimes some is placed on the surface.
Area for beneficiation wastes	Tailings ponds or dry-stack tailings storage facility	Tailings ponds or dry-stack tailings storage facility

Source: self-elaboration

Landsat images do not always allow the identification of each element on its own; this was done with the support of high spatial resolution images on Google Earth. In cases of historic mines in which mining towns have developed and became a separate entity of the mine, the perimeter of the town was not included as a part of the mine (e.g. Super Pit gold mine and the adjacent Kalgoorlie-Boulder town).

Exploration traits (drilling) were not included in the measurements; access roads were measured only up to 500 m from the mine industrial area (MIA). Areas affected by subsidence (if present) were also not measured. The detailed account of elements included in the measurement of each mine´s cumulative net area disturbed can be consulted in the Appendix in the Section 8.3 under the "Observation / Detail on mine elements included in the net area disturbed measurement" column.

Measurements were not done for each element but for the entire mining area as a whole. In this study area measurements on Landsat images are all two-dimensional, namely, there is no height or depth measured; if a mine is located over a mountain, the area calculated belongs to the 2D (two-dimensional) satellite image.

After visually identifying the above-depicted elements on each mine scene, the subset was loaded as a project into the eCognition Developer software (Trimble 2011a). A rule set was applied to each subset following four steps: i) segmentation; ii) classification of segments; iii) merging of the mine area, and iv) creation of one image object. The multiresolution segmentation was applied creating 13 levels and classes[35]. For segmentation, the most appropriate level was chosen by trial and error from the 13 levels created.

Preference was given to image objects produced with low scale parameters (e.g. Figure 27B) as such were small enough to delineate the boundaries of the "mine" class and provided higher accuracy than bigger ones (e.g. Figure 27C and D).

For classification purposes, different band combination(s) complement each other and provide the best method to visually interpret the mine site boundaries. All segments belonging to the cumulative net area disturbed were manually classified using eCognition´s Manual Editing Toolbar.

---

[35] Levels were defined with the following characteristics: image layer weights were equally assigned by 10,10,10,10,10,10, shape was 0.1 and compactness 0.5 for all levels. From Level 0 to Level 13 scale parameters assigned were as follows: Level 0 with scale parameter of 5, Level 1 10, Level 2 20, Level 3 30, Level 4 40, Level 5 50, Level 6 60, Level 7 70, Level 8 80, Level 9 90, Level 10 100, Level 11 110, Level 12 120, Level 13 130.

Figure 27: Comparison of segmentation levels at Bajo de la Alumbrera mine.

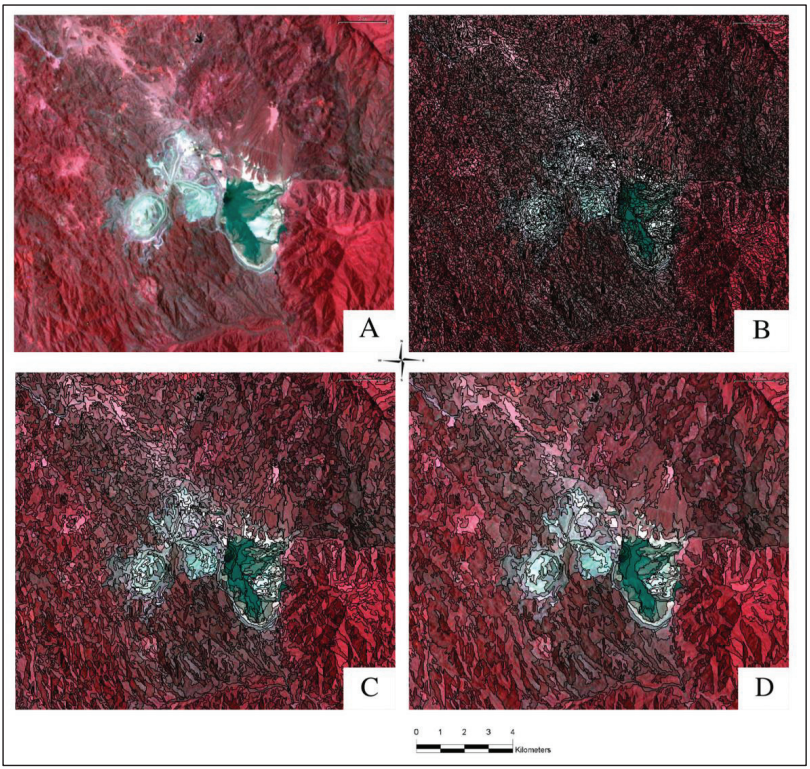

Note: Comparison of segmentation levels for Bajo de la Alumbrera open pit mine, Landsat 5 TM image acquired February 02 2010, segments are delimited with black lines: A) Subset displaying a shortwave infrared composite (712) image, band combination R-Mid-infrared, G-Blue, B-Green, the open pit, waste dumps and tailings pond can be recognized due to color, shape and size contrast with the surroundings; B) Subset image segmentation (MRS scale 20); C) Subset image segmentation (MRS scale 60); D) Subset image segmentation (MRS scale 120).

The subsets in Figure 28 and Figure 29 cover the area of the Robinson copper-gold open pit mine in Nevada (U.S.) and are a false color composite with colors, patterns and textures providing elements to differentiate the spatial continuum of the mine from the surroundings.

In the first image (Figure 28) open pits, adjacent waste dumps and the mine infrastructure area are clearly visible due to a different color in comparison to its

surroundings, to the shape, sizes and tones of the elements which differentiate them and allow visually observing the spatial continuum occupied by the mine.

Figure 28: Robinson OP Cu-Au mine. Mine elements. 2012.

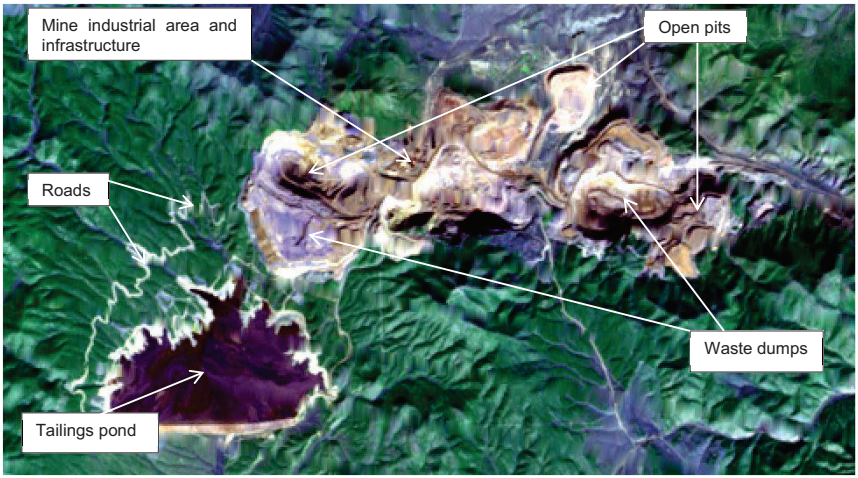

Source: self-elaboration on a L7 image (Acquisition date: 03/11/2012). Band combination (RGB): 345.

Figure 29: Robinson OP Cu-Au mine. Cumulative net area disturbed. 2012.

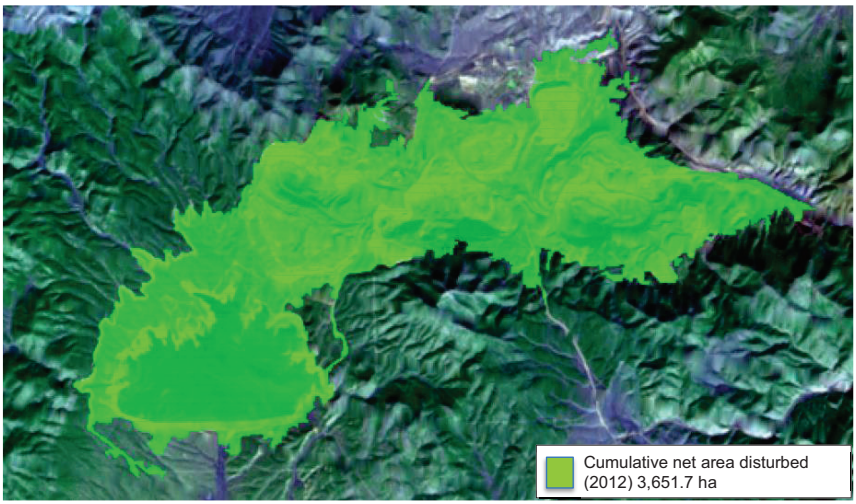

Source: self-elaboration on a L7 image (Acquisition date: 03/11/2012). Band combination (RGB): 345.

Association also plays an important role since objects become identifiable when they are analyzed with their spatial associations; in this case, e.g. the white lines (low tonal variation) connecting the tailings pond with the pits clearly allows concluding that they belong to the mine. Once all elements have been visually identified and verified as belonging to the mine with a Google Earth image and technical reports, the spatial continuum can be classified by manually selecting segments resulting in the cumulative net area disturbed shown in Figure 29. The light green area in the Figure 29 below accounts for the merged area of the Robinson mine which totaled 40,575 pixels, equivalent to 3,651.7 ha (in 2012).

The images below for the Musselwhite gold mine (in northwestern Ontario, Canada) (Figure 30) display that for UG mines, smaller in surface disturbances, the spatial resolution of the Landsat satellites does not allow an easy differentiation of elements but it does allow the creation of one merged area accounting for the cumulative net area disturbed. This includes the mine infrastructure, the airstrip, the tailings pond (in reddish color due to having unclear water) and the access road (white color belonging to cleared soil). All this elements appear in the image to the left in a reddish tone due to the band combination used.

Figure 30: Musselwhite UG gold mine elements (left) and classification (right). 2011.

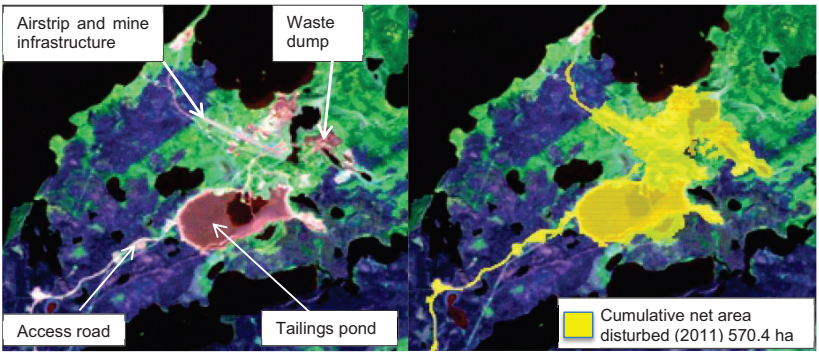

Source: self-elaboration based on a L5 image (Acquisition date: 20110927). Band combination (RGB): 123.

The image to the right shows in yellow colour the area classified as the cumulative net area disturbed of the Musselwhite mine by the end of 2011 totaling 6,338 pixels (570.4 ha). Other colours (resulting from a band combination different for instance in comparison to Figure 28 or Figure 29) show clear water belonging to lakes (in dark black), green areas (with different tones) belong to vegetation and blue-violet range colored areas to naturally bare soil or soil with sparse vegetation. Further examples of calculations of cumulative net area disturbances are provided for the Boddington bauxite mine, the Yandi iron ore open pit mine, Burnstone underground gold mine and the Super Pit open pit gold mine in the Appendix, Section 8.2.

In the case of a historic mine with two images, the classification procedure began with the most recent one which in all cases encompassed the old area disturbed. By subtracting the net area calculated in the most recent from the oldest, the cumulative net area disturbed in the period considered was obtained. All data were calculated by counting pixels contained in segments. All segments forming the mining cumulative net area disturbed were merged as one area, and were later converted to hectares using the conversion factors listed in Table 10.

Table 10: Pixel-hectares conversion factors used.

Landsat Sensor	Bands used	Pixel size (m)	1 pixel equals (ha)
TM/ETM+	1-5 and 7	30	0.09
OLI	2-7	30	0.09

Source: self-elaboration based on http://landsat.gsfc.nasa.gov/?page_id=2401

The final results of the (unallocated) cumulative net area disturbed per mine can be consulted in the Appendix at Section 8.3. For results of the period considered for calculations please refer to the Appendix, Section 8.1.

3.1.4 Estimating specific land requirements by regression analysis

3.1.4.1 Theoretical assumption and model fitting by regression analysis

The unallocated and allocated cumulative net area disturbed and cumulative ore produced are continuous quantitative variables which were examined in

scatterplots to test the theoretical assumption that the cumulative ore extracted determines the cumulative net area disturbed under a power function, following the notation by Bronshtein et al., (2004), as shown in Eq. 3:

$$S_{ad} = a * x^k \qquad \text{Eq. 3}$$

where S_{ad} (y) is the (cumulative) surface area disturbed, *a* (beta) and *k* (gamma) are constant parameters and *x* is the (cumulative) ore extracted (mass).

Previous research has determined that the surface area disturbed by large metal mines (open pit and underground) is directly dependent on the amount of annual ore extracted (Martens et al. 2002; Ruhrberg 2002; Sliwka 2001). Consequently, it is argued that, at a mine site, the extraction mass directly corresponds to the extraction volume which is a three-dimensional measure that can be expressed as z^3 if z is distance such as length (l), width (w) and depth (d) of a mine as shown in Figure 31.

Figure 31: Dimensions of extraction volume at an open pit mine.

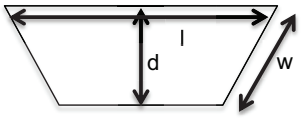

Nevertheless, the area disturbed measured on a satellite image is only a two-dimensional (z^2) measure, i.e. length and width. Therefore, the hypothesis argues that the cumulative net area disturbed (y) is a function of the cumulative ore extracted (x) under a power function like that in Eq. 3, with the constant *k* having a value in the range of 2/3 (0.666) (Figure 32).

Figure 32: Power function for $y=x^{2/3}$.

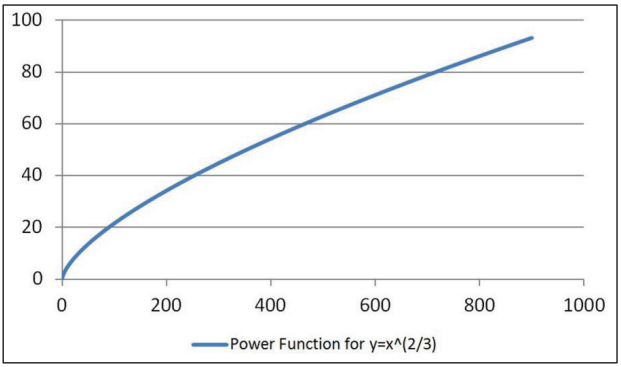

This hypothesis was tested by means of either linear or non-linear least squares regression analysis. The selection of a linear or nonlinear regression was based on the ordinary least squares method yielding the lowest sum of squares. As described in the Results (Section 4.1.2), the nonlinear method proved to be the one with the lowest sum of squares in all cases.

The model fitting was performed first for all mines (not differentiating by extraction method) and then, for copper, gold and silver separating by open pit and underground methods. Results separated by open pit and underground methods were not used for scenario construction, yet, they were computed and are reported to show differences between both. In all cases, the regression analysis was performed using the nonlinear ordinary least squares (OLS) estimation module within the Stata® software package version 11.1 (Stata Corp LP 2009). Initial value for parameterization of beta was set at a = 50, doubling the value set by Ruhrberg (2002:70) for open pit mines (a = 23.86). Such value was used as the first estimate and, after testing other initial values (a = 5, a = 25), the lack of statistically significantly different results led to the use of a = 50 as common initial value for all regressions. For gamma, the initial value was set at k = 0.666.

Given that regressions are potentially affected by influential points, results were bootstrapped in order to obtain robust estimates of p-values and conduct hypothesis testing to test the null hypothesis that the regression parameters equal

zero. The bootstrap (Efron 1979; Efron and Tibshirani 1993) is a nonparametric random resampling method that uses the information of a number of resamples from the original sample to estimate the population distribution. It is based on the idea that the original sample represents the population from which it was drawn, so resamples from this sample represent the result if many samples were taken from the population. Thus, the bootstrap distribution of a statistic, based on many resamples, represents the sampling distribution of the statistic, based on many samples (Hesterberg et al. 2006). Bootstrapping was chosen as the correct statistical technique as it does not assume normal distributions (Hesterberg 2007; Schmidheiny 2012) and works well for small samples (Fisher and Hall 1991). This technique has been successfully applied in nonlinear regression models (Davidson and MacKinnon 1999; Roy 1994) and has been proven to yield robust estimates of standard errors and confidence intervals (Sohn and Menke 2002). Bootstrapping was applied using Stata´s built-in module (Stata Corp LP 2009) running 50 replications to test the statistical significance of results. When in suspicion, the impact of outliers which could be considered influential points was graphically analysed to verify that none were substantially changing the function equation, i.e. an observation is said to be influential "if removing the observation substantially changes the estimate of the regression coefficients" (UCLA Statistical Consulting Group 2007). If an observation was determined to be an influential point, it was removed (this was the case in the copper, silver and bauxite samples).

For each sample undergoing a regression, the average ore grade was calculated. Ore grades did not play a role during the regression analysis but were calculated and are reported to disclose the average quality of the ore processed in the samples. Ore grades informed are based on the annual information available at the SNL Metals & Mining database during the period 1998-2014. Results are expressed in percentage of iron (Fe) or copper (Cu) content for iron and copper mines and in grams per metric ton (gpt) for gold and silver mines. No information of ore grades for bauxite is reported as it is not available. It must be highlighted that results for each regression curve are only valid for mines with a cumulative ore production within the range of applicability determined by the curves.

Principal assumptions underlying OLS regression analysis comprise the normality of residuals (their distribution should be approximately normal) and the homoscedasticity of the variance (data should show a homoscedastic pattern); otherwise heteroscedasticity (nonuniform error variance) means that observations with lower variance are more informative than others (higher variance) making the standard error and hypothesis tests not that reliable (Barreto and Howland 2006).

After fitting the model, such assumptions were tested by means of:

- **Plots of residuals against fitted values.** The presence of heteroscedasticity was visually assessed by plotting the residuals against the fitted values. Patterns in residual plots allow observing whether the variance of residuals varies constantly or non-constantly. If the points are randomly distributed, it indicates that the variance is constant;
- **Histograms**. Frequency histograms were created to test whether the distribution of the residuals looks approximately close to normal (bell-shaped or Gaussian); a normal distribution curve and a kernel density estimate (a non-parametric estimator used to smooth the density estimate while retaining the overall structure) (Thomson 2006) were superimposed in the graph to show how curves differ from each other, i.e. how close to normality is the distribution of residuals.

3.1.4.2 Calculating the global cumulative new net area disturbed per year

The specific land requirements (also called the new net area disturbed factors), were calculated by means of a weighted disturbance rate computed from the sample following five steps:

1. **Calculating mine-specific slopes**: based on the non-linear regression curve fitted for each sample, the slope of each data point of the primary data was computed using the equation given by the first derivative (Eq. 4) of the power function presented in Eq. 3:

$$y' = a * k * x^{k-1} \qquad \text{Eq. 4}$$

The mine-specific slope (y´) was thus calculated for each data point for a specific reference year (the last year of the period used to compute the cumulative ore produced) by applying the function in Eq. 4 to the total amount of cumulative ore produced until that year (see for instance Table 21 in the Appendix);

2. **The new net area disturbed per mine per year (A_i)** was calculated by multiplying the mine-specific slope by the amount of (average) annual ore extracted in the next two years following the reference year (O_i); if the reference year was 2013, and given the lack of data for 2014, it was assumed that the production in 2014 equaled that in 2013. Mines which were suspended or closed after the reference year were excluded;

3. **The sum of all new net area disturbances per year (A_p) was computed for all mines in each sample**; this indicator provides the total new net area disturbed in one year by the mines in the sample;

4. **The sum of all ore extracted as average in the two years following the reference year (O_p) was computed for all mines in each sample**; this indicator provides the total amount of ore extracted in one year by all mines in the sample;

5. **Compute the weighted disturbance rate (WDR)** following Eq. 5:

$$WDR = \frac{A_p}{O_p} \qquad \text{Eq. 5}$$

This weighted disturbance rate indicates the specific land requirements, i.e. the average annual amount of hectares newly disturbed caused by the annual extraction of a certain amount of ore. In other words, it represents how many hectares are newly disturbed per year given a certain amount of mass extracted, based on the given global distribution of mines according to size and age (duration of production). It is expressed in hectares per million metric ton of ore extracted (ha/Mt_{ore}) and the ore refers to the total amount of ore milled in a mine (allocated

to a certain metal according to the main metal in the case of polymetallic mines). Using the afore-mentioned WDR rate, the global annual amount of new hectares disturbed (per metal) was calculated by multiplying the WDR with the world mine production of ore per metal. This amount of new hectares disturbed per year was used for the construction of scenarios departing from the global status quo and adding such amount cumulatively during the modeling period (2010-2050).

3.2 Calculating the global status quo in 2011

3.2.1 Sample size

The samples used are based on those mines selected and measured for the specific land requirements section. However ten additional mines were included to increase the sample size; these mines were not included in the specific land requirements sampling due to lack of historical production data. Final sample sizes of mines for the global status quo were: bauxite (n=13), iron ore (n=27), copper, gold and silver (n=76), in total 116 mines widely distributed worldwide (Figure 33).

Figure 33: Spatial distribution of the mines sampled for the global status quo.

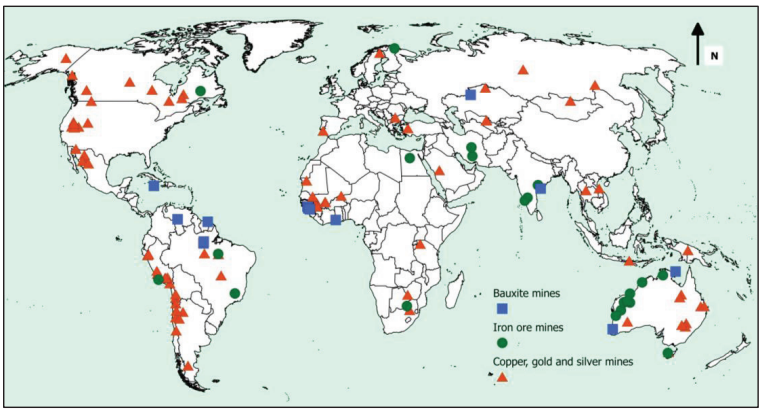

Source: own cartographical representation based on the database by SNL Mining & Metals.

The sample, and the global area disturbed calculated based on it, includes mines in operation, closed or suspended but does not include abandoned or orphaned mines which are numerous in countries such as Canada or Australia.

The groups of mines sampled are considered to be representative of the world mine production in terms of the amount of ore extracted. On the one hand, the sample was selected randomly from the available mines and follows the frequency distribution of the world industrial metal mines population (by ore extraction per mine). On the other hand, the average sample share in the world mine production achieved for all five metals is 17.6%. As shown in Table 33, Table 31, Table 35, Table 37 and Table 39 (all in Appendix, Section 8.5), the average of the sample share (or proportion) of the world mine production in the period 2010-2012 per metal was: Fe (14.3%), Al (29.2%), Cu (18.3%), Au (15.7%) and Ag (8.6%).

3.2.2 Method applied

The calculation of the global cumulative net area disturbed in 2011 per sample is based on the cumulative net area disturbed by all active mines in each sample and its interrelation with the world production.

The first step encompassed calculating the global cumulative net area disturbed (2011) per sample. The area occupied by the active mines sampled was calculated using 44 Landsat 5 TM, 46 Landsat 7 ETM+, and 26 Landsat 8 OLI image subsets captured mostly for the years 2011, 2012 and 2013. It was attempted to work only with images belonging to the year 2011 but whenever this was not possible (due to lack of cloud or haze-free images or lack of enough spatial resolution), images from nearby years were used and an adjustment was applied to approach a 2011 value. One image per mine was employed. The list of mines used and the (unallocated) cumulative net area disturbed for 2011 can be consulted in the Appendix, Section 8.3.2.

A second step was approaching the relation between sample and world production by calculating an annual proportion factor between world mine production and the material mined by the mines in each sample for the period 2010-2012. Such period was chosen to cover fluctuations in a year previous and another after 2011. The year 2011 was chosen given that it provides the largest number and diversity of L5 satellite images hosting enough spatial resolution to detect and measure large mines.

For bauxite and iron, the annual proportion factor was determined by dividing the world mine production of ore by the sample production of ore[36]; this was based on the U.S. Geological Survey (USGS) data. In contrast, for copper, gold and silver, no world statistics of ore production exist; the USGS and the BGS provide world mine production in terms of metal content. In such cases the annual proportion factor was calculated dividing the metal content in the world production and that in the sample. Results of annual proportion factors are found in the Appendix (Section 8.5). An average annual proportion factor was computed per sample.

The third step involved using such 3-year average proportion factor to multiply it with the cumulative net area disturbed by mines in the sample in 2011. This determined the global cumulative net area disturbed per metal in 2011 (does not include the area disturbed by abandoned or orphaned mines). The sum of the five samples resulted in the global area disturbed by all of them.

3.3 Scenarios on global cumulative net area disturbed by 2050

The construction of scenarios and scenario corridors is based on existing data modeled by colleagues at the Norwegian University of Science and Technology, the Commonwealth Scientific and Industrial Research, the Lund University, and the University of Iceland. Stock-based models were preferred to flow-driven ones. Projections were built by multiplying the specific land requirements to the projected global annual ore extraction. This resulted in three to six scenarios or a scenario corridor which show different potential paths of future global cumulative net area disturbed (excluding the area disturbed by abandoned mines).

3.3.1 Iron ore

Introduction

Globally, around 98% of iron ore mined is used in steelmaking. Therefore, all forecasts of iron ore extraction in the decades to come are directly linked to

[36] For iron ore, run-of-mine (ROM) numbers were used and, for bauxite, ore production (no ROM given in the database). ROM and ore produced (milled) can be different in some cases since the mine might extract and stockpile the ore, leading in some cases to years of more milling than extracting. Yet, for iron ore mines, in most cases ROM and ore produced were the same or nearly the same.

steelmaking projections. World crude steel production has been yearly increasing in the last four decades at an average growth rate of 2.4% per annum, jumping from 595 Mt/a in 1975 to 1,500 Mt/a in 2012. Most predictions agree that the final demand will keep on increasing up until 2050 (Hatayama et al. 2010; IEA 2009; Yellishetty et al. 2010). This issue raises concerns as the social and environmental impacts of materials production and processing are rapidly becoming critical and can be ameliorated to some extent by the pursuit of efficiency increases. However, if final steel demand doubles by 2050 as projected by the IEA (IEA 2009), the socio-environmental pressures exerted by mining will not be ameliorated and targets (e.g. carbon emissions reduction) will not be reached unless noticeable energy and material efficiency efforts take place.

If the past world production of iron ore is considered, Figure 34 shows that it increased gradually during the first part of the 20th century and then doubled in the period 1960-1990.

Figure 34: World annual production of iron ore. 1904-2013.

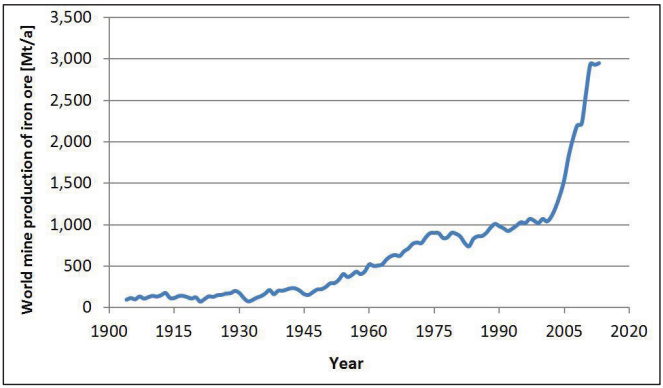

Source: USGS and Kelly and Matos (2013)

Another big jump occurred in the decade 2002-2012 as production almost tripled from 1,100 Mt/a (2002) to 2,930 Mt/a (2012). Given the tight link between steel demand and iron ore production, it seems wise to follow models which prioritize this relationship, assume saturation levels and pay attention to novel technologies

and ratios of primary and secondary steel production. Not many models exist taking into account so many variables.

Recently, and because of the fact that steelmaking accounts for one quarter of all industrial CO_2 emissions globally (Cullen et al. 2012), research has been conducted constructing normative scenarios in order to evaluate what kind of policy-alternatives are required to increase energy and material efficiency in the steel supply chain so as to achieve IPCC carbon emission reduction targets by 2050 (set to less than 1 Gt CO_2/a for the steel sector). Milford et al. (2013) have published seven scenarios based on a dynamic stock model estimating future final demand for steel and post-consumer scrap published in an accompanying paper by Pauliuk et al. (2013).

In this dissertation it was decided to use such model and the related seven scenarios given that they take into account per capita in-use stocks rather than consumption flows to make projections. The model is quite optimistic in many ways and assumptions but at the same time complex enough to provide possible industry pathways depending on how investment decisions are led.

According to the USGS (USGS 2014b) global iron ore resources are estimated to exceed 230,000 Mt whilst reserves reach 170,000 Mt which are supposed to last for another 57 years if extraction levels continue at the 2013 one (2,950 Mt/a). This means that for scenarios up until 2050 no shortages of iron ore are assumed.

Scenarios of global annual iron ore extraction

This dissertation is based on the seven scenarios modeled by Milford et al. (2013) anticipating changes in future mass-flows. Regarding mass flows, such authors assume the following:

- based on historical evidence, the model assumes a future stock saturation and extrapolates historical steel use patterns in the developed world to the entire globe and assumes that eventually “all world regions will benefit from the same services provided by steel stocks as industrialized countries do today” (Pauliuk et al. 2013:3449);

- all available end-of-life scrap is recycled, with iron production used to top-up the level of steel production required to meet demand;
- steel production from end-of-life scrap can be a perfect substitute to steel produced from ore, which is currently not true.

Milford et al. claim that steel services may be delivered in the future with less liquid steel by means of implementation (at different speeds and degrees of implementation) of six material efficiency strategies as defined in Allwood et al. (2011):

- Less metal, same service: lightweight product design could reduce the average mass of material per product;
- More intense use;
- Life extension (increasing product lifespan);
- Fabrication scrap diversion, rather than melting;
- Reuse: components from unwanted products and buildings could be reused without melting;
- Fabrication yield improvement: better manufacturing processes could reduce yield losses.

Taking into account that all such strategies could be applied to different extents in the future, the authors investigated seven scenarios:

- One business-as-usual (BAU), where it was assumed that recovery rates increase to 90% (nowadays estimated at 83%) and scrap input to the BOF increases from 10% to 20% by 2050, and that best available technology is reached by 2020;
- Three "energy efficiency" scenarios with, in addition to the BAU improvements, low, medium, or high deployment of novel technologies[37] and electricity decarbonization;

[37] Refers to a number of technologies which could substantially reduce emission intensities: top-gas recycling, fuel substitution, smelt reduction, advanced direct reduction, electrolysis, and a decarbonization (a decrease in the emission intensity of electricity if the grid is decarbonized through implementation of CCS, nuclear power or increased renewable capacity).

- Three “energy & material efficiency” scenarios, with a medium level of energy efficiency, and the full technical potential (theoretical limits) of material efficiency strategies mentioned in the bullet points above attained at slow, moderate, and fast rates. The names of the scenarios reflect the speed of attainment of such material efficiency strategies: in the 2050 scenario, material efficiency strategies are applied fast (by the year 2050 all strategies have been successfully applied), in the 2100 one at a moderate speed and in the 2150 scenario are very slowly attained (they are effectively implemented only by the year 2150);
- For each of the strategies, and based on case studies, interviews and literature, the authors established upper bounds (theoretical limits) to the impact of the strategies to different product categories.

The seven scenarios of iron ore extraction in this dissertation were created with raw data from the Mining Module of the model published by Stefan Pauliuk and colleagues (Pauliuk et al. 2013). The data as delivered refers to flows of beneficiated iron ore (iron oxide) to sintering and iron making by smelting and electrolysis. These data assume a 15% loss during beneficiation; therefore, in order to obtain flows of iron ore to beneficiation, and as recommended by S. Pauliuk, data were divided by 0.85. When comparing these results with those reported by the USGS for world iron ore production for the period 2008-2013 (Kelly and Matos 2013), there was an average difference of –23.8% for the modeled data; if the period 2011-2013 is considered, the difference adds up to –34.1% since in those years the difference was bigger as the iron ore extraction grew significantly (from 2,590 Mt/a in 2010 to 2,950 Mt/a in 2013). Since scenarios depart from the base year 2011, in order to make the modeled data come closer to the actual iron ore extracted as reported by the USGS, it was decided to adjust the modeled data by adding a compromise number of +25%. This adjustment may introduce some bias to the modeled data but makes it come much closer to the actual data and was agreed by the model´s authors as a reasonable solution (pers. comm. with Stefan Pauliuk, 22 April 2014).

The seven scenarios projecting annual quantities of global iron ore mine extraction until 2050 are displayed below in Figure 35. In general, all scenarios show, at different rates, a decline in the global volume of iron ore extraction over time. In the first scenario (BAU) and in all Energy Efficiency ones annual extraction peaks around 2025 at a level slightly higher than current extraction levels (3,000 Mt/a in 2012).

Figure 35: Seven scenarios of global annual iron ore extraction. 2010-2050.

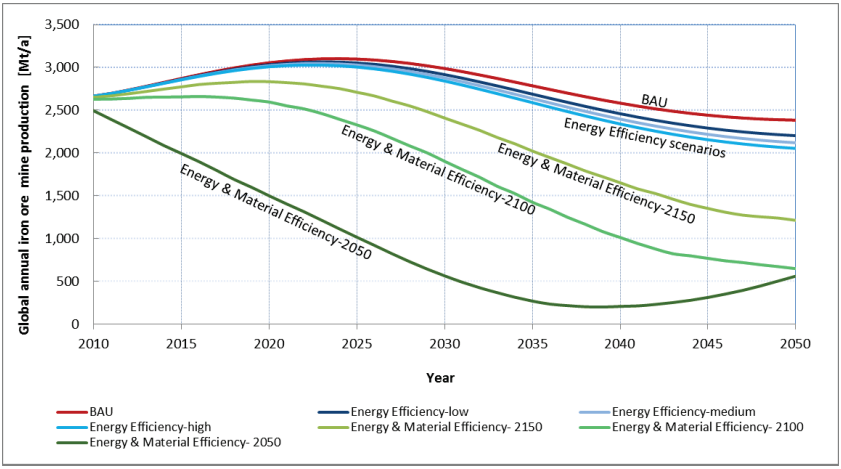

Source: self-elaboration based on data by Milford et al. (2013) and Pauliuk et al. (2013).

After 2025, despite increasing final steel demand, iron ore extraction is reduced gradually, reaching an annual extraction of less than 2,500 Mt/a by 2050; this is due to the increased availability of scrap, mainly from China which has quickly built up stocks until then and secondary steel production which considerably reduces the demand for iron ore. The difference between these three Energy Efficiency scenarios lies in the level of deployment (or aggressiveness) with which novel technologies (aimed at emissions reductions) are applied, more specifically, the amount of steel produced in electric arc furnaces (EAF) (used for secondary steelmaking).

According to the predictions of the model, electric arc furnace (EAF) steel production grows significantly until 2050, actually with a chance to surpass basic oxygen furnace (BOF) steel output (primary steel production) between 2050 and 2060, leading the way towards what the model´s authors call “the steel scrap age”.

The three “Energy & Material Efficiency” scenarios show much more aggressive scenarios. In the first two (2150 and 2100), iron ore production remains relatively constant until 2020 and then falls uninterruptedly to very low levels by 2050. This is the result of an aggressive implementation of energy and material efficiency strategies coupled with the availability and usage of scrap. The last scenario, the Energy & Material Efficiency 2050, shows the most theoretical (and perhaps most unlikely) picture as demand falls quickly until 2035, and then experiences a rebound after 2040 as the rapid implementation of lightweight design and life extension restricts subsequent scrap availability.

Scenarios on the global cumulative net area disturbed by iron ore mining

The seven scenarios projecting levels of global annual iron ore extraction (Figure 35) were combined with the specific land requirement computed for iron ore mines. The global annual iron ore extracted was multiplied by the weighted disturbance rate of iron ore and the output represents the annual amount of new hectares disturbed by mining of iron ore globally. Starting from the global status quo for 2011, such amount of new hectares disturbed annually was added cumulatively over the modelling period (2011-2050). The result consists of seven scenarios depicting a BAU scenario and alternatives on the potential global cumulative net area disturbed by iron ore mining until 2050.

3.3.2 Bauxite

Scenarios on global annual bauxite ore extraction

As a first step existing literature was reviewed focusing on scenarios of future global bauxite ore extraction. Only one scientific study (Liu et al. 2012) was found forecasting bauxite ore supply until 2050; most others forecast consumption or demand of aluminium or bauxite ore. Existing forecasts of global aluminium demand are usually based on extrapolated assumptions of market growth (IEA

2009; Schwarz et al. 2001) or economic indicators (for example, price, per-capita GDP) (Luo and Soria 2008; Menzie et al. 2010); others also use the same method but only consider BRICs or G6 countries (Halada, Shimada, and Ijima 2008).

In the model by Liu et al., (2012), the future aluminium cycle (2010-2100) was calculated employing a stock-driven approach, assuming that the global aluminium in-use stocks per capita eventually saturate. In contrast to supply or consumption-driven models which do not consider stock dynamics (e.g. Allwood et al., 2010; GARC, 2011), stock-driven ones integrate into the analysis anthropogenic stocks (in-use stocks), stocks in the lithosphere (in-ground reserves and resources) and their flows by primary (from ore) and secondary (from scrap) use.

The model by Liu et al., (2012) was constructed to explore GHG emission pathways and mitigation potentials, it considers pre-consumer and post-consumer scrap availability, its influence on primary production, and it includes bauxite ore extraction calculated from the mass balance. The model outputs different levels of aluminium demand according to nine no-action wide-ranging scenarios that vary in assumed saturation levels and time. Saturation levels are set to represent a low (200 kg per capita), medium (400 kg per capita), and high (600 kg per capita) level of future global aluminium use. Saturation times (approximated by the time when the stocks reach 98% of the saturation level) were chosen to reflect a fast (2050), medium (2075), and slow (2100) stock growth.

The nine no-action (or business-as-usual) scenarios of global annual bauxite ore demand modeled by Liu et al (2012) are shown in Figure 36. They are based on modeled data of bauxite ore demand until 2100 which was obtained by personal communication with Dr. Gang Liu (May 2014) in metal content units of bauxite. It was then converted to bauxite ore backwards using the static conversion factors assumed by the authors in constructing the model: Al-to-Alumina conversion factor of 1.923 and an Alumina-to-Bauxite factor of 2.739[38], and a mining loss of 8%.

[38] The factor is slightly high if compared, for instance, with Alumina Limited which estimates an average of 2.5 tons of bauxite per ton of alumina (Wasow and Thiris 2014).

As can be seen in Figure 36, the saturation level and the saturation time both play an important role. If the saturation level is first considered, the low-level scenarios all remain around a mining rate of 250-300 Mt/a by 2050, namely, a bauxite ore extraction rate in the range of the present one (258 Mt/a in 2012) or slightly larger; the Low-2100 scenario shows the smallest increase due to a late saturation and provides actually the best possible situation in terms of low environmental pressures due to bauxite extraction.

Figure 36: Nine no-action scenarios of global annual bauxite ore demand. 2010-2050.

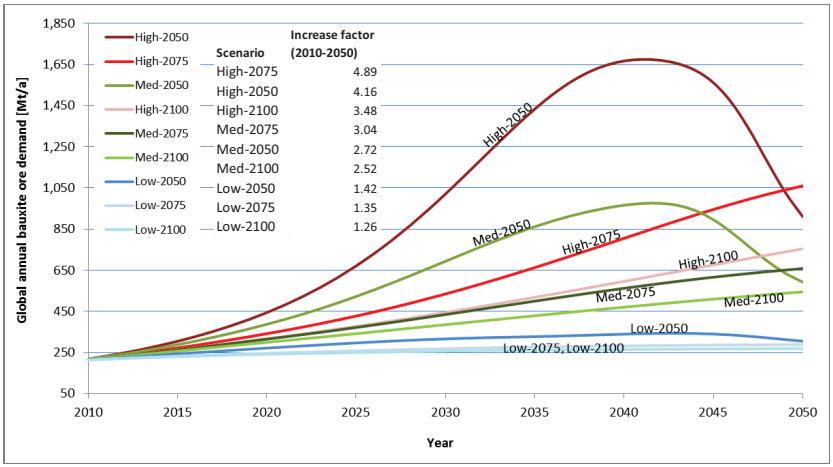

Source: self-elaboration based on data modeled by Liu et al. (2012)

The medium-level saturation scenarios all show by 2030 a significant increase in the extraction with the scenario reaching saturation most quickly (Med-2050) requiring an increase in the production of bauxite ore with a factor of 3.1 by 2030. The two medium level scenarios saturating in 2075 and 2100 (Med-2075 and Med-2100) at least double the current annual global bauxite ore demand by 2050 and still show an increase by then.

The no-action scenarios with high saturation levels, namely, with aluminium in-use per-capita stock levels similar to Netherlands or U.S. today, are more different in terms of bauxite ore demand as the curves enter into a concave up phase quickly, especially for the two scenarios saturating in 2050 and 2075 (High-2050 and High-2075). The most bauxite-intensive one, saturating globally very early and at a very high level (High 2050), would require extraordinary increases in ore extraction from 2025 onwards, with an increase factor (in comparison to 2010 extraction levels) of 4.6 by 2030, reaching a factor of 7.6 in the peak (2040) and of 4.1 by 2050, going down in the curve as recycling takes over. Medium and low saturation times (High-2075 and High-2100) still require significant increases in bauxite ore extraction with increase factors spanning between 3 and 5 by 2050.

With regards to the saturation time, all three scenarios which reach a saturation point by 2050 (Low-, Med- and High-2050) show an early turning point taking place by 2030, they peak in the period 2040-2045 and display a concave down phase in the curve afterwards. Concerning those scenarios reaching a saturation in the year 2075 or 2100 (Low, Med and High-2075 and 2100), they all peak in bauxite ore demand after 2050, namely, they show a gradual increase along the curve until 2060 or longer for the 2100 ones.

The dynamics of the stock model show that when the global aluminium stock saturation is reached, virgin (or primary) production is required only to replace material lost during collection, reprocessing, and final deposition. For those scenarios with global bauxite ore demand peaking by 2040-2045 this means that secondary production will overtake primary production, which then either declines or levels off (in Low-2075 and Low-2100 scenarios). From a land disturbances point of view, the best possible option would be to quickly achieve a low saturation level globally so that the primary production and land disturbances are reduced to a minimum.

Selection of three representative no-action scenarios

Given the variability in the nine no-action scenarios, three representative scenarios are selected with the aim of establishing a potential development corridor under BAU conditions with a realistic low, medium and high variant.

The three selected no-action (or BAU) scenarios depicting possible pathways of annual bauxite ore demand are: **High-2075, Med-2075** and **Low-2050** (Figure 37).

Figure 37: Three selected no-action scenarios on global bauxite ore demand. 2010-2050.

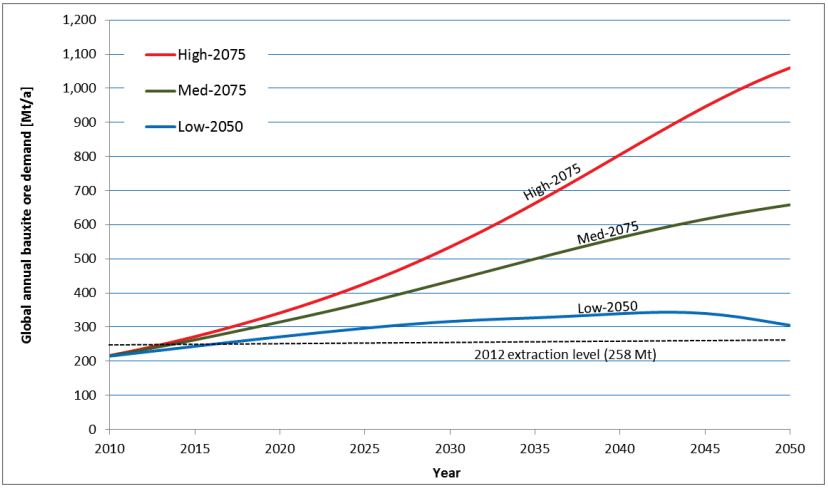

Source: self-elaboration based on data modeled by Liu et al. (2012)

The High-2075 scenario was selected because it represents a maximum range with a medium saturation time which seems more plausible than a fast stock growth. The Med-2075 scenario was chosen as it is in line with the industry middle-term publicly available projections which forecast that bauxite ore demand is expected to be close to 500 Mt/a by 2035 (Wasow and Thiris 2014). Moreover, such scenario is compatible with the projections of a tripling or quadrupling of aluminium demand by 2050 made by the IEA (IEA 2009) and Sinden et al. (2011). Of the available Low-saturation-level scenarios, the Low-2050 was chosen given its early saturation and because it represents the best possible option for minimizing pressures on land due to bauxite ore extraction. The High-2050 scenario was not selected because it appears unrealistic as the cumulative bauxite

ore extraction would reach 39,142 Mt of ore by 2050 while global reserves are currently estimated at 29,000 Mt.

Scenarios on global bauxite ore demand with inclusion of mitigation measures

In addition to the business-as-usual (or no-action) scenarios, Liu et al., (2012) modeled alternative scenarios which would result out of implementing four kinds of mitigation measures designed to reduce future GHG emissions. For this dissertation only the scenarios resulting from implementing measures to increase collection rates of product waste to a near-perfect level and improve manufacturing and semi-manufacturing yields are considered as they are the ones reducing the demand for primary production of aluminium and bauxite.

According to the model by Liu et al. (2012) current collection rates of product waste belonging to building and construction, automobiles and light trucks, aerospace and other transportation means (railway cars, marine vessels, motorcycles and bicycles) equal 88%, 88%, 83% and 83% respectively, while the collection rate of all other products considered (packaging cans and others, machinery and equipment, electrical cables and other devices, consumer durables and other uses) varies between 65% and 11%. The model by Liu et al. is quite optimistic and assumes that via aggressive implementation of mitigation measures (wedges), the collection rates of the both above-mentioned waste products would gradually reach 95% and 90% respectively in 2050 (these are called near-perfect collection rates, abbreviated as M1-NPC).

If such a measure was implemented simultaneously with a gradual increase in yield ratios in semi-manufacturing and manufacturing processes to reach 90% and 95% respectively by 2050 (a wedge abbreviated as M2-TYI), then the level of global bauxite ore demanded would gradually decline and would considerably reduce the bauxite ore demand levels for each of the three selected no-action scenarios. This would imply a diminishing extraction of bauxite ore and less pressure on land. In order to account for these potential measures, the three previously selected scenarios were complemented by adding their respective alternative by including the two mitigation measures (M1-NPC & M2-TYI).

As shown in Figure 38, all scenarios with both mitigation measures applied (scenario name with M1-NPC & M2-TYI) describe a substantially lower pathway in comparison to those business-as-usual.

Figure 38: Global annual bauxite ore demand with mitigation measures (dashed lines).

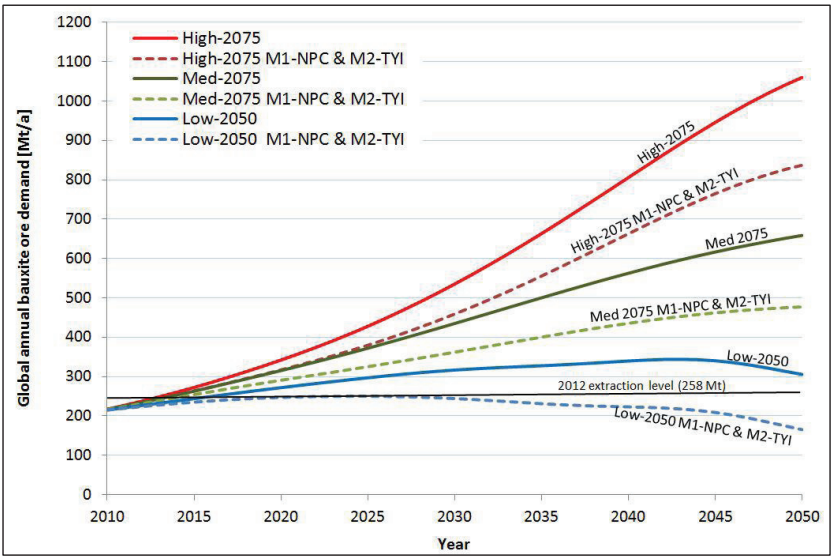

Source: self-elaboration based on data modeled by Liu et al. (2012)

Scenarios on global cumulative net area disturbed by bauxite ore extraction

These six scenarios of possible trajectories of global annual bauxite ore demand until 2050 (Figure 38) are multiplied with the weighted disturbance rate for bauxite mines. This determines the amount of hectares newly disturbed per year globally due to bauxite ore extraction. Then, these values of new hectares disturbed per year are cumulated over the modelling period (2010-2050) starting from the global status quo in 2011. The output is six scenarios showing different levels of an increasing global cumulative net area disturbed until 2050. Three scenarios

represent BAU conditions and three alternatives arising from the application of mitigation measures.

3.3.3 Copper

Copper remains to be considered a cornerstone and one of the most important strategic metals for mankind. Given the rapid industrialization in China in recent years, India following a similar path and other regions expected to follow in the medium term (e.g. South America), it can be reasonably expected that demand for copper will continue to stay strong and grow in the decades to come (Northey et al. 2014).

Few studies have developed models to explore long-term scenarios for global primary copper demand, and even fewer to explore copper supply. As claimed by Northey et al., global or regional models presenting scenarios have often been demand-focused (Ayres et al. 2003; Kapur 2005), with little attention given to copper mining supply constraints with the output extraction rates by 2050 very high and unlikely considering the current reserve base. More recently, Sverdrup et al. (2014b) have published a stock-driven model based on system dynamics which provides a one-scenario forecast of how the global copper production might behave. Nonetheless, such authors did not include in the model saturation levels or saturation times, neither at global nor at regional (e.g. developing and developed countries) levels.

A recent publication by Northey et al. (2014) depicts a supply-focused model which takes the resource base into account by defining the ultimate recoverable copper resource (URR)[39] from mineral deposits (estimated at 2,096 Mt Cu) and models the future copper demand using the model GeRS-DeMo which forecasts static and dynamic supply and demand levels for individual countries and deposit types. The supply side of the model works by determining when to put idealized mines online (until the URR of a country is exhausted) and the demand side is determined by the per capita demand times the population projections. The main

[39] Defined as an estimate of the total copper that society will globally recover from mineral deposits, both historically and into the future. In other words, it is an estimate of the cumulative mined Cu production for each country or major region of the world until 2100.

advantage of this model is that modelling results accurately reproduce historical production trends (peaks and troughs) for each country. Given that the data on reserves and future production is modeled at a country and deposit-specific level, the model was deemed more adequate for middle-term projections (up until 2050) than Svedrup et al´s.

A limitation of the Northey et al. (2014) model is that it does not explicitly determine a copper recovery from secondary resources; however, the model assumes the maintenance of the current recycling rate for copper (EOL-RR >50%) (UNEP 2011b) and of the current share of recycled copper (new and old scrap) which accounts for nearly one third of global demand (Glöser et al. 2013). According to the output of the model in Figure 39 global copper production from primary mining will increase over the decades and is expected to peak by 2030 or 2033.

Figure 39: Global Cu production modeled by GeRS-DeMo in dynamic demand mode.

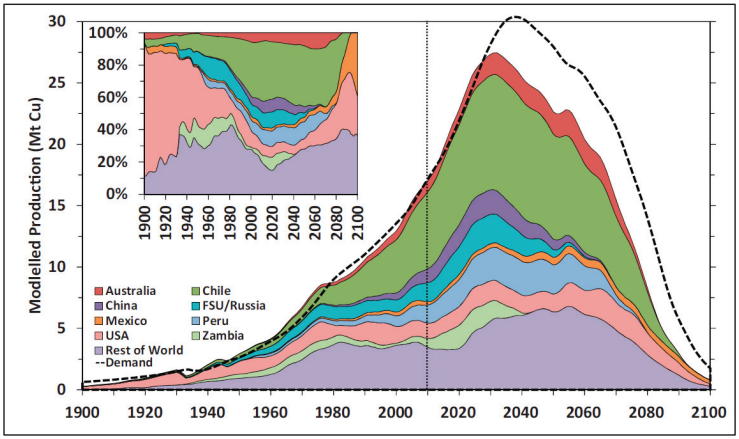

Source: Northey et al. (2014)

After the peak, it is expected a falling off gradually until 2100 as reserves get exhausted and recycling flows gain in importance. The dynamics of the modeled

copper production are simultaneously followed by a general historical trend of an ore grade decline over time as observed below in Figure 40.

Figure 40: Actual historical and projected Cu ore grade for selected countries.

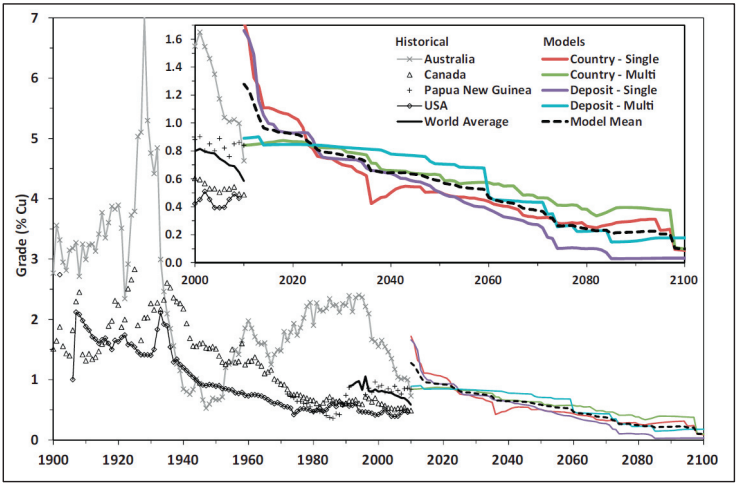

Source: Northey et al. (2014)

As copper ore grades decline further, more ore is required to be extracted and beneficiated to obtain the same amount of copper content. Thus, mines will tend to be more surface, water and emissions-intensive (in absolute terms) creating additional social and environmental impacts. According to Northey et al., these socio-environmental pressures coupled with potential increases in production costs associated with rising oil prices may present continued barriers to the primary mining business, providing further argumentation as to why a peak mined copper is expected in the decades to come.

Construction of a BAU scenario and a scenario corridor

In order to construct the BAU scenario, the modeled data on copper mine production until 2050 was obtained from Stephen Northey by personal communication. The delivered data (on Cu content produced) sourced from the dynamic mode of the model was used to construct the BAU scenario projecting

future global copper production until 2050. For the BAU scenario on future copper ore production, the data was transformed to copper ore using the modeled annual mean ore grade, adjusting to account for an ore milling copper recovery rate of 85% as advised in the publication by Northey et al. (2014).

A scenario corridor (two projections covering an uncertainty range around a main scenario) was created to cater for uncertainties in the behavior of the BAU scenario assuming a ±30% of deviation, a deviation percentage similar to that used by other authors for sensitivity analysis (e.g. Pauliuk et al. 2013). In order to cover the alternative of a potential increase in the global resources base, in metal prices or a decrease in production costs (lowering the cut-off grade), the upper limit, projection number 1, is included (BAU +30%). It assumes that the BAU scenario provides annual copper production levels lower than actual production; consequently, the projection is created by applying a moving adjusting factor to the BAU scenario over the 41 years of the modeled period (2010-2050). The adjusting factor equals a +0.73% in the first year and then it increases gradually over the years to a reach a +30% in the last year. On the other hand, the lower projection number 2 (BAU -30%) is created. It caters for increases in material efficiency (e.g. increasing scrap) reducing the quantity of copper mined. This projection is generated in a similar way to the projection number 1 but progressively reducing the annual copper mined. Both projections are set to progressively escalate the uncertainty as decades go by; this is based on the assumption that in scenario construction uncertainty grows into the future.

The BAU scenario depicted below in Figure 41 forecasts an increase in copper mining rates until the curve reaches a peak mined copper by 2032 (at a mining rate of 27 Mt/a) with a subsequent decline in mine production to reach a level of 22 Mt/a by 2050. The upper and lower projections around the BAU cover for the uncertainty range of ±30%, achieving mining rates of 31.5 Mt/a and 23.1 Mt/a by the 2030 and between 29.4 Mt/a and 15.8 Mt/a by 2050. Both projections of the uncertainty range follow a similar trajectory to the BAU with a gradual growth in copper primary production until 2030, peaking around the year 2032 and the falling off gradually.

Figure 41: Global annual Cu mine production. BAU scenario and corridor. 2010-2050.

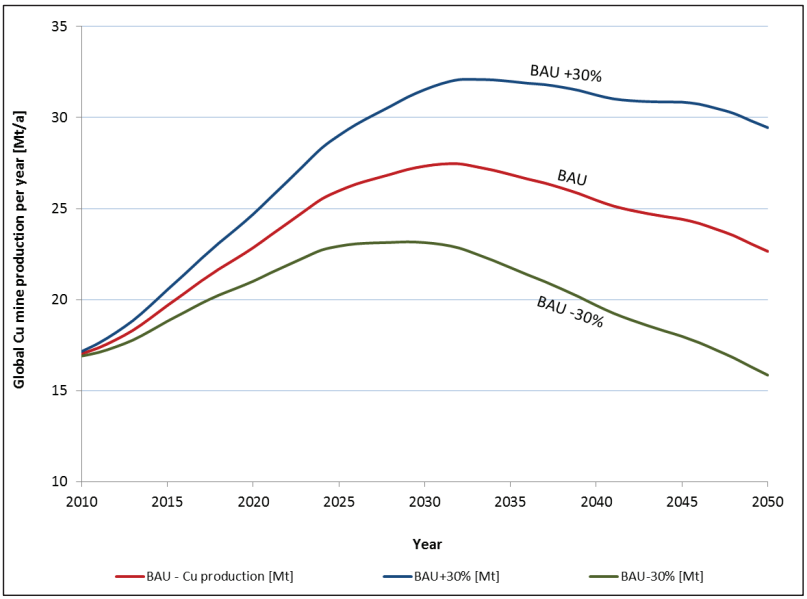

Source: self-elaboration based on Northey et al. (2014)

The lower projection (BAU -30%) caters for a steep fall in the mine extraction of copper reaching a level of 15.8 Mt/a by 2050; this can only happen if larger shares of scrap became available to cover a bigger share of the global copper supply by 2050. Even though global yearly mining rates of primary copper are forecast to decline as shown in Figure 41, such trends are coupled with the fact that they will be possible only by the exploitation of declining ore grades, namely, low ore grades averaging less than 1% copper content, achieving a modeled mean ore grade of 0.59% by 2050.

Henceforth, the lower ore grades will trigger an increase in the amount of ore processed which will inexorably drive the amount of ore extracted up until 2036 and then slowly downwards as observed in the BAU scenario shown in Figure 42.

Only if material efficiency measures were successfully implemented and recycling was enough to cater for a larger share of the global copper supply would the ore extraction be reduced according to the BAU -30% projection in Figure 42. Otherwise, if ore grades continued to decline even more, the annual amounts of ore extracted may behave in between the BAU and the upper limit set by the BAU +30%.

Figure 42: Global annual Cu ore mine extraction. 2010-2050.

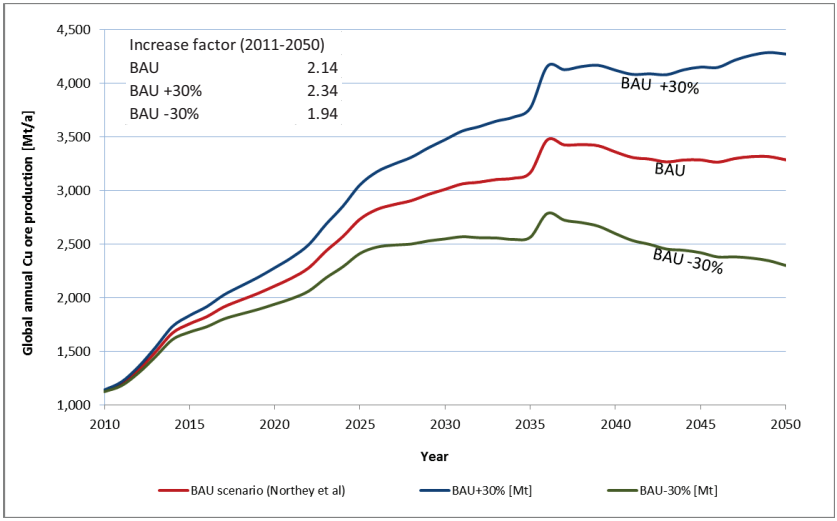

Source: self-elaboration based on Northey et al., (2014)

The BAU scenario (Figure 42) shows a pronounced growth in global annual copper ore extraction until 2036 and then gradually declines and levels off by 2040 as ore grades reach very low levels and do not decline so quickly. The BAU +30% projection shows a similar growing trajectory until 2036 but it does not peak by then; it stabilizes but resumes growth to reach a mining rate of 4,271 Mt ore/a by 2050. In contrast, the BAU -30% projection shows a peak by the year 2036 and then falls off to reach a mining rate of 2,300 Mt ore/a by 2050.

Scenario corridor on global cumulative net area disturbed by copper mining

Using the scenario corridor with possible pathways of future world mine extraction of copper ore (Figure 42), a BAU scenario and an uncertainty range was created showing possible pathways of evolution for the global cumulative net area disturbed by copper mining. This was done multiplying the amount of global annual copper ore extracted with the weighted disturbance rate which yielded the annual amount of new hectares disturbed by copper mining globally. Departing from the global status quo in 2011, such quantity of new hectares disturbed was added cumulatively during the period 2011-2050. This resulted in a BAU scenario and an uncertainty range for the global cumulative net area disturbed by copper mining until 2050.

3.3.4 Gold

Similar to other metals, the world mine production of gold has been framed by a general historical trend of declining (average) ore grades of gold-bearing ores (Figure 43). High grade deposits like those placer deposits mined in the past at the Witwatersrand basin in South Africa (2 to 10 g Au/t) or in Berelekh in Russia (12 g Au/t) (Frimmel 2008) are becoming rare to be found. Nowadays, the discovery of Tier 1 and 2[40] deposits are very unusual events (MinEx Consulting Pty Ltd 2011). Global average gold ore grades have fallen from over 2 g Au/t in the 1960s to the 1980s (MinEx Consulting Pty Ltd 2011) to average values between 1.8 and 1 g Au/t at presently gold producing mines (Visual Capitalist and Nature Resource Holdings 2013). This is due to a range of factors, including changes in gold prices and mining practices that make it economic to mine gold from low grade ores.

In the future, it is expected that the ore grade will keep on falling; whereas the average grade of undeveloped deposits was around 2.08 g Au/t in 1979 (MinEx Consulting Pty Ltd 2011), it is currently estimated at 0.89 g Au/t (Visual Capitalist and Nature Resource Holdings 2013).

[40] Tier 1 deposits are world-class mines (large, long-life, and low cost). Tier 2 deposits are not quite as large or long life or profitable as Tier 1 but are economically attractive.

Figure 43: Gold ore grades over time for selected countries. 1830-2005.

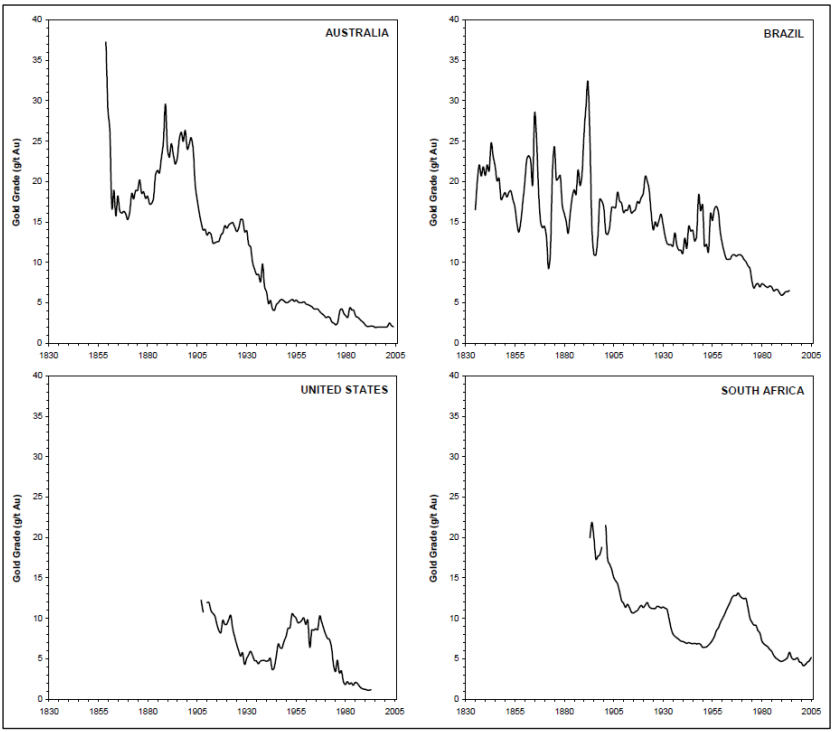

Source: Mudd (2007a)

Modeled projections on future gold extraction

Forecasts of world gold primary supply and demand are rarely found in the academic or business-related literature in longer terms than five years ahead given that, unlike base metals, the gold market trades gold in physical and paper form (certificates, account statements, forward contracts, etc.) and gold plays a significant role as a financial investment, making projections of future demand or extraction more complex than for other commodities chiefly used for the industry.

Some of the few existing studies assessing potential future supply of primary gold have used static methods like extrapolation of historical production curves (Menzie et al. 2013) or burn-off rates (or burn-off time, defined as the known reserves

divided by the present production) (Shafiee and Topal 2010). However, they have only provided short-term projections or simple depletion times. Out of the literature review only the model by Sverdrup et al. (2012) provides a long-term simulation into the past and of the future primary and secondary gold supply (until 2050 and beyond); the model is not expected to reproduce short-term variations but to capture the overall long-term trends which makes it suitable for the creation of explorative scenarios or scenario corridors depicting broad trends. Nevertheless, it must be underlined that the modelling results by Sverdrup and colleagues reflect a possible future development but heavily rely on the modelling assumptions. Consequently, the one scenario developed in the model will be employed as the BAU but attention must be paid to stocks and flows dynamics underlying the model (for further details see Sverdrup et al. 2012).

The model by Sverdrup and colleagues is built using system dynamics, is based on mass balances and reproduces a systemic mapping of gold flows in the world gold trade system using historical data. It employs in-use stocks of gold being traded, stored in central banks, amounts locked in industrial processes, held on private hand and reserves (stocks) in the ground (high, low and ultra-low grade deposits) and in mining processing plants. In the model, the metal from mines is moved to the market based on the gold price and world population numbers; metal is mobilized from public holding depending on the gold price whereas the latter depends on the gold amount physically present in the market (Sverdrup et al. 2012).

If simulation results from the model are inspected for the period 1950-2050 (Figure 44), it can be observed that the model reproduces fairly well the past real world mine production of gold, with a small deviation around 2010 and some years beyond. The model predicts a peak in the world mine production of gold around the year 2010 and an irregular falling off afterwards with ups (peaks) and downs (troughs) until the year 2032 when the production is expected to continuously fall off, reaching a level of 1 kt/a in the year 2050.

Figure 44: Simulated and real world annual gold mine production. 1950-2050.

Source: self-elaboration based on data by Sverdrup et al. (pers. comm.) and Kelly and Matos (2013)

With regards to the ore grades, the model forecasts that presently producing mines (exploiting high grade reserves) (almost) run empty after 2030 (Figure 45). Then gold must come to a larger degree from low-grade reserves as the modeled price is not sufficiently high for mining of ultra-low reserves (Sverdrup et al. 2012).

Figure 45: Simulated remaining world gold-bearing reserves.

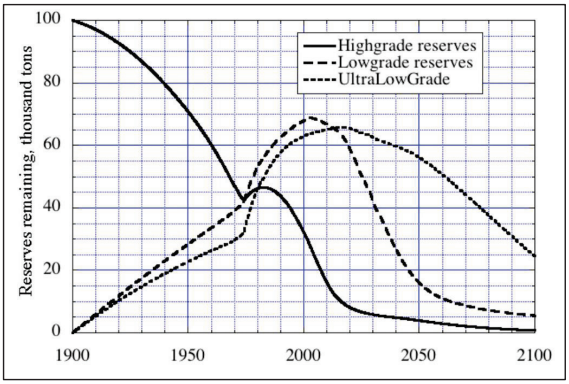

Source: Sverdrup et al. (2012)

The model assumes a total in-use stock of 147,000 tons of gold retained in the anthroposphere as a product of mankind´s extraction from the litosphere during the last 7,000 years and an estimated amount of 13,000 tons which have been lost due to dissipative uses and are therefore not included.

With regards to reserves in the litosphere, the model is based on the reserve base from the USGS for 2008 (90,000 tons) (USGS 2008b) but adds potential hidden reserves. It assumes known and hidden reserves (in 2010) of 170,000 tons. These comprise 40,000 tons of gold in high grade ores (includes 10,000 tons in ore bodies not yet discovered), 70,000 tons of low-grade ores (20,000 tons estimated as available and 50,000 low-grade reserves as hidden reserves to be found by prospecting) and 60,000 tons in ultra-low grade reserves (10,000 tons known and 50,000 tons hidden to be discovered by geological prospecting). An assumption underlying the model is that, for gold, “there is no reason to expect any new substantial finds of unexploited resources” (Sverdrup et al. 2012:15).

The downward trend in the gold mine production is contrasted by an upward trend in the recycling of gold which is expected, according to the simulations in the model, to gradually increase and surpass the gold primary production by 2040. Although not specified in the model, jewelry is expected to play one of the biggest roles as a source of recycled gold as it accounts for half of the gold above ground, followed by private investment (18.7%) and official holdings (17.2%) (World Gold Council 2011). Jewelry also explains around a 43% of the world gold demand (largely driven by India and China as the main consuming countries) (PriceWaterhouseCooper 2013).

Construction of BAU scenario and limits for the scenario corridor

Based on the dynamic simulation of the future world mine production of gold shown in Figure 44, a BAU scenario is constructed using the modeled data for mine production of gold (Au content) in the period 2010-2050. Given the lack of alternative scenarios in the paper by Sverdrup et al. (2012), a scenario corridor is constructed using the BAU as the basis and by adding an upper (No 1) and a lower (No 2) projection which cover for deviations from the BAU scenario. Both projections increase over time and are set to progressively escalate the

uncertainty as decades go by; this is based on the assumption that in scenario construction uncertainty grows into the future.

The projection No 1 (BAU +30%) considers that the model has systematically predicted a production smaller than the actual and thus the curve depicts an annual production larger than the BAU scenario for all years (Figure 46). It is constructed assuming an increasing uncertainty which reaches an additional 30% in the production by the last year of the period considered (2010-2050); the uncertainty is smallest in the first year of the period (2010, starting at +0.73% resulting from dividing 30 in 41 years), then it grows in the subsequent years to reach the 30% difference with the BAU scenario in the last year (2050).

The projection No 2 (BAU –30%) represents the lower curve of the uncertainty range with gold production smaller all over the years in comparison to the BAU scenario. It is constructed in a similar way to the projection No 1; it progressively reduces the forecasted production reaching a -30% less in the gold annual production by the last year of the period (2050). The actual gold production may move in the uncertainty range as the share of recycling is increased more quickly or more slowly than predicted or according to changes in the gold market prices which to some extent determine the gold mining activities.

The BAU scenario and the upper and lower projections (Figure 46) depict a predicted general overall fall in the annual world mine production of gold with some short-term peaks at the years 2018, 2023, 2030 and 2033. From the year 2035 it is expected that the mine production will keep on steadily falling and reach a mining rate between 1.3 kt/a (BAU +30%) and 0.7 kt/a (BAU -30%).

The BAU scenario and its upper and lower projections on future world mine production of gold (Au content, in metric tons) need to be converted to world production of gold-bearing ore (in Mt) in order to be able to create a BAU scenario and a range of global cumulative area disturbances. An average ore grade for the world mine production is required. Given the trend of historically declining ore grades, it is assumed that the global average ore grade for currently producing

mines (set at 1.8 g Au/t[41]) is expected to gradually decrease until 2030 when the model predicts that most high-grade reserves will be exhausted.

Figure 46: Modeled global annual gold mine production. BAU scenario and corridor.

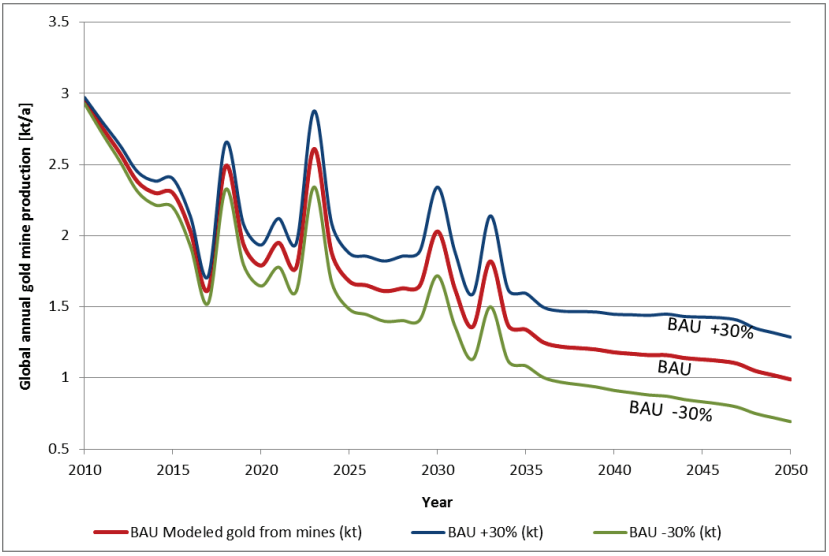

Source: self-elaboration based on data by Sverdrup (pers. comm.)

Accordingly, by 2030 the average ore grade is estimated to be at 0.7 g Au/t and may keep on decreasing to reach a 0.5 g Au/t by 2050 (combining remaining low grade and ultra-low grade reserves)[42]. Based on these estimations, a BAU

[41] This value originates from averaging three different sources with estimates on the average ore grade of currently producing gold mines (open pit and underground): 1.18 g Au/t (Visual Capitalist and Nature Resource Holdings 2013), 1.4 g Au/t (Mudd et al. 2012), and 2.8 gpt (average grade Au in ore production of 2012 and 2013 in the SNL Metals & Mining database).

[42] These numbers are estimations based on the best available knowledge and the curves for remaining gold reserves in Figure 45. They result from annually reducing the average global gold ore grade by a 5% until 2030 and from 2030 annually reducing it by a 1.5% until 2050.

scenario and its uncertainty range on future world mine gold ore extraction are constructed.

Given the trend of a declining average (global) gold ore grade, the amount of gold ore extracted tends to increase (with peaks) along the years (Figure 47). This appears logical as more ore needs to be extracted and milled to produce a similar amount of net metal content. According to the BAU scenario (Figure 47), by 2050 the average amount of ore required to produce 1 kt of Au (metal content) from mines is estimated to be around 1,900 Mt ore with an average ore grade expected at 0.5 g Au/t ore.

Figure 47: Global Au ore extraction and ore grade. BAU scenario and corridor. 2010-2050.

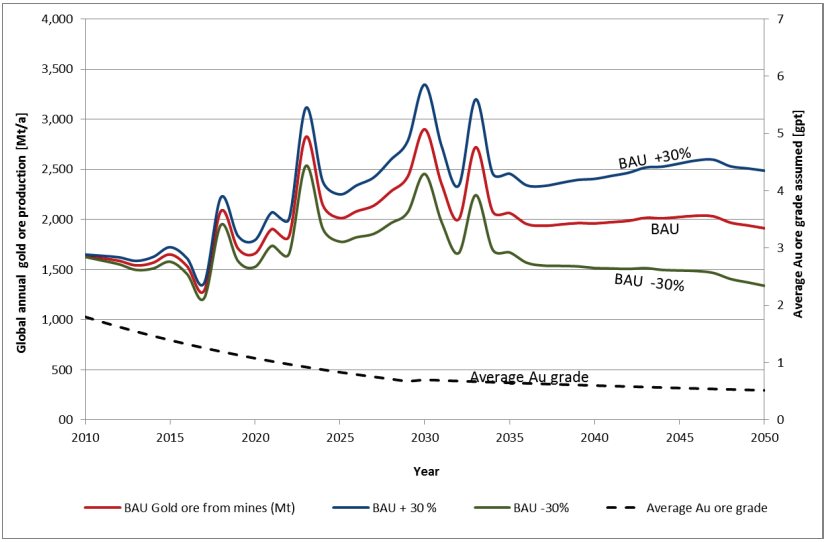

Source: self-elaboration based on data by Sverdrup (pers. comm.)

For the BAU scenario in Figure 47 the absolute amount of ore extracted is expected to upsurge by a factor of 1.2 by the end of the period 2010-2050; for the upper and lower projections the factors are 1.5 (BAU +30%) and 0.8 (BAU -30%) by 2050.

Projections on global cumulative net area disturbed by gold mining

The resulting three projections on future global annual gold ore extraction until 2050 (Figure 47) are used as the basis for constructing a BAU scenario and an uncertainty range on global cumulative net area disturbances by gold mining until 2050. First, the modeled amount of global annual gold ore extraction is multiplied with the weighted disturbance rate. This yields the global amount of newly disturbed hectares per year by gold mining. Departing from the global status quo in 2011, such newly disturbed hectares area cumulatively added to create a BAU scenario and its uncertainty range of how the global cumulative net area disturbed by gold mining might evolve until 2050.

3.3.5 Silver

Around 60% of the silver extracted comes from copper, zinc and lead mining, being the two latter the carrier metals and main fractions from which silver is co-produced. Gold is another important carrier metal from which silver is co-produced; deposits with silver as the only constituent are extremely rare.

Figure 48: Australia. Average lead, zinc and silver ore grades. 1880-2000.

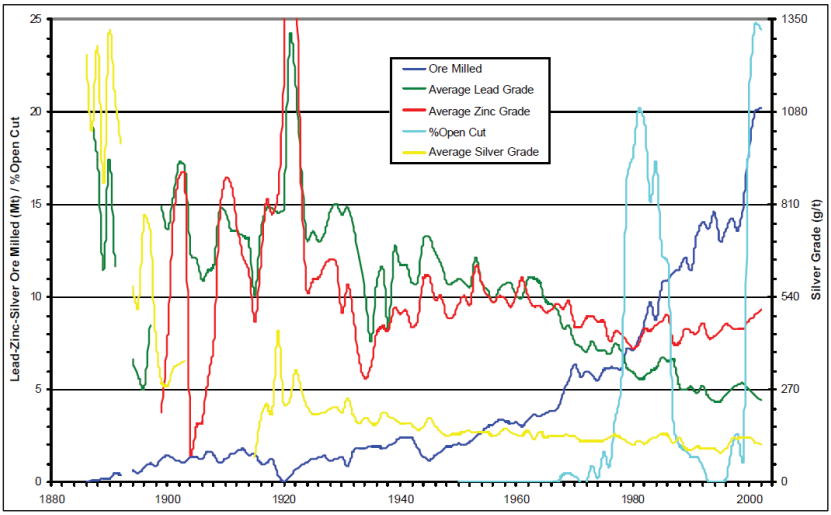

Source: Mudd (2004b)

The ore grades of copper, zinc and lead have been steadily declining for the last 100 years and seem now to be levelling off at very low content (Sverdrup et al. 2014a). Following this trend, the evolution of silver ore grades also shows a decline over time, as exemplified for instance by the Australian case (Figure 48).

Modeled projections on future silver extraction

Similar to prospects on future world gold supply, forecasts or scenarios of future silver extraction at a global scale are scarce to find, with the exception of very short-term forecasts made by the industry (e.g. GFMS 2012; Krebs 2013).

During the literature review, only the model by Sverdrup et al. (2014a) based on system dynamics of silver stocks and flows, makes long-term projections of how the world mine production of silver might evolve. The model is based on a systematic mapping of world silver material fluxes, including all sources of supply and demand in the global market. The silver metal demand in the model is driven by population growth and silver use per person in society which was related to global GDP change over time. Demand is affected by market price which in turn depends on how much silver is available in the market.

With regards to the primary mining of silver, the reserves in the geosphere are divided into known and hidden ones and are stratified according to four levels of ore quality: extra high quality (10,000 – 6,000 g Ag/t), high grade (1,100-800 g Ag/t), low grade (100-80 g Ag/t), and ultra-low grade (below 10-8 g Ag/t). Reserves include silver extracted from silver, copper, zinc, and lead couple production mines.

According to the simulated model results world silver mine production per year has been steadily increasing (though with fluctuations) and is expected to peak around 2030. It is then anticipated to fall off (also with fluctuations) until passing the year 2040 when production is predicted to continuously fall to annual production levels lower in 2100 than in 1950. After 2100 most silver supply to society is expected to come from recycling and urban mining.

Figure 49: Simulated and real global annual mine production of silver. 1950-2100.

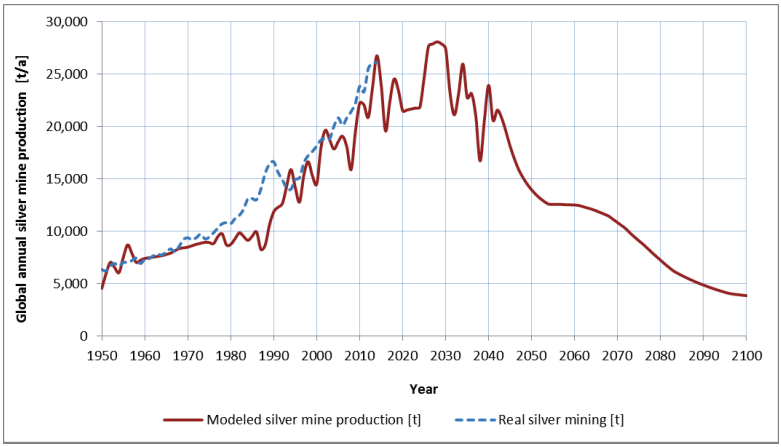

Source: self-elaboration based on data modeled by Sverdrup (pers. communication) and Kelly and Matos (2013)

The expected downward production after 2030 is explained mainly because low grade reserves start to decline rapidly along with ultra-low grade ones (Figure 50).

Figure 50: Simulated remaining world silver-bearing reserves. 1840-2340.

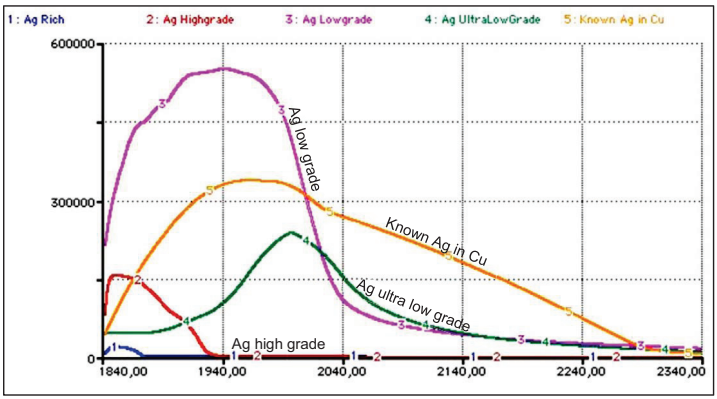

Source: Sverdrup et al. (2014a)

According to the predictions by the model, after 2040, most of the silver input to the market is expected to come from recycling (Figure 51).

Figure 51: Modeled shares of world primary and secondary silver production. 1840-2340.

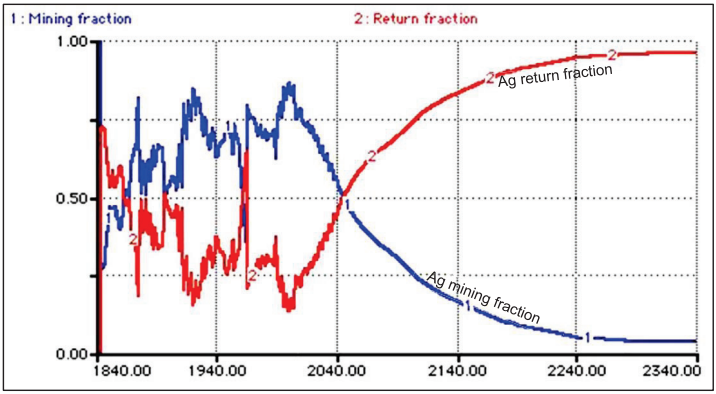

Source: Sverdrup et al. (2014a)

Construction of BAU scenario and its uncertainty range (period 2010-2050)

The modeled world silver mine production for the period 2010-2050 (Figure 52) is used as the BAU scenario; it represents the results of the model according to Sverdrup et al. best´s understanding of how the silver market and the supply from mines may behave over time. The global annual silver mine production is expected to fluctuate along the years (Figure 52) and only start steadily falling from 2040 as recycling surpasses primary production.

Careful consideration must be given to the modelling results by Sverdrup and colleagues as they reflect a possible future development but heavily rely on the modelling assumptions, e.g. assumptions of in-use and on-the-ground stocks. Were these to significantly deviate during the years, future developments may also considerably differ. In order to cater for these uncertainties, a scenario corridor with an uncertainty range is constructed.

Figure 52: Evolution of world modeled silver mined and Ag ore grade. 2010-2050.

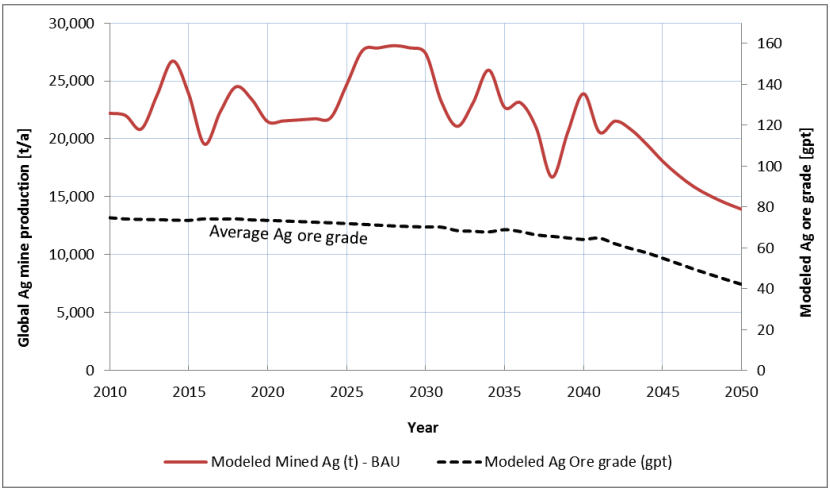

Source: self-elaboration based on data by Sverdrup et al. (pers. comm.)

Sverdrup et al. (2014a) did not publish a sensitivity analysis or alternative scenarios increasing supply from recycling or different price ranges. Therefore, two additional projections are created using the BAU as the basis to cater for uncertainties or unexpected changes in the silver production according to changes in the levels of on-the-ground stocks, silver market prices, increases in material efficiency leading to a higher or lower recycling levels or other factors.

The first and upper projection No 1 (BAU +30%) (Figure 53) implies that the annual silver mine production for the period 2010-2050 has been under represented; it caters for an increasing uncertainty over time. Accordingly, an annual moving adjusting factor is applied to each value of the BAU scenario over the 41 years of the period. The adjusting factor equals a +0.73% in the first year and then it increases gradually over the years to reach a +15% in 2030 and a +30% in the last year. Likewise, the lower projection No 2 (BAU -30%) is created

in a similar way (using the same adjusting factor) but reducing (instead of increasing) the world silver mine production in the same period of years.

These potential deviations from the BAU scenario are considered possible given that silver is mostly used for industrial purposes which could considerably improve their material efficiency performances, requiring less silver for the same products (e.g. by substitution). On the other hand, recycling of silver might considerably improve its share in the global market input.

The BAU scenario and the upper and lower projections (Figure 53) all depict a predicted general fall in the annual world mine production of silver from 2040 onwards; yet, from 2010 until then there are oscillations with peaks at the years 2014, 2018, 2029, 2034, and 2040.

Figure 53: Global annual silver mine production. BAU scenario and corridor. 2010-2050.

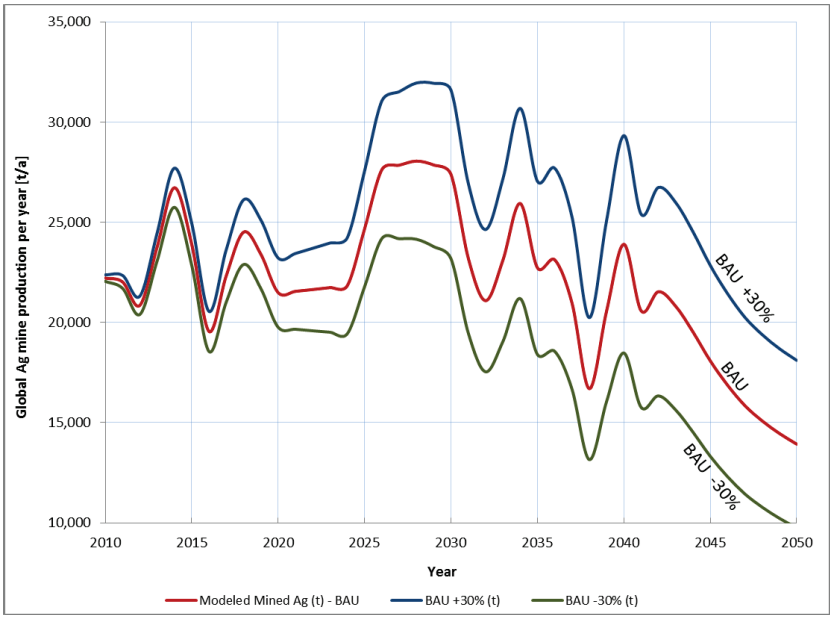

Source: self-elaboration based on data by Sverdrup et al. (pers. comm.)

The modelled BAU scenario and its uncertainty range of future world silver mine production require conversion to an equivalent scenario corridor of future silver ore mine production. The conversion is performed using the modeled average silver ore grade from Sverdrup et al. (2014a) which combines ore grades from known and hidden reserves and from the different (polymetallic) sources of silver.

The results for the BAU scenario and the uncertainty range for silver ore mining (Figure 54) show large fluctuations over the years as the overall amount of mining fluctuates while the average ore grade declines (Figure 52). Although ore extraction is considerably reduced by the year 2038 (due to the decrease in silver production shown in Figure 53 and due to an increasing recycling) it then increases considerably and achieves levels higher than 2010 by 2050 due to steeper decline in the modeled average ore grade (modeled grades change from 74 gpt in 2010 to 42 gpt by 2050) (Figure 52).

Figure 54: Global annual silver ore mined. BAU scenario and corridor. 2010-2050.

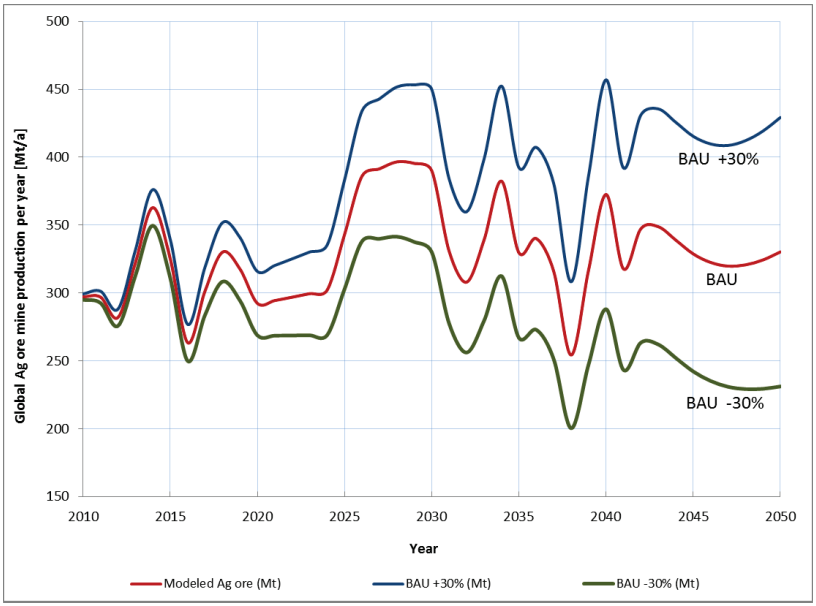

Source: self-elaboration based on data by Sverdrup et al. (pers. comm.)

Scenario corridor on global cumulative net area disturbed by silver mining

Using the scenario corridor showing possible pathways of the future world mine production of silver ore (Figure 54), projections on possible developments of the global cumulative net area disturbed by silver mining were created. This was done by multiplying the global annual amount of silver ore mined with the weighted disturbance rate calculated from the sample of silver mines. This yields the annual global amount of newly disturbed hectares due to silver mining. Departing from the global status quo in 2011, such amount is cumulatively added resulting in a BAU scenario and an uncertainty range of the global cumulative net area disturbed by silver mining until 2050.

3.4 Assessing mining pressures on biodiversity: method and dataset

The method consisted in overlaying the location of mines and geological deposits listed in the SNL Metals & Mining database with the plant diversity zones in the global map by Barthlott et al. (2007). In such map species numbers are calculated for a standard unit area of 10,000 km^2 using the equation for the species-area relationship introduced by Arrhenius (1921). The standardized richness estimates are delineated into ten Diversity Zones distinguished by different colours (Figure 21). The species numbers calculated cover a spectrum of less than 100 species up to approximately 17,000 species per 10,000 km^2. Only five global endemism-rich centers of mega-diversity host more than 5,000 species per 10,000 km^2 and are represented by the diversity zone number 10; these centers are: Costa Rica-Chocó, Atlantic Brazil, Tropical Eastern Andes, Northern Borneo, and New Guinea. Since species numbers refer to political rather than natural units, the diversity zones and the isotaxas (lines which encompass equal numbers of taxa) which represent their boundaries were adjusted using an overlay from climatic and vegetation maps (Barthlott et al. 1996). Mountain regions, elements which increase geodiversity (abiotic factors like climate, orogeny, geology), have a special status as a rapid succession of diversity zones and were influential in the delineation of the global centers of biodiversity, all of which are located in

mountainous regions within the humid tropics where suitable climatic conditions and high levels of geodiversity coincide (Kier et al. 2009).

The overlay of the point location of mines and deposits over the plant diversity map was done to test the null hypothesis asserting that the spatial occurrence of industrial metal mines and deposits in the world´s land terrestrial surface (excluding Antarctica) is random. In other words, the null hypothesis asserts that the frequency distribution of the observed data (across diversity zones) equals the frequency distribution of a null or random model (representing a random spatial distribution of mines and deposits across diversity zones):

> H_o hypothesis = the frequency distribution between the observed data (mines and deposits) and the expected one (null model) are equal (implies randomness)
>
> H_1 hypothesis = the frequency distribution between the observed and the expected data are not equal (are different; this implies the spatial distribution is not random)

The null hypothesis was tested by comparing the frequency distribution of mines and deposits per diversity zone against the frequency distribution of the null model. The latter was constructed by the proportion (percentage) of the global terrestrial surface area (excluding Antarctica) occupied by each DZ. Such share of each DZ in the world terrestrial area was calculated using QGis software (QGIS Development Team 2012); results are expressed in km^2 and percentages.

The observed frequency distribution of mines and deposits per DZ was computed by determining only one point location per observation and counting the number of entries per DZ using the QGis Vector Analysis tool (QGIS Development Team 2012). It is expressed in absolute numbers and in percentages. No differentiation between open pit and underground mines was done for mines or deposits, all records were included. Deposits were not straightforward to use and required some data preparation (for details on how data was prepared see Section 8.6.1 in the Appendix); the final dataset summary for mines and deposits used per mineral

can be appreciated in the Table 11 below. The final dataset employed comprised 2,860 mines and 2,055 deposits.

Table 11: Summary of the final dataset used for the biodiversity analysis.

Metal	Total amount of entries in SNL Metals & Mining	Active, Non active, Status not available	Number of entries with coordinates not available	Final dataset MINES	Final dataset DEPOSITS	Observation on data preparation
Al	186	6	63	90	27	Coordinates were found for 11 deposits
Fe	1,104	20	261	479	322	22 records were deleted to avoid double accounting
Cu	1,186	18	187	539	384	58 records were deleted to avoid double accounting
Au	3,614	82	649	1,614	1,223	46 records were deleted to avoid double accounting
Ag	314	6	67	138	99	4 records were deleted to avoid double accounting

Source: SNL Metals & Mining database, Mines & Projects entry (update April 2014).

The null hypothesis was tested visually via bar charts and statistically by means of a Pearson´s chi square goodness-of-fit test (using significance levels of .05 and .01) and a Fisher´s exact test of independence by means of a Monte Carlo simulation (10,000 iterations) using the statistics package SAS® version 9.1.3 (SAS Institute Inc. 2005). The analysis of the distribution of mines and deposits per DZ was conducted by classifying Barthlott et al. (2007)´s diversity zones for operational purposes into three categories: low, intermediate and high diversity (DZs 1-3, 4-6, and 7-10 respectively). Special attention was given in the analysis to the DZ 10, the mega-diversity zone (red color).

Based on the results of the graphical and the statistical test, the possibility of proposing a shift of future new mines from areas of high biodiversity towards areas of lower one was also analyzed.

CHAPTER FOUR

This results chapter first addresses the specific land requirements calculations by summarizing the final samples used per metal, results of the nonlinear regression analysis, and presents the computed weighted disturbance rates per metal. Subsequently the global status quo per metal and for all five metals is presented. The following section presents the scenarios (iron and bauxite) and scenario corridors (copper, gold and silver) with the possible future pathways of the global cumulative net area disturbed by the mining of each metal until 2050. The final section presents the results of the comparison of the frequency distribution of mines and deposits per biodiversity zone for each of the metals with the frequency distribution by the null model.

4 Results

4.1 Specific land requirements per metal

4.1.1 Sample sizes

The final sample size employed for quantifying specific land requirements comprised 106 mines. If classified per mining method, the sample is led by open pit mines (share of 80%, Table 12).

Table 12: Number of mines for specific land requirement calculations.

Metal	Number of mines per mining method		Sample size total
	OP	UG	OP+UG
Fe	27	0	27
Al	13	0	13
Cu	13	6	19
Au	29	15	44
Ag	3	0	3
Total	85	21	106

Of the 106 mines, 62 were monometallic and 44 polymetallic (applies only to copper, gold and silver mines). Once polymetallic mines were allocated, the number of observations increased to 165 (increased by 59 observations, 9 observations in Cu, 19 in gold, and 31 in silver). The Table 13 below shows the details per metal and mining method. Again, the sample size is inclined towards OP mines reflecting the trend in the metal mining industry.

Table 13: Number of observations for specific land requirement calculations per metal.

Metal	NCP or CP	Number of (allocated) observations employed for land requirements		Total number of observations
		OP	UG	OP+UG
Fe	NCP	27	0	27
Al	NCP	13	0	13
Cu	CP	17	11	28
Au	NCP+CP	44	19	63
Ag	CP	22	12	34
Total	NCP+CP	123	42	165

The sample of iron ore producing mines was divided into two groups: direct shipping ore grade ones (DSO) and non-direct shipping ones (NDSO). In the first ore does not undergo a beneficiation process given that the grade is high enough to be directly shipped, after minor primary processing; however, NDSO mines require beneficiation before the final product is shipped. In some cases it occurred that mines were mining and processing ore with a high grade (average of 60% Fe) and were classified as NDSO since beneficiation activities were still taking place, examples of this are Capitão do Mato and Tamanduá mines in Brazil or Kudremukh mine in India, with a high average ore grade being currently mined but low in the reported resources and reserves.

In the case of the copper sample, all 28 mines sampled are polymetallic (21 have copper, six gold, and one silver as main metal produced). For gold, 22 mines are monometallic and 41 are polymetallic; in the latter, 20 mines have gold, 18 have copper, and three have silver as the main metal produced. For silver, all mines are

polymetallic and only three mines have silver as the main metal (17 have gold and 14 have copper assigned as main metal).

The global spatial distribution of all mines sampled is random with a certain bias in the case of iron ore towards a high number of mines (ten out of 27) in Australia[43] and a low number for instance in Brazil´s Iron Quadrangle, a rainy area for which obtaining cloud-free satellite images becomes difficult. The sample is limited in the case of silver-production given that no lead or zinc mines were sampled producing silver as a co-product.

The total number of Landsat satellite images used was 119 distributed as: 56 Landsat 5 (TM) images, 42 Landsat 7 (ETM+) and 21 Landsat 8 (OLI) images. The list of images per mine employed can be consulted in the Appendix, Section 8.3.1.

4.1.2 Model fitting by regression analysis

An examination of the scatterplots of the raw data (allocated) for each sample (Figure 55) reveals that, in general, there is a positive association between the predictor and response variable because the cumulative net area disturbed increases as the cumulative ore produced grows.

Scatterplots show that linear and non-linear regressions might provide a good model fit. The best model fit was decided for each metal based on the minimum sum of squared residuals after model fitting. Plots also suggest some points may be outliers with a high leverage and influence as they are located far away from the cloud of points; this is particularly striking for copper, gold and silver. This can be explained due to the inclusion of a few very large mines within the sample (e.g. Escondida-Zaldivar copper mine, Chuquicamata copper mine, Yanacocha gold mine).

[43] Australian mines represent a large part of the iron ore mines sample. The main reasons for that include: i) the availability of cloud-free Landsat images since much of the territory is arid; ii) the availability of public technical reports which allow for a clear delimitation of the mine and its facilities, plus the verification of the used extraction flows; iii) the fact that in many cases mines are located in remote areas, with no other adjacent land covers, making it easy to delimit the boundary of the mine from other land uses. The opposite reasons (many days of the year with rainfall and thus few cloud-free images available, mixed land cover types which make it impossible to clearly establish the limit between a mine and other mines or kinds of land covers and lack of technical data on the mine) made it very hard to use mines located, e.g. in Brazil´s Iron Quadrangle.

Figure 55: Five metals. Scatterplots of raw data.

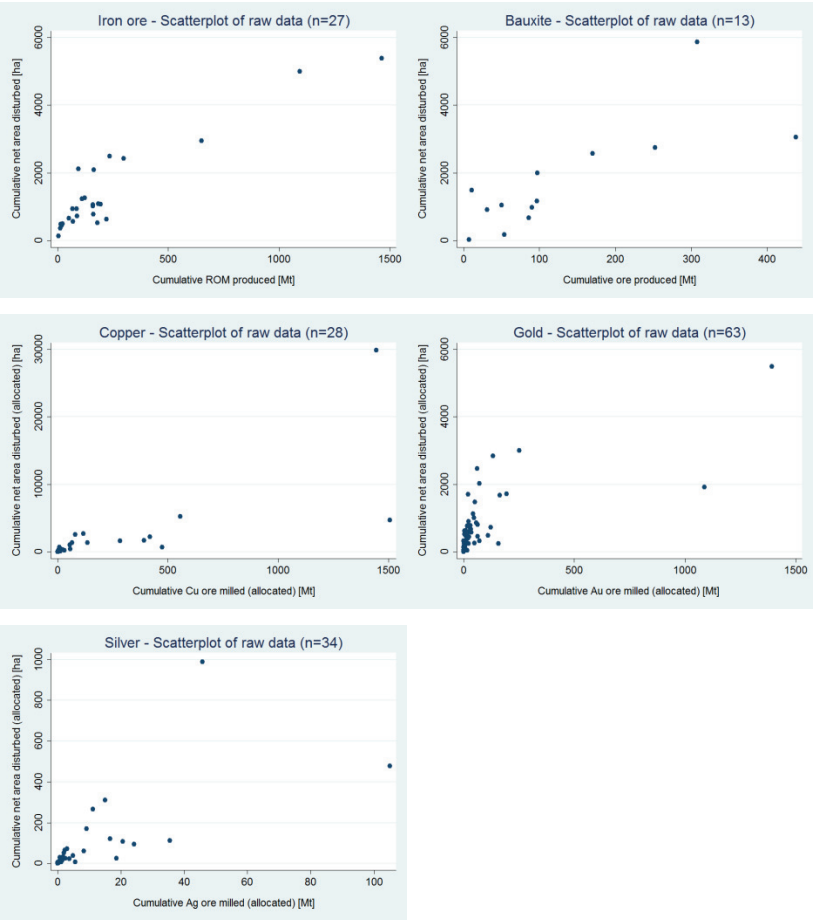

The existence of a reduced number of giant mines explains the right skewed distribution of the world´s metal mining sector consisting of multiple small and medium-sized mines and only a few very big deposits and mines. This pattern is reproduced by the random sampling procedure and can be viewed in the histograms (Figure 56) belonging to all mines sampled.

Figure 56: Five metals. Histograms of (allocated) primary data (n=165).

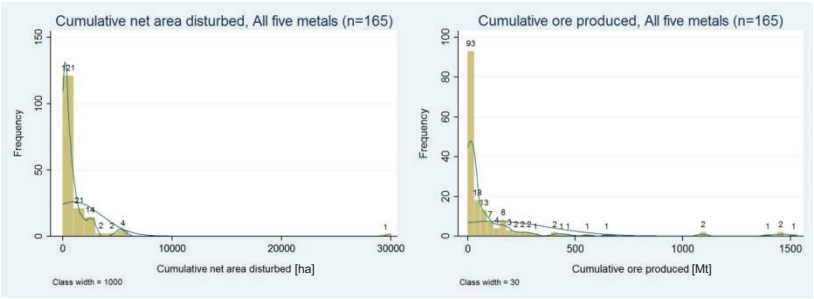

4.1.2.1 Specific land requirements - Iron

Fitting the model

In order to determine the best fit, an ordinary least square linear and non-linear fit was run as a regression. The minimum sum of squared residuals was found for the non-linear (5877401.07) against the linear regression (6360108.76).

Then, the nonlinear regression analysis was first split into DSO and NDSO mines to evaluate if the fitted models for each group were statistically significantly different. As shown in Figure 57 the results for DSO iron ore mines show a positive correlation between the cumulative ROM produced and the cumulative net area disturbed (R^2 = 0.9240[44]). If NDSO mines are considered, as observed in Figure 58, results also show a positive strong correlation between both variables (R^2 = 0.9652).

Given the similarity of the coefficients of determination, the hypothesis of no statistically significant differences among both types of mines in terms of specific land requirements was tested. A Wilcoxon-Mann-Whitney test (not assuming any normality of the dependent variable, also called two-sample Wilcoxon rank sum

[44] The usage of the coefficient of determination (R^2) to evaluate the fit of nonlinear models is contested by some (for pharmacological and biochemical nonlinear data) (e.g. Spiess and Neumeyer 2010); yet, it is frequently used by convention and thus it is reported (rounded to two digits).

test) was applied to the two groups (DSO and NDSO mines) to compare the means of the cumulative net area disturbed.

Figure 57: Specific land requirement of DSO iron ore mines (n=16).

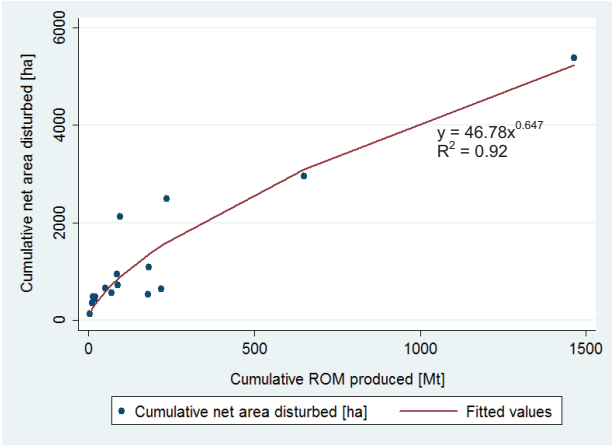

Figure 58: Specific land requirement of NDSO iron ore mines (n=11).

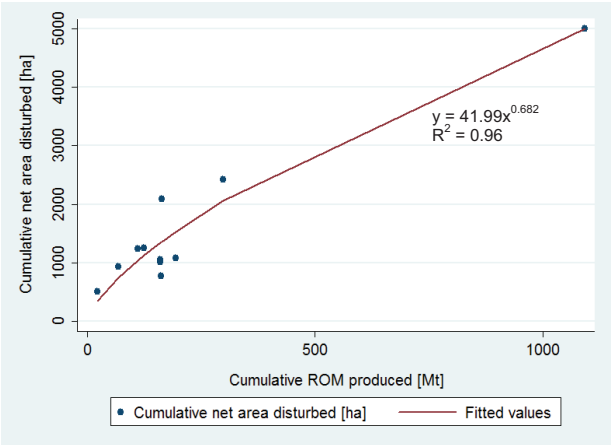

The null hypothesis asserts that the medians (mean ranks) of the two groups are equal. The results of the test suggest that the null hypothesis is accepted (z = -

1.678, p = 0.0934) and there is no statistically significant difference between the underlying distributions of the cumulative net area disturbed by DSO or NDSO.

Hence, it does not become necessary to separate mines according to the ore grades. The result of the regression combining DSO and NDSO mines (Figure 59) displays again a positive strong correlation (R^2 = 0.9391).

Figure 59: Non-linear regression for DSO and NDSO iron ore mines (n=27).

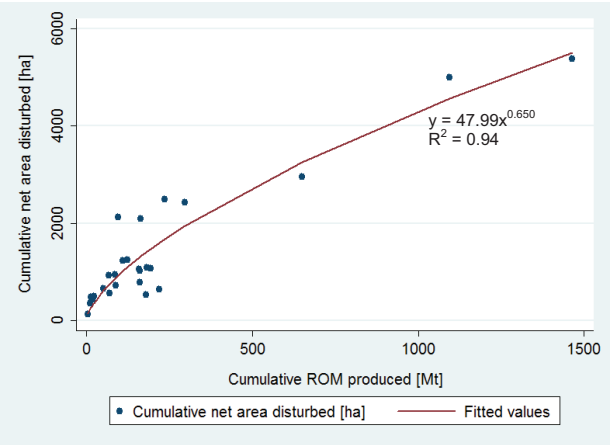

The model´s null hypothesis (asserting that the regression parameters equal zero) was rejected as the bootstrapped regression yielded statistically significant results at a 99% confidence level for the beta (p = 0.008) and gamma (p < 0.0001) parameters (seed set at 50). The average ore grade for all iron mines was 59.6% (Fe content).

Testing homoscedasticity and normality of residuals

The fitted model (DSO and NDSO) was found to be slightly heteroscedastic as the variance of the residuals changes across levels of the predicted values (Figure 60). The pattern of the data points becomes wider around the fitted value of 1,500 and then narrower. The distribution of residuals was not substantially different from normality (Figure 61).

Figure 60: Iron ore. Residuals vs fitted values (n=27).

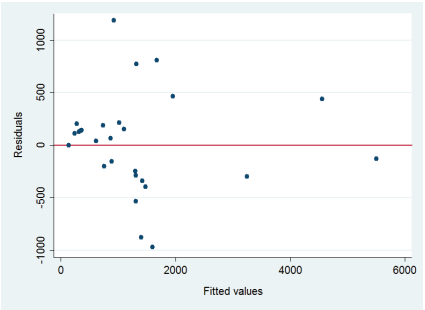

Figure 61: Iron ore. Normality of residuals (n=27).

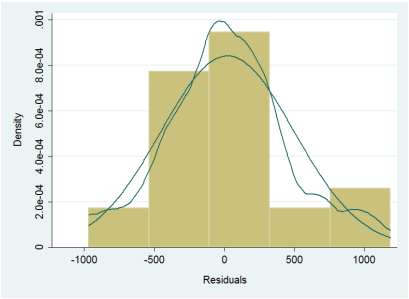

Calculating the weighted disturbance rate

The weighted disturbance rate for iron ore producing mines was based on the 27 mines of the original sample given that they were all producing the two years after the reference year (last year of the period used to calculate cumulative values). Based on the Table 21 and Table 22 (see Appendix, Section 8.4.2), the weighted disturbance rate, which indicates the annual amount of new hectares disturbed according to the mass extracted (Mt of ROM), was estimated at 4.25 ha/Mt_{ore}.

4.1.2.2 Specific land requirements - Bauxite

Fitting the model

In order to determine the best fit, an ordinary least square linear and non-linear fit was run as a regression. The minimum sum of squared residuals was found for

the latter (11072612.2) against the linear regression (11462421.1). The scatterplot with the non-linear regression shows a positive association (R^2 = 0.8391).

Figure 62: Bauxite. Non-linear regression (n=13).

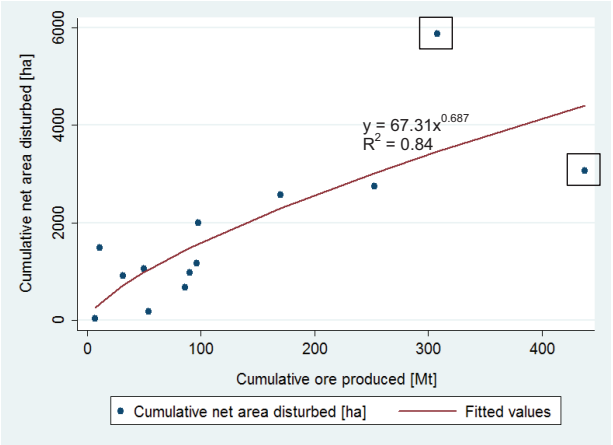

However, the points most distanced from the fitted values curve (marked with rectangles) may be influential points. In order to test it an analysis was performed running the regression excluding each of the points at a time (Figure 63).

Figure 63: Bauxite. Results restricting potential influential points.

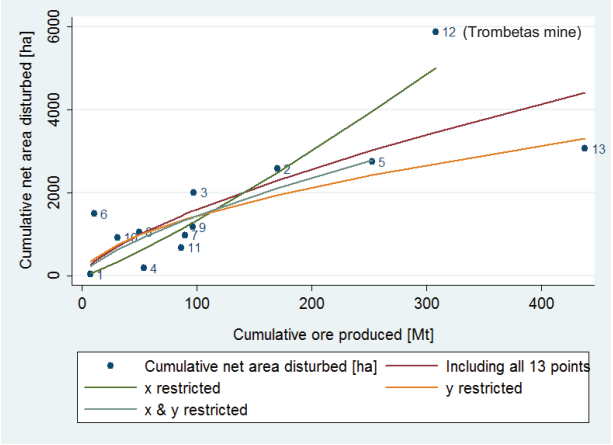

Regressions were run first restricting the Trombetas mine ("y restricted" = excluding point with id 12), excluding the Boke Sangaredi mine ("x restricted" = excluding point with id 13), and then excluding both of them ("x & y restricted").

Results show that only the point with id=12 (Trombetas mine) is an influential point changing the direction of the curve. Accordingly, it was decided to run the regression excluding this influential point. Results excluding such influential point (n=12) show again a positive strong correlation (R^2 = 0.8987) (Figure 64).

Figure 64: Bauxite. Non-linear regression excluding point 12 (n=12).

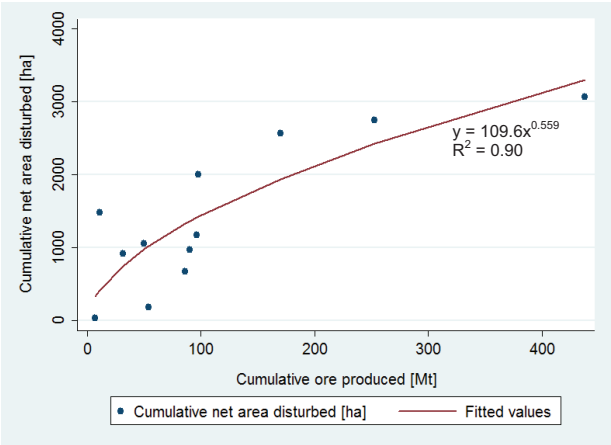

The null hypothesis (asserting that the regression parameters equal zero) was rejected as the bootstrapped regression yielded statistically significant results at a 95% confidence level for the gamma (p = 0.01) parameter but not for the beta parameter (p = 0.5) (seed set at 50). For bauxite mines the average ore grade could not be calculated due to lack of data in the SNL Metals & Mining database.

Testing homoscedasticity and normality of residuals

The fitted model does not display a substantial degree of heteroscedasticity and the distribution of the residuals is approximately normal (Figure 66).

Figure 65: Bauxite. Residuals vs fitted values (n=12).

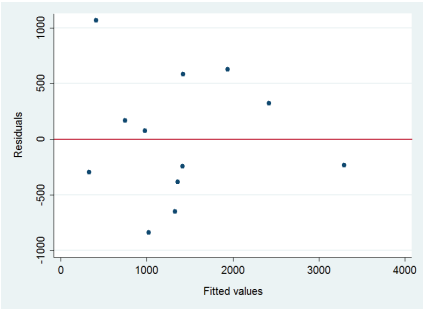

Figure 66: Bauxite. Distribution of residuals (n=12).

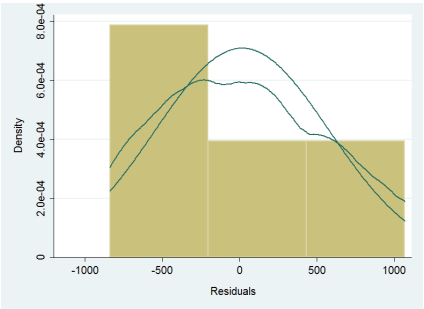

Calculating the weighted disturbance rate

The weighted disturbance rate for bauxite producing mines was based on the 12 mines of the sample given that they were all producing the two years after the reference year (last year of the period used to calculate cumulative values). Based on the Table 23 and the Table 24 (see Appendix, Section 8.4.2), the weighted disturbance rate was estimated at 7.98 ha/Mt_{ore}.

4.1.2.3 Specific land requirements - Copper

All copper-producing mines (open pit and underground)

In order to determine the best fit, an ordinary least square linear and non-linear fit was run as a regression. The minimum sum of squared residuals was found for the non-linear (363541422) against the linear regression (374938903).

A first non-linear regression was run for all data points (n=28). After 21 iterations the model converged to the regression curve shown in Figure 67. The curve appears highly influenced by two outlier points, one circled (in red) and the other squared (in green).

Figure 67: Copper. Non-linear regression (n=28).

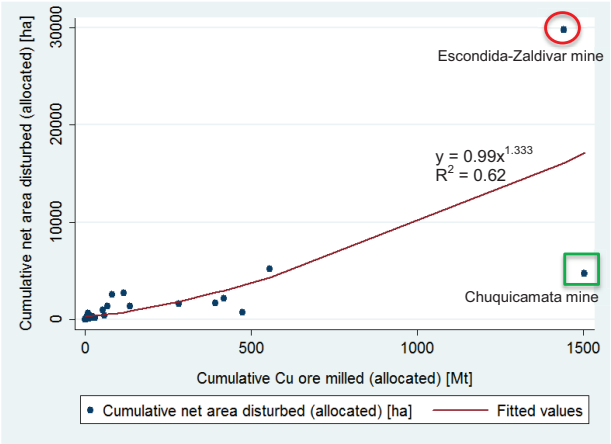

A more detailed examination of the points reveals that the point circled in red (the Escondida-Zaldivar mine, cumulative net area disturbed close to 30,000 ha) is an outlier which substantially distorts the function equation (presented in Eq. 3 and which explains the association of variables in all models).

The influence of this point, considered an extreme outlier[45], is high enough to make the curve not consistent with the basic theoretical form of the function presented in Eq. 3 (thus it is considered an influential point). Further inquiry of this point revealed that its outlying value is explained given that the Escondida-Zaldivar entity represents the only measurement in this study covering two mines together: the Escondida mine and the Zaldivar mines. Both mines were considered together because during the measurement it was not possible to establish the visual

[45] According to the definition by Hamilton (Hamilton 2008) used by the "iqr" module in Stata® (Stata Corp LP 2009), extreme or severe outliers are any data values which lie more than three times the interquartile range below the first quartile or above the third quartile.

boundary between them; thus, cumulative area disturbances and ore extraction represent the sum of values of both mines.

Given that this entity is not actually one mine but two mines combined into one and given that it is far distant from any other observation, it was decided to be removed from the dataset. In contrast, the Chuquicamata copper mine (square in green) (Figure 67) was also found to be an extreme outlier (according to the interquartile range method applied to cumulative copper ore produced defined in Hamilton 2008) but it was decided to be maintained in the dataset given that it represents a point belonging to one mine and covers part of the "very big mines" which explain the right skewed distribution of metal mine production in the world.

The model fit module was run again and after nine iterations, the non-linear regression excluding the Escondida-Zaldivar mine converged to the equation shown in Figure 68. The graph shows a positive association between variables and a relatively strong coefficient of determination (R^2 = 0.8135).

Figure 68: Copper. Non-linear regression excluding Escondida-Zaldivar mine (n=27).

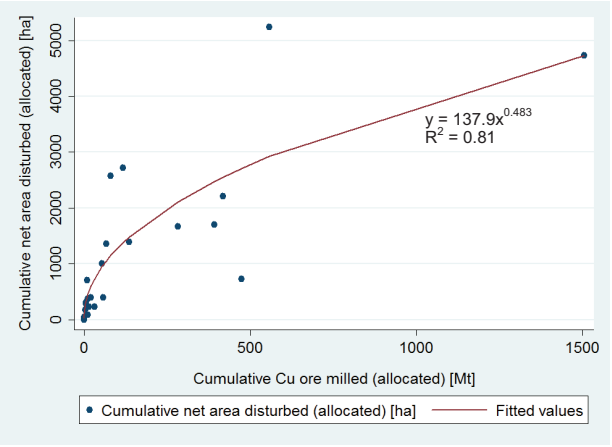

The null hypothesis (asserting that the regression parameters equal zero) was rejected as the bootstrapped regression yielded statistically significant results at a 95% confidence level for beta (p = 0.043) and gamma (p < 0.0001) parameters

(seed set at 50). The average ore grade (excluding Escondida-Zaldivar) was 1.17% Cu.

Testing homoscedasticity and normality of residuals

The fitted model shows a slight degree of heteroscedasticity as the values increase towards the fitted value of 3,000.

Figure 69: Copper. Residuals versus fitted values (n=27).

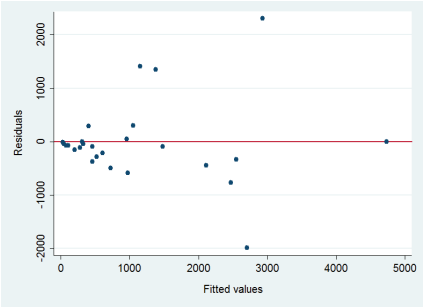

With regards to the distribution of residuals, it tends to follow an approximately normal one.

Figure 70: Copper. Distribution of residuals (n=27).

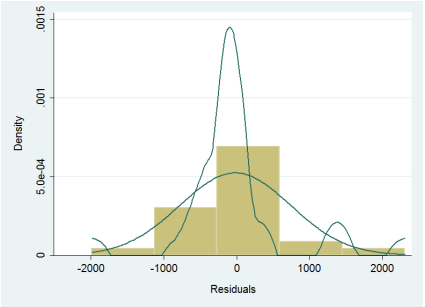

Calculating the weighted disturbance rate

The weighted disturbance rate for copper ore producing mines was in principle based on the 27 mines of the used sample; yet, three additional mines were

excluded because they were either suspended or closed after the reference year (the last year used for computing the regression in Figure 68). Thus, the calculation was made on 24 mines. Based on the Table 25 and the Table 26 (see Appendix, Section 8.4.2), the weighted disturbance rate was estimated at 4.5 ha/Mt Cu ore extracted.

4.1.2.3.1 Open pit copper-producing mines

After eight iterations the non-linear regression analysis for open pit copper-producing mines provided the equation and curve given in Figure 71. The graph shows a positive association between variables and a relatively strong coefficient of determination (R^2 = 0.8264). The null hypothesis (asserting that the regression parameters equal zero) was rejected as the bootstrapped regression yielded statistically significant results at a 95% confidence level for gamma ($p < 0.0001$) but not for beta ($p = 0.08$) parameters (seed set at 23).

Figure 71: Copper. Non-linear regression for open pit mines (n=16).

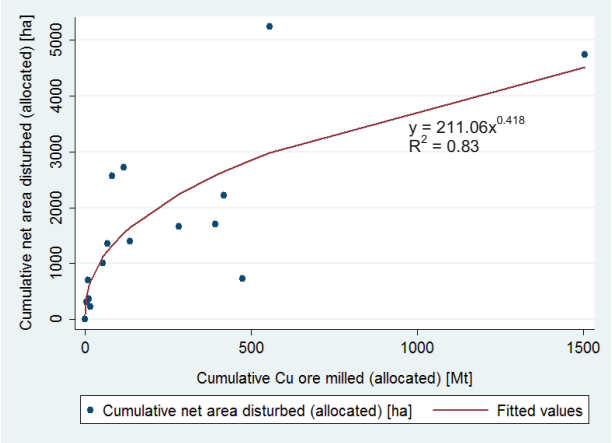

4.1.2.3.2 Underground copper-producing mines

After seven iterations the non-linear regression analysis for underground mines provided the equation and curve given in Figure 72. The graph shows a positive association between variables and a relatively strong coefficient of determination (R^2 = 0.8751).

Figure 72: Copper. Non-linear regression for underground mines (n=11).

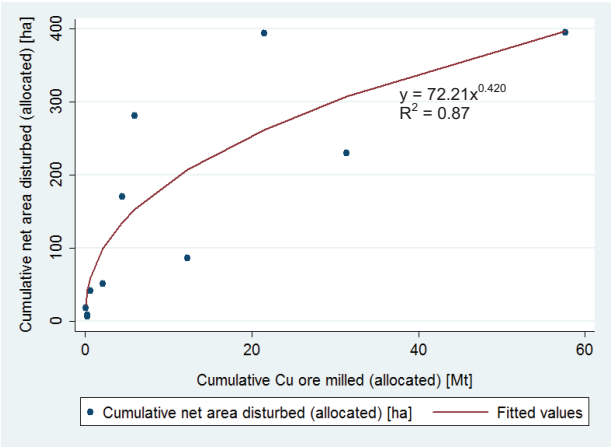

The bootstrapped regression analysis shows that results are statistically significant at a 99% confidence level for beta ($p = 0.0002$) and gamma ($p < 0.0001$) parameters (seed set at 21).

4.1.2.4 Specific land requirements - Gold

4.1.2.4.1 All gold-producing mines (open pit and underground)

Fitting the model

In order to determine the best fit, an ordinary least square linear and non-linear fit was run as a regression. The minimum sum of squared residuals was found for the nonlinear (18662404.6) against the linear regression (24155114.5).

After seven iterations the model fitting operation converged to the non-linear regression curve shown in Figure 73 depicting a positive and relatively strong correlation ($R^2 = 0.7773$). The points on the x axis beyond the 1,000 could be considered influential points. Yet, the output of the bootstrapped regression allows verifying that results for beta ($p = 0.01$) and gamma ($p < 0.0001$) are statistically significant at a 95% confidence level (seed set at 50). The average ore grade for gold mines was 3.11 grams of gold per metric ton of ore extracted.

Figure 73: Gold. Non-linear regression (n=63).

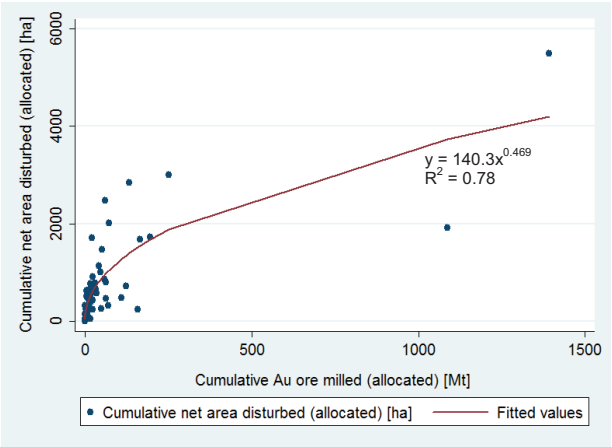

Testing homoscedasticity and normality of residuals

The fitted model was tested for heteroscedasticity and the residuals plotted against the fitted values reveal a certain degree of heteroscedasticity. Points gain in spread along the fitted values axis.

Figure 74: Gold. Residuals versus fitted values (n=63).

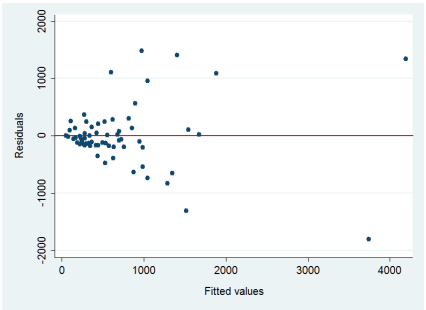

With regards to the distribution of residuals, it is approximately normal (Figure 75).

Figure 75: Gold. Distribution of residuals (n=63).

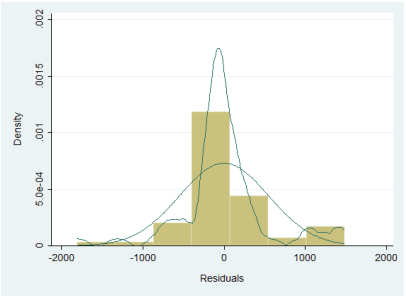

Calculating the weighted disturbance rate

The weighted disturbance rate for gold producing mines was based on 57 mines; out of the original sample (n=63), six mines were excluded because they were either suspended or closed after the reference year. Based on the Table 27 and the Table 28 (see Appendix, Section 8.4.2), the weighted disturbance rate was estimated at 6.70 ha/Mt Au ore extracted.

4.1.2.4.2 Open pit gold-producing mines

After eight iterations, the model fitting gold-producing open pit mines converged to a non-linear regression depicting a positive association (R^2 = 0.78).

Figure 76: Gold. Non-linear regression for open pit mines (n=44).

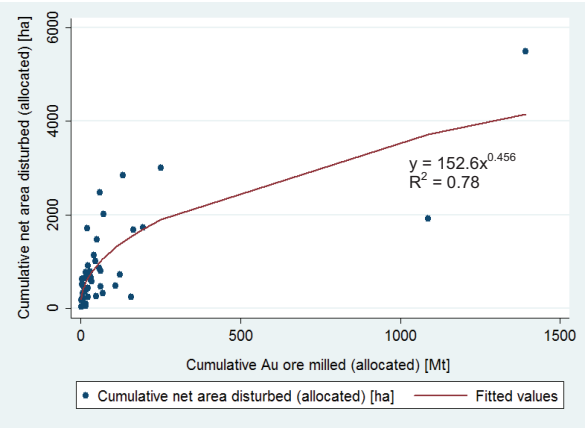

The null hypothesis was rejected as the bootstrapped regression yielded statistically significant results at a 95% confidence level for gamma ($p < 0.0001$) but not for the beta ($p = 0.05$) parameter (seed set at 50).

4.1.2.4.3 Underground gold-producing mines

After ten iterations, the model fit converged with a non-linear regression whose coefficient of determination was $R^2 = 0.7476$.

Figure 77: Gold. Non-linear regression for underground mines (n=19).

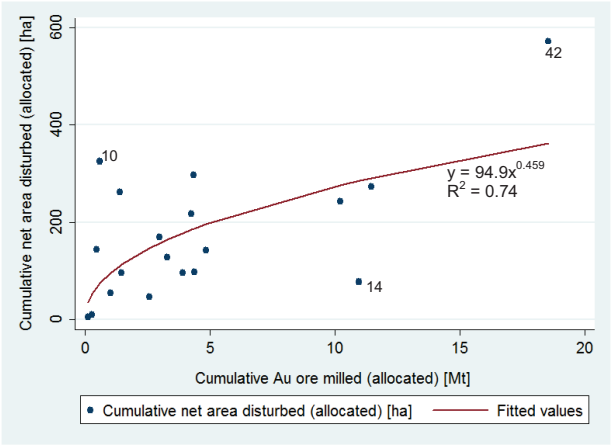

The graph shows that the points with id 42, 14 and 10 are outliers and may be an influential point substantially changing the regression model. They were graphically evaluated (Figure 78) and it was found that none of them is exerting an influence strong enough to noticeably change the form of the curve.

Hence, it was decided to use all points for the regression. Using all points (n=19), the boostrapped regression allows concluding that the null hypothesis was rejected as results are statistically significant at a 95% confidence level for beta ($p = 0.01$) but not for the gamma ($p = 0.08$) parameter (seed set at 23).

Figure 78: Gold. Non-linear regression for underground mines excluding outliers (n=19).

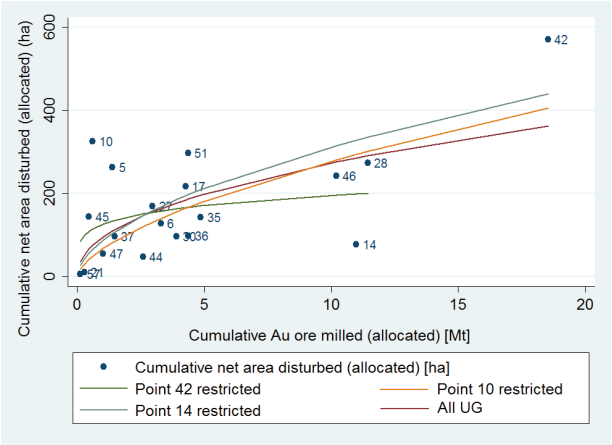

4.1.2.5 Specific land requirements - Silver

4.1.2.5.1 All silver-producing mines (open pit and underground)

In order to determine the best fit, an ordinary least square linear and non-linear fit was run as a regression. The minimum sum of squared residuals was found for the nonlinear (553814.89) against the linear (594667.26).

The model fitting operation converged to the non-linear regression curve shown in Figure 79 depicting a positive correlation (R^2 = 0.6067). However, the observations within a rectangle are outliers which may be acting as influential points.

Nonlinear regressions were run excluding (restricting) such points (first each at a time and then the two together) and it can be concluded from the graphical analysis (Figure 80) that the observation with almost 1,000 ha of cumulative net area disturbed (La Coipa mine, id 16) is acting as an influential point. Therefore, it was decided to run the regression excluding such point.

Without the influential point, the regression shows a positive strong correlation (R^2 = 0.8174) (Figure 81).

Figure 79: Silver. Non-linear regression (n=34).

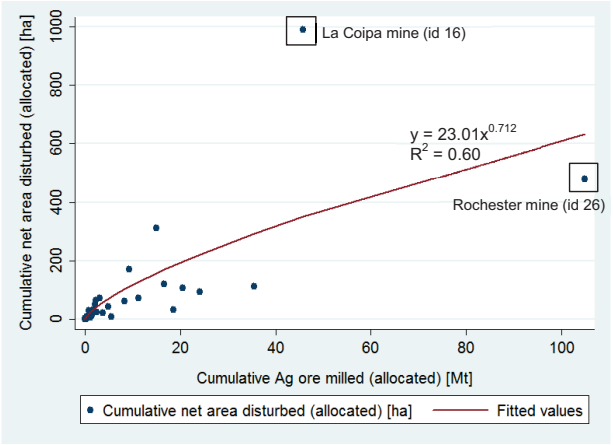

Figure 80: Silver. Non-linear regression excluding different potential influential points.

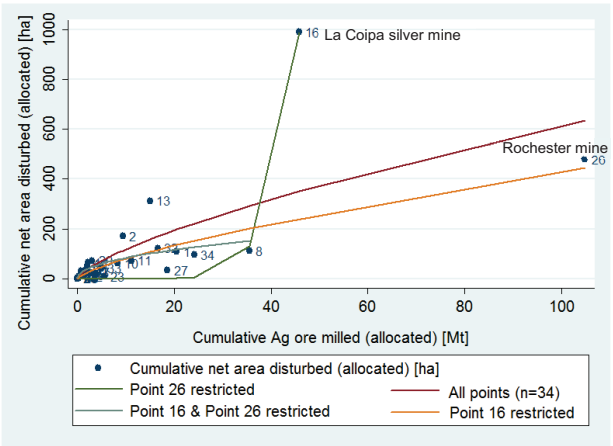

Figure 81: Silver. Non-linear regression excluding the influential point La Coipa (n=33).

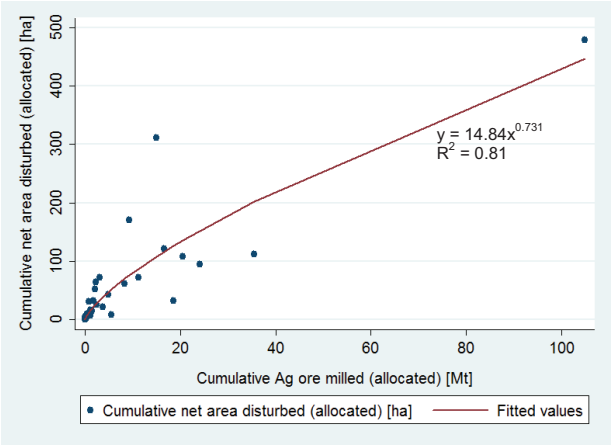

The null hypothesis was rejected as the bootstrapped regression yielded statistically significant results at a 95% confidence level for the gamma ($p < 0.0001$) parameter but not for beta ($p = 0.09$) (seed set at 50). Due to the lack of significance of the beta parameter, the Rochester point was tested and it resulted to be an extreme outlier (according to the definition by Hamilton, cf. Hamilton 2008).

Given such characteristic, the lack of significance of the bootstrapped regression and the fact that the point is the only much distanced from the cloud of points, it was removed. The regression curve excluding the Rochester mine shows a positive correlation ($R^2 = 0.6577$) as shown in Figure 82.

The null hypothesis was rejected as the bootstrapped regression (excluding Rochester) yielded statistically significant results at a 95% confidence level for gamma ($p = 0.02$) and at a 99% confidence level for beta ($p < 0.0001$) (seed set at 50). The average ore grade for silver mines was 37.2 grams of silver per metric ton of ore extracted (only polymetallic mines).

Figure 82: Silver. Non-linear regression excluding the Rochester mine (n=32).

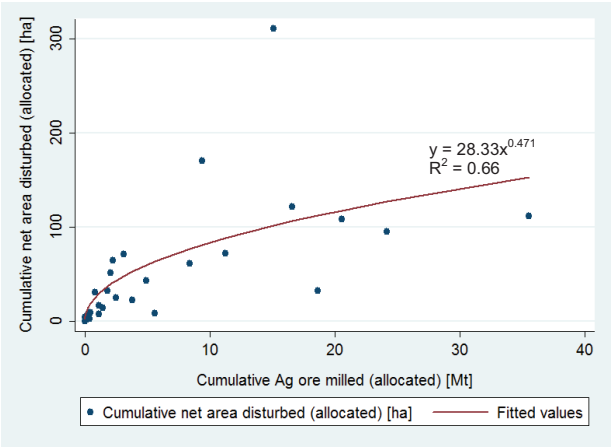

Testing homoscedasticity and normality of residuals

The fitted model was tested for heteroscedasticity with the residuals plotted against the fitted values. The plot (Figure 83) reveals an increase in the spread of the data from the left to the right, i.e. it shows a certain degree of heteroscedasticity.

Figure 83: Silver. Residuals versus fitted (n=32).

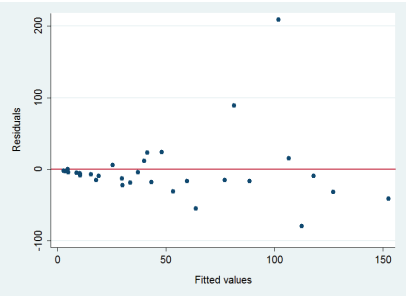

With regards to the distribution of residuals, it is approximately normal (Figure 84).

Figure 84: Silver. Distribution of residuals (n=32).

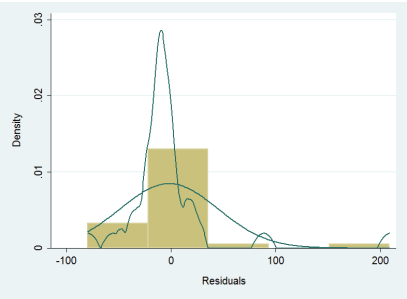

Calculating the weighted disturbance rate

The weighted disturbance rate for silver producing mines was based on 27 mines; of the sample (n=32), five mines were excluded because they were either suspended or closed after the reference year. Based on the Table 29 and the Table 30 (Appendix, Section 8.4.2) the WDR was 5.53 ha/Mt Ag ore extracted.

4.1.2.5.2 Open pit silver-producing mines

After ten iterations, the model fitting converged and produced the non-linear regression curve shown below. It depicts a positive association (R^2 = 0.6356).

Figure 85: Silver. Non-linear regression for open pit mines (n=20).

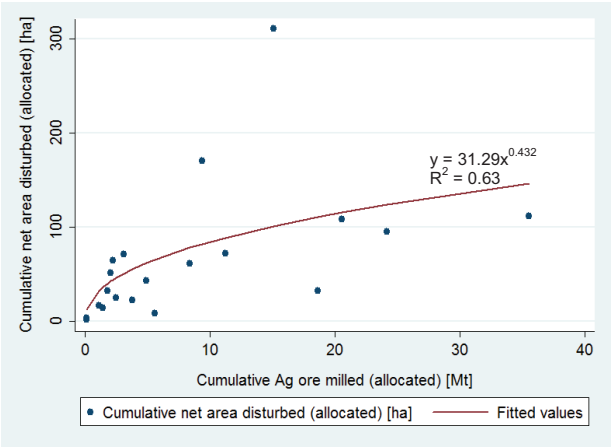

The null hypothesis was rejected as the bootstrapped regression yielded statistically significant results at a 99% confidence level for the beta (p = 0.002) but not for the gamma parameter (p = 0.1) (seed set at 21).

4.1.2.5.3 Underground silver-producing mines

After three iterations, the model fitting operation converged and produced the non-linear regression curve shown in Figure 86. It depicts a positive association of variables (R^2 = 0.9733). Yet, bootstrapped p-values confirm that results are statistically not significant at a 95% confidence level for beta (p = 0.1) and for gamma (p = 0.1) parameters (seed set at 50).

Figure 86: Silver. Non-linear regression for underground mines (n=12).

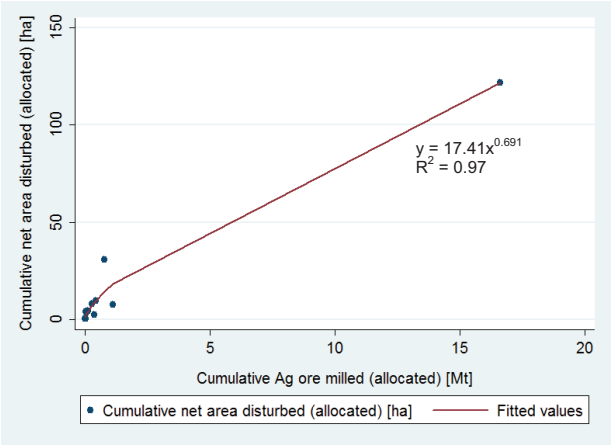

4.1.3 Summary of weighted disturbance rates for the five metals

A comparison of the five metals investigated (Table 14) allows concluding that iron ore mining generates the lowest new net area disturbances per unit of (allocated) mined ore (weighted disturbance rate) whereas bauxite mining has the largest one. Gold and silver mining also have larger disturbance rates than copper and iron.

Table 14: Summary of weighted disturbance rates per metal and per mine.

Metal	Annual new net area disturbed per mine (average) [ha/a]	Annual (allocated) ore extraction per mine (average) [Mt/a]	Weighted disturbance rate [ha/Mt ore]	Observation
Al	39.7	4.98	7.98	Only OP mines.
Au	36.42	5.44	6.70	Encompasses OP and UG mines.
Ag	3.189	0.576	5.53	Encompasses OP and UG mines.
Cu	46.29	10.3	4.5	Encompasses OP and UG mines.
Fe	70.56	16.59	4.25	Only OP mines. Includes DSO and NDSO mines.

4.2 Global status quo in 2011

The amount of Landsat images used for calculating the global status quo was 116 distributed as of: 44 Landsat 5 (TM), 46 Landsat 7 (ETM+) and 26 Landsat 8 (OLI). The full list of images employed per metal and per mine can be consulted in the Appendix, Section 8.3.2.

The calculation of the average proportion factor per metal for the years 2010-2012 (Table 15) shows the highest values for silver and iron, i.e. these are the metal samples with the smallest share in the world production. Bauxite has the largest share.

Table 15: Average proportion factor and global cumulative net area disturbed (2011).

	Bauxite	Iron	Copper	Gold	Silver	5 metals
Average proportion factor (2010-2012)	3.43	6.99	5.54	6.39	11.69	-
Global cumulative area disturbed in 2011 (ha)	95,780	267,344	415,245	371,815	45,357	1,195,541

Source: based on data in Table 31 to Table 40 in Appendix Section 8.5.

The per-metal global cumulative net area disturbed in 2011 calculated is shown in Figure 87.

Figure 87: Global cumulative net area disturbed per metal in 2011 (rounded numbers).

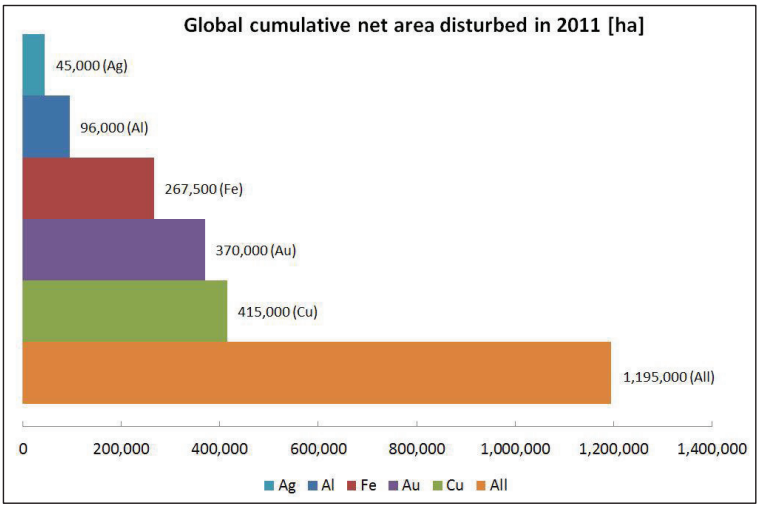

Copper shows the largest topographical footprint surpassing the 400,000 ha followed by gold and iron ore extracting operations. The surface disturbances assigned to silver use (45,000 ha) represents the smallest surface area affected. If all five metals are considered, the global cumulative net area disturbed reaches almost 1.2 Mha, an area slightly bigger than half the state of Hessen (2.1 Mha) in Germany, slightly smaller than Montenegro´s area (1.3 Mha) or less than half of Belgium (3.05 Mha).

4.3 Scenarios on global cumulative net area disturbed until 2050

4.3.1 Iron ore

Scenarios on global cumulative net area disturbed by iron ore mining

All scenarios shown in Figure 88 indicate that the global cumulative net area disturbed by iron ore mining is expected to rise until 2050, at a minimum (almost) doubling and at a maximum multiplying the area disturbed (in 2010) by a factor of 2.85. Except for the “Energy & Material Efficiency-2050” scenario which shows a

leveling off by 2025, all other scenarios suggest that the cumulative net area disturbed is expected to increase and double (or almost double) the area currently disturbed (2010 level) already by 2035.

Figure 88: Scenarios of global cumulative area disturbed by iron ore mining. 2010-2050.

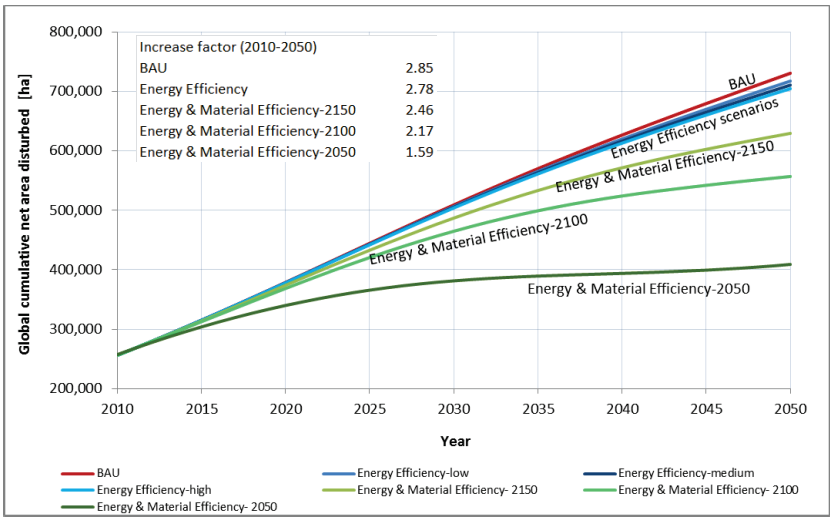

Source: self-elaboration based on data by Milford et al. (2013).

BAU and Energy Efficiency scenarios show a similar path, converging by 2050, doubling the global cumulative net area disturbed by 2035 and achieving 2.8 or 2.7 increase factors by 2050.

The more aggressive Energy and Material efficiency scenarios show a slower growth rate, especially after 2025 when scrap flows surpass primary mining ones. The least aggressive of those three Energy and Material Efficiency scenarios (Energy & Material Efficiency-2150) assumes the deployment of material efficiency strategies at a slow rate, with a doubling of the global area disturbed already by 2038 and by a factor of 2.4 by 2050. The Energy & Material Efficiency 2100 shows a slower growth rate, with the doubling of the area disturbed only by 2043. The most novel-tech aggressive scenario (Energy & Material Efficiency-2050)

represents the least impacting one in terms of land disturbances with a slow growth until 2025 and a subsequent growth at a slow pace, reaching a total land disturbance over 400,000 ha by 2050 (multiplying the current status by only 1.59).

4.3.2 Bauxite

Scenarios on global cumulative net area disturbed by bauxite mining

As observed in Figure 89, all scenarios display a steady ramp up of the global area disturbed without signs of leveling off by 2050 in line with the forecasts of increasing primary extraction. The high-level saturation scenarios show an increase in the global area disturbed by a factor of 2.89 by 2050 (High-2075) or 2.59 (High-2075 with M1-NPC & M2-TYI), namely, far more than doubling the global area currently disturbed.

Figure 89: Scenarios on global cumulative net area disturbed by bauxite mining. 2012-2050.

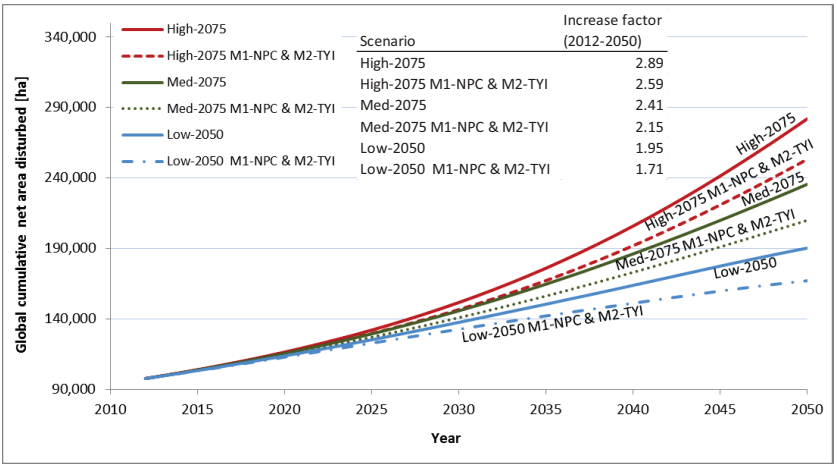

Source: self-elaboration based on data modeled by Liu et al. (2012)

Medium-level saturation scenarios demand a bit more than a doubling of the land disturbed by bauxite mining (increase factors of 2.1 and 2.4) whereas the low-level saturation scenarios show a trend towards a doubling or even less than that (increase factor of 1.7 by 2050) for the low scenario with the implementation of

mitigation measures. The effect of an early saturation (by 2050) with the consequent concave down phase of bauxite ore demand from 2045 onwards in the two low-level scenarios presented in Figure 38 (Low-2050 and Low-2050 M1-NPC & M2-TYI), does not seem to outweight the trend of an increasing demand for land for bauxite ore mining.

4.3.3 Copper

According to the BAU scenario displayed in Figure 90, the global cumulative net area disturbed is expected to increase by a factor of 2.1, i.e. to double the current status by 2050. According to the uncertainty range defined by the BAU +30% and BAU -30% projections (Figure 90), the global area disturbed might otherwise increase by factors between 2.3 and 1.9, namely, the area currently disturbed is still expected to at least double by the year 2050.

Figure 90: Scenarios on global cumulative net area disturbed by Cu extraction. 2012-2050.

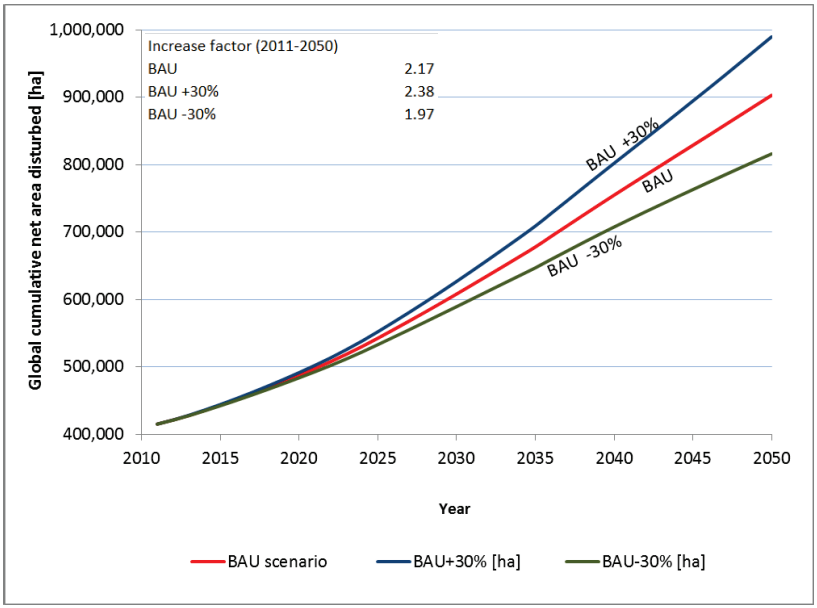

Source: self-elaboration based on Northey et al. (2014)

4.3.4 Gold

According to the BAU scenario (Figure 91), large-scale gold mining activities are anticipated to double the global cumulative net area disturbed by gold mining by the year 2039 and keep on increasing to reach an increase factor of almost 2.5 by 2050 (in comparison to the 2010 level computed at 359,000 ha).

Considering the uncertainty range, this may vary by rising the area disturbed globally by a factor of 2.7 or 2.2; yet, it can be anticipated that, in general and if gold production behaves within a similar trend to that modeled in Figure 47, the land currently disturbed by gold mining is expected to more than double by 2050.

Figure 91: Global cumulative area disturbed by Au mining. BAU scenario and corridor.

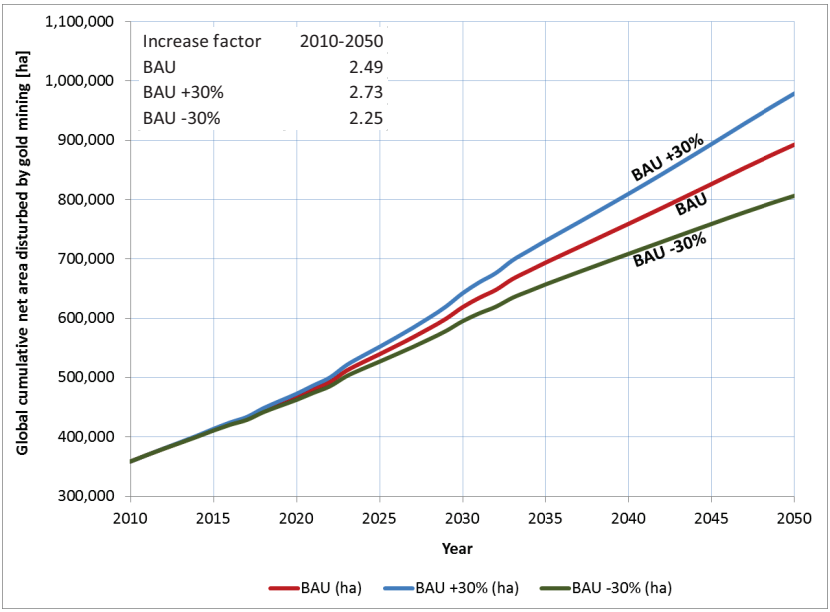

Source: self-elaboration based on modeled data by Sverdrup et al. (2012)

4.3.5 Silver

With regards to the scenario corridor for the global cumulative net area disturbed by silver mining (Figure 92), the BAU scenario shows that the global cumulative net area currently disturbed (computed at 43,300 ha for 2010) is expected to be multiplied by a factor of almost 2.7 by 2050.

Projections covering the uncertainty range depict an increase by factors of 2.95 or 2.4. This means that, in general, the area disturbed by large-scale silver mining is expected to at most almost triple by 2050 and at a minimum more than double. The tripling projection represents one of the highest projections in terms of increase of the area currently disturbed (if compared to the other metals).

Figure 92: Global cumulative area disturbed by Ag mining. BAU scenario and corridor.

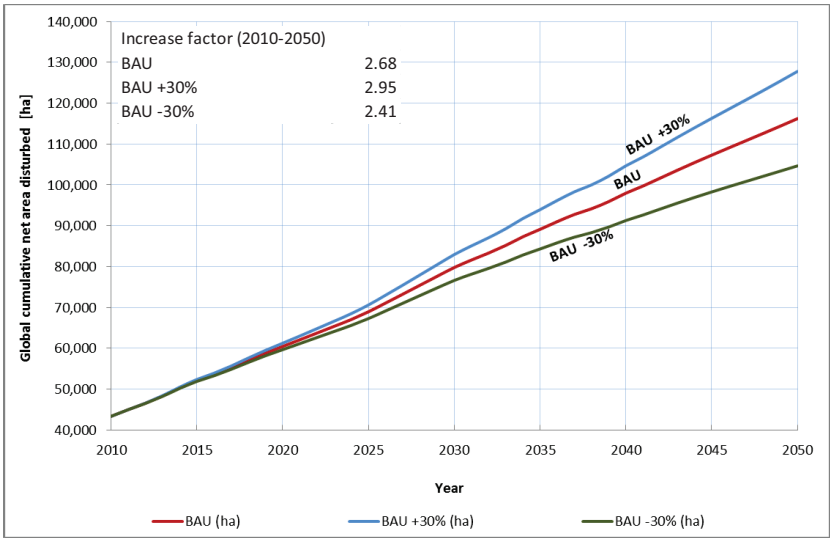

Source: self-elaboration based on data by Sverdrup et al. (pers. comm.)

4.4 Distribution of mines and deposits across biodiversity zones

4.4.1 Iron ore

As the overall picture in Figure 93 below shows, iron ore mines and deposits appear to follow, in general terms, the expected natural spatial pattern (null model) represented by blue-colored bars (bar to the left in each diversity zone), with the exception of mines largely deviating from it in DZs 8 and 9, areas of high biodiversity and often a priority for conservation.

Focusing in mines, in DZs 1-3 they occur less frequently than expected (by chance), only surpassing the expected frequency in the DZs 4-5 and more importantly in DZs 7-9. Regarding iron ore deposits, they are surpassing expected values only in the DZ 4 and 8, remaining in DZs 5, 6, 8 and 9 very close to the natural or expected spatial pattern. The DZ 10 does not host any iron ore mine or deposit.

Figure 93: Graphical frequency distribution of Fe mines and deposits per DZ.

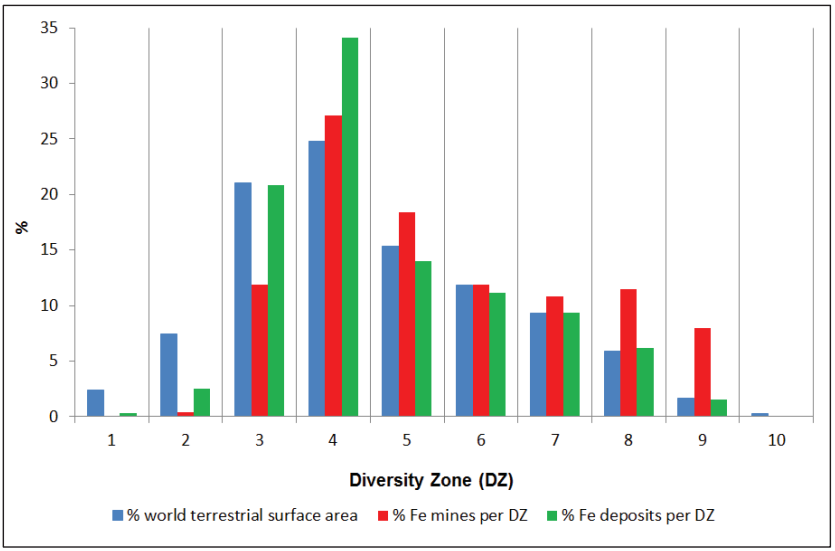

Source: self-elaboration based on SNL Metals & Mining and Barthlott et al. (2007)

The relative high concentration of iron ore deposits in DZs 3 and 4 (together accounting for roughly 55% of all data on iron deposits) indicates the option to shift future new iron ore mining activities towards those areas with lower biodiversity.

If the percentages of the iron ore mines column are observed as probabilities (Table 41, Appendix, Section 8.6.2), they express the probability of each metric ton of iron ore extracted today of exerting a pressure on an area of high diversity of plants (DZs 7-10). Consequently, there is around 30% probability that a ton of iron ore extracted today has been derived from a high-biodiversity area; this percentage may decrease in the future as deposits tend to be available in areas of lower diversity.

The chi-square test revealed that the distribution of observed iron ore mines was not equal to the expected one (natural spatial pattern) either for a significance level of 95% or 99% ($\chi^2(9)=210.57$, $p < 0.0001$). As can be observed below in the table, the value of the test statistic is greater than the critical values portrayed by the chi-square distribution table at both significance levels and the significance levels are both greater than the p-value, hence, the null hypothesis gets rejected and the alternative accepted.

Table 16: Statistical testing of frequency distribution of Fe mines and deposits.

Category	Chi-square test statistic	Critical value Significance level 0.05 (*df* = 9)	Critical value Significance level 0.01 (*df* = 9)	Chi-square Test p-value (chitest)	Monte Carlo estimate for the Exact Test p-value
Iron ore mines	210.57	16.919	21.666	< 0.0001	< 0.0001
Iron ore deposits	29.37	16.919	21.666	0.0005	0.0015

Source: self-elaboration

The results of the Fisher test provided further evidence to reject the null hypothesis (p-value < 0.0001), namely, that there is a statistically significant difference between the observed frequency distribution of iron ore mines and the null model. Consequently, it can be argued that the distribution of iron ore mines is

not random; it is concentrated in different diversity zones. In the case of iron ore deposits, also the chi-square statistic is greater than the critical values at both significance levels. The p-value is smaller than both significance levels, and even though the p-value by the Fisher test is higher, it is still below the significance levels of .05 and .01. This provides evidence to reject the null hypothesis and accept the alternative one.

4.4.2 Bauxite

Results of the frequency distribution of bauxite mines and deposits per DZ indicate that both do not follow the natural pattern and are actually highly concentrated in DZs 5 to 8, namely, zones of intermediate and high importance for biodiversity conservation; no current or future project can be observed in the zone of mega diversity (DZ 10, which occupies only 0.25% of the global terrestrial surface excluding Antarctica, slightly larger than the area of Germany).

Figure 94: Graphical frequency distribution of Al mines and deposits per DZ.

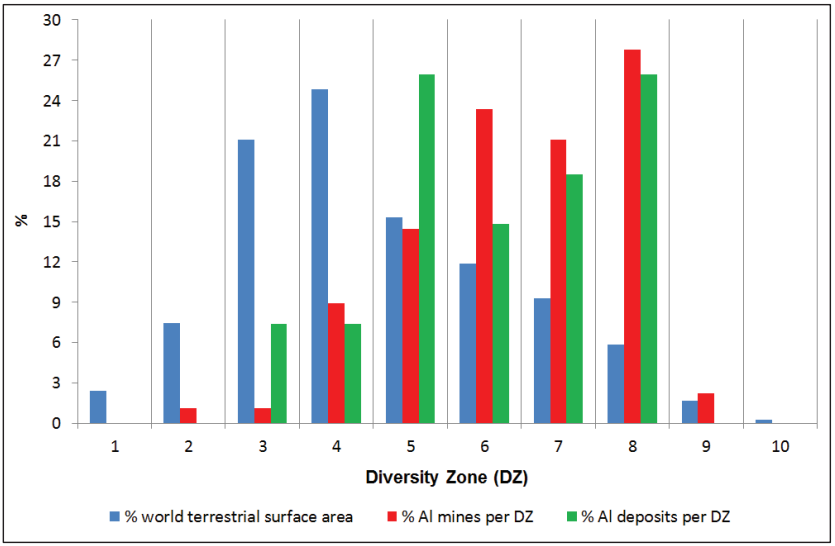

Source: self-elaboration based on SNL Metals & Mining and Barthlott et al. (2007)

The frequency distribution of bauxite mines progressively increases between DZs 2-6, showing a less than expected occurrence in DZs 2-5 and a higher than expected in DZs 6-9. This can be explained due to the main concentration of bauxite deposits in tropical and sub-tropical areas.

With regards to bauxite ore deposits, the graph shows that deposits occur much less frequently than expected in DZs 3-4, and then far-more frequently than expected in DZs 5 to 8. Hence, it can be directly concluded that current and future bauxite ore mining will be exerting a relative stronger pressure on biodiversity areas of higher priority for conservation.

Given the relative low presence of bauxite deposits in areas of low diversity, it becomes difficult to consider the viability of shifting new mining activities to low biodiversity areas of the world, although a certain shift from higher DZs towards DZ 5 may be theoretically possible.

If observed as probabilities and if DZs 7-10 are considered (Table 42, Appendix, Section 8.6), there exists a 51.1% probability that each new ton of bauxite ore mined nowadays comes from an area with a high diversity of vascular plants; even higher (74.3%) if DZ 6 (covering part of the Brazilian and Vietnamese rainforests) is included. In the long run (considering only deposits once the currently operating mines are exhausted) it is expected that the probability will slightly decrease to 44.4%.

This overview indicates that the frequency distributions of both mines and deposits are clearly non-matching with the natural spatial pattern for most of the diversity zones. The conclusions from the graphical analysis were complemented by a statistical one. For bauxite ore mines the chi-square test revealed that the distribution was not equal to the expected one, neither for a significance level of 95% nor of 99% ($\chi^2(9)=131.07$, $p < 0.0001$). The value of the test statistic is greater than the critical value and the significance levels are both greater than the p-value, hence, the null hypothesis gets rejected. The results of the Fisher test provide further evidence to reject the null hypothesis (p-value < 0.0001). As for geological bauxite ore deposits, also the test statistic is greater than the critical values and the p-value is smaller than the significance levels.

Table 17: Statistical testing of frequency distribution of Al mines and deposits.

Category	Chi-square test statistic	Critical value Significance level 0.05 (*df* = 9)	Critical value Significance level 0.01 (*df* = 9)	Chi-square Test *p*-value (chitest)	Monte Carlo estimate for the Exact Test *p*-value
Al ore mines	131.07	16.919	21.666	< 0.0001	< 0.0001
Al ore deposits	32.08	16.919	21.666	0.00019	0.0047

Source: self-elaboration.

The Monte Carlo estimate provides a p-value more than double but still below both significance levels. The null hypothesis is rejected and the alternative accepted.

4.4.3 Copper

The overall picture in the Figure 95 below shows that copper deposits seem to follow by and large the natural spatial pattern whereas mines have a higher frequency in DZs 4, 6, 7 and 8.

Figure 95: Graphical frequency distribution of Cu mines and deposits per DZ.

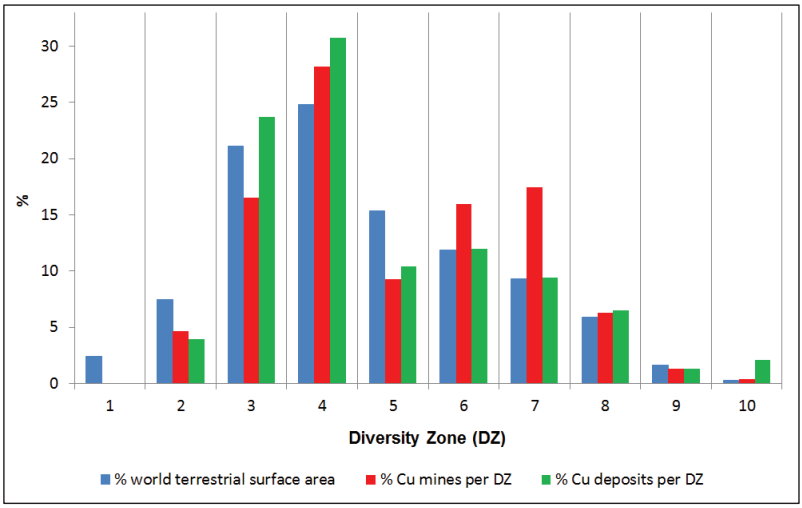

Source: self-elaboration based on SNL Metals & Mining and Barthlott et al. (2007)

With regards to copper deposits, they tend to be more spatially concentrated than expected mainly in DZs 3 and 4 (also slightly in DZs 5 and 8) which indicates again the option of a possible shift of new mines (and exploration) from areas of high diversity towards low-biodiversity ones. The mega-diversity zone is also of high interest for copper deposits given that there are more deposits than expected, indicating a certain concentration which might be the cause of future environmentally-motivated social disputes.

According to the probabilities, there exists a 25% probability that a new ton of copper ore extracted comes from a high biodiversity area if DZs 7-10 are considered (Table 43, Appendix, Section 8.6.2). If deposits are considered, the probability declines to a 19%.

The hypothesis testing results show that frequency distribution of mines and deposits does not match the frequency distribution of the null model.

Table 18: Statistical testing of frequency distribution of Cu mines and deposits.

Category	Chi-square test statistic	Critical value Significance level 0.05 (*df* = 9)	Critical value Significance level 0.01 (*df* = 9)	Chi-square Test p-value (chitest)	Monte Carlo estimate for the Exact Test p-value
Cu mines	86.66	16.919	21.666	< 0.0001	< 0.0001
Cu deposits	80.16	16.919	21.666	< 0.0001	< 0.0001

Source: self-elaboration

Both chi-square test statistic values are higher than the critical values of the significance levels analyzed. The p-value resulting from the chitest and from the Fisher exact test is lower than significance levels, i.e. falls in the rejection region. Therefore the null hypothesis is rejected and the alternative accepted.

4.4.4 Gold

Results show that gold mines and deposits follow by and large the distribution of the natural pattern with the exception of a higher frequency of mines in DZs 4-6 and deposits in DZs 4-6 and 8 and less saliently in DZs 9-10 (Figure 96). The

areas of high biodiversity (DZs 7-10) do not particularly show a concentration higher than expected, except for the DZ 8 which has a higher-than-expected number of mines and deposits.

Figure 96: Graphical frequency distribution of Au mines and deposits per DZ.

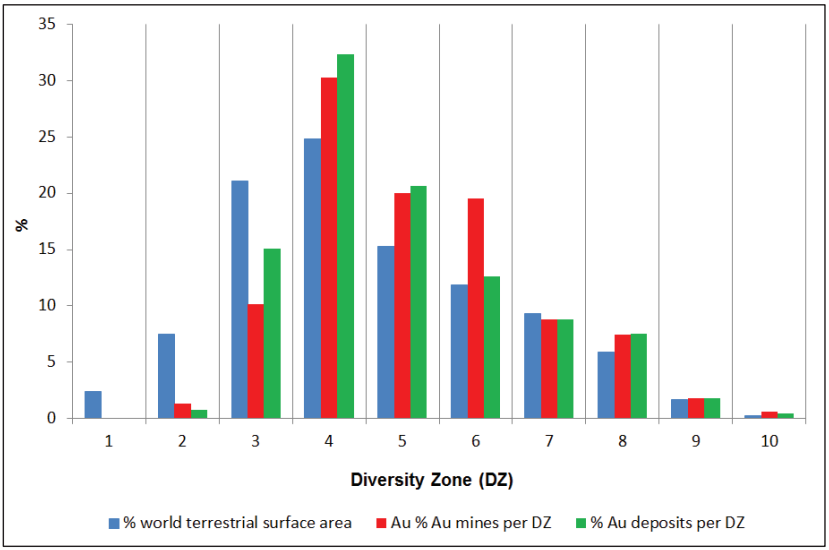

Source: self-elaboration based on SNL Metals & Mining and Barthlott et al. (2007)

Currently, there exists an 18% probability that a metric ton of mined gold is sourced from an area of high biodiversity (DZs 7-10) (Table 44, Appendix, Section 8.6.2). The relative concentration of gold mines in the DZ 6 and slightly in DZ 8 indicate the option that a shift of new mines in the future might be possible towards areas of lower biodiversity, like DZs 3 or 4 in which there exists a relative abundance of gold deposits, probably linked to polymetallic copper deposits already mentioned above in the same DZs.

The results of the hypothesis testing procedure reveals a chi-square test statistic, both for mines and deposits, higher than the critical values, and a p-value smaller than the significance levels. Given these results are straightforward; there was no

need to implement a Fisher exact test. According to results, the null hypothesis is rejected and the alternative accepted.

Table 19: Statistical testing of frequency distribution of Au mines and deposits.

Category	Chi-square test statistic	Critical value Significance level 0.05 (*df* = 9)	Critical value Significance level 0.01 (*df* = 9)	Chi-square Test *p*-value (chitest)
Gold mines	352.47	16.919	21.666	< 0.0001
Gold deposits	184.08	16.919	21.666	< 0.0001

Source: self-elaboration

4.4.5 Silver

For silver, the Figure 97 shows that, in general and similar to bauxite mines, mines and deposits do not follow the natural pattern, largely surpassing the null model for mines and deposits in DZs 6 to 8.

Figure 97: Graphical frequency distribution of Ag mines and deposits per DZ.

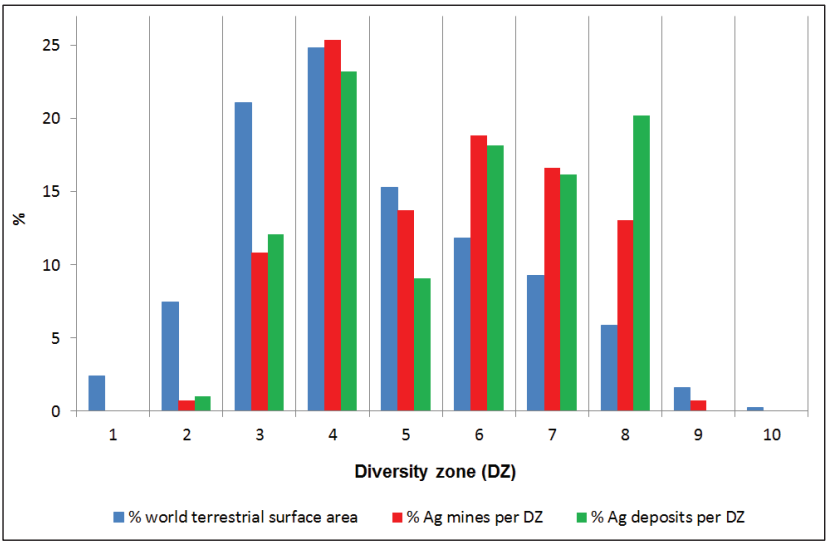

Source: self-elaboration based on SNL Metals & Mining and Barthlott et al. (2007).

In terms of potential future conflicts, no silver mine or deposit was registered in the mega-diversity area (DZ 10). Nevertheless, the relative high concentration of mines and deposits in DZs 6 to 8 (accounting for 48.5% of mines and 54% of deposits) and the low frequencies in DZs 1 to 3 indicate a difficulty to attempt a shift in the opening of new mines towards areas of lower biodiversity.

According to the hypothesis testing procedures, both the chi-square statistic value for silver mines and deposits is greater than the critical values.

Table 20: Statistical testing of frequency distribution of Ag mines and deposits.

Category	Chi-square test statistic	Critical value Significance level 0.05 (*df* = 9)	Critical value Significance level 0.01 (*df* = 9)	Chi-square Test p-value (chitest)
Silver mines	45.79	16.919	21.666	< 0.0001
Silver deposits	59.31	16.919	21.666	< 0.0001

Source: self-elaboration

The p-value from the chi-square test is smaller than significance levels and the null hypothesis is rejected in both cases. There was no need to perform a Fisher exact test as results are straightforward.

CHAPTER FIVE

This discussion chapter first focuses on a review of the hybrid methodology applied for measuring the cumulative net area disturbances by large mines in Landsat images. This is followed by a comprehensive section which discusses results of hypothesis testing and of the specific land requirement calculations with existing literature and provides available references to discuss global status quo and scenario results on a per metal basis. The subsequent section discusses the global status quo for all five metals with available literature. The final section is centered on discussing the results of the analysis of biodiversity pressures on mining; firstly, the approach to operationalize the biodiversity concept is discussed, followed by a general and per-metal review of possibilities to shift future new mining operations towards areas of low biodiversity, and finally a brief discussion is provided on the implications for different actors of such proposal.

5 Discussion

5.1 On the hybrid methodology for quantifying area disturbances

Combining object-based image analysis and visual image interpretation provides the opportunity to quickly and accurately quantify mining-affected areas if local knowledge is available to the trained analyst on the area, either through field work or ancillary information. One of the main advantages of this hybrid method is that it allows the interpreter control over the segments classified and it provides a higher degree of confidence in that the feature being extracted belongs to the mine area. Another advantage is that, if required and allowed by the image´s spatial resolution, the interpreter can make separate measurements of the infrastructure at the mine in a relatively rapid and reliable way. The main applications in the eCognition Developer software (Trimble 2011a) which enable a fast selection comprise the line and polygon tools which allow the accurate classification, even of small segments, of linear infrastructure like haul roads, circular tailings ponds or open pits much faster. Yet, one of the main drawbacks of the method is the time-consuming task of finding mines which fulfil the selection criteria for which

sufficient ancillary information is available. These requirements limit the number of eligible mines reducing the sample sizes. Another disadvantage is the laborious manual classification of segments guided by the contextual information; this is a mine-per-mine specific task which might be regarded as time-intensive and subjective in comparison to more automated methods for feature extraction.

The new hybrid method may come under criticism by arguing that the manual delineation of discrete areal units could be implemented by loading the image subsets into a geographical information software (GIS) for digitizing the mine area. I contend that this method might prove more straightforward but it undermines the reproducibility of results because it introduces subjectivity from the very beginning (the classification is done at the pixel-level). In contrast, the segmentation of the image subset using the MRS algorithm (Trimble 2011b) provides a more consistent and objective basis for the classification. Likewise, it could be claimed that feature extraction could be performed based only on ancillary information, e.g. using Google Earth imagery and technical reports, avoiding the use of Landsat or other proper satellite data. This does not seem plausible given that Google Earth images (actually only pictures) is so far only available in sufficient detail for some locations, does not allow the execution of MRS algorithms (Google Earth does not provide the data for each band, only a picture of the actual satellite image) and hinders an effective visual interpretation based on the different reflectance of mine infrastructure by mixing band combinations.

Despite the success of this new hybrid methodology, the development of a semi-automatic algorithm or rule set over multiple Landsat data (in very different environments) to extract features belonging to a mine (e.g. to be run in eCognition server) remains a challenge. Using radiometrically normalized image subsets, it was attempted to develop such a rule set based on features and thresholds identified by the iterative feature analysis implemented by the SEaTH (Separability and Thresholds) tool. Even though the tool appeared to work relatively satisfactorily for single mines, thresholds were mine and environment-specific determined and could not be readily transferred from one image subset to the other. This hampered the creation of a semi-automatic rule set for feature extraction. A main reason impeding the development of such an automated rule

set to date may be the medium spatial resolution of Landsat data which impedes the successful development of rule sets in eCognition; such software and object-based image analysis in general was predominantly developed as a method to analyse very high resolution imagery (Blaschke 2010). If this type of imagery was to be available at reasonable costs, much could be advanced in developing a semi-automatic rule for extracting mine´s areas.

Using Landsat imagery for mapping metal mines resulted adequate but time-intensive due to the constraints of finding eligible mines and the contextual information; yet, these constraints would not be eliminated by having very high resolution imagery freely available. However, the availability of it would certainly enable the creation of more sophisticated rule sets unleashing the potential of the semantic network in the eCognition Developer or other object-based analysis software.

Despite the inherent drawbacks the new method might involve, its usage reinforces a trend towards transdisciplinary research projects and opens up possibilities for, for instance, crowdsourcing, which is expected to become an effective research method in transdisciplinary research (Wechsler 2014). In the last years crowdsourcing projects have put an emphasis on making the most out of available information, communication technologies and high resolution imagery for several scientific purposes. Projects like the Geo-Wiki or the environmental monitoring (inclusive of mining and fracking) implemented by the Sky Truth Foundation[46] are only a few examples of applied visual image interpretation using the role of the human eye for classification and extraction of specific features (though using mostly high resolution imagery). If such high spatial resolution images were available, students could be engaged in participative monitoring of mines, providing not only manpower but also local knowledge to improve accuracy and other mine-affected features besides the area disturbance.

[46] The Geo-Wiki Project can be visited at: http://www.geo-wiki.org/ and the Skytruth foundation at: http://skytruth.org/index.htm (Websites accessed: May 2015).

5.2 Specific land requirements, global status quo and scenarios per metal

Results from the regression analysis for each metal (without separating per mining method) allowed rejecting the null hypothesis (asserting that regression parameters equal zero). Consequently, the alternative hypothesis arguing that the cumulative net area disturbed is determined by the cumulative ore extracted at the mine site was accepted. Thus, the nonlinear regression analysis corroborates the underlying theoretical assumption illustrated by Eq. 3 given that the fitted values of the gamma parameter were close to the value of 0.666 in all regressions. Furthermore, in most cases (with the exception of the beta parameter in bauxite) bootstrapped parameters were statistically significant at least at a 95% confidence level. Samples, particularly those of copper, gold and silver show some degree of heteroscedasticity but the parameters estimated remain unbiased (this was validated by the bootstrapped results). Findings confirm, in agreement with previous work by Ruhrberg (2002), that a power function best represents the fit between the variables. The specific land requirement metric of this study could be used as a multi-locational updatable standard to approach other site-specific impacts associated with large-scale metal mining around the globe.

5.2.1 Iron ore

In this thesis the specific land requirement for iron ore mines was estimated (rounded) at 0.04 m^2/t_{ore}[47]. No references have been found in the literature accounting for specific land requirements of global iron ore mining. In the Ecoinvent database (version 2.0) (Classen et al. 2007), the land use phase is based on one mine (Carajás mine, ore mining rate of 40 Mt/a, 46% Fe content in ore) sourced from Roth et al. (1999). With regards to area disturbances, the study by Roth and colleagues only reports the annual area disturbances for Carajás (0.16 km^2/a) (Roth et al., 1999:40) but no references for specific land requirements exist for comparison. In the GaBi software (University of Stuttgart 2011) there are references of land use productivity (land occupied by mining to produce an annual

[47] 4.25 ha/Mt_{ore}

amount of ore) for Australia, Brazil and Canada and all share the value of 0.92 $m^2/t_{\text{iron ore}}$ based on data reported by the companies BHP Billiton and Rio Tinto; these numbers result from dividing the cumulative area disturbed at a certain year by the annual ore production of a mine (or a region) run by the company. For instance, if Rio Tinto´s land use productivity for iron ore in 2011 in Western Australia is considered, the company reports for the whole region a cumulative area disturbance ("land area in use") of around 17,000 ha and a shipping of 225 Mt ore in 2011 (Rio Tinto 2011), which results in a factor of 0.75 $m^2/t_{\text{ore shipped}}$. This factor cannot be compared with the specific land requirement calculated in this dissertation given that they are computed in different ways (annual/cumulative vs cumulative/cumulative) and refer to different units of analysis (mine vs a region). However, these are the only references found to frame results by this study.

In relation to the global status quo and scenarios for iron ore mines, no other references in the literature were found to discuss them. The scenarios presented are based on a model which presents pathways to cut the CO_2 emissions of the steel sector and actually achieve by 2050 the targets set by the IPCC (Milford et al. 2013). This requires deploying as soon as possible energy and material efficiency strategies. Were this achieved, not only would CO_2 emissions be significantly reduced, but this would be coupled with a significant reduction in the amount of iron ore extracted and consequently of the global area disturbed by its mining activities.

Concerning the issue of reclamation, although not directly a primary objective of this research, the visual interpretation of multiples images allowed observing that reclamation has been less successful than in the case of bauxite mining. This is in line with evidence from the mining industry, for instance, for the Western Region in Australia under operation by Rio Tinto in which, in 2011, only 14.8% of the land disturbed was under active rehabilitation (Rio Tinto 2011).

5.2.2 Bauxite

In this thesis, the specific land requirement for bauxite ore mines was estimated at (rounded) 0.08 m^2/t_{ore}[48]. Specific land requirement calculations in the scientific literature have only been found in studies by Sliwka and colleagues. The first study by Sliwka (2001) carried out an in-depth analysis of two mines, of which only the Trombetas was approached in this study. His results covering the land dynamics of such mine were calculated to be of 0.21 m^2/t (Sliwka 2001) considering the ore production during the entire mine life, a specific land requirement larger than the one calculated in this study (0.1 m^2/t). The difference might be due to the calculation method as Sliwka considered theoretical disturbances based on a fixed bauxite density (1.7 t/m^3) and average depth (4.5m) to calculate the theoretical pits´ specific land requirements (0.13 m^2/t, increased to 0.18 m^2/t given that 28% of the bauxite is washed away) which contrast the actual surface disturbances measured on satellite images in two dimensions (not accounting for the depth of the pits and tailings ponds). Another reason explaining the difference is that Sliwka computed such value for the entire expected mine life (66 years) while this study only covered half of it. The second study published by Sliwka and colleagues (Sliwka et al. 2001) calculated a new area disturbance factor of 0.13 m^2/t of bauxite ore for the year 1997[49] (and for 52 mines) which is higher than the one calculated in this study; yet the comparison is methodologically not fully adequate as Sliwka and colleagues employed annual values of production while this study relied on cumulative production values.

Another reference to area disturbances by bauxite mining exists from the International Aluminium Institute (IAI) which some years ago performed a multi-year bauxite mine rehabilitation survey and assessment study on global bauxite mining, during a 5-year period (2002-2006), using a sample of 14 mines spanning from small to large mines. Such land use value calculations show that, on average

---

[48] 7.98 ha/Mt_{ore}

[49] Authors argue that in 1997, the "annual occupation of new land (specific land requirement) by bauxite mining sums up to 1,650 ha" (Sliwka et al. 2001). The factor originates from a world bauxite ore production of 122 Mt in 1997.

and for the year 2006, approximately 162m^2 of land was required to produce 1,000 tons of bauxite ore (International Aluminium Institute 2009) which translates to a land use of 0.16 m^2/t$_{ore}$; furthermore, the same study established that over the 15 year period (1991-2006), the factor had ranged between 0.20 and 0.16 m^2/t of ore[50]. The difference between the results by the IAI and this thesis (0.08 m^2/t ore) may be due to the fact that the IAI has computed gross area disturbances while this study has only worked with net area disturbances.

With regards to the global cumulative net area disturbed by bauxite mining in 2011 (computed in this study at rounded 96,000 ha), no other references have been found to make a comparison. Relating to the area reclaimed by bauxite mining, the IAI contends that, yearly, a similar amount of area mined is rehabilitated (International Aluminium Institute 2009), yielding then a no net loss of area disturbed (or "land area footprint neutral" condition) in quantitative terms for mines in operation. This postulate does not seem to reflect reality in so far all operating mines sampled in this study using two satellite images showed a growth in the net area disturbed during the periods considered; although successful reclamation could be ascertained in some cases (e.g. Moengo Coermotibo or Trombetas mines), no evidence of a steady area disturbance or no net loss was found; yet this specific topic remains outside the scope of this investigation.

As regards the final scenarios displayed in Figure 89, no other sources have been found for comparison. It can be concluded that in order to keep the global cumulative net area disturbed as low as possible several measures need to be implemented. First and related to the mining operations, more investments in terms of land rehabilitation are needed in order to increase successful reclamation of already disturbed areas. However, this overall measure needs to be complemented by promoting a low level saturation of global stock of aluminium-in-

[50] Using this land use factor of 0.16 m^2/t for the year 2006 (world production of bauxite ore totaled 193 Mt), in the same study, the IAI contends that during 2006 a global area of 30 km^2 (3,000 ha or half the size of Manhattan island) had been used for bauxite mining operations with a similar amount of mined land being rehabilitated. This measurement does not indicate the global cumulative area disturbed in 2006, it only refers to the new (gross) area disturbed for the mining of 193 Mt of bauxite ore in 2006. According to this thesis, for those 193 Mt of ore extracted in 2006 and using the specific land requirement factor of 7.98 ha/Mt ore, the new (net) area disturbed by global bauxite mining in 2006 should have been 15.4 km^2 (1,540 ha).

use per capita and a saturation time as soon as possible. An increase in collection rates of waste products and manufacturing yields (M1-NPC & M2-TYI) should be encouraged. Increasing collection rates is one of the most daunting tasks, and actually the assumption of reaching 90-95% for waste products, as Liu et al. (2012) argue, is very optimistic or only theoretically possible. With regards to increasing yield ratios[51] of semi-manufacturing and manufacturing process, some strategies which might be promoted include developing new manufacturing processes with higher yields, operating existing processes more effectively or designing components with geometries more similar to those of semi-finished products (Liu et al. 2012). However, achieving 90-95% yield ratios by 2050 is also very optimistic or only theoretically possible, which indicates a trend toward scenarios without a full implementation of such assumptions.

If implemented, all such strategies would increase the amount of recycled bauxite and lower the amount of mined one. Consequently, this would reduce the specific land requirements of annual newly hectares disturbed. On the other hand, if rehabilitation of mined land was more aggressively implemented, this would reduce the cumulative net area disturbances.

5.2.3 Copper

In this dissertation the specific land requirement for copper producing mines was estimated at 0.04 m^2/t_{ore}[52]. Martens et al. (2002a) are the main reference for comparison. The authors investigated the specific land requirements of surface copper mining operations by means of an estimation model (using volumes of waste and production) for a fictitious large-scale open pit copper mine. They applied this model to 89 surface mines spread around the world (accounting for 94% of total surface copper ore production in 1998). Results were provided according to five continents; the specific land requirement of surface copper mining was calculated at: Africa 0.025 m^2/t_{ore}, Asia and Oceania 0.034 m^2/t_{ore}, Europe 0.031 m^2/t_{ore}, Latin America 0.023 m^2/t_{ore}, North America 0.018 m^2/t_{ore}, and

[51] Defined as the efficiency of metal to downstream processes relative to the sum of all process inputs.

[52] 4.5 ha/Mt Cu ore

Total (all continents) 0.023 m^2/t_{ore}. The "Total" metric is almost half of the specific land requirement determined in this dissertation (0.04 m^2/t_{ore}). In his Ph.D. thesis, following a similar methodological approach to Martens and colleagues, Ruhrberg (2002) calculated specific land requirements by relating mass extraction and the area occupied by mining surface infrastructure (estimated by calculating the volume of the deposit). He either used field data or, for mines with unknown field data, used a fictive model for a typical open pit mine estimating the volume of the pit by multiplying the volume of the annual ore and waste production with the number of the years in operation. His result yielded an average specific land requirement of 0.02 m^2/t_{ore} (Ruhrberg, 2002:119). Both values are lower than the estimation for copper-producing mines in this investigation. This may be due to different measurement procedures, to the different distribution of the sample used and to the fact that Martens et al. did not include underground operations.

Concerning the global status quo, Martens et al. (2002) estimated a world total land disturbed to date (1998) for surface copper mining operations of 93,800 ha, much lower than the one estimated in this study (415,000 ha). This might be explained due to the increasing nature of the status quo from 1998 until 2011 and also because the authors only calculated the area disturbances associated with open pit mining.

With regards to the scenarios, the supply-driven model by Northey et al. captured the peaks and troughs in historical production for each country analyzed with a high to very high coefficients of determination. But as the authors argue, the estimated ultimate recoverable resource (URR), with different definitions of resources and reserves, is the major source of uncertainty and sensitivity for the scenarios modeled. However, if compared with other demand-driven models by Ayres et al. (2003) or Kapur (2005), the reported copper resources appear insufficient to meet the demand modeled by such two authors. The model by Northey indicates that there is potential to grow (or sustain) mine production beyond the forecasted peak; however, the study only accounts for copper mine extraction without considering effects of increasing secondary copper production.

Such limitation is overcome in the system dynamics COPPER model run by Sverdrup et al. (2014b) which examines the range of possible peak years of copper production and, similar to the forecasts by Northey et al. (2014), the authors share the forecast of a peak copper production in the next decades. The peak might occur within a time interval between the years 2030 and 2045 depending on ore grades, production costs (depending on oil prices), and the minimum supply price to society; the lower the cut-off, the higher the URR; the higher the URR, the later the peak occurs. A main difference between Northey et al. and Sverdrup et al. is that Sverdrup´s model refers to reserves whereas Northey´s to resources and the fact that Sverdrup considers recycling within the model. In any case, forecasts of a certain peak copper in the next decades are shared by both investigations with a decreasing copper demand and production as reserves get exhausted as shown in Figure 39. No studies addressing future global cumulative areas disturbed by copper mining have been found to discuss the results of the scenario (and scenario corridor) presented in this study.

5.2.4 Gold and Silver

Gold (6.70 ha/$Mt_{Au\ ore}$) and silver (5.53 ha/$Mt_{Ag\ ore}$) have the highest weighted disturbances rates after bauxite (7.98 ha/Mt_{ore}). The high rates may be explained due to the lower amount of allocated ore per mine in comparison to copper or iron (see Table 14); for instance, the average amount of new copper ore extracted per year and per mine (10.3 Mt/a) (Table 14) is much higher than that for gold (5.44 Mt/a), silver (0.556 Mt/a) or bauxite (4.98 Mt/a). Given that, for gold, 41 out of 63 mines sampled are polymetallic and that, for silver, all mines are polymetallic, the results of the allocation procedure of ore can explain the comparatively higher weighted disturbance rates for gold and silver in comparison to copper.

With regards to literature investigating specific land requirements for gold, the only source tackling the land use by gold mines refers to the work of Spitzley and Tolle (2004). They have approached the calculation of the surface area occupation for three gold mines (none studied in this dissertation) and have assumed that they could accurately estimate the time required for site reclamation. Thus, they have proposed a metric, the acre-years used per ton of resource extracted until the land

is reclaimed back to similar conditions. For calculating such metric, they have used average annual disturbance rates (constant annual change) based on an updated area disturbed measurement and the number of years passed since the mine started production. However, they have not used a functional unit similar to this study which could be used for comparison. In relation to specific land requirements for silver, no references have been found in the literature. Related studies exist in the field of life cycle assessment. The Ecoinvent database (version 2.0) (Classen et al. 2007) refers to gold and silver together and provides references to data originating from reports of the Swedish company Boliden belonging to the mines Aitik, Boliden and Garpenberg which produce gold, silver and other metals. Nevertheless, no data on specific land requirements is provided; the database provides estimations on the disturbed area in activity (during 50 years which is the assumed mine life employed) but it does not determine the cumulative or annual mass extracted.

With regards to the global status quo no sources for comparison have been found, either in academic or business-related literature.

Concerning the gold scenario, existing literature agrees with the modeled overall trend of a decline in the future amount of world gold mined. According to Müller and Frimmel (2010), the historical world gold production has evolved under four individual sub-cycles (following Hubbert-style sub cycles) showing that production reached a peak gold in 2001 and it is predicted to subsequently fall to a mining rate of 1,600 t/a by the year 2018. No other studies have been found discussing long-term trends of declining (or rising) future global gold production. With regards to short-term predictions for gold extraction, the model forecasts by Sverdrup tend to agree with existing forecasts up until the year 2015 but the subsequent fall to annual extraction levels lower than 2 kt Au/a contradict some few short-term forecasts available (e.g. Menzie et al. 2013 forecasted an increase to 3.2 kt/a by 2017). However, some more recent forecasts are in line with the model´s prediction of a peak gold taking place soon (e.g. in 2015, see Goldcorp 2014).

With regards to the ore grades, the industry and the academia agree on the historically falling ore grades for metals, inclusive for gold. Yet, there is some

disagreement with regards to the absolute average ore grade amount. While Müller and Frimmel (2010) claim a mean ore grade by the year 2010 around 3 g Au/t and argue it may fall to 2 g Au/t by 2050 (by extrapolation), Mudd et al. (2012) establish the current grade at 1.4 g Au/t. No publicly available industry forecasts could be found predicting the mid or long-term evolution of global average (gold) ore grades or scenarios of global cumulative net area disturbances.

In relation to the silver scenario, short-term projections are in line with the modeled mine production in 2013 and 2014 (approximately 26,000 t/a). Yet, the industry´s short-term forecasts (e.g. Krebs 2013) do not forecast a steep fall in the production after 2015 as the model by Sverdrup (Sverdrup et al. 2014a) does. In relation to the ore grades, there is a lack of sources to discuss the results by Sverdrup et al. The industry agrees on the evidence of historically declining ore grades (e.g. GFMS 2014) but there is no research on the possible development in the future. Concerning the global cumulative area disturbed, no research was found to discuss results. It must be underlined that results of the scenario corridor might be modified if the weighted disturbance rate was increased or reduced, e.g. by a stronger policy of land rehabilitation once mining ceases.

5.3 Global status quo of all five metals

This dissertation´s estimate of the global cumulative area disturbed for all five metals (1.2 million hectares, 0.007% of the world´s land ice-free surface) falls well within and below previous broad approximations of the area directly disturbed by mining. For instance, it was estimated that mining would occupy considerably less than 1% of the world´s terrestrial land surface (Bridge 2004) or that mining and quarrying had transformed (by 2007) around 40 million hectares (Hooke and Martín-Duque 2012). No other sources were found to provide a more refined comparison of results.

It must be stressed that the global cumulative net area disturbed does not include areas potentially disturbed (gross areas e.g. for bauxite) and also does not include areas disturbed by abandoned or orphaned mines. In the USA, as of January 2015, the number of known abandoned mines (most of them hardrock mines) reached over 48,000 sites and 89,000 features (U.S. Bureau of Land Management

2015). In Canada and Australia it is estimated that their number (including small and large mines, and all minerals) reach over 10,000 (Mackasey 2000) and over 50,000 (Vella 2015) respectively. Thus if such sites were included in the sample, the global area disturbed (including legacy mines) would be substantially higher.

5.4 Global pressures on biodiversity by metal mining activities

Results allow concluding that, for all metals, the null hypothesis (asserting that the observed distribution of mines and deposits equals the expected by the natural pattern or null model) could be rejected, thereby accepting the alternative hypothesis of an unequal spatial distribution across biodiversity zones around the world. Results were statistically significant at least at a 95% confidence level and are in agreement with previous works stating that the spatial distribution of mines does not follow a random pattern around the world (e.g. Durán et al. 2013).

5.4.1 Adequacy of the mapping approach and coordinates precision

In the last decades the biodiversity conservation planning discipline has been dominated by nine major institutional templates of global biodiversity conservation prioritization which have yielded global priority maps that cover from less than one-tenth to more than a third of the Earth´s land surface (Brooks et al. 2006), among them the Biodiversity Hotspots, Crisis Ecoregions or Centers of Plant Diversity. Nonetheless, if all nine are overlapped, 79% of the land is highlighted by at least one of such prioritization systems. In contrast, in this study it was decided to use a world map of phytodiversity covering a 100% of the land terrestrial surface as a contribution to schemes prioritizing areas of high irreplaceability. Among existing approaches, the inventory-based top-down approach by Barthlott et al. (2007) is regarded as suitable for large scale conservation approaches and matches most grid-based mapping schemes which use a one degree resolution (~12,300 km^2 at the equator and below 10,000 km^2 in temperate regions) (Barthlott et al. 2005).

One of the main advantages of the approach lies in that, at a global scale, the spatial distribution of vascular plants is strongly correlated with the distribution of vertebrate richness and insect diversity, and thereby, their diversity as observed per diversity zone can be used as an approximate indicator for overall biodiversity (Koch 2010). Another gain comes from the fact of being based on a species-area

relationship, which provides justification that habitat loss, e.g. due to land conversion to allow mining, translates into biodiversity loss (Brooks et al. 2006).

However, the main drawback of the method is that it does not include values for all species but only for higher plants. Similarly, it does not consider abundance or conservation value (Baan et al. 2013). In addition, the limits of the applied method lie in the constraints of the data for some tropical and subtropical regions because only fragmentary, outdated or incomplete floras data exist (e.g. Brazil, Madagascar) (Barthlott et al. 1996). Moreover, the use of the Barthlott approach may be controversial with priority-setting schemes prioritizing certain areas of low biodiversity, for instance, proactive approaches like Frontier Forests (Bryant et al. 1997) or Lasts of the Wild (Sanderson et al. 2002). These two approaches prioritize the last large, ecologically intact and relatively undisturbed natural forests in northern Canada and Russia, which, in contrast, are classified as low-biodiversity zones by species richness of vascular plants according to the Barthlott approach.

With regards to the precision of the mine locations sourced from the SNL Metals & Mining database, it was assumed that they were precise enough to fit within the biodiversity areas; this is based on previous research (Kobayashi et al. 2014). Same as this study, such authors acknowledged the lack of precision in the coordinates but, after conducting a sensitivity analysis on the location data of mines, concluded that they were acceptably accurate.

5.4.2 Potential shift of mining activities to lower-biodiversity zones

Results by this dissertation indicate a clear non-random spatial co-occurrence of metal mines and deposits across diversity zones with spatial concentrations in areas of high plant diversity for some metals (Al, Ag, partly for Cu and Fe) and a generally lower-than-expected (or high potential) existence of mining activities in zones of low diversity. This very uneven spatial distribution of mining activities might be explained because the location of metallic ore deposits follows the existence of regional metallogenic provinces (Evans 2009) and because metal provinces, particularly in the case of copper (porphyry deposits), gold and silver, tend to coincide with orogenic belts (Sillitoe 1972). In the case of bauxite, the

majority of economic reserves (around 90%) are located in tropical and sub-tropical regions, namely, between 25° N and 20° S (Bárdossy and Aleva 1990), a fact that explains its spatial coincidence with relative higher plant diversity.

The state of global biodiversity is continuing to decline, with declines being most rapid in the tropics (Armenteras and Finlayson 2012). This may be an incentive to divert mining activities from such areas, especially from the mega-diversity ones. The global spatial distribution of biodiversity and metal mining activities provides an opportunity for re-orienting the mining business towards a higher prioritization of halting biodiversity losses. First and foremost, for all five metals together, results point to the lower-than-expected (by chance) quantity of currently operating mines in low-biodiversity zones (slightly over 13%) and the large availability of metallic ore deposits in such zones (nearly 19% of the total amount of deposits). If the intermediate diversity zone (DZ) 4 is additionally counted, the proportion of deposits available in low and intermediate DZs increases to over 50% of all available deposits considered. These numbers suggest that it is geologically possible to promote a shift of new mining activities from high to low-biodiversity zones.

A more detailed examination of each metal provides a more concrete and regional-based picture. In the case of iron ore, numerous deposits are available in low diversity zones which are already active in Australia (Western Australia, Pilbara region), Russia (Central Russia, Urals and Siberia), Saharan-Africa (Mauritania, Egypt), Mongolia or Chile (Figure 99); future iron ore mining in such zones could be made preferable to those located in rainforest areas like in Brazil´s Iron Quadrangle, Indonesia, Vietnam, Gabon, Congo or Cameroon. This would prevent exerting further pressure on high-biodiversity areas.

If bauxite is considered (Figure 100), while some of the high plant diversity areas already house a high concentration of mines and deposits, e.g. in Vietnam or Brazil, others less biodiverse areas in Australia (regions in the north and north-east), Guinea, Russia, India, the United States or Kazakhstan have the potential of attracting investments and shifting the extractive pressure towards areas with lower biodiversity.

Figure 98: Global location of iron ore mines per DZ. 2014.

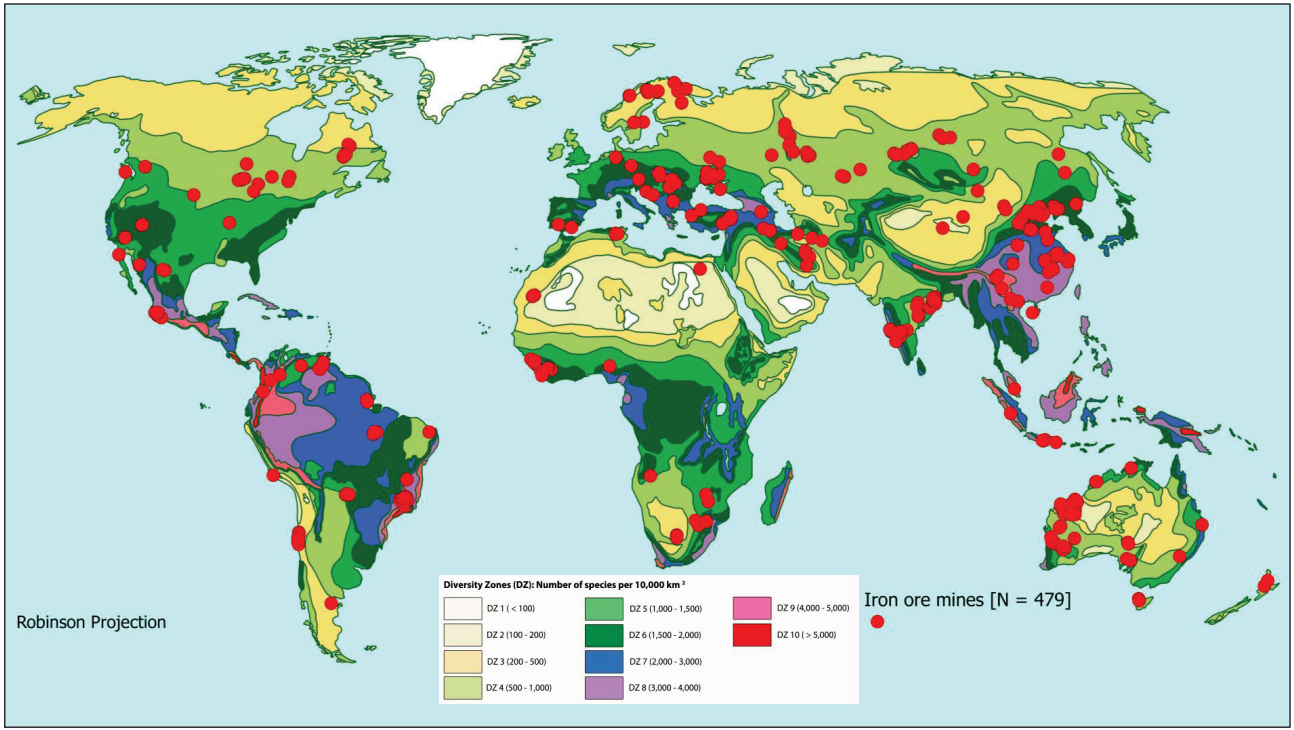

Source: self-elaboration based on Barthlott et al. (2007) and the SNL Metals & Mining database.

Figure 99: Global location of iron ore deposits per DZ. 2014.

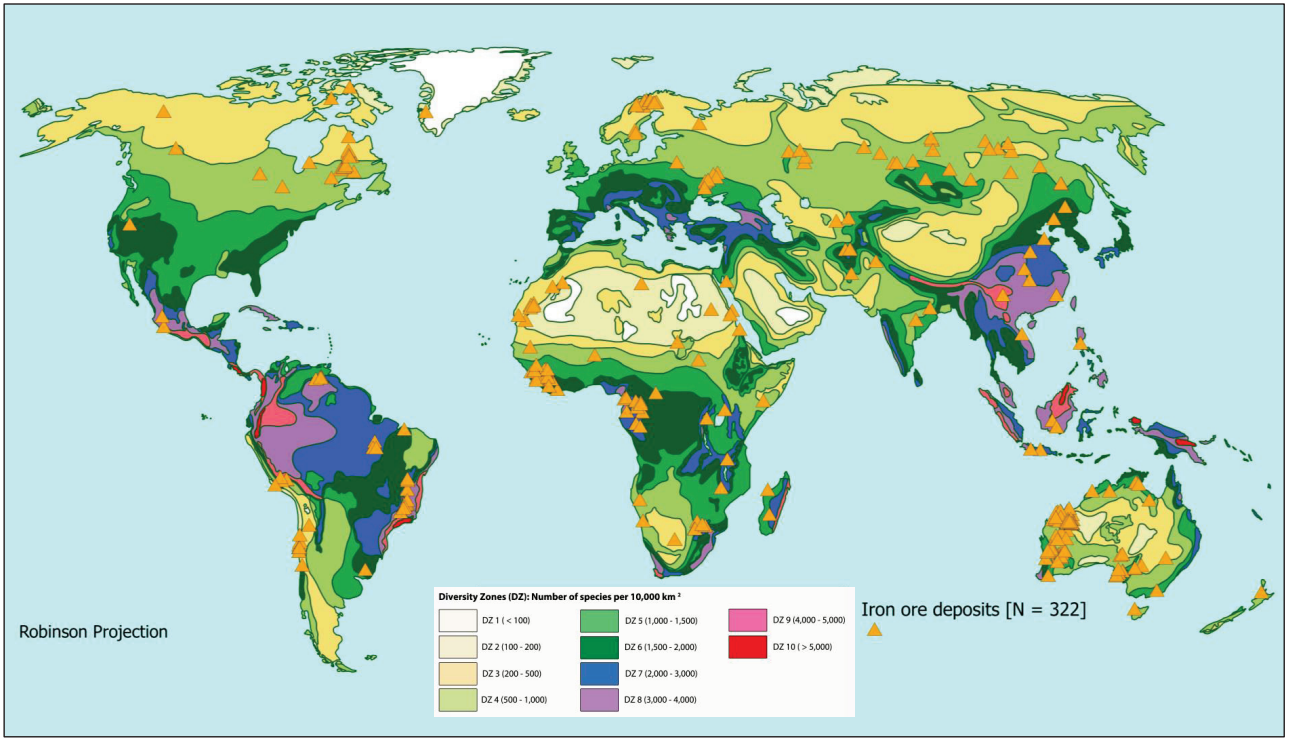

Source: self-elaboration based on Barthlott et al. (2007) and the SNL Metals & Mining database.

Figure 100: Global location of bauxite mines and deposits per DZ. 2014.

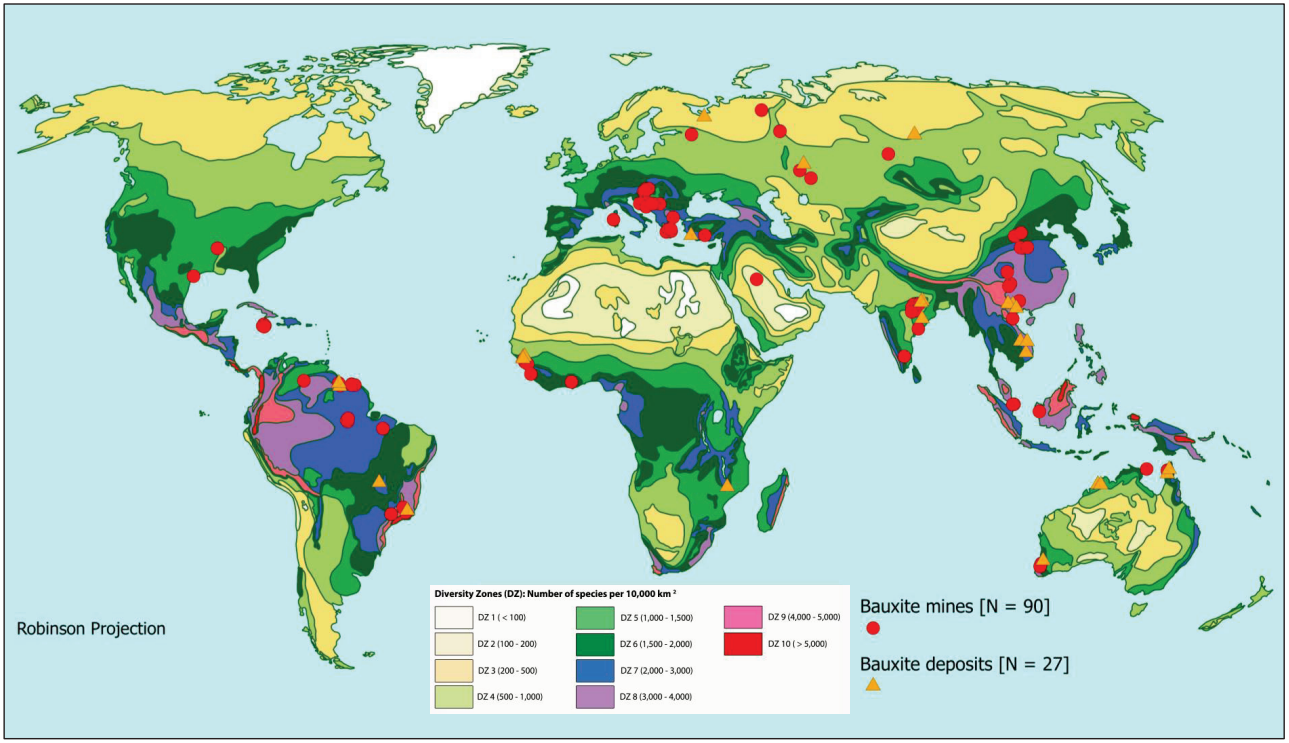

Source: self-elaboration based on Barthlott et al. (2007) and the SNL Metals & Mining database.

Regarding copper, current operations (Figure 101) show already a concentration in low-biodiversity zones: much of the global mine copper is extracted in low-biodiversity areas in Chile, China, Peru, the U.S., Australia and Russia; if low-biodiversity areas within such countries were promoted with deposits located in the Scandinavian countries, Canada, Russia, Kazakhstan or Mongolia, it would become possible to avoid the development of deposits located in biodiversity-rich and often badly-managed zones, e.g. in South East Asia.

With regards to gold mining, the industry is currently exerting a strong pressure on biodiversity-rich regions in the Asia-Pacific and the South-American portions of the rainforest, particularly in three of the mega-diverse regions: Tropical Eastern Andes, Costa Rica-Chocó, and Northern Borneo (Figure 103). However, the option of re-distributing the pressures toward low plant diversity zones is given by the large availability of deposits in Scandinavian countries, Russia, Northern Canada, the U.S., Australia, Chile or Argentina (Figure 104); this could help prevent repeating bad social and environmental practices associated with gold mining in high-biodiversity areas, e.g. riverine tailings disposal, in countries like Indonesia or Papua New Guinea (Cardiff et al. 2012; Banks 2002; Van Zyl et al. 2002b, 2002c).

Given that silver is often produced as a co-product of copper, lead, zinc and gold, a shifting of copper and gold operations would certainly also lower the pressure by silver mining in high diversity zones; moreover, a shift in the case of silver seems feasible given that numerous deposits exist in Australia, Poland, Peru and Chile (the four countries with the largest available silver reserves) to encourage further new mining activities there (Figure 106).

Figure 101: Global location of copper mines per DZ. 2014.

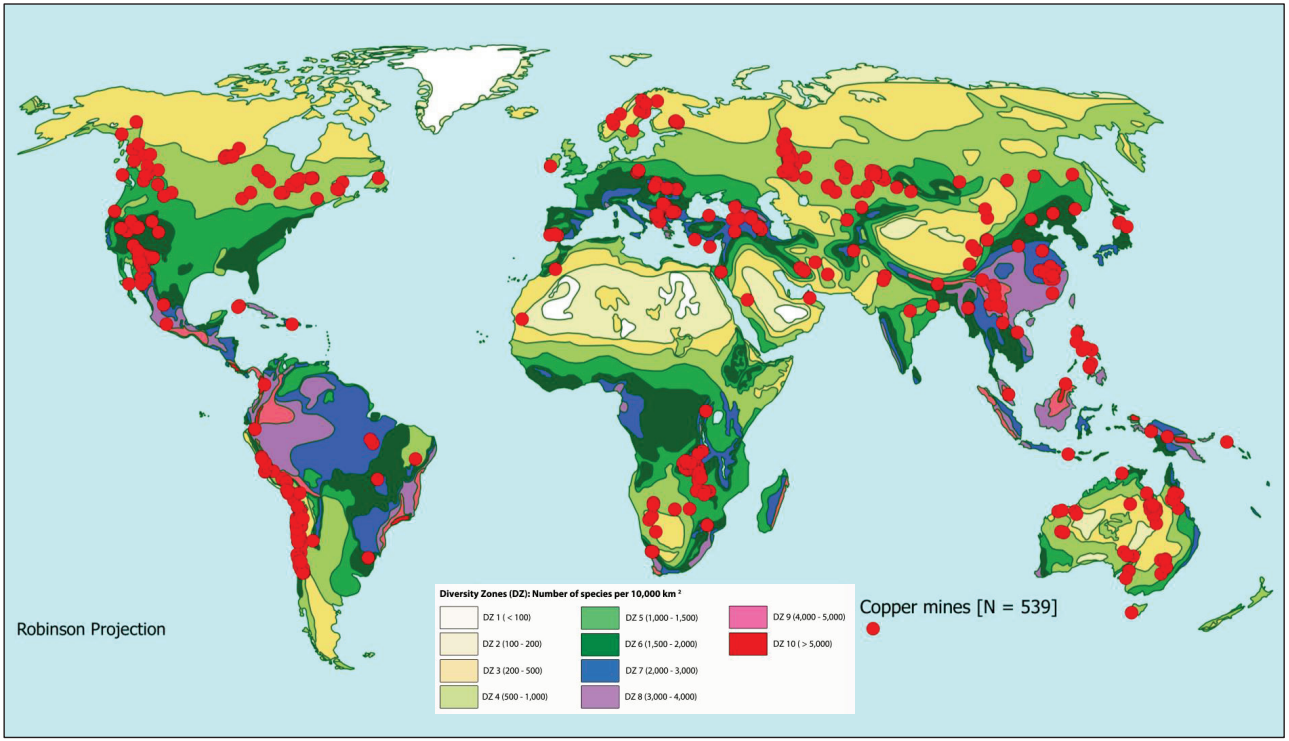

Source: self-elaboration based on Barthlott et al. (2007) and the SNL Metals & Mining database.

Figure 102: Global location of copper deposits per DZ. 2014.

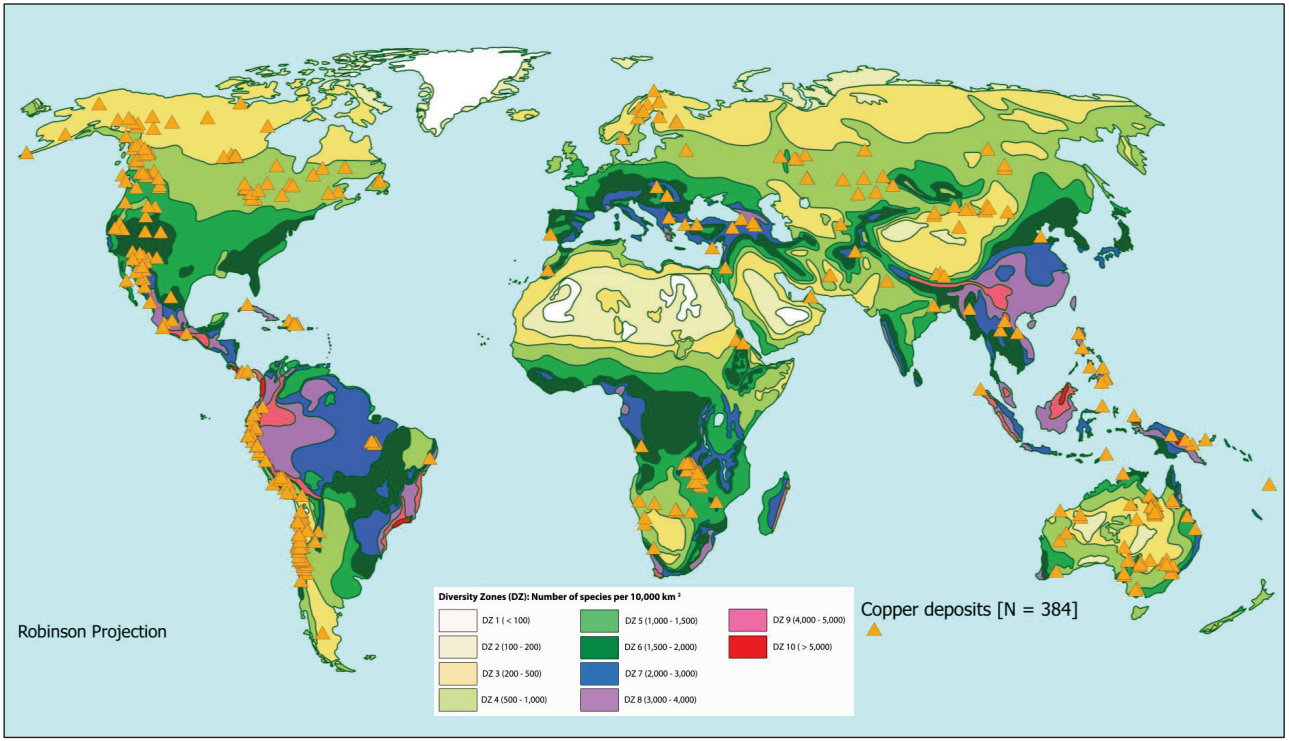

Source: self-elaboration based on Barthlott et al. (2007) and the SNL Metals & Mining database.

Figure 103: Global location of gold mines per DZ. 2014.

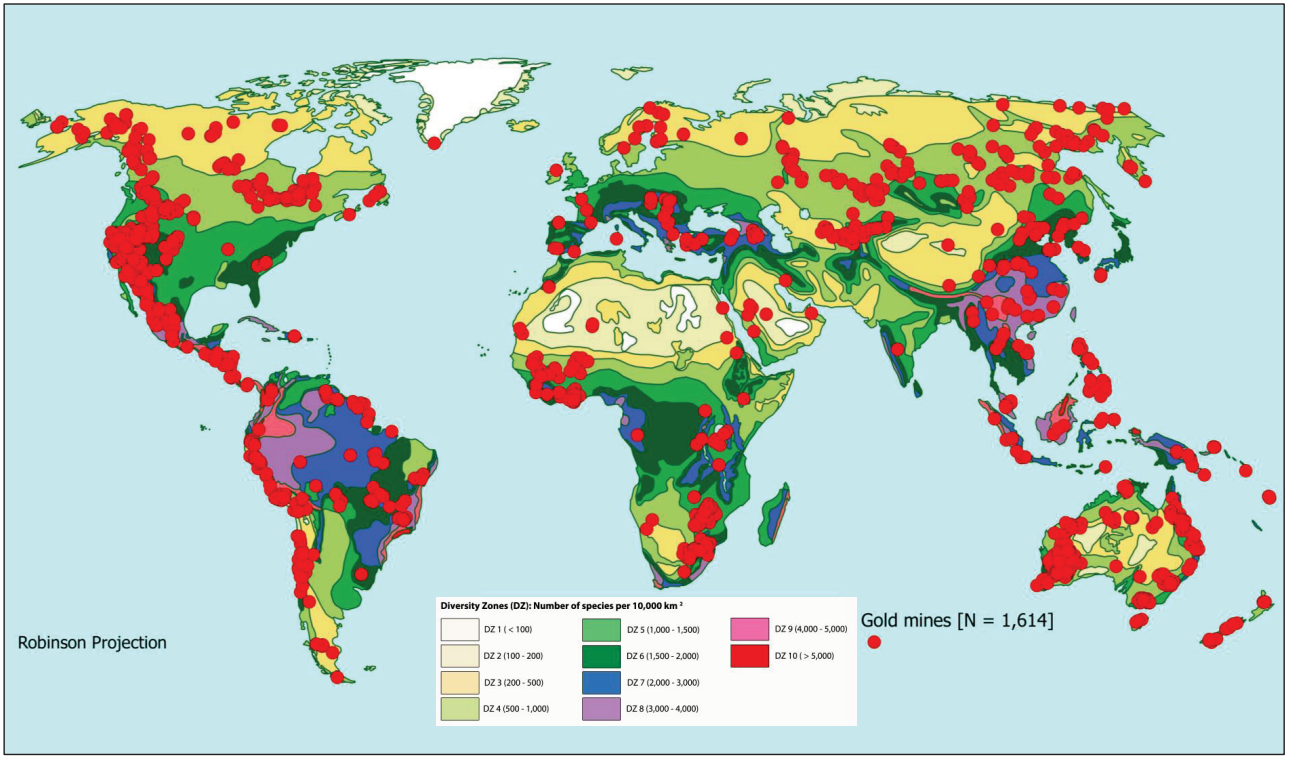

Source: self-elaboration based on Barthlott et al. (2007) and the SNL Metals & Mining database.

Figure 104: Global location of gold deposits per DZ. 2014.

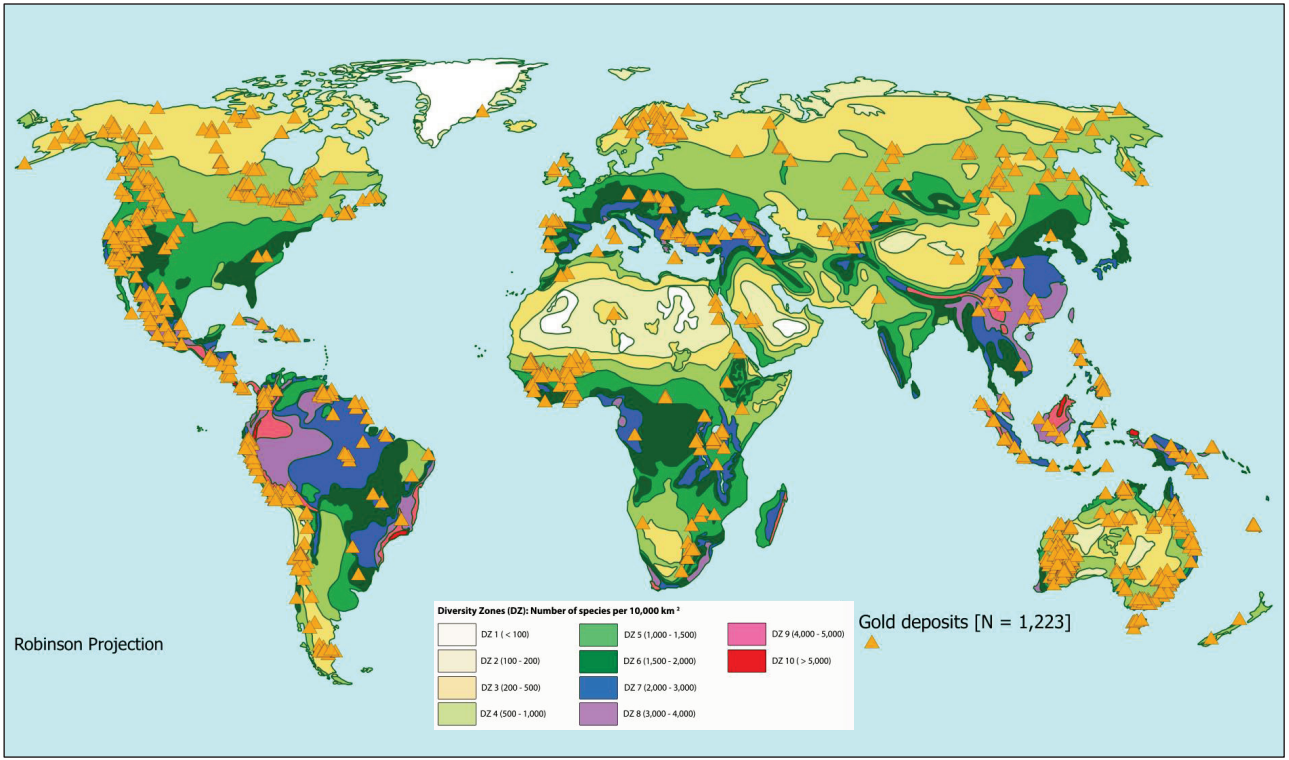

Source: self-elaboration based on Barthlott et al. (2007) and the SNL Metals & Mining database.

Figure 105: Global location of silver mines per DZ. 2014.

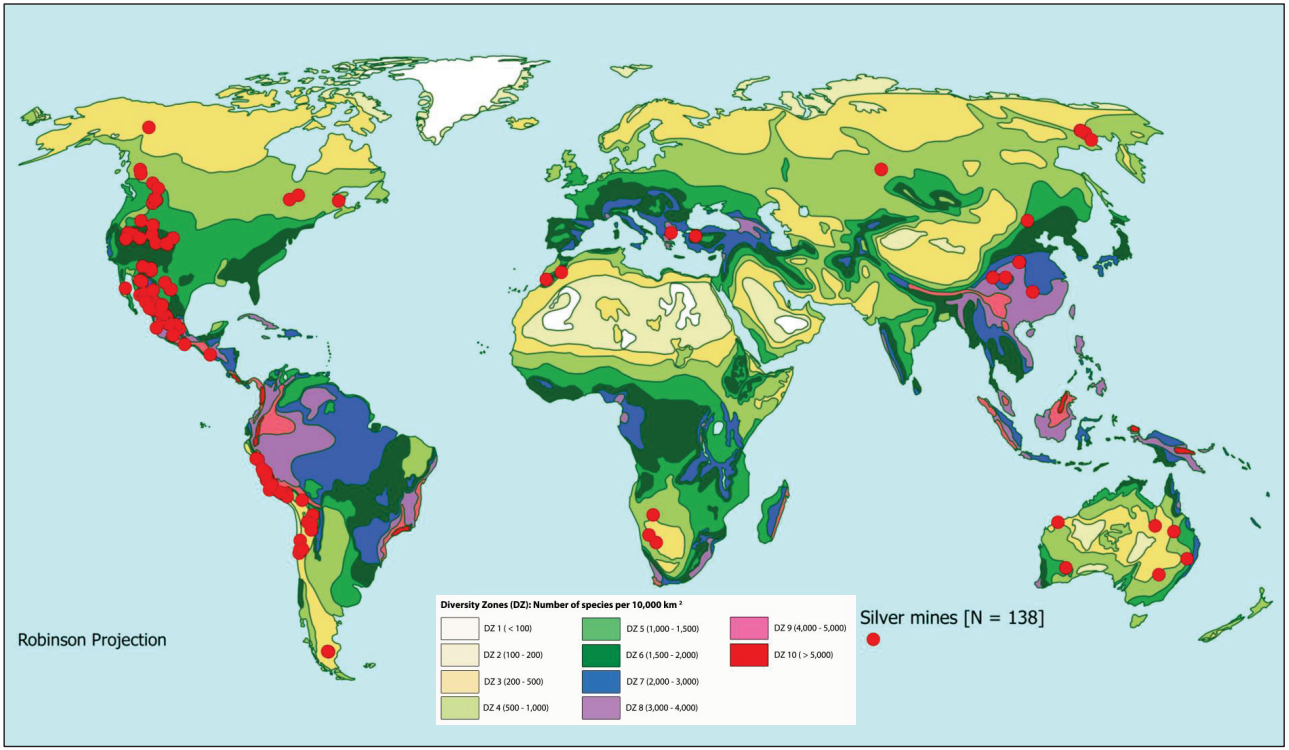

Source: self-elaboration based on Barthlott et al. (2007) and the SNL Metals & Mining database.

Figure 106: Global location of silver deposits per DZ. 2014.

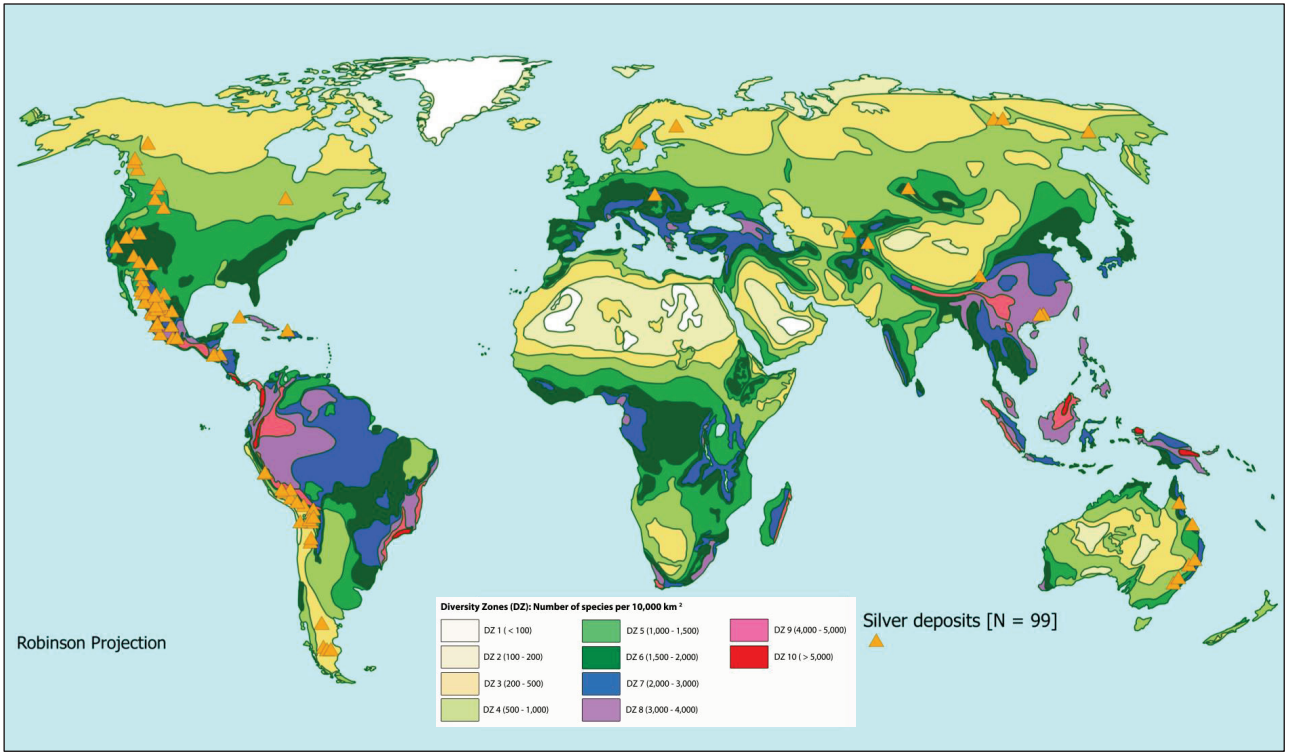

Source: self-elaboration based on Barthlott et al. (2007) and the SNL Metals & Mining database.

5.4.3 Implications for different actors

From a global biodiversity management perspective, the suggestion to support a shift of prospecting-exploration and ore extraction (new mining operations) from higher to lower biodiversity areas may be considered by international organizations like the Intergovernmental Science-Policy Platform on Biodiversity & Ecosystem Services (IPBES). Such a shift would imply that activities are deviated from one region to the other, thereby alleviating pressures and not multiplying them. Firstly, this will require further research in order to specify the conditions under which a mere problem shifting can be avoided and to devise effective management mechanisms, e.g. incentives to encourage exploration and mining investments in low biodiversity areas.

Secondly, such idea would most likely be contested from a national point of view of developing resource-rich countries which may prioritize the extraction of metal ores catering for domestic metal needs or delivering short-term economic profits to long-term biodiversity conservation. For instance, Brazil, third largest producer and second largest holder of iron ore reserves in the world, and home to Vale do Rio Dolce, the world´s largest iron ore producer, is investing to increase production in the coming years following the mounting demand. Both major iron ore deposits (reserves) and producing areas (States of Pará and Minais Gerais) are placed within high biodiversity zones. In lack of any economic incentives (or disincentives such as carbon or deforestation taxes), the proposal to avoid mining in such areas would surely be controversial and it would most likely be disregarded by mining companies and authorities as it goes against a traditional mining culture.

Thirdly, authorities in developing countries may argue that the lack of income derived from mining may act against biodiversity conservation due to lack of funds to stop other extensive land use activities (e.g. land conversion for agriculture, pulp and paper or biodiesel production) or illegal activities associated with unregulated deforestation of diverse ecosystems (e.g. illegal logging or illegal mining which may be much more degrading for the rainforests than industrial mining as exemplified by the Madre de Dios area in Peru, see Asner et al. 2013).

Fourthly, the mining sector may be reluctant to modify investments and feasibility criteria to prioritize low biodiversity regions. On the one hand, results indicate a higher-than-expected spatial concentration of metal mines and deposits in zones of high plant diversity which signals the role the large-scale metal mining sector has and will likely have in the near future as an additional direct cause of human-induced land cover and land-use change (Sonter et al. 2014b), as competitor with other land uses, and potential trigger of land-use disputes (Hilson 2002; Schueler et al. 2011; Smith et al. 2010). On the other hand, the mining industry is much aware of the risks of financial losses due to disruptions in projects developments (Franks et al. 2014), has been for long engaged in dialogue with environmental and social development organizations to address these conflicts and seems open to discuss alternative options for investments. At the same time, however, mining is a capital intensive industry with high sunk costs (Runge 2012) in which the availability of existing infrastructure due to other projects in the region becomes of importance in order to reduce extraction and transportation costs of the mined material. Consequently, ore grades and other economic considerations being equal, when opening up new deposits in mining, areas already active are more attractive than distant areas where greenfield projects and more up front investment would be required.

Fifth, results may be contested by followers of other approaches to determining areas of interest for conservation of biodiversity. For instance, those following the Frontier Forests approach might disagree with the suggestion of encouraging the mining of deposits located in northern Canada or Russia, areas considered of priority for conservation due to the ecologically intact character of the forests. These approaches do not need to confront with the suggestions by this study, a more refined analysis is necessary to apply various criteria to the mines and deposits database and classify deposits according to multiple-criteria.

Sixth, and following from the above paragraph, besides biodiversity richness, other criteria should be considered at local or regional scales before making recommendations of land use and where mining should be encouraged. Metal mining is currently an important cause of social conflict due to various reasons, among them the clash of values among different actors. In South America, in the

Andes mountains, the binational Pascua-Lama gold-silver mega project is located in the border of Chile and Argentina. Such project has been heavily criticized and its construction was suspended on the Chilean side due to claims of pollution and glaciers destruction by indigenous communities. Although the project is located in a comparatively low biodiversity zone (DZ 3), it is home to glaciers which act as regulators of water basins and which deserve protection. This has aroused much concern and rendered, for some stakeholders, incompatible the exploitation of ore deposits located (parcially) below such glaciers (Taillant 2013, 2015; Urkidi and Walter 2010; Fields 2006), with the project still halted for indefinite time. Thus, before any specific recommendations are given, the local situation must be carefully considered.

Finally, if mining was displaced towards areas more distant from the consumption centers and with less developed seaborne transportation routes, this would imply a change in transportation costs and carbon emissions. All these implications require further analysis outside the scope of this investigation.

CHAPTER SIX

This last chapter addresses the dissertation´s limitations, general and specific conclusions per metal. Then some implications of the analysis and conclusions for the metal mining industry are briefly reviewed and the dissertation is closed with some proposals for future research avenues.

6 Conclusions and Implications

6.1 Study limitations

The results, analysis, conclusions and implications derived of this Ph.D. dissertation are delimited by the following aspects:

- **Mine life cycle and indirect impacts**: the study is delimited in the specific land requirement calculations to area disturbances directly caused by mines in operation, suspended or closed, excluding impacts associated with exploration and indirect impacts such as the areas disturbed elsewhere to produce inputs for the mining process (e.g. to produce electric energy);
- **Large-scale metal mines**: results by this study only apply to large-scale metal mines; therefore results should be used neither for artisanal and small-scale mines nor for large-scale mines extracting other metals different from the five major metals investigated;
- **Sample limitations**: the mines included in the samples are limited to industrial mine operations available at the SNL Metals & Mining database. The selection of eligible mines was constrained by the availability of public technical information in Spanish, Portuguese, French, German or English language. During the sampling procedure for the calculation of new net area disturbance factors, mines randomly selected in Russia, China or even India could not be considered eligible because: i) no data or contradictory data was found as to its opening year or annual ore production; ii) the area affected by mine operations could not be (by visual interpretation) spatially separated from other land covers due to lack of relevant information. This

created a certain bias in the geographical location of samples towards mines located in countries with availability of public information like Australia, the U.S., Canada, Brazil, Chile, Peru or some African countries; the bias is particularly high in the case of iron ore mines. This means that specific land requirement calculations may not accurately represent mines in China, Russia or India;

- **Silver specific land requirements**: A particular limitation applies to silver specific land requirement calculations as they were implemented on a sample limited to silver as a co-product of gold and copper. No lead or zinc mines producing silver as a by-product were investigated;
- **Reclamation rates**: the issue of post-mining reclamation was not explicitly addressed in this study because it was not a main aim and because of the limitation in Landsat images to visually identify areas already reclaimed or expected to be reclaimed. Net areas disturbed were measured, excluding any area already reclaimed (if the area was disturbed, it was assumed no successful reclamation had taken place by the time of the measurement);
- **Static specific land requirements**: this study has created scenarios based on a static value of specific land requirements, which could increase in the future due to declining ore grades (requiring more hectares per ton of ore extracted) or be reduced due to increased investments in land rehabilitation;
- **Limitation of the biodiversity pressures analysis**: the analysis and the derived implications associated with pressures on biodiversity are only based on the analysis of the point location of mines and deposits across diversity zones. However, any policy implication needs to assess multiple aspects, namely, an area believed to house low biodiversity might still be very important from a social point of view (e.g. from a religious, historical or cultural stance), a hydrological (as a source of water), from another biodiversity-conservation perspective, among many other perspectives which need to be evaluated before pinpointing a recommendation towards the exploitation of certain deposits against others.

6.2 General conclusions

This dissertation explored the direct specific land requirements by the large-scale metal mining of five major metals in the context of a sustainable management of mineral resources at a global scale. The large-scale metal mining industry has widely embraced the concepts of sustainability, sustainable and responsible mining; yet, at the same time much controversy around social and environmental impacts remain. Land use conflicts are one of these and given the trends of declining ore grades, relative low production costs and an increasing global demand for metals, it is expected that the land use by mines, along with energy and water consumption (main inputs for metal mining) will remain relevant indicators. Energy and water inputs have been extensively studied but land use impacts are in need of a global outlook, hence the motivation for this work.

Conclusions from the methodological development:

- Landsat satellite images (Landsat 5 TM, Landsat 7 ETM+, and Landsat 8 OLI) supported by ancillary information (e.g. high resolution imagery or technical reports) can be reliably used to measure the cumulative net area disturbed by large-scale metal mines, also for less land-intensive underground mines;
- Visually determining and linking the spatial limits of a mine-affected area to a single mine can become very difficult in historic mining districts where several mines and infrastructures are operating together creating a spatial continuum in which individual mines cannot be separated; therefore, single mines in such settings are not eligible for measuring the area disturbances directly linked to them; e.g. the spatial continuum by the Jangada, Itaminas and Córrego de Feijão mines in the state of Minais Gerais in Brazil;
- Identifying successfully reclaimed areas in Landsat images using only visual image interpretation is not possible; for this task, precise ancillary information is required along with ground observations; similar conditions apply to identification of areas affected by subsidence;

- Rule set procedures for the automatic (or semi-automatic) detection and classification of large-scale mines in multiple Landsat images (batch processing) in the eCognition Definiens software remains a challenge for future studies; main reasons for this are the medium spatial resolution of the Landsat images and the lack of a clear spectral signature or other distinct features that can be readily applied to different images in different regions of the world and for different metals;
- In lack of precise pixel-based algorithms, visual image interpretation and manual classification using object-based image analysis, for instance via segmentation in the eCognition Definiens software, can act as a quick and sufficiently precise technique for the classification of and net area measurement of large-scale mines in Landsat image subsets;
- Area measurements resulting from manual classification of segments in Landsat images are influenced by errors stemming from the subjectivity of the analyst; however, for global analyses approaching orders of magnitude in the land transformed by the large-scale mining industry such errors are not significant;
- Combining image-object analysis with visual image interpretation applied to Landsat images provides a low-cost method to monitor the surface dynamics of large-scale metal mines.

General conclusions of this thesis assert that:

- Remote sensing techniques are a useful tool for the monitoring of mining landscapes and their evolution in time;
- Material flow analysis can be combined with remote sensing techniques in order to update and improve MFA and LCA databases according to site-specific measurements in multiple mines around the world;
- Mined material and net area disturbances at mine sites can be correlated via nonlinear regression analysis obtaining moderately to highly significant correlation depending on the mining method. As expected, the more material extracted, the bigger the net area occupied and transformed during

mining; this is in line with assumptions by other studies (e.g., for copper, Martens et al. 2002) and applies much better to open pit mines than to underground mines;

- Active large-scale metal mining activities (excluding abandoned mines) directly occupy a relatively small proportion of the global land surface although it has significant impacts at the local level associated with the transformation of the area. This indicator may be used as a proxy variable to approach other direct impacts (e.g. land degradation, land use change);
- The global cumulative net area disturbed by active large-scale metal mines is forecast to increase by 2050, at a minimum doubling and at a maximum tripling the area in 2011 (in the case of silver). In order to achieve the scenarios with the minimum area disturbances, land rehabilitation and measures to reduce the demand for primary metals (in particular material efficiency increase measures) are required;
- The analysis of bauxite and iron ore mining have shown that there exist theoretical options to reduce the future global cumulative net area disturbed to less than double by 2050 in comparison to 2010 levels; for that energy and material efficiency measures require an urgent deployment, with a double gain if implemented: not only global land disturbances would be significantly reduced but also IPCC´s sectoral CO_2 emission targets could be achieved by 2050;
- The global cumulative net area disturbed by copper, gold and silver mining is also likely to double 2010 levels by 2050 unless recycling increases its global market input share significantly or land rehabilitation is strongly implemented (if land rehabilitation increases, the cumulative net area disturbed decreases and so do the specific land requirements);
- The increasing pressure on land will also exert it on biodiversity-rich zones; mines and deposits are not randomly distributed around the world plant diversity zones but are instead concentrated in certain zones;

- Pressures by mining on biodiversity-rich zones are particularly noteworthy in the cases of bauxite and silver, although iron and copper-producing mines also show a particular concentration in two high-diversity zones; bauxite mines and deposits show the highest spatial concentration in high-biodiversity zones if compared with the other four metals analyzed;
- According to the spatial distribution of deposits and particularly for bauxite, copper and gold, it is expected that further pressures on biodiversity due to mining-induced land conversion will continue in the rainforests of the Amazon and those in Vietnam, Indonesia, Papua New Guinea, the Philippines and some African countries housing promising deposits; the megadiversity zone (DZ 10) is expected to be under pressure due to copper and gold mining, the only metals with deposits located within it;
- The analysis in this thesis indicated the possibility to shift the exploration and opening of new mines from areas of high biodiversity towards low-biodiversity zones; this is particularly salient in the case of copper and gold which host a large number of deposits in zones of low biodiversity.

6.3 Specific conclusions per metal

Iron ore

- Iron ore mines have the lowest specific land requirements (4.25 ha/Mt_{ore}) of all five metals investigated;
- Stock-driven scenarios forecast a peak of global iron ore extraction by 2025 with a reduction in the extraction levels and an increase in the supply of steel scrap recycling, particularly led by developing countries, especially China; however, the global cumulative net area disturbed by iron ore mining is expected to significantly increase (likely more than doubling the 2010 level) by 2050;
- Such global cumulative net area disturbed can be considerably reduced if energy and material efficiency measures are aggressively deployed as soon as possible; the successful implementation of such measures could

not only attain a cut in CO_2 emissions by the steel sector within IPCC´s 2050 targets but also considerably reduce the pressures on land;

- The pressures on biodiversity might be diminished by promoting a spatial de-concentration and a shift of new mining licenses (for expansion of operating mines or development of new deposits) from areas of high biodiversity (DZ 8 and 9) towards areas of relative low biodiversity (DZs 3 and 4); deposits in the latter two zones are abundant and account for roughly 55% of all data analyzed on iron ore deposits.

Bauxite

- Due to the extraction method applied in bauxite mining (large-scale removal of a shallow soil and sub-soil layer) bauxite mines disturb extensive surface areas and have a specific land requirement 1.87 times higher than iron ore mines;
- Bauxite mines have the highest specific land requirement (7.98 ha/Mt_{ore}) of all five metals investigated;
- Unless early and low-level global saturation of per capita in-use aluminium stocks occurs coupled with increases in material efficiency, scenarios project a considerable rise of the global cumulative net area disturbed at least doubling by 2050 the global status quo in 2011;
- Bauxite mines and deposits are located far-more than expected by chance in diversity zones 6 to 8 and in zones 5 to 8 respectively; in contrast, low biodiversity zones 1-4 host a small and far less than expected number of mines and deposits;
- Consequently, the option of shifting new mines towards low-biodiversity zones may be possible but appears more difficult (and unlikely) due to the geographical concentration of mines and deposits in tropical areas around the world, i.e., the low amount of deposits in low biodiversity zones; nevertheless, the analysis shows that options exist, e.g. with deposits located in low-biodiversity zones in regions of Australia, Russia and Kazakhstan.

Copper

- Similar to iron ore, copper-producing mines have a comparatively low specific land requirement (4.25 ha/$Mt_{Cu\ ore}$), lower than gold (6.70 ha/$Mt_{Au\ ore}$) and silver mines (5.53 ha/$Mt_{Ag\ ore}$).
- This can be explained because of the prevalence of polymetallic mines in all three samples: for copper and silver, all mines sampled are polymetallic and for gold 41 mines out of 63 are polymetallic. By allocating ore and area disturbances for polymetallic mines using average metal prices, much of the material has been allocated to copper, which explains the higher amount of annual average copper ore extracted per mine (10.3 Mt/a) in comparison to average annual gold ore (5.44 Mt/a) and silver ore (0.74 Mt/a) extracted per mine; given similar annual average area disturbances per mine (e.g. 46.2 ha/a for copper and 36.4 ha/a for gold, see Table 14), the higher annual ore extraction rate explains the lower weighted disturbance rate of copper (compared to gold);
- Even though global annual primary copper extraction is expected to peak between the years 2030-2040 (depending on cut-off grades, production costs, and the ultimate recoverable copper resources) with a subsequent decrease in the global extraction, the declining ore grades push the global cumulative net area disturbed upwards, at least doubling by 2050 the area disturbed by copper mining (compared to the 2011 level);
- When compared with the null model, pressures on biodiversity by copper mining show a stronger concentration of mines in diversity zones 6 and 7, whereas deposits are more equally distributed;
- The relative high absolute number of copper deposits in low biodiversity zones (mainly DZs 3 and 4 with deposits available in Canada, Scandinavia, Russia, Chile or Australia) indicates the option of a shift in new mines towards these areas, thereby decreasing the pressure and risk of biodiversity loss in tropical areas in Ecuador, Peru, Indonesia, the Philippines or Papua New Guinea, inclusive of mega diversity zones.

Gold

- Due also to declining ore grades and the availability of gold in disseminated deposits, the specific land requirement for gold mines was computed to be high (6.70 ha/$Mt_{Au\ ore}$), the second highest of the five metals investigated;
- Gold operating mines account for the largest absolute number of metal-producing mines in the world with 1,482 large-scale gold-producing mines (coupled and no-coupled production) currently (April 2014) in operation. The number is far larger than for the other metals investigated (second come operating silver-producing mines with 698 records). Nevertheless, the global cumulative net area occupied in 2011 by gold (around 370,000 ha) comes second after copper-producing mines (around 415,000 ha);
- Even though the global annual gold extraction is expected to decline, global annual gold ore extraction is expected to increase in the middle-term driven by declining ore grades; thus, the global cumulative net area disturbed by gold mining activities is expected to at least double by 2050 in comparison to the 2010 level;
- Gold mines and deposits are by and large randomly distributed across the diversity zones around the world, with a concentration of gold-producing mines in DZs 4-6; in absolute terms, there exist many gold-bearing deposits located in low-biodiversity DZs 3 and 4 which indicate the possibility of a shifting of environmentally-risky new gold-mining operating towards these lower-biodiversity regions.

Silver

- Primary silver production is strongly coupled with gold production worldwide and therefore, its specific land requirement (5.53 ha/$Mt_{Ag\ ore}$) is the third largest after those of bauxite (7.98 ha/Mt ore) and gold (6.70 ha/$Mt_{Au\ ore}$);
- The global cumulative net area disturbed by silver mines was found to be the smallest (around 45,000 ha); this may be explained because of the small area disturbances allocated to silver in polymetallic mines via economic value relationships;

- Similar to gold, declining ore grades will irregularly drive up the global annual silver ore extraction. Given the expected growth in silver ore extraction, the global cumulative net area disturbed by silver mining is expected to at a minimum double and at a maximum triple by 2050 in comparison to the 2010 level;
- Substitution of silver with other metals may not be as easy in the future as it would seem today; the metals that may serve as substitutes for silver (gold, nickel) will have similar production peaks and a similar decline in primary production, making substitution a challenge (Sverdrup et al. 2014a), therefore, material efficiency measures (doing more with less) need quick encouragement and deployment;
- Similar to bauxite, the silver sector shows the second highest spatial concentration of mines and deposits in high-biodiversity zones around the world; the frequency distribution was far higher than expected in diversity zones 6 to 8, particularly due to a concentration of mines and deposits in regions of Mexico, Western of the U.S., and Peru. Nonetheless, at the same time, there seems to be enough silver reserves and deposits in lower-biodiversity regions in Australia, Poland, Peru and Chile (the four largest silver-containing reserves countries) to encourage a geographical shift in the new mine production towards these areas.

6.4 Implications for the metal mining industry

The metals mining industry is currently framed by the Sustainable Development Goals (UN Open Working Group 2014), the internationally accepted view that there exist planetary boundaries which constraint human activities (Rockström et al. 2009; Steffen et al. 2015) and the increasing scrutiny of the extractive industry by the civil society (Oxfam America 2014; Earthworks and Oxfam America 2004). Within this frame, the large-scale metal mining industry needs to constantly re-adapt its practice to reduce its pressures on the environment and community´s livelihoods and enhance its benefits to society.

In order to reduce pressures on biodiversity, the industry might consider this dissertations´ recommendations of modifying decision-making processes which

consider predominantly economic aspects when comparing the attractiveness of deposits in feasibility studies towards a more balanced multi-criteria methodology which includes “threats or risks of unacceptable biodiversity losses” in areas of high importance for the conservation of biodiversity. This would imply considering a shift of some mining investments towards areas of lower-biodiversity, setting a new benchmark in the catalogue of good biodiversity management practices, which currently encompass: i) company biodiversity commitments (“no net loss” or “net positive impact” to biodiversity initiatives); ii) “no go” policies (company-wide commitments to avoid mining within areas where harm to biodiversity is unacceptable); iii) mitigation hierarchies; iv) biodiversity action plans, and v) biodiversity reporting (ICMM 2010).

Then, in order to reduce cumulative area disturbances, the industry might increase its investment in land rehabilitation practices; this is actually a trend within the industry which should be reinforced, following for instance, the leading example of bauxite mining in which the industry has announced the goal of achieving a “no net loss area”, namely, a rate of 1:1 between area disturbed by mining and area rehabilitated (International Aluminium Institute 2009). However, the actual practice shows that for other metals, particularly in developing countries, land reclamation rates are low and should be more encouraged, for instance in China. This country is expected to be the main driver of metals´ demand in the next couple of decades while at the same time is anticipated to be a strong producer; however, the land reclamation rate is currently reported to be less than 10% (Liu et al. 2013b). In the case of Australia, a leading country in environmental regulation and protection, Mudd (2004b) determined that, by 2003, of the total cumulative land disturbed by mining in Western Australia, only close to 22% had been preliminary rehabilitated and 15% had been revegetated. This shows the need for more widespread and effective land reclamation practices.

Thirdly, given the forecasts of medium and long-term peaks in primary metal production coupled with a subsequent increase in the scrap flows of metals, mining companies might consider a larger involvement and investments in the secondary metal production business in order to accelerate the deployment of resource efficiency strategies towards a circular economy. Innovation, recycling,

re-using and ecodesign are considered important milestones towards circular economies (European Commission 2014a). Designing for recyclability (e.g. accessible components and easy opening of fastenings) requires cooperation with recycling companies and manufacturing ones which adapt their design process to account for material availability and increased recycling (Graedel and Erdmann 2012) in order to head towards closing the material loop. This is a challenging task since it involves cooperation among producers and suppliers along obscure and complex global supply chains. Therefore, the minerals industry sector (investors, mining companies, smelters and refiners) may consider cooperating more strongly with the different sectors of the metals value chain towards closing the material loop, thereby reducing pressures on land and biodiversity losses.

6.5 Future research avenues

Firstly, future research may develop further the measurement workflow and attempt an application to other metals with substantial direct global mass flows (e.g. manganese, nickel, zinc, chromium), for mineral fuels (coal, oil, oil sands and shales) or industrial minerals in order to refine the research and determine the direct global land use by mineral extraction. Strategic minerals like lithium (battery applications), phosphorus (core component of mineral fertilizers) or uranium (still essential for long-term energy generation) may also be targeted. Scenarios on future global cumulative net area disturbances may also be envisaged for some of these minerals.

Secondly, land rehabilitated might be seeked to be included in the calculations in order to achieve the quantification of cumulative gross area disturbances; this may be done by the integration of field work data or precise geographically-referenced data obtained from Geological Surveys or from mining companies themselves;

Thirdly, the global status quo for metals might be refined by including a larger number of small and medium scale operations which can also be land-intensive (e.g. the Madre de Dios ASM illegal gold mining activities in Peru extend over thousands of hectares) (Asner et al. 2013). These areas can also be visually detected and measured by means of Landsat satellite imagery. Also the global status quo of the area disturbed by metal mining would be substantially improved if

abandoned and orphaned mines (e.g. estimated to be over 50,000 in Australia) were included in the calculation.

Fourthly, in order to reduce the time-consuming activity of dealing with manual classification, crowdsourcing with trained analysts may be an option. Yet, further research should seek to obtain very high resolution imagery for these purposes, e.g. through foundations which can freely provide this kind of imagery for scientific purposes, for instance the Digital Globe foundation (Digital Globe Foundation 2015). Having such imagery available automatic or semi-automatic rule set may be developed in the eCognition Definiens software to increase the number of sample mines processed.

Fifth, in order to verify and refine specific land requirement calculations, future research calculations of new net area disturbances might include investigating variables excluded from this study. It could be hypothesized that the amount of land directly disturbed by mining is not only depending on the amounts of material extracted but also in the country where the mines are located since mining practices depend on countries´ regulations. For instance, countries or regions with stricter environmental regulations might be influencing the areal extent of the landforms (compactness) created by mining companies. The research could be approached by performing multiple regressions with more terms to the right of the regression equation, for instance using human development indexes per country. In order to perform such task, the bias in the sample caused by the availability of public information to verify the land dynamics should also be overtaken by expanding the sample towards mines operating in China, Russia and other countries excluded from the samples analysed.

Finally, with regards to the analysis of pressures on biodiversity, future research may seek to make a multi-criteria spatial analysis combining the Barthlott et al. approach with other criteria to define which areas have a high value for conservation, thereby enhancing the richness of the approach and the likelihood of acceptance of the proposal to shift future new mining operations towards areas of lower-biodiversity.

CHAPTER SEVEN

7 References

Abd El-Kawy, O.R., J.K. Rød, H.A. Ismail, and A.S. Suliman. 2011. Land use and land cover change detection in the western Nile delta of Egypt using remote sensing data. *Applied Geography* 31(2): 483–494.

Alcamo, J. 2001. *Scenarios as Tools for International Environmental Assessment*. Environmental Issue Report. Copenhagen: European Environment Agency.

Alcamo, J., K. Kok, G. Busch, J.A. Priess, B. Eickhout, M. Rounsevell, D.S. Rothman, and M. Heistermann. 2006. Searching for the Future of Land: Scenarios from the Local to Global Scale. In *Land-Use and Land-Cover Change*, ed. by Eric F. Lambin and Helmut Geist, 137–155. Global Change - The IGBP Series. Springer Berlin Heidelberg. http://link.springer.com/chapter/10.1007/3-540-32202-7_6. Accessed May 12, 2015.

Ali, S.H. 2009. *Mining, the Environment, and Indigenous Development Conflicts*. University of Arizona Press, August 1.

Allison, P. 2009. Missing Data. In *Handbook of Quantitative Methods in Psychology*, ed. by Roger Millsap and Alberto Maydeu-Olivares. Thousand Oaks, CA: Sage Publications INc.

Allwood, J.M., M.F. Ashby, T.G. Gutowski, and E. Worrell. 2011. Material efficiency: A white paper. *Resources, Conservation and Recycling* 55(3): 362–381.

Almeida-Filho, R. and Y.E. Shimabukuro. 2002. Digital processing of a Landsat-TM time series for mapping and monitoring degraded areas caused by independent gold miners, Roraima State, Brazilian Amazon. *Remote Sensing of Environment* 79(1): 42–50.

Anderson, A.T., D. Schultz, N. Buchman, and H.M. Nock. 1977. Landsat imagery for surface-mine inventory. *Photogrammetric Engineering and Remote Sensing* 43(8). http://trid.trb.org/view.aspx?id=59686. Accessed November 14, 2014.

Andresen, T., C. Mott, S. Zimmermann, T. Schneider, and A. Melzer. 2002. Object-oriented information extraction for the monitoring of sensitive aquatic environments. In *Geoscience and Remote Sensing Symposium, 2002. IGARSS '02. 2002 IEEE International*, 5:3083–3085 vol.5.

Andrews-Speed, C.P., R. Bleischwitz, T. Boersma, C. Johnson, G. Kemp, and S.D. Van Deveer. 2014. *Want, waste or war?: the global resource nexus and the struggle for land, energy, food, water and minerals*. Abingdon, Oxon ; New York, NY: Routledge.

Andrews-Speed, P., R. Bleischwitz, T. Boersma, C. Johnson, G. Kemp, and S.D. VanDeveer. 2012. *The Global Resource Nexus. The Struggles for Land, Energy, Food, Water, and Minerals*. Washington D.C.: Transatlantic Academy, May.

ArcelorMittal. 2012. ArcelorMittal Mining Canada Expansion June.

Armenteras, Dolores, and Max Finlayson, eds. 2012. Chapter 5. Biodiversity. In *Global Environmental Outlook 5. Environment for the Future We Want.* Malta: Progress Press Ltd.

Arrhenius, O. 1921. Species and area. *Journal of Ecology* 9: 95–99.

Asner, G.P., A.J. Elmore, L.P. Olander, R.E. Martin, and A.T. Harris. 2004. Grazing Systems, Ecosystem Responses, and Global Change. *Annual Review of Environment and Resources* 29(1): 261–299.

Asner, G.P., W. Llactayo, R. Tupayachi, and E.R. Luna. 2013. Elevated rates of gold mining in the Amazon revealed through high-resolution monitoring. *Proceedings of the National Academy of Sciences* 110(46): 18454–18459.

Avila de Moura, A. 2007. Chapada mine. Minera Mineração Marac ão Maracá Ind. e Com. November.

Ayres, R.U. 1989. Industrial Metabolism. In *Technology and Environment*, ed. by Jesse Ausubel and Hedy Sladovich. National Academy of Engineering.

Ayres, R.U. 1993. *Industrial Metabolism - closing the materials cycle*. Ed. by Tim Jackson. Boca Raton/New York: CRC Press. http://www.crcpress.com/product/isbn/9780873718844. Accessed December 9, 2014.

Ayres, R.U. 1994a. Industrial metabolism: Theory and practice. In *The Greening of Industrial Ecosystems*, ed. by B.R. Allenby and Deanna Richards, 23–37. Washington D.C.: National Academy Press.

Ayres, R.U. 1994b. Industrial Metabolism: Theory and Policy. In *Industrial Metabolism: Restructuring for Sustainable Development*. Tokyo ; New York: United Nations University.

Ayres, R.U., L.W. Ayres, and I. Råde. 2003. *The life cycle of copper, its co-products and byproducts*. Dordrecht, The Netherland: Kluwer Academic Publishers.

Azapagic, A. 2004. Developing a framework for sustainable development indicators for the mining and minerals industry. *Journal of Cleaner Production* 12(6): 639–662.

Baan, L. de, R. Alkemade, and T. Koellner. 2013. Land use impacts on biodiversity in LCA: a global approach. *The International Journal of Life Cycle Assessment* 18(6): 1216–1230.

Banks, G. 2002. Mining and the Environment in Melanesia: Contemporary Debates Reviewed. *The Contemporary Pacific* 14(1): 39–67.

Bárdossy, G. and G.J.J. Aleva. 1990. *Lateritic Bauxites*. Developments in Economic Geology 27. Amsterdam, The Netherlands: Elsevier Science Ltd.

Barreto, H. and F. Howland. 2006. *Introductory Econometrics Using Monte Carlo Simulation with Microsoft Excel*. Cambridge University Press, March. http://www.cambridge.org/gb/academic/subjects/economics/econometrics-statistics-and-mathematical-economics/introductory-econometrics-using-monte-carlo-simulation-microsoft-excel. Accessed January 19, 2015.

Barthlott, W., A. Hostert, G. Kier, W. Kueper, H. Kreft, J. Mutke, M.D. Rafiqpoor, and J.H. Sommer. 2007. Geographic patterns of vascular plant diversity at continental to global scales. *Erdkunde* 61(4): 305–315.

Barthlott, W., W. Lauer, and A. Placke. 1996. Global distribution of species diversity in vascular plants: Towards a world map of phytodiversity. *ERDKUNDE* 50(4): 317–327.

Barthlott, W., J. Mutke, M.D. Rafiqpoor, G. Kier, and H. Kreft. 2005. Global Centers of Vascular Plant Diversity. *Nova Acta Leopoldina* 92(342): 61–83.
Bateman. 1998. *Feasibility Study Varvarinskoye Gold-Copper Project. Summary Report*. Kazakhstan Minerals Corporation, June.
Bauer, T. and G. Kaiser. 2006. Knowledge Transfer - Formalising an interpretation key. In *1st International Conference on Object-Based Image Analysis (OBIA 2006)*. Salzburg, July 4.
Beadell Resources Ltd. 2008. Cracow gold mine. A Unique investment opportunity. April.
Beaubien, J. 1986. Visual interpretation of vegetation through digitally enhanced LANDSAT-MSS images. *Remote Sensing Reviews* 2(1): 111–143.
Bebbington, A. 2011. *Social Conflict, Economic Development and the Extractive Industry: Evidence from South America*. Routledge, October 13.
Bebbington, A., L. Hinojosa, D.H. Bebbington, M.L. Burneo, and X. Warnaars. 2008. Contention and Ambiguity: Mining and the Possibilities of Development. *Development and Change* 39(6): 887–914.
Bebbington, A.J. 2014. Socio-environmental conflict: an opportunity for mining companies. *Journal of Cleaner Production* 84. Special Volume: The sustainability agenda of the minerals and energy supply and demand network: an integrative analysis of ecological, ethical, economic, and technological dimensions: 34.
Bebbington, A. and M. Williams. 2008. Water and Mining Conflicts in Peru. *Mountain Research and Development* 28(3/4): 190–195.
Behre Dolbear. 2010. *NMDC Ltd. JORC equivalent reserve estimate statement (Behre Dolbear Project Number J10-012)*. Kent, UK, January 21.
Belanger, M. 2003. *Technical Report La Coipa Mine, Chile*. Toronto, Canada: Kinross Gold Corporation, May 5.
Bellard, C., C. Bertelsmeier, P. Leadley, W. Thuiller, and F. Courchamp. 2012. Impacts of climate change on the future of biodiversity: Biodiversity and climate change. *Ecology Letters* 15(4): 365–377.
BGR. 2013. *Aluminium/Bauxite*. Rohstoffwirtschaftliche Steckbriefe. Hannover, Germany: Bundesanstalt für Geowissenschaften und Rohstoffe, November. http://www.bgr.bund.de/DE/Themen/Min_rohstoffe/Downloads/rohstoffsteckbrief_al.pdf?__blob=publicationFile&v=7.
BHP Billiton. 2002. *Mining Area C Development. Port Hedland Port & Capacity Expansion*. Briefing Paper. April.
BHP Billiton. 2012. BHP Billiton Iron Ore - Growth and Outlook March 20.
Blaschke, T. 2010. Object based image analysis for remote sensing. *ISPRS Journal of Photogrammetry and Remote Sensing* 65(1): 2–16.
Blaschke, T., G.J. Hay, M. Kelly, S. Lang, P. Hofmann, E. Addink, R. Queiroz Feitosa, et al. 2014. Geographic Object-Based Image Analysis - Towards a new paradigm. *Isprs Journal of Photogrammetry and Remote Sensing* 87(100): 180–191.
Blaschke, T. and J. Strobl. 2001. What's wrong with pixels? Some recent developments interfacing remote sensing and GIS. *GeoBIT/GIS* 6: 12–17.
Bleischwitz, R., B. Bahn-Walkowiak, F. Ekardt, H. Feldt, and L. Fuhr. 2012. *International Resource Politics: New challenges demanding new governance approaches for a green economy*. Publication Series on

Ecology. Berlin: Heinrich Böll Stiftung and Wuppertal Institute. http://www.boell.de/en/content/international-resource-politics. Accessed April 22, 2014.
Boge, V. 1998. Mining, Environmental Degradation and War: the Bougainville Case. In *Ecology, Politics and Violent Conflict*, ed. by M. Suliman. London: Zed Books.
Boliden Mineral. 2014. *Updated Mineral Reserves and Resources estimate for the Aitik Copper-Gold Operation, Northern Sweden*. May 5.
Boon, M. 2013. Mt Rawdon May.
Börjeson, L., M. Höjer, K.-H. Dreborg, T. Ekvall, and G. Finnveden. 2006. Scenario types and techniques: Towards a user's guide. *Futures* 38(7): 723–739.
Bowles, A.A. and G.T. Prickett. 2001. Footprints in the jungle: natural resource industries, infrastructure, and biodiversity conservation.: xix + 332 pp.
Brattebø, H., H. Bergsdal, N.H. Sandberg, J. Hammervold, and D.B. Müller. 2009. Exploring built environment stock metabolism and sustainability by systems analysis approaches. *Building Research & Information* 37(5-6): 569–582.
Bridge, G. 2004. Contested Terrain: Mining and the Environment. *Annual Review of Environment and Resources* 29(1): 205–259.
Briggs, D. 2005. *Mining Operations Report. Yanacocha Complex*. October 5.
Bringezu, S. 2015. Possible Target Corridor for Sustainable Use of Global Material. *Resources* 4(1): 25–54.
Bringezu, S. and R. Bleischwitz. 2013. Preventing a resource curse fuelled by the green economy. In *Global Corruption Report: Climate Change*, ed. by Transparency International. Routledge, November 26.
Bringezu, S. and Y. Moriguchi. 2002. Material flow analysis. In *A Handbook of Industrial Ecology*, ed. by Robert U Ayres and Leslie W. Ayres. Cheltenham, UK ; Northampton, MA: Edward Elgar Publishing Ltd.
Bringezu, S., M. O'Brien, and H. Schütz. 2012. Beyond biofuels: Assessing global land use for domestic consumption of biomass. *Land Use Policy* 29(1): 224–232.
Bringezu, S., I. van de Sand, H. Schütz, R. Bleischwitz, and S. Moll. 2009. Analysing global resource use of national and regional economies across various levels. In *Sustainable Resource Management*, ed. by Stefan Bringezu and Raimund Bleischwitz. Sheffield, UK: Greenleaf Publishing.
Bringezu, S. and H. Schütz. 1995. Wie mißt man die ökologische Zukunftsfähigkeit einer Volkswirtschaft? Ein Beitrag der Stoffstrombilanzierung am Beispiel der Bundesrepublik Deutschland. In *Neue Ansätze Der Umweltstatistik: Ein Wuppertaler Werkstattgespräch*, ed. by Stefan Bringezu, 26–54. Berlin: Birkhäuser Verlag.
Bringezu, S., H. Schütz, P. Schepelmann, U. Lange, J. von Geibler, K. Bienge, K. Kristof, et al. 2008. *Optionen einer nachhaltigen Flächennutzung und Ressourcenschutzstrategien unter besonderer Berücksichtigung der nachhaltigen Versorgung mit nachwachsenden Rohstoffen*. Wuppertal: UBA/Wuppertal Institute.
Bringezu, Stefan, and Raimund Bleischwitz, eds. 2009. *Sustainable Resource Management. Global Trends, Visions and Policies.* Sheffield, UK: Greenleaf Publishing, September.

Bronshtein, I.N., Semendayev, G. Musiol, and H. Muehlig. 2004. *Handbook of mathematics*. 4th ed. Berlin ; New York: Springer.

Brooks, T. 2010. Conservation planning and priorities. In *Conservation Biology for All*, ed. by Navjot S. Sodhi and Paul R. Ehrlich, 199–219. Oxford University Press, January 1. http://www.oxfordscholarship.com/view/10.1093/acprof:oso/9780199554232.001.0001/acprof-9780199554232-chapter-12. Accessed January 2, 2015.

Brooks, T.M., R.A. Mittermeier, G.A.B. da Fonseca, J. Gerlach, M. Hoffmann, J.F. Lamoreux, C.G. Mittermeier, J.D. Pilgrim, and A.S.L. Rodrigues. 2006. Global Biodiversity Conservation Priorities. *Science* 313(5783): 58–61.

Brown, T.J., N.E. Idoine, E.R. Raycraft, R.A. Shaw, E.A. Deady, J. Rippingale, T. Bide, C.E. Wrighton, and J. Rodley. 2014. *World mineral production 2008-12*. Nottingham: British Geological Survey.

Brummit, N. and S. Bachman. 2010. *Plants under pressure - a global assessment. The first report of the Sampled Red List Index for Plants.* Richmond, Surrey, UK: Kew, Natural History Museum, IUCN, Missouri Botanical Garden, ZSL.

Bryant, D., D. Nielsen, and L. Tangley. 1997. *Last Frontier Forests: Ecosystems and economies on the edge*. World Resources Institute Forest Frontiers In, March 1. http://forests.wri.org/pubs_description.cfm?PubID=2619. Accessed November 27, 2014.

Buchert, M., D. Schüler, and D. Bleher. 2009. *Critical Metals for Future Sustainable Technologies and their Recycling Potential*. July.

BUND, and MISEREOR, eds. 1997. *Zukunftsfähiges Deutschland: Ein Beitrag zu einer global nachhaltigen Entwicklung*. Auflage: 4. Aufl. Basel u.a.: Birkhäuser Verlag.

Bureau of International Recycling. 2014. *World Steel Recycling in Figures 2009-2013. Steel scrap - a raw material for steelmaking*. Brussels, May. http://www.bdsv.org/downloads/weltstatistik_2009_2013.pdf.

Burt, C.N. 2008. An optimisation approach to materials handling in surface mines. PhD Thesis, Curtin University of Technology, August.

Campbell, J. 2007. *Introduction to Remote Sensing*. London: Taylor & Francis.

Cardiff, S., C. Coumans, R. Hart, P. Sampat, and B. Walker. 2012. *Troubled Waters. How mine waste dumping is poisoning our oceans, rivers and lakes.* Earthworks and Mining Watch Canada.

Cardinale, B.J., J.E. Duffy, A. Gonzalez, D.U. Hooper, C. Perrings, P. Venail, A. Narwani, et al. 2012. Biodiversity loss and its impact on humanity. *Nature* 486(7401): 59–67.

Chelopech Mining EAD. 2010. *Chelopech Mine Expansion Project. Non-Technical Summary*. Sofia, August.

Chen, J., X. Zhu, J.E. Vogelmann, F. Gao, and S. Jin. 2011. A simple and effective method for filling gaps in Landsat ETM+ SLC-off images. *Remote Sensing of Environment* 115(4): 1053–1064.

Chitade, A. and S.K. Katyar. 2010. Impact analysis of open cast coal mines on land use/land cover using remote sensing and GIS technique: a case study. *International Journal of Engineering Science and Technology* 2(12): 7171–7176.

Classen, M., H.-J. Althaus, M. Tuchschmid, N. Jungbluth, G. Doka, M. Faist Emmenegger, W. Scharnhorst, and S. Blaser. 2007. *Life Cycle Inventories*

of Metals. Final report ecoinvent data v.20, No 10. Dübendorf, CH: EMPA Dübendorf, Swiss Centre for Life Cycle Inventories.
Coffey Mining Pty Ltd. 2010. *Corihuarmi gold project. National Instrument 43-101 Technical report*. April 6.
Cohen, W.B., Z. Yang, and R. Kennedy. 2010. Detecting trends in forest disturbance and recovery using yearly Landsat time series: 2. TimeSync — Tools for calibration and validation. *Remote Sensing of Environment* 114(12): 2911–2924.
Comber, A.J. 2008. Land use or land cover? *Journal of Land Use Science* 3(4): 199–201.
Convention on Biological Diversity. 2014. Article 2. Use of Terms. http://www.cbd.int/convention/articles/default.shtml?a=cbd-02.
Cooke, J.A. and M.S. Johnson. 2002. Ecological restoration of land with particular reference to the mining of metals and industrial minerals: A review of theory and practice. *Environmental Reviews* 10(1): 41–71.
Copper One. 2014. Expanding our Quebec Copper Portfolio. Investor Presentation May.
Craig Vogt Inc. 2012. International Assessment of Marine and Riverine Disposal of Mine Tailings. Draft report. September 30 2012 presented at the Meeting of the 34th London Convention & the 7th Meeting of the London Protocol, November 1.
Cristiane, F. and F. Fabrina. 2013. *Mineração e Violações de Direitos: O Projeto Ferro Carajás S11D, da Vale S.A. Relatório da Missão de Investigação e Incidência.*
Crompton, P. 1999. Forecasting steel consumption in South–East Asia. *Resources Policy* 25(2): 111–123.
Crowson, P. 2012. Some observations on copper yields and ore grades. *Resources Policy* 37(1): 59–72.
Cullen, J.M., J.M. Allwood, and M.D. Bambach. 2012. Mapping the Global Flow of Steel: From Steelmaking to End-Use Goods. *Environmental Science & Technology* 46(24): 13048–13055.
Curi, A. and H. Mota de Lima. 2002. Qualitative analysis of mining environmental sustainability: myth and reality. In *Indicators of Sustainability for the Mineral Extraction Industry*, ed. by Roberto C. Villas Bôas and Christian Beinhoff, 47–60. Rio de Janeiro: CNPq/CYTED, June.
Davidson, R. and J.G. MacKinnon. 1999. Bootstrap Testing in Nonlinear Models. *International Economic Review* 40(2): 487–508.
Davis, G.A. 1995. Learning to love the Dutch disease: Evidence from the mineral economies. *World Development* 23(10): 1765–1779.
Davis, G.A. and J.E. Tilton. 2005. The resource curse. *Natural Resources Forum* 29(3): 233–242.
Demirel, N., M.K. Emil, and H.S. Duzgun. 2011. Surface coal mine area monitoring using multi-temporal high-resolution satellite imagery. *International Journal of Coal Geology* 86(1). Applications of Remote Sensing and GIS for Monitoring of Coal Fires, Mine Subsidence, Environmental Impacts of Coal-mine Closure and Reclamation: 3–11.

Department of Environment and Conservation. 2012. *Environmental Protection Act 1986, - Amendment to Conditions of Licence L5960/1983/10. Boddington Bauxite mine*. February.
Digital Globe Foundation. 2015. How to apply for an imagery grant. http://www.digitalglobefoundation.org/application-process.
Dingle Robertson, L. and D.J. King. 2011. Comparison of pixel- and object-based classification in land cover change mapping. *International Journal of Remote Sensing* 32(6): 1505–1529.
Dittrich, M., S. Giljum, S. Lutter, and C. Polzin. 2012. *Green economies around the world? Implications of resource use for development and the environment.* Vienna.
Dolman, A.J., A. Verhagen, and C.A. Rovers. 2003. *Global Environmental Change and Land Use*. Dordrecht: Springer Netherlands. http://dx.doi.org/10.1007/978-94-017-0335-2. Accessed December 3, 2014.
Douglas, I. and N. Lawson. 2002. Material flows due to mining and urbanization. In *A Handbook of Industrial Ecology*, ed. by Robert U Ayres and Leslie W. Ayres. Gloucestershire, UK: Edward Elgar Publishing Ltd.
Dubovyk, O., G. Menz, C. Conrad, F. Thonfeld, and A. Khamzina. 2013. Object-based identification of vegetation cover decline in irrigated agro-ecosystems in Uzbekistan. *Quaternary International* 311. Hydrological and Ecological Responses to Climatic Change and to Land-use/land-cover changes in Central Asia: 163–174.
Dundee Precious Metals Inc. 2011. *Technical report for the Chelopech Project, Bulgaria*. Toronto, Canada, March 24.
Durán, A.P., J. Rauch, and K.J. Gaston. 2013. Global spatial coincidence between protected areas and metal mining activities. *Biological Conservation* 160: 272–278.
Duro, D.C., S.E. Franklin, and M.G. Dubé. 2012. A comparison of pixel-based and object-based image analysis with selected machine learning algorithms for the classification of agricultural landscapes using SPOT-5 HRG imagery. *Remote Sensing of Environment* 118: 259–272.
Du, X. and T.E. Graedel. 2011. Global In-Use Stocks of the Rare Earth Elements: A First Estimate. *Environmental Science & Technology* 45(9): 4096–4101.
Düzgün, Ş. and N. Demirel. 2011. *Remote Sensing of the Mine Environment.* Leiden, The Netherlands: CRC Press/Balkema.
EAA, IAI, OEA. 2009. *Global Aluminium Recycling: a Cornerstone of Sustainable Development.*
Earthworks and Oxfam America. 2004. *Dirty Metals. Mining, Communities and the Environment.* Washington D.C.
Ebbels, A.-M., P. Fairfield, R. Lewis, and P. Munro. 2012. *NI 43-101 Technical Report for Osborne Copper-Gold Project located in northwest Queensland Region of Australia*. Melbourne, Vic.: SRK Consulting, November 2.
Ecologia Environment. 2005. *Koolan Island Iron Ore mine and port facility. Conceptual closure plan.* West Perth, November.
EEA. 2009. *Looking back on looking forward: a review of evaluative scenario literature.* Technical Report.
Efron, B. 1979. Bootstrap Methods: Another Look at the Jackknife. *The Annals of Statistics* 7(1): 1–26.

Efron, B. and R. Tibshirani. 1993. *An introduction to the bootstrap*. Monographs on statistics and applied probability 57. New York: Chapman & Hall.

Environmental Protection Authority. 1995. *Jimblebar rationalisation and planned expansion (formerly McCamey´s Monster Iron Ore mining proposal). BHP Iron Ore (Jimblebar) Pty Ltd. Proposed changes to environmental conditions. Report and recommendations of the Environmental Protection Authority*. Perth, WA, Australia, March.

Environmental Protection Authority. 1998. *Multiple iron ore mine development, Mining Area C-Northern Flank, 100km Northwest of Newman. Report and recommendations of the Environmental Protection Authority. BHP Iron Ore Pty Ltd*. Perth, WA, Australia, November.

Environmental Protection Authority. 2001. *Hope Downs Iron Ore Mine, 75 km north-west of Newman, Pilbara Region. Report and recommendations of the Environmental Protection Authority*. Bulletin 1024. Perth, WA, Australia, August.

Environmental Protection Authority. 2005. *Marillana Creek (Yandi) Life of Mine Proposal, Mining Leases 270SA and 47/292, 90 km north-west of Newman. BHP Billiton Iron Ore Pty Ltd. Report and Recommendations of the Environmental Protection Authority*. Perth, WA, Australia, April.

Environmental Protection Authority. 2008. *Pardoo iron ore mine & direct shipping from Port Hedland. Statement that a proposal may be implemented.* October 3.

Environmental Protection Authority. 2010. *Jimblebar Iron Ore Project. BHP Billiton Iron Ore Pty Ltd. Report and recommendations of the Environmental Protection Authority.* Perth, WA, Australia, October.

Environmental Protection Authority. 2011. *Report and recommendations of the Environmental Protection Authority. Jack Hills Expansion Project. Crosslands Resources Ltd*. August.

Ericsson, M. 2012. *Mining technology – trends and development*. Version 1.0. March. http://www.polinares.eu/docs/d2-1/polinares_wp2_chapter17.pdf.

Ericsson, M. and A. Hodge. 2012. *Trends in the mining and metals industry.* InBrief. London: International Council on Mining and Metals.

ERM. 2013. *International Cyanide Management Code Gold Mining Operation Recertification Audit Musselwhite mine, Ontario, Canada. Summary Audit Report.* Greenwood Village, Colorado, US, April.

European Commission. 2009. *Reference Document on Best Available Techniques for Management of Tailings and Waste-Rock in Mining Activities.* Seville, January.

European Commission. 2014a. *Towards a circular economy: a zero waste programme for Europe.* Communication from the Commission to the European Parliament, the Council, the European Economic and Social Committee and the Committee of the Regions.

European Commission. 2014b. On the review of the list of critical raw materials for the EU and the implementation of the Raw Materials Intiative. SWD(2014) 171 final. May 26.

Eurostat. 2011. *Economy Wide Material Flow Accounts (EW-MFA): Compilation Guidelines for Eurostat´s 2011 EW-MFA Questionnaire*.

Eurostat. 2013. *Economy-wide Material Flow Accounts (EW-MFA). Compilation Guide 2013.* September.
Evans, A.M. 2009. *Ore Geology and Industrial Minerals: An Introduction*. John Wiley & Sons, July 10.
Ewen, C. and Öko-Institut. 1998. Flächenverbrauch als Indikator für Umweltbelastungen. Darmstadt/Freiburg: TU Darmstadt.
Exelis Visual Information Solutions. 2009. *ENVI Version 4.7*.
Exner, A., P. Fleissner, L. Kranzl, and W. Zittel. 2013. *Multiple Crises in Land and Resource Use: Capitalism, Struggle and Well-being in a World without Fossil Fuels*. Routledge, March 5.
Feddema, J.J., K.W. Oleson, G.B. Bonan, L.O. Mearns, L.E. Buja, G.A. Meehl, and W.M. Washington. 2005. The Importance of Land-Cover Change in Simulating Future Climates. *Science* 310(5754): 1674–1678.
Feizi, F. and E. Mansouri. 2013. Introducing the Iron Potential Zones Using Remote Sensing Studies in South of Qom Province, Iran. *Open Journal of Geology* 03(04): 278–286.
Fields, S. 2006. The Price of Gold in Chile. *Environmental Health Perspectives* 114(9): A536–A539.
Figuereido e Silva, R.C., L.M. Lobato, C.A. Rosière, and S. Hagemann. 2011. Petrographic and geochemical studies at giant Serra Norte iron ore deposits in the Carajás mineral province, Pará State, Brazil. *Geonomos*.
Fischer-Kowalski, M. 2011. Analyzing sustainability transitions as a shift between socio-metabolic regimes. *Environmental Innovation and Societal Transitions* 1(1): 152–159.
Fischer-Kowalski, M. and H. Haberl. 2007. *Socioecological Transitions and Global Change: Trajectories of Social Metabolism and Land Use*. Cheltenham, UK ; Northampton, MA: Edward Elgar Publishing Ltd, July 7.
Fisher, B.S. and S. Schnittger. 2012. Autonomous and remote operation technologies in the mining industry. BAeconomics Pty Ltd, February.
Fisher, N.I. and P. Hall. 1991. Bootstrap algorithms for small samples. *Journal of Statistical Planning and Inference* 27(2): 157–169.
Five Winds, ICMM & IISD. 2011. *Sustainable Development and the Global Copper Supply Chain: International research team report.* June.
Foley, J.A., R. DeFries, G.P. Asner, C. Barford, G. Bonan, S.R. Carpenter, F.S. Chapin, et al. 2005. Global Consequences of Land Use. *Science* 309(5734): 570–574.
Frank, P. 2000. Evaluation of different methods for glacier mapping using Landsat TM. In *Proceedings of 20th EARSeL Symposium—land Ice and Snow.*, 239–245. Dresden: European Association of Remote-Sensing Laboratories, June.
Franks, D.M., R. Davis, A.J. Bebbington, S.H. Ali, D. Kemp, and M. Scurrah. 2014. Conflict translates environmental and social risk into business costs. *Proceedings of the National Academy of Sciences*: 201405135.
Freudenberger, L., P. Hobson, M. Schluck, S. Kreft, K. Vohland, H. Sommer, S. Reichle, C. Nowicki, W. Barthlott, and P.L. Ibisch. 2013. Nature conservation: priority-setting needs a global change. *Biodiversity and Conservation* 22(5): 1255–1281.

Friis, I. and H. Balslev. 2005. *Plant Diversity and Complexity Patterns: Local, Regional, and Global Dimensions : Proceedings of an International Symposium Held at the Royal Danish Academy of Sciences and Letters in Copenhagen, Denmark, 25-28 May, 2003*. Kgl. Danske Videnskabernes Selskab.

Frimmel, H.E. 2008. Earth's continental crustal gold endowment. *Earth and Planetary Science Letters* 267(1–2): 45–55.

Gaston, K.J. 1998. Biodiversity -the road to an atlas. *Progress in Physical Geography* 22(2): 269–281.

Geneletti, D. and B.G.H. Gorte. 2003. A method for object-oriented land cover classification combining Landsat TM data and aerial photographs. *International Journal of Remote Sensing* 24(6): 1273–1286.

Gerst, M.D. 2009. Linking Material Flow Analysis and Resource Policy via Future Scenarios of In-Use Stock: An Example for Copper. *Environmental Science & Technology* 43(16): 6320–6325.

GFMS. 2010. *World Silver Survey 2010.* Washington D.C.: The Silver Institute.

GFMS. 2012. *The outlook for silver industrial demand*. The Silver Institute, November.

GFMS. 2014. Supply & Demand | The Silver Institute. https://www.silverinstitute.org/site/supply-demand/. Accessed December 9, 2014.

Gignac, L., I.M. Glacken, J. Hawxby, L.-P. Gignac, and P. Bedell. 2009. *IAMGOLD Corporation: Updated Feasibility Study - Essakane Gold Project Burkina Faso*. March 3.

Gilliam, M. 2012. *Revised Greens Creek Mine Proposed Tailings Disposal Facility Expansion*. February 29.

Gillstrom, G. 2004. *43-101 Technical Report. Mount Polley Mine 2004 Feasibility Study*. Vancouver, BC: Imperial Metals Corporation, August 1.

GISAgMaps. 2014. Landsat vs. Aster Satellite Imagery Comparison. http://www.gisagmaps.com/aster-vs-landsat-imagery-comp/.

Giurco, D. 2005. Towards sustainable metal cycles: the case of copper. Ph.D. Thesis, University of Sydney, March.

Global Footprint Network. 2014. Glossary. http://www.footprintnetwork.org/en/index.php/GFN/page/glossary/.

Global Reporting Initiative. 2013. *G4 Sector Disclosures. Mining and Metals.* Amsterdam, The Netherlands.

Glöser, S., M. Soulier, and L.A. Tercero Espinoza. 2013. Dynamic Analysis of Global Copper Flows. Global Stocks, Postconsumer Material Flows, Recycling Indicators, and Uncertainty Evaluation. *Environmental Science & Technology* 47(12): 6564–6572.

GME. 2013. *Technical review of the Chatree Gold Project*. September 6.

Goldcorp. 2007. *Musselwhite Mine Sustainability Report 07*.

Goldcorp. 2014. Goldcorp. November 20. http://www.goldcorp.com/files/Goldcorp_GoldmanSachs-2014_November_v001_p220b4.pdf.

Golder Associates. 2008. *Declaración de Impacto Ambiental. Proyecto Planta de Molibdeno. Minera Escondida Limitada. II Región de Antofagasta.* April.

Gold Fields. 2011. *Cerro Corona Mine. Technical Short Form Report.* December 31.
Gold Field Tourism. 2015. The Super Pit lookout. http://www.goldfieldstourism.com.au/Attractions/tabid/62/articleType/ArticleView/articleId/8/The-Super-Pit-Lookout.aspx.
Google Earth Pro v. 7.1.4. 2015. *Google Earth Pro v. 7.1.4*. March 30.
Google Earth V.7. 2013. *Google Earth V. 7.1.2.*
Gordon, S.I. 1980. Utilizing LANDSAT imagery to monitor land-use change: A case study in ohio. *Remote Sensing of Environment* 9(3): 189–196.
Graedel, T.E. and B.R. Allenby. 1995. *Industrial Ecology*. New Jersey, EEUU: Prentice Hall.
Graedel, T.E. and L. Erdmann. 2012. Will metal scarcity impede routine industrial use? *MRS Bulletin* 37(04): 325–331.
Great Basin Gold Ltd. 2011. *Technical report update on the mineral resource and mineral reserve estimates for the Burnstone gold mine. Mpumalanga Province of the Republic of South Africa*.
Gutman, Garik, Anthony C. Janetos, Christopher O. Justice, Emilio F. Moran, John F. Mustard, Ronald R. Rindfuss, David Skole, Billy Lee Turner, and Mark A. Cochrane, eds. 2004. *Land Change Science*. Vol. 6. Remote Sensing and Digital Image Processing. Dordrecht: Springer Netherlands.
Gutman, N. 2013. *Argentina en la frontera minera*. 1ra ed. Buenos Aires: Ediciones del Centro Cultural de la Cooperación Floreal Gorini y Centro de Estudios Económicos y Monitoreo de las Políticas Públicas.
Guzmán, C. and R. Mello. 2012. *Preliminary Economic Assessment for the Jardim do Ouro Project, Pará State, Brazil. Technical Report NI 43-101*. NCL Ingeniería y Contrucción Ltda, June.
Haberl, H., K.-H. Erb, F. Krausmann, S. Berecz, N. Ludwiczek, J. Martínez-Alier, A. Musel, and A. Schaffartzik. 2009. Using embodied HANPP to analyze teleconnections in the global land system: Conceptual considerations. *Geografisk Tidsskrift-Danish Journal of Geography* 109(2): 119–130.
Haigh, M.J. 1992. Degradation of “reclaimed” lands previously disturbed by coal mining in Wales: Causes and remedies. *Land Degradation & Development* 3(3): 169–180.
Halada, K., M. Shimada, and K. Ijima. 2008. Forecasting of the Consumption of Metals up to 2050. *Materials Transactions* 49(3): 402–410.
Hamilton, L. 2008. *Statistics with STATA*. Cengage Learning, October 16.
Hanson, W. 2006. *Round Mountain Mine Technical Report*. Kinross Gold Corporation, March 30.
Harvey, M. and S. Pilgrim. 2011. The new competition for land: Food, energy, and climate change. *Food Policy* 36, Supplement 1. The challenge of global food sustainability: S40–S51.
Hatayama, H., I. Daigo, Y. Matsuno, and Y. Adachi. 2010. Outlook of the World Steel Cycle Based on the Stock and Flow Dynamics. *Environmental Science & Technology* 44(16): 6457–6463.
Hatch. 2003. *El Dorado gold corporation. Technical report Kisladag Project. Feasibility Study.* March.
Hecheltjen, A., B. Waske, F. Thonfeld, M. Braun, and G. Menz. 2010. Support Vector Machines for multitemporal and multisensor change detection in a

mining area. In *Deutsche Gesellschaft Für Geographie (DGfG), Arbeitskreis Fernerkundung*. Heidelberg.
Hendry, J.W., L. Evans, and G. Wiatzja. 2005. *Technical report on the Ok Tedi mining limited, Mt. Fubilan copper-gold mine, mineral resource estimate and mineral reserve estimates, Papua New Guinea. Prepared for Inmet Mining Corporation. NI 43-101 Report*. Toronto, Canada: Roscoe Postle Associates Inc., August 2.
Hennessey, B.T., D. Verma, and D.T. Wells. 2009. *An updated technical report on the mineral reserves of Minera Alumbrera Ltd., Catamarca, Argentina. February 13, 2009*. Toronto, Ontario, Canada: Micon International Ltd. & Goldcorp Inc.
Hernández, A.J. and J. Pastor. 2008. Relationship between plant biodiversity and heavy metal bioavailability in grasslands overlying an abandoned mine. *Environmental Geochemistry and Health* 30(2): 127–133.
Hesterberg, T. 2007. Bootstrap. In *Wiley Encyclopedia of Clinical Trials*. John Wiley & Sons, Inc.
Hesterberg, T., D.S. Moore, S. Monaghan, A. Clipson, and R. Epstein. 2006. Bootstrap Methods and Permutation Tests. Chapter 14. In *Introduction to the Practice of Statistics*. W.H. Freeman & Company, January 1.
Hilário, J.., T. Abdala, M.G. Alves de Carvalho, and E. Lúcia. 2008. *Reconciliação: estudo de caso nas minas de ferro de Carajás*. Brasil Mining Site, February 3.
Hilson, G. 2002. An overview of land use conflicts in mining communities. *Land Use Policy* 19(1): 65–73.
Hoekstra, J.M., T.M. Boucher, T.H. Ricketts, and C. Roberts. 2004. Confronting a biome crisis: global disparities of habitat loss and protection: Confronting a biome crisis. *Ecology Letters* 8(1): 23–29.
Honaker, J. and G. King. 2010. What to Do about Missing Values in Time-Series Cross-Section data. *American Journal of Political Science* 54(2): 561–581.
Hooke, R.L. and J.F. Martín-Duque. 2012. Land transformation by humans: A review. *GSA Today* 12(12): 4–10.
Horning, N. 2004. *Justification for using photo interpretation methods to interpret satellite imagery.* New York: Center for Biodiversity and Conservation, American Museum of National History. Accessed November 13, 2014.
Horning, N., J.A. Robinson, E.J. Sterling, W. Turner, and S. Spector. 2010. *Remote sensing for ecology and conservation: a handbook of techniques*. Techniques in ecology and conservation series. Oxford ; New York: Oxford University Press.
Howarth, P.J. and G.M. Wickware. 1981. Procedures for change detection using Landsat digital data. *International Journal of Remote Sensing* 2(3): 277–291.
Huang, C., S.N. Goward, J.G. Masek, N. Thomas, Z. Zhu, and J.E. Vogelmann. 2010. An automated approach for reconstructing recent forest disturbance history using dense Landsat time series stacks. *Remote Sensing of Environment* 114(1): 183–198.
Hurtt, G.C., L.P. Chini, S. Frolking, R.A. Betts, J. Feddema, G. Fischer, J.P. Fisk, et al. 2011. Harmonization of land-use scenarios for the period 1500–2100:

600 years of global gridded annual land-use transitions, wood harvest, and resulting secondary lands. *Climatic Change* 109(1-2): 117–161.
ICMM. 2010. *Mining and Bidiversity. A collection of case studies - 2010 edition.* London, UK. http://www.icmm.com/document/1246.
ICSOBA. 2011. *Bauxite residue seminar field trip to Belgaum´s rehabilitated storage area.* Newsletter. International Committee for Study of Bauxite, Alumina and Aluminium, December 15.
IEA. 2009. *Energy Technology Transitions for Industry: Strategies for the Next Industrial Revolution*. International Energy Agency.
IEEP, Alterra, Ecologic, PBL, and UNEP-WCMC. 2009. *Scenarios and models for exploring future trends of biodiversity and ecosystem services changes. Final report to the European Commission, DG Environment on Contract EBV.G.1/ETU/2008/0090r.* Institute for European Environmental Policy, Alterra, Wageningen UR, Ecologic, Netherlands EAA, UNEP and WCMC.
International Aluminium Institute. 2004. *Third Bauxite Mine Rehabilitation Survey*. Sustainable Development Series. London, UK, June.
International Aluminium Institute. 2009. *Fourth Sustainable Bauxite Mining Report.* London, UK: IAI.
International Copper Study Group. 2012. *The World Copper Factbook 2012*. Lisbon, Portugal.
International Copper Study Group. 2013. *The World Copper Factbook 2013*. Lisbon, Portugal.
Japan Association of Remote Sensing, ed. 1999. *Remote Sensing Note*. http://wtlab.iis.u-tokyo.ac.jp/~wataru/lecture/rsgis/rsnote/contents.htm.
Jiping, Z., Z. Yili, L. Linshan, D. Mingjun, and Z. Xueru. 2012. Identifying Alpine Wetlands in the Damqu River Basin in the Source Area of the Yangtze River using Object-Based Classification Method. Research-article. *BioOne*. January 24.
Johansson, A. 2002. Industrial ecology and industrial metabolism: use and misuse of metaphors. In *A Handbook of Industrial Ecology*, ed. by Robert U Ayres and Leslie W. Ayres. Cheltenham, UK ; Northampton, MA: Edward Elgar Publishing Ltd.
Kalgoorlie Consolidated Gold Mines Pty Ltd. 2007. *Fimiston Gold Mine Operations Extension (Stage 3) and Mine Closure Planning. Report and recommendations of the Environmental Protection Authority, pursuant to the Minister for the Environment remittal under Section 43.* Perth, WA, Australia, December.
Kampouraki, M., G.A. Wood, and T.R. Brewer. 2008. Opportunities and limitations of object based image analysis for detecting urban impervious and vegetated surfaces using true-colour aerial photography. In *Object-Based Image Analysis*, ed. by Thomas Blaschke, Stefan Lang, and Geoffrey J. Hay, 555–569. Lecture Notes in Geoinformation and Cartography. Springer Berlin Heidelberg, January 1.
Kapur, A. 2005. The future of the red metal - scenario analysis. *Futures* 37: 1067–94.
Kelly, M. and K. Tuxen. 2009. Remote Sensing Support for Tidal Wetland Vegetation Research and Management. In *Remote Sensing and Geospatial Technologies for Coastal Ecosystem Assessment and Management*, ed. by

Xiaojun Yang, 341–363. Lecture Notes in Geoinformation and Cartography. Springer Berlin Heidelberg, January 1.
Kelly, T.D. and G.R. Matos. 2013. *Historical Statistics for Mineral and Material Commodities in the United States*. Open-File Report. Data Series 140. U.S. Geological Survey. http://minerals.usgs.gov/ds/2005/140/.
Kemp, D., C.J. Bond, D.M. Franks, and C. Cote. 2010. Mining, water and human rights: making the connection. *Journal of Cleaner Production* 18(15): 1553–1562.
Kennedy, R.E., Z. Yang, and W.B. Cohen. 2010. Detecting trends in forest disturbance and recovery using yearly Landsat time series: 1. LandTrendr — Temporal segmentation algorithms. *Remote Sensing of Environment* 114(12): 2897–2910.
Kenwright, M., A. Allen, J. Marley, and L. Fusher. 2013. *Updated CPR report on the Berezitovy Asset, Russian Federation*. Norgold, April.
Keramidas, K., A. Kitous, and B. Griffin. 2012. *Future availability and demand for oil gas and key minerals.* POLINARES Working Paper. March.
Kier, G., H. Kreft, T.M. Lee, W. Jetz, P.L. Ibisch, C. Nowicki, J. Mutke, and W. Barthlott. 2009. A global assessment of endemism and species richness across island and mainland regions. *Proceedings of the National Academy of Sciences* 106(23): 9322–9327.
Kobayashi, H., H. Watando, and M. Kakimoto. 2014. A global extent site-level analysis of land cover and protected area overlap with mining activities as an indicator of biodiversity pressure. *Journal of Cleaner Production* 84. Special Volume: The sustainability agenda of the minerals and energy supply and demand network: an integrative analysis of ecological, ethical, economic, and technological dimensions: 459–468.
Koch, J. 2010. Modeling the impacts of land-use change on ecosystems at the regional and continental scale. Ph.D. Thesis, Kassel, Germany: University of Kassel. http://www.uni-kassel.de/upress/online/frei/978-3-89958-964-1.volltext.frei.pdf.
Koellner, T., L. de Baan, T. Beck, M. Brandão, B. Civit, M. Margni, L.M. i Canals, R. Saad, D.M. de Souza, and R. Müller-Wenk. 2013. UNEP-SETAC guideline on global land use impact assessment on biodiversity and ecosystem services in LCA. *The International Journal of Life Cycle Assessment* 18(6): 1188–1202.
Koruyan, K., A.H. Deliormanli, Z. Karaca, M. Momayez, H. Lu, and E. Yalçin. 2012. Remote sensing in management of mining land and proximate habitat. *The Journal of The Southern African Institute of Mining and Metallurgy* 112: 667–672.
Koziell, I. and E. Omosa. 2003. *Room to Manoeuvre?: Mining, Biodiversity, and Protected Areas*. IIED.
KPMG. 2013. *Global Metals Outlook*. http://www.kpmg.no/arch/_img/9839533.pdf.
Krausmann, F., S. Gingrich, N. Eisenmenger, K.-H. Erb, H. Haberl, and M. Fischer-Kowalski. 2009. Growth in global materials use, GDP and population during the 20th century. *Ecological Economics* 68(10): 2696–2705.
Krebs, M. 2013. The future of silver mining. October.

Kreft, H. and W. Jetz. 2007. Global patterns and determinants of vascular plant diversity. *Proceedings of the National Academy of Sciences* 104(14): 5925–5930.

Kupfer, J.A. and G.P. Malanson. 2004. The Biodiversity Crisis. In *WorldMinds: Geographical Perspectives on 100 Problems*, ed. by Donald G. Janelle, Barney Warf, and Kathy Hansen, 273–277. Springer Netherlands, January 1.

Lamb, A.D. 2000. Earth observation technology applied to mining-related environmental issues. *Mining Technology* 109(3): 153–156.

Lambin, E.F. and H. Geist. 2006. *Land-use and land-cover change local processes and global impacts*. Berlin; New York: Springer.

Lambin, E.F. and P. Meyfroidt. 2011. Global land use change, economic globalization, and the looming land scarcity. *Proceedings of the National Academy of Sciences* 108(9): 3465–3472.

Lang, S., E. Schöpfer, and T. Langanke. 2009. Combined object-based classification and manual interpretation–synergies for a quantitative assessment of parcels and biotopes. *Geocarto International* 24(2): 99–114.

Lapola, D.M., R. Schaldach, J. Alcamo, A. Bondeau, J. Koch, C. Koelking, and J.A. Priess. 2010. Indirect land-use changes can overcome carbon savings from biofuels in Brazil. *Proceedings of the National Academy of Sciences* 107(8): 3388–3393.

Latifovic, R. 2009. *Mining and the Environment. Satellite remote sensing in assessing the environmental impact of large-scale surface mining operations.* Leipzig, Germany: VDM Verlag Dr. Müller Aktiengesellschaft & Co. KG, Amazon Distribution GmbH.

Latifovic, R., K. Fytas, J. Chen, and J. Paraszczak. 2005. Assessing land cover change resulting from large surface mining development. *International Journal of Applied Earth Observation and Geoinformation* 7(1): 29–48.

Laurance, W.F., M. Goosem, and S.G.W. Laurance. 2009. Impacts of roads and linear clearings on tropical forests. *Trends in Ecology & Evolution* 24(12): 659–669.

Laurance, W.F., T.E. Lovejoy, H.L. Vasconcelos, E.M. Bruna, R.K. Didham, P.C. Stouffer, C. Gascon, R.O. Bierregaard, S.G. Laurance, and E. Sampaio. 2002. Ecosystem Decay of Amazonian Forest Fragments: a 22-Year Investigation. *Conservation Biology* 16(3): 605–618.

Lee, B., F. Preston, J. Kooroshy, R. Bailey, and G. Lahn. 2012. *Resource Futures. A Chatham House Report.* London, UK: The Royal Institute of International Affairs, December.

Lehne, R.W. 1993. Copper, its nature, its extraction. In *Die Welt Der Metalle, Kupfer. The World of Metals, Copper*, 1.: 1st Edition. Frankfurt Am Main, Germany: Metallgesellschaft AG.

Lifset, R. and T.E. Graedel. 2002. Industrial ecology: goals and definitions. In *A Handbook of Industrial Ecology*, ed. by Robert U Ayres and Leslie W. Ayres. Cheltenham, UK ; Northampton, MA: Edward Elgar Publishing Ltd.

Lindeijer, E. 2000. Review of land use impact methodologies. *Journal of Cleaner Production* 8(4): 273–281.

Liu, G., C.E. Bangs, and D.B. Müller. 2012. Stock dynamics and emission pathways of the global aluminium cycle. *Nature Climate Change* 3(4): 338–342.
Liu, J., V. Hull, M. Batistella, R. DeFries, T. Dietz, F. Fu, T.W. Hertel, et al. 2013a. Framing Sustainability in a Telecoupled World. *Ecology and Society* 18(2).
Liu, Y., Y. Liu, and L. Ma. 2013b. Iron mine land reclamation measures: Niu Xi River iron ore. In *Advances in Earth and Environmental Sciences*, ed. by Y. Yang, 1156. Southampton: WIT Press.
Lloyd, P., R. Berthelsen, and E. Strom. 2009. *Technical report on Peak Gold Mines, New South Wales, Australia*. January 1.
Longo, P. and B. Skanderberg. 2012. *Mineral Resource and Mineral Reserve Estimate Seabee Gold Operation Saskatchewan, Canada. 2011 Year End NI 43-101 Technical Report*. Claude Resources Inc., April 28.
Loveland, T.R. and R. DeFries. 2004. Observing and Monitoring Land Use and Land Cover Change. In *Ecosystems and Land Use Change*. Geophysical Monograph 153. American Geophysical Union.
Lunding Mining. 2012. Neves-Corvo Site Tour February.
Luo, Z. and A. Soria. 2008. *Prospective Study of the World Aluminium Industry.* JRC Scientific and Technical Reports. JRC IPTS. http://ftp.jrc.es/EURdoc/JRC40221.pdf. Accessed May 26, 2014.
Lutter, S., C. Polzin, S. Giljum, T. Pálfy, T. Patz, M. Dittrich, L. Kernegger, and A. Rodrigo. 2011. *Under pressure. How our material consumption threatens the planet´s water resources.* REdUSE, Friends of the Earth Europe, Global 2000, SERI, Friends of the Earth.
Mace, G.M., J.L. Gittleman, and A. Purvis. 2003. Preserving the Tree of Life. *Science* 300(5626): 1707–1709.
Mackasey, W.O., 2000. Abandoned mines in Canada. WOM Geological Associates, Mining Watch Canada, Ontario.
MAGSA. 2009. *Proyecto Veladero. Monitoreos Ambientales. Julio 09 - Diciembre 09*. Barrick Veladero.
Malyshev, L.I. 1975. The quantitative analysis of flora: spatial diversity, level of specific richness, and representativity of sampling areas (in Russian). *Botanicheskiy Zhurn.* 60: 1537–1550.
Martens, P.N., M. Ruhrberg, and M. Mistry. 2002. Assessing global land requirement for surface copper mining. *Mineral Resources Engineering* 11(04): 337–348.
Maurice-Bourgoin, L., I. Quiroga, J.L. Guyot, and O. Malm. 1999. Mercury Pollution in the Upper Beni River, Amazonian Basin: Bolivia. *AMBIO* 28(4): 302–306.
MBS Environmental. 2006. *Frances Creek Project, Northern Territory: Public Environmental Report.* August.
Meli, P., J.M. Rey Benayas, P. Balvanera, and M. Martínez Ramos. 2014. Restoration Enhances Wetland Biodiversity and Ecosystem Service Supply, but Results Are Context-Dependent: A Meta-Analysis. *PLoS ONE* 9(4): e93507.
Memarian, H., S.K. Balasundram, and R. Khosla. 2013. Comparison between pixel- and object-based image classification of a tropical landscape using

Système Pour l'Observation de la Terre-5 imagery. *Journal of Applied Remote Sensing* 7(1): 073512–073512.
Menzie, W.D., J.J. Barry, D.I. Bleiwas, E.L. Bray, T.G. Goonan, and G. Matos. 2010. *The global flow of aluminum from 2006 through 2025.* Open-File Report. U.S. Geological Survey.
Menzie, W.D., Y. Soto-Viruet, O. Bermúdez-Lugo, P. Mobbs, A.A. Perez, M. Taib, S. Wacaster, and Staff. 2013. *Review of Selected Global Mineral Industries in 2011 and an Outlook to 2017*. USGS.
Mesa de Diálogo Espinar. 2013. *Hacia una gestión ambiental que garantiza derechos y desarrollo sostenible de Espinar. Informe final integrado de monitoreo sanitario ambiental participativo de la Provincia de Espinar*. Lima, Peru, June.
Meyfroidt, P., E.F. Lambin, K.-H. Erb, and T.W. Hertel. 2013. Globalization of land use: distant drivers of land change and geographic displacement of land use. *Current Opinion in Environmental Sustainability* 5(5): 438–444.
Miao, Z. and R. Marrs. 2000. Ecological restoration and land reclamation in open-cast mines in Shanxi Province, China. *Journal of Environmental Management* 59(3): 205–215.
Mikesell, R.F. 2013. *The World Copper Industry: Structure and Economic Analysis*. Routledge, November 26.
Milford, R.L., S. Pauliuk, J.M. Allwood, and D.B. Müller. 2013. The Roles of Energy and Material Efficiency in Meeting Steel Industry CO_2 Targets. *Environmental Science & Technology* 47(7): 3455–3462.
MinEx Consulting Pty Ltd. 2011. Recent trends in gold discovery. Perth, WA, Australia, November 22.
Mining Atlas. 2015. Mining Atlas. https://mining-atlas.com.
Mining Ore Consultants. 2008. *Savage River mine. Australian bulk minerals. Independent expert report on resources, mine geotechnical and mining.* West Perth, October 23.
Mining Technology. 2015a. Collahuasi Copper Mine, Chile. http://www.mining-technology.com/projects/collahuasi/collahuasi2.html. Accessed September 18, 2015.
Mining Technology. 2015b. Sadiola Gold Mine, Mali. http://www.mining-technology.com/projects/sadiola-gold-mine-mali/. Accessed September 19, 2015.
Mining Technology. 2015c. Fimiston Open Pit "Super Pit" Gold Mine, Australia. http://www.mining-technology.com/projects/superpitgoldmineaust/.
Mirajkar, M.A. and T.R. Srinjvasan. 1975. Landsat photo-interpretation for preparation of small scale soil maps through a multistage approach. *Journal of the Indian Society of Photo-Interpretation* 3(2): 87–92.
Miranda, M., P. Burris, J. Froy Bingcang, P. Shearman, J.O. Briones, A. La Viña, and S. Menard. 2003. *Mining and critical ecosystems: mapping the risks.* Washington D.C.: World Resources Institute.
MIT. 2010. *Critical Elements for New Energy Technologies. An MIT Energy Initiative Workshop Report*. April.
Mittermeier, R.A., C.G. Mittermeier, T.M. Brooks, J.D. Pilgrim, W.R. Konstant, G.A.B. da Fonseca, and C. Kormos. 2003. Wilderness and biodiversity

conservation. *Proceedings of the National Academy of Sciences* 100(18): 10309–10313.
Mittermeier, R.A., P. Robles Gil, M. Hoffman, J. Pilgrim, T. Brooks, C. Geottsch Mittermeier, J. Lamoreux, and G. da Fonseca. 2005. *Hotspots Revisited: Earth´s biologically richest and most endangered terrestrial ecoregions.* Chicago: University of Chicago PRess.
Mittermeier, R. A., P. Robles-Gil, and C. G. Mittermeier, eds. 1997. *Megadiversity. Earth's Biologically Wealthiest Nations*. Mexico City: CEMEX/Agrupación Sierra Madre.
Mittermeier, R.A., W.R. Turner, F.W. Larsen, T.M. Brooks, and C. Gascon. 2011. Global Biodiversity Conservation: The Critical Role of Hotspots. In *Biodiversity Hotspots*, ed. by Frank E. Zachos and Jan Christian Habel, 3–22. Springer Berlin Heidelberg, January 1.
Mora, C., D.P. Tittensor, S. Adl, A.G.B. Simpson, and B. Worm. 2011. How Many Species Are There on Earth and in the Ocean? *PLoS Biol* 9(8): e1001127.
Mount Gibson Iron Limited. 2006. *Quarterly Report for the period ending March 2006*. April 20.
Mount Gibson Iron Limited. 2013. *Koolan Island Optimisation Completed*. March 18.
Mudd, G., D. Giurco, S. Mohr, and L. Mason. 2012. *Gold resources and production: Australia in a global context*. Prepared for CSIRO Minerals Down Under Flagship. Department of Civil Engineering (Monash University) and the Institute for Sustainable Futures (University of Technology, Sydney), October.
Mudd, G.M. 2004a. One Australian Perspective on Sustainable Mining: Declining Ore Grades and Increasing Waste Volumes. In *11th International Conference on Tailings & Mine Waste ´04*, 359–369. Taylor & Francis Group.
Mudd, G.M. 2004b. Sustainable mining: An evaluation of changing ore grades and waste volumes. In *International Conference on Sustainability Engineering and Science*. Auckland, New Zealand, July.
Mudd, G.M. 2007a. Resource Consumption Intensity and the Sustainability of Gold Mining. In . Auckland, New Zealand, February 20.
Mudd, G.M. 2007b. Global trends in gold mining: Towards quantifying environmental and resource sustainability. *Resources Policy* 32(1–2): 42–56.
Mudd, G.M. 2007c. *The Sustainability of Mining in Australia: key production trends and their environmental implications for the future.* Research Report. Department of Civil Engineering, Monash University, and Mineral Policy Institute, October.
Müller, D. 2006. Stock dynamics for forecasting material flows—Case study for housing in The Netherlands. *Ecological Economics* 59(1): 142–156.
Müller, E., L.M. Hilty, R. Widmer, M. Schluep, and M. Faulstich. 2014. Modeling Metal Stocks and Flows: A Review of Dynamic Material Flow Analysis Methods. *Environmental Science & Technology* 48(4): 2102–2113.
Müller, J. and H.E. Frimmel. 2010. Numerical Analysis of Historic Gold Production Cycles and Implications for Future Sub-Cycles. *The Open Geology Journal* 4: 29–34.

Murguía, D. 2014. *Sustainability Reporting in the Mining Industry: Revealing or Hiding Conflics? The Case of Bajo de la Alumbrera in Argentina.* Buenos Aires: Libros en Red.

Murguía, D.I. and K. Böhling. 2013. Sustainability reporting on large-scale mining conflicts: the case of Bajo de la Alumbrera, Argentina. *Journal of Cleaner Production* 41: 202–209.

Myers, N. 1996. The biodiversity crisis and the future of evolution. *Environmentalist* 16(1): 37–47.

Myers, N., R.A. Mittermeier, C.G. Mittermeier, G.A.B. da Fonseca, and J. Kent. 2000. Biodiversity hotspots for conservation priorities. *Nature* 403(6772): 853–858.

Myint, S., T.A. Kyaw, and I. Takashima. 2005. *Application of Remote Sensing Techniques on Iron Oxide Detection from ASTER and Landsat Images of Tanintharyi Costal Area, Myanmar*. Scientific and Technical Reports of Faculty of Engineering and Resource Science. Akita University, Akita.

Myint, S.W., C.S. Galletti, S. Kaplan, and W.K. Kim. 2013. Object vs. pixel: a systematic evaluation in urban environments. *Geocarto International* 28(7): 657–678.

Myint, S.W., P. Gober, A. Brazel, S. Grossman-Clarke, and Q. Weng. 2011. Per-pixel vs. object-based classification of urban land cover extraction using high spatial resolution imagery. *Remote Sensing of Environment* 115(5): 1145–1161.

MYMA. 2012. *Declaración de Impacto Ambiental. Proyecto Depositación de Relaves Filtrados Interior Mina.* Santiago, Chile.

Naidoo, R., A. Balmford, R. Costanza, B. Fisher, R.E. Green, B. Lehner, T.R. Malcolm, and T.H. Ricketts. 2008. Global mapping of ecosystem services and conservation priorities. *Proceedings of the National Academy of Sciences* 105(28): 9495–9500.

National Research Council (U.S.). 2011. *Assessment of impediments to interagency collaboration on space and earth missions*. Washington, D.C: National Academies Press.

Newmont. 2013. Yanacocha Site Visit. September 28, 2013.

Norgate, T.E., S. Jahanshahi, and W.J. Rankin. 2007. Assessing the environmental impact of metal production processes. *Journal of Cleaner Production* 15(8-9): 838–848.

Norris, C., P. Hobson, and P.L. Ibisch. 2011. Microclimate and vegetation function as indicators of forest thermodynamic efficiency: Forest thermodynamic efficiency. *Journal of Applied Ecology*: no–no.

Northey, S., S. Mohr, G.M. Mudd, Z. Weng, and D. Giurco. 2014. Modelling future copper ore grade decline based on a detailed assessment of copper resources and mining. *Resources, Conservation and Recycling* 83: 190–201.

Nowicki, T.E., J.A. Carlson, B.B. Crawford, G.D. Lochart, P.A. Oshust, and D.R. Dyck. 2003. Field guide to the Ekati Diamond Mine. In . Victoria, CA, June 22.

Nussbaum, S. and G. Menz. 2008a. Satellite Imagery and Methods of Remote Sensing. In *Object-Based Image Analysis and Treaty Verification*, 17–27. Springer Netherlands, January 1.

Nussbaum, S. and G. Menz. 2008b. SEaTH – A New Tool for Feature Analysis. In *Object-Based Image Analysis and Treaty Verification*, 51–62. Springer Netherlands, January 1.

Nuss, P., E.M. Harper, N.T. Nassar, B.K. Reck, and T.E. Graedel. 2014. Criticality of Iron and Its Principal Alloying Elements. *Environmental Science & Technology*. http://dx.doi.org/10.1021/es405044w. Accessed March 27, 2014.

OECD. 2008. *OECD Environmental Outlook to 2030*. OECD Environmental Outlook. OECD Publishing, March 5.

OECD. 2012. OECD Environmental Outlook to 2050. The Consequences of Inaction. In *OECD Environmental Outlook*, 19–33. Organisation for Economic Co-operation and Development, March 15.

OECD. 2015. *Material Resources, Productivity and the Environment*. OECD Green Growth Studies. OECD Publishing, February 12.

Olson, D.M. and E. Dinerstein. 1998. The Global 200: A Representation Approach to Conserving the Earth's Most Biologically Valuable Ecoregions. *Conservation Biology* 12(3): 502–515.

Olson, D.M. and E. Dinerstein. 2002. The Global 200: priority ecoregions for global conservation. *Annals of the Missouri Botanical Garden* 89: 199–224.

Olson, D.M., E. Dinerstein, E.D. Wikramanayake, N.D. Burgess, G.V.N. Powell, E.C. Underwood, J.A. D'amico, et al. 2001. Terrestrial Ecoregions of the World: A New Map of Life on Earth A new global map of terrestrial ecoregions provides an innovative tool for conserving biodiversity. *BioScience* 51(11): 933–938.

Oxfam America. 2014. *Geographies of Conflict. Mapping overlaps between extractive industries and agricultural land uses in Ghana and Peru*.

Ozkaynak, Begum, Lazlo Pinter, and Detlef van Vuuren, eds. 2012. Scenarios and Sustainability Transformation. In *Global Environmental Outlook 5. Environment for the Future We Want.* Malta: UNEP.

Pagot, E., M. Pesaresi, D. Buda, and D. Ehrlich. 2008. Development of an object-oriented classification model using very high resolution satellite imagery for monitoring diamond mining activity. *International Journal of Remote Sensing* 29(2): 499–512.

Park, C.C. 1992. *Tropical Rainforests*. Routledge.

Patterson, S., H. Kurtz, J. Olson, and C. Neeley. 1986. *World Bauxite Resources*. Professional Paper. USGS.

Pauliuk, S., R.L. Milford, D.B. Müller, and J.M. Allwood. 2013. The Steel Scrap Age. *Environmental Science & Technology* 47(7): 3448–3454.

Pauliuk, S. and D.B. Müller. 2014. The role of in-use stocks in the social metabolism and in climate change mitigation. *Global Environmental Change* 24: 132–142.

Petropoulos, G.P., P. Partsinevelos, and Z. Mitraka. 2013. Change detection of surface mining activity and reclamation based on a machine learning approach of multi-temporal Landsat TM imagery. *Geocarto International* 28(4): 323–342.

Pilbara Iron. 2011. *Channar Mining Project. Environmental Referral Supporting Document. Adjustment of the Defined Ground Disturbances Boundaries*

and Removal of Mining Rate and Life of Mine. Perth, WA, Australia: Rio Tinto, March.
Plunkert, P. 2000. *USGS Mineral Yearbook. Bauxite and Alumina.* USGS.
Poenaru, V.D., A. Badea, E. Savin, D. Teleaga, and V. Poncos. 2011. Land degradation monitoring in the Ocnele Mari salt mining area using satellite imagery. http://dx.doi.org/10.1117/12.898022. Accessed December 3, 2014.
Polinares. 2012. *Fact Sheet: Iron Ore.* POLINARES Working Paper. March.
PriceWaterhouseCooper. 2013. *The direct economic impact of gold*. October. https://www.pwc.com/en_GX/gx/mining/publications/assets/pwc-the-direct-economic-impact-of-gold.pdf.
PwC. 2012. *Mine. The growing disconnect. Review of global trends in the mining industry - 2012.* PricewaterhouseCoopers LLP.
QGIS Development Team. 2012. *QGIS Geographic Information System.* Open Source Geospatial Foundation Project. https://hub.qgis.org/.
Quandt, D., C. Ekstrom, and K. Triebel. 2008. *Technical report for the Fort Knox Mine*. Kinross Gold Corporation, March 31.
Rajaram, Vasudevan, Subijoy Dutta, and Krishna Parameswaran, eds. 2011. *Sustainable mining practices - a global perspective*. New Delhi, India: Nutech Photolitographers.
Raponi, T.R. and D. Redmond. 2009. *Technical report on the Boroo gold mine Mongolia*. Toronto, Canada: Centerra Gold Inc., December 17.
Raskin, P., T. Banuri, G. Gallopin, P. Gutman, A. Hammond, R. Kates, and R. Swart. 2002. *Great Transition. The Promise and Lure of the Times Ahead. A report of the Global Scenario Group.* Stockholm Environment Institute. http://tellus.org/documents/Great_Transition.pdf.
Raskin, P., G. Gallopin, P. Gutman, A. Hammond, and R. Swart. 1998. *Bending the curve: toward global sustainability. A report of the Global Scenario Group.* Boston, USA: Stockholm Environment Institute-Boston, November.
Rathmann, R., A. Szklo, and R. Schaeffer. 2010. Land use competition for production of food and liquid biofuels: An analysis of the arguments in the current debate. *Renewable Energy* 35(1): 14–22.
Raw Materials Group. 2004. Raw Materials Data Handbook. 2004.
Reichl, C., M. Schatz, and G. Zsak. 2013. *World mining data. Welt Bergbau Daten.* Vienna: Bundesministerium für Wirtschaft, Familie und Jugend / International Organizing Committee for the World Mining Congresses. http://www.wmc.org.pl/sites/default/files/WMD2013.pdf.
Rio Tinto. 2006. *Reclaiming the environment from a century of mining: A status report on the Last Century Cleanup Program Kennecott Utah Copper Corporation*.
Rio Tinto. 2011. *Iron Ore in Western Australia. Sustainable development report 2011.*
Rockström, J., W. Steffen, K. Noone, Å. Persson, F.S. Chapin, E.F. Lambin, T.M. Lenton, et al. 2009. A safe operating space for humanity. *Nature* 461(7263): 472–475.
Rose, S.K., H. Ahammad, B. Eickhout, B. Fisher, A. Kurosawa, S. Rao, K. Riahi, and D.P. van Vuuren. 2012. Land-based mitigation in climate stabilization. *Energy Economics* 34(1): 365–380.

Rothman, K.J. 2012. *Epidemiology. An introduction.* 2nd ed. New York: Oxford University Press.

Roth, W., T. Atmaca, G. Mori, W. Neumann, and A. Thormann. 1999. *Stoffmengenflüsse und Energiebedarf bei der Gewinnung ausgewählter mineralischer Rohstoffe. Teilstudie Eisen.* Hannover: BGR & Staatliche Geologische Dienst in der Bundesrepublik Deutschland.

Rounsevell, M.D.A., B. Pedroli, K.-H. Erb, M. Gramberger, A.G. Busck, H. Haberl, S. Kristensen, et al. 2012. Challenges for land system science. *Land Use Policy* 29(4): 899–910.

Roy, A.K. 1978. LANDSAT (MSS) imagery interpretation: A new perspective tool aiding regional hydromorphic mapping for groundwater exploration. *Journal of the Indian Society of Photo-Interpretation* 6(2): 79–86.

Roy, T. 1994. Bootstrap accuracy for non-linear regression models. *Journal of Chemometrics* 8(1): 37–44.

RSG Global Consulting Pty Ltd. 2007. *Independent Technical Report on the Norwegian Mineral Properties of Northern Iron Limited*. October 24.

Ruhrberg, M. 2002. Entwicklung eines betriebsübergreifenden Ressourcenmanagementsystems für metallische Rohstoffe am Beispiel des Kupferbergbaus. PhD Thesis, Aachen: RWTH Aachen.

Runge, I. 2012. Mining Economics. In *Discover Mongolia 2012: International Mining Conference and Investors Forum*.

Sampaio, J.A., M.J. Kesley, and M.T. Moreira Penna. 2002. *Ferro - Mina N5 - Carajás/CVRD*. Rio de Janeiro, Brasil: CETEM, December.

Sanderson, E.W., M. Jaiteh, M.A. Levy, K.H. Redford, A.V. Wannebo, and G. Woolmer. 2002. The Human Footprint and the Last of the Wild. *BioScience* 52(10): 891–904.

Santi, E., S. Maccherini, D. Rocchini, I. Bonini, G. Brunialti, L. Favilli, C. Perini, et al. 2010. Simple to sample: Vascular plants as surrogate group in a nature reserve. *Journal for Nature Conservation* 18(1): 2–11.

SAS Institute Inc. 2005. *SAS 9.1.* Cary, NC, USA.

Schafer, J.L. and J.W. Graham. 2002. Missing data: Our view of the state of the art. *Psychological Methods* 7(2): 147–177.

Schlomer, G.L., S. Bauman, and N.A. Card. 2010. Best practices for missing data management in counseling psychology. *Journal of Counseling Psychology* 57(1): 1–10.

Schmidheiny, K. 2012. *The Bootstrap.* Short Guides to Microeconometrics. University of Bassel.

Schmidt, G., C. Jenkerson, J. Masek, E. Vermote, and F. Gao. 2013. *Landsat ecosystem disturbance adaptive processing system (LEDAPS) algorithm description*. United States Geological Survey.

Schmidt, H. and C. Glaesser. 1998. Multitemporal analysis of satellite data and their use in the monitoring of the environmental impacts of open cast lignite mining areas in Eastern Germany. *International Journal of Remote Sensing* 19(12): 2245–2260.

Schueler, V., T. Kuemmerle, and H. Schroder. 2011. Impacts of Surface Gold Mining on Land Use Systems in Western Ghana. *Ambio* 40(5): 528–539.

Schütz, H. 2003. *Economy-Wide Material Flow Accounts, Land Use Accounts and Derived Indicators for Germany: MFA Germany*. Final Report to the Commission of the European Communities. Eurostat/Wuppertal Institute.
Schwarz, H.-G., S. Briem, and P. Zapp. 2001. Future carbon dioxide emissions in the global material flow of primary aluminium. *Energy* 26(8): 775–795.
Scott E. Wilson Consulting Inc. 2009. *Technical report Allied Nevada Gold Corp. Hycroft mine, Winnemucca, Nevada, USA*. May 15.
Scott Wilson Mining. 2005. *Guelb Moghrein Copper Gold Project. Environmental and Social Impact Assessment Report*. Mauritanian Copper Mines SARL, June.
Seto, Karen Ching-Yee, and Anette Reenberg, eds. 2014. *Rethinking global land use in an urban era*. Strüngmann forum reports. Cambridge, MA: The MIT Press.
Seto, K.C., A. Reenberg, C.G. Boone, M. Fragkias, D. Haase, T. Langanke, P. Marcotullio, D.K. Munroe, B. Olah, and D. Simon. 2012. Urban land teleconnections and sustainability. *Proceedings of the National Academy of Sciences* 109(20): 7687–7692.
Shafiee, S. and E. Topal. 2010. An overview of global gold market and gold price forecasting. *Resources Policy* 35(3): 178–189.
Shangoni Management Services. 2011. *Sishen Iron ore Thabazimbi mine. Review and update of the environmental management programme LP 30/5/1/3/2/1 (45) and (47) EM*. July 28.
Short, N.M. 1982. *The Landsat Tutorial Workbook: Basics of Satellite Remote Sensing*. National Aeronautics and Space Administration, Scientific and Technical Information Branch.
Sibaud, P. and GAIA Foundation. 2013. *Short Circuit: the lifecycle of our electronic gadgets and the true cost to Earth*. London, UK.
Sidjak, R.W. 1999. Glacier mapping of the Illecillewaet icefield, British Columbia, Canada, using Landsat TM and digital elevation data. *International Journal of Remote Sensing* 20(2): 273–284.
Sillitoe, R.H. 1972. A Plate Tectonic Model for the Origin of Porphyry Copper Deposits. *Economic Geology* 67(2): 184–197.
Simonis, U.E. and R.U. Ayres. 1994. *Industrial Metabolism: Restructuring for Sustainable Development*. Tokyo ; New York: United Nations University.
Sinden, G.E., G.P. Peters, J. Minx, and C.L. Weber. 2011. *International Carbon Flows: Aluminium*. The Carbon Trust.
Sliwka, P. 2001. *Quantifizierung der Umwelteinwirkungen des Bauxitbergbaus unter besonderer Berücksichtigung der Flächeninanspruchnahme*. Aachen: Lehrstuhl für Ingenieurgeologie und Hydrogeologie der RWTH Aachen.
Sliwka, P., C. Bauer, K. Eden, J. Grassman, M. Mistry, M. Röhrlich, M. Ruhrberg, and H. Sievers. 2001. A global environmental impact assessment for bauxite mining. Land use and soil erosion. In *Proceedings of Light Metals 2001*, 85–90. New Orleans, Louisiana (USA), February 11.
Smart, S.M., P.A. Henrys, B.V. Purse, J.M. Murphy, M.J. Bailey, and R.H. Marrs. 2012. Clarity or confusion? – Problems in attributing large-scale ecological changes to anthropogenic drivers. *Ecological Indicators* 20: 51–56.
Smith, P., P.J. Gregory, D. van Vuuren, M. Obersteiner, P. Havlik, M. Rounsevell, J. Woods, E. Stehfest, and J. Bellarby. 2010. Competition for land.

Philosophical Transactions of the Royal Society B: Biological Sciences 365(1554): 2941–2957.
SNL Metals & Mining. 2015. SNL Metals & Mining Database. http://www.snl.com/Sectors/metalsmining/Default.aspx.
Sohn, I. 2005. Long-term projections of non-fuel minerals: We were wrong, but why? *Resources Policy* 30(4): 259–284.
Sohn, R.A. and W. Menke. 2002. Application of maximum likelihood and bootstrap methods to nonlinear curve-fit problems in geochemistry. *Geochemistry, Geophysics, Geosystems* 3(7): 1–17.
Sonter, L.J., D.J. Barrett, C.J. Moran, and B.S. Soares-Filho. 2013. A Land System Science meta-analysis suggests we underestimate intensive land uses in land use change dynamics. *Journal of Land Use Science*: 1–14.
Sonter, L.J., D.J. Barrett, and B.S. Soares-Filho. 2014a. Offsetting the Impacts of Mining to Achieve No Net Loss of Native Vegetation: Offsets, Mining, and No Net Loss. *Conservation Biology*: n/a–n/a.
Sonter, L.J., D.J. Barrett, B.S. Soares-Filho, and C.J. Moran. 2014b. Global demand for steel drives extensive land-use change in Brazil's Iron Quadrangle. *Global Environmental Change* 26: 63–72.
Spiess, A.-N. and N. Neumeyer. 2010. An evaluation of R2 as an inadequate measure for nonlinear models in pharmacological and biochemical research: a Monte Carlo approach. *BMC Pharmacology* 10(1): 6.
Spitzley, D.V. and D.A. Tolle. 2004. Evaluating Land-Use Impacts: Selection of Surface Area Metrics for Life-Cycle Assessment of Mining. *Journal of Industrial Ecology* 8(1-2): 11–21.
SRK Consulting. 2005. *Independent Technical Report on the Troy Cu-Ag Project, Montana*. Toronto, Canada: Revett Silver Company, January 27.
SRK Consulting. 2007. *An independent mineral experts´ report on the gold mining and exploration assets of Saudi Arabian mining company (Ma´aden)*. November.
SRK Consulting. 2009. *NI 43-101 Technical Report Minera Andes Inc. San José Silver-Gold Project Santa Cruz, Argentina*. Minera Andes Inc, May 29.
Stata Corp LP. 2009. *Stata Statistical Software: Release 11*. Special Edition. College Station, TX, USA. http://www.stata.com/.
Stattersfield, A.J., M.J. Crosby, A.J. Long, and D.C. Wege. 1998. *Endemic Bird Areas of the World. Priorities for biodiversity conservation*. Cambridge, UK: BirdLife International.
Steffen, W., K. Richardson, J. Rockstrom, S.E. Cornell, I. Fetzer, E.M. Bennett, R. Biggs, et al. 2015. Planetary boundaries: Guiding human development on a changing planet. *Science* 347(6223): 1259855–1259855.
Stehfest, E. and Planbureau voor de Leefomgeving. 2014. *Integrated assessment of global environmental change with IMAGE 3.0: model description and policy applications*. The Hague: PBL Netherlands Environmental Assessment Agency.
Steinberger, J.K., F. Krausmann, and N. Eisenmenger. 2010. Global patterns of materials use: A socioeconomic and geophysical analysis. *Ecological Economics* 69(5): 1148–1158.

Sutton, P.C. and R. Constanza. 2002. Global estimates of market and non-market values derived from nighttime satellite imagery, land cover, and ecosystem service valuation. *Ecological Economics* 41(3): 509–527.

Sverdrup, H.U., D. Koca, and C. Granath. 2012. Modelling the gold market, explaining the past and assessing the physical and economical sustainability of future scenarios. St Gallen, Switzerland, July 22.

Sverdrup, H.U., D. Koca, and K.V. Ragnarsdottir. 2014a. Investigating the sustainability of the global silver supply, reserves, stocks in society and market price using different approaches. *Resources, Conservation and Recycling* 83: 121–140.

Sverdrup, H.U., K.V. Ragnarsdottir, and D. Koca. 2014b. On modelling the global copper mining rates, market supply, copper price and the end of copper reserves. *Resources, Conservation and Recycling* 87: 158–174.

SVS Ingenieros. 2012. *Segunda modificación del Estudio de Impacto Ambiental para el recrecimiento del depósito de relaves de la planta de beneficio Ares. Resúmen Ejecutivo*. Compañia Minera Ares SAC, November.

Taillant, J.D. 2013. *Los Glaciares de Barrick Gold. Informe Técnico sobre el Impacto de Barrick Gold en Glaciares en los Proyectos Mineros de Veladero y Pascua Lama.* Córdoba, Argentina: Centro de Derechos Humanos y Ambiente (CEDHA), May 20.

Taillant, J.D. 2015. *Glaciers: the politics of ice*. New York, NY: Oxford University Press.

Teršič, T., F. Andriamasinoro, E. Ben-Dor, F. Blanchard, A. Bourguignon, H. Coetzee, C. Ehrler, et al. 2013. *Indicators and Earth Observation Products for the Assessment of the Extractive Industry Environmental and Societal Impacts. Material and information for the EO-MINERS workshop at the eMalahleni Coalfied demonstration site.* EO-MINERS, April. DOI: 10.5474/eo-miners.2013.02. Accessed March 10, 2015.

Thomson, M. 2006. Representing data distributions with kernel density estimates. Royal Society of Chemistry, March. http://www.rsc.org/images/data-distributions-kernel-density-technical-brief-4_tcm18-214836.pdf.

Tomkinson, M.J. and L.J. Putland. 2006. *Technical report on the Mupane Gold Project. NI 43-101 Report*. January 18.

Townsend, P.A., D.P. Helmers, C.C. Kingdon, B.E. McNeil, K.M. de Beurs, and K.N. Eshleman. 2009. Changes in the extent of surface mining and reclamation in the Central Appalachians detected using a 1976–2006 Landsat time series. *Remote Sensing of Environment* 113(1): 62–72.

Trimble. 2011a. *eCognition Developer 8.7*. Munich, Germany: Trimble Germany GmbH.

Trimble. 2011b. eCognition Developer 8.7. Reference Book. Trimble Documentation, September.

Trimble. 2013. eCognition Server. September 17. http://www.ecognition.com/suite/ecognition-server. Accessed April 24, 2015.

Tukker, A., T. Bulavskaya, S. Giljum, A. de Koning, S. Lutter, M. Simas, K. Stadler, and R. Wood. 2014. *The Global Resource Footprint of Nations. Carbon, water, land and materials embodied in trade and final consumption calculated with EXIOBASE 2.1*. Leiden/Delft/Vienna/Trondheim.

Turner, W.R., K. Brandon, T.M. Brooks, R. Constanza, G. da Fonseca, and R. Portela. 2007. Global conservation of biodiversity and ecosystem services. *BioScience* 57: 868–873.

Tutu, H., T.S. McCarthy, and E. Cukrowska. 2008. The chemical characteristics of acid mine drainage with particular reference to sources, distribution and remediation: The Witwatersrand Basin, South Africa as a case study. *Applied Geochemistry* 23(12): 3666–3684.

UCLA Statistical Consulting Group. 2007. Introduction to SAS. http://www.ats.ucla.edu/stat/stata/dae/rreg.htm.

UN-DESA. 2010. *Trends in Sustainable Development - Chemicals, Mining, Transport, Waste Management 2010-2011*.

UNEP. 2011a. *Recycling rates of metals - a status report. A Report of the Working Group on the Global Metal Flows to the International Resource Panel. Graedel, T.E.; Allwood, J.; Birat, J.-P.; Reck, B.K.; Sibley, S.F.; Sonnemann, G.; Buchert, M.; Hagelüken, C.*

UNEP. 2011b. *Decoupling natural resource use and environmental impacts from economic growth. A Report of the Working Group on Decoupling to the International Resource Panel. Fischer-Kowalski, M., Swilling, M., von Weizsäcker, E.U., Ren, Y., Moriguchi, Y., Crane, W., Krausmann, F., Eisenmenger, N., Giljum, S., Hennicke, P., Romero Lankao, P., Siriban Manalang, A., Sewerin, S.*

UNEP. 2014. *Assessing Global Land Use: Balancing Consumption with Sustainable Supply. A Report of the Working Group on Land and Soils of the International Resource Panel. Bringezu S., Schütz H., Pengue W., O´Brien M., Garcia F., Sims R., Howarth R., Kauppi L., Swilling M., and Herrick*.

UNEP-GEAS. 2014. *Sand, rarer than one thinks*. Thematic Focus: Ecosystem management, Environmental governance, Resource efficiency. March. http://na.unep.net/geas/archive/pdfs/GEAS_Mar2014_Sand_Mining.pdf.

University of Stuttgart. 2011. Documentation of Land use Indicator Values in GaBi. http://www.gabi-software.com/fileadmin/Documents/landuse.pdf.

UN Open Working Group. 2014. *Open Working Group Proposal for Sustainable Development Goals, 2014.*

Urkidi, L. and M. Walter. 2010. A glocal environmental movement against gold mining: Pascua–Lama in Chile. *Ecological Economics* 70(2): 219–227.

USAID. 2005. *Minerals & Conflict. A toolkit for intervention.* Washington D.C., April.

U.S. Bureau of Land Management. 2015. Abandoned Mine Lands Inventory. http://www.blm.gov/wo/st/en/prog/more/Abandoned_Mine_Lands/abandoned_mine_site.html

U.S. EPA. 2009. *First five year review report. Kennecott South Zone*.

USGS. 2008a. Opening the Landsat Archive. http://landsat.usgs.gov/documents/USGS_Landsat_Imagery_Release.pdf.

USGS. 2008b. *Mineral Commodity Summaries. Gold.* January. http://minerals.usgs.gov/minerals/pubs/commodity/gold/mcs-2008-gold.pdf.

USGS. 2014a. *Copper. Statistics and Information.* http://minerals.usgs.gov/minerals/pubs/commodity/copper/.

USGS. 2014b. Mineral Commodity Summaries. Iron ore. February. http://minerals.usgs.gov/minerals/pubs/commodity/iron_ore/mcs-2014-feore.pdf.
USGS. 2014c. *Mineral Commodity Summary. Bauxite and Alumina.* Mineral Commodiy Summaries. USGS, February. http://minerals.usgs.gov/minerals/pubs/commodity/bauxite/mcs-2014-bauxi.pdf.
USGS. 2014d. *Mineral Commodity Summaries. Copper.* February. http://minerals.usgs.gov/minerals/pubs/commodity/copper/mcs-2014-coppe.pdf.
USGS. 2014e. *Mineral Commodity Summaries. Gold.* February. http://minerals.usgs.gov/minerals/pubs/commodity/gold/mcs-2014-gold.pdf.
USGS. 2014f. *Mineral Commodity Summaries. Silver.* February. http://minerals.usgs.gov/minerals/pubs/commodity/silver/mcs-2014-silve.pdf.
USGS. 2015. Landsat Project Description. http://landsat.usgs.gov/about_project_descriptions.php.
Van Zyl, D., M. Sasoon, C. Digby, A.-M. Fleury, and S. Kyeyune. 2002a. *Mining for the Future. Appendix A: Large Volume Waste Working Paper*.
Van Zyl, D., M. Sasoon, C. Digby, A.-M. Fleury, and S. Kyeyune. 2002b. *MMSD Working Paper No. 68b. Mining for the Future. Appendix I: Porgera Riverine Disposal Case Study.* IIED and WBCSD, April.
Van Zyl, D., M. Sasoon, C. Digby, A.-M. Fleury, and S. Kyeyune. 2002c. *MMSD Working Paper No. 68a. Mining for the Future. Appendix H: Ok tedi Riverine Disposal Case Study.* IIED and WBCSD, April.
Vella, H., 2015. Managing Australia's 50,000 abandoned mines. Mining Technology, April 13.
Verburg, P.H., K. Neumann, and L. Nol. 2011. Challenges in using land use and land cover data for global change studies. *Global Change Biology* 17(2): 974–989.
Vîjdea, A.-M., S. Sommer, and W. Mehl. 2004. *Use of remote sensing for mapping and evaluation of mining waste anomalies at national to multi-country scale. A case study to integrate remote sensing information with thematic data layers and national inventories on mining features in pre-accession countries.* Ispra, Italy: EU Joint Research Center (DG JRC).
Villas Bôas, R.C. and M. Barreto. 1996. Clean technologies for the minerals industries: the need of P2 solutions. In *Clean Technology for the Mining Industry*, ed. by M. Sanchez, F. Vergara, and S. Castro. Concepción, Chile.
Visual Capitalist and Nature Resource Holdings. 2013. *Global 2013 Gold. Mine & Deposit Rankings. A meticulous examination of existing and future gold supply.* http://www.visualcapitalist.com/wp-content/uploads/2013/11/global-gold-mine-and-deposit-rankings-2013.pdf.
Voet, E. van der. 2002. *Land use in LCA.* CML-SSP Working Paper. Leiden, The Netherlands: Center of Environmental Science, Leiden University.
Voet, E. van der, R. Kleijn, R. Huele, M. Ishikawa, and E. Verkuijlen. 2002. Predicting future emissions based on characteristics of stocks. *Ecological Economics* 41(2): 223–234.

Vuuren, D.P. van, B.J. Strengers, and H.J.M. De Vries. 1999. Long-term perspectives on world metal use—a system-dynamics model. *Resources Policy* 25(4): 239–255.
Walsh Peru SA. 2011. *Estudio de Impacto Ambiental "Ampliación de la concentradora Toquepala y recrecimiento del embalse de relaves de Quebrada HOnda."* Lima, Peru: Southern Copper Peru.
Wang, L., W.P. Sousa, and P. Gong. 2004. Integration of object-based and pixel-based classification for mapping mangroves with IKONOS imagery. *International Journal of Remote Sensing* 25(24): 5655–5668.
Wasow, P. and C. Thiris. 2014. Alumina Limited presented at the 2014 Global Metals, Mining & Steel Conference, May, Miami.
Wechsler, D. 2014. Crowdsourcing as a method of transdisciplinary research—Tapping the full potential of participants. *Futures* 60:14-22.
Weitzel, N. 2013. Detektion von Aktivitäten im Goldbergbau mit multispektralen Satellitenbildern. Master Thesis, Bonn: Rheinische Friedrich-Wilhelms Universität Bonn, October.
Wellmer, F.-W., M. Dalheimer, and M. Wagner. 2008. *Economic Evaluations in Exploration*. 2nd ed. Berlin, Heidelberg: Springer.
West, J. 2011. Decreasing Metal Ore Grades. *Journal of Industrial Ecology* 15(2): 165–168.
World Economic Forum. 2010. *Mining & Metals. Scenarios to 2030.* World Scenario Series. Cologny/Geneva, Switzerland.
World Gold Council. 2011. *Liquidity in the global gold market.* London, UK.
World Gold Council. 2014a. *Gold Demand Trends. Full Year 2013.* February.
World Gold Council. 2014b. *China´s gold market: progress and prospects.* London, April 15.
World Steel Association. 2012. *Sustainable Steel: at the core of a green economy.* Brussels: World Steel Association.
Wulder, M.A., J.G. Masek, W.B. Cohen, T.R. Loveland, and C.E. Woodcock. 2012. Opening the archive: How free data has enabled the science and monitoring promise of Landsat. *Remote Sensing of Environment* 122. Landsat Legacy Special Issue: 2–10.
Wulff, E.W. 1935. Versuch einer Einteilung der Vegetation der Erde in pflanzengeographische Gebiete auf Grund der Artenzahl. *Repertorium Specierum Novarum Regni Vegetabilis* 12: 57–83.
WWF and IUCN. 1997. *Centres of Plant Diversity . A Guide and Strategy for their Conservation (1994–1997)*. Cambridge, UK.
Yellishetty, M., G.M. Mudd, P.G. Ranjith, and A. Tharumarajah. 2011. Environmental life-cycle comparisons of steel production and recycling: sustainability issues, problems and prospects. *Environmental Science & Policy* 14(6): 650–663.
Yellishetty, M., P.G. Ranjith, and A. Tharumarajah. 2010. Iron ore and steel production trends and material flows in the world: Is this really sustainable? *Resources, Conservation and Recycling* 54(12): 1084–1094.
Zhang, F.-P., C.-F. Li, L.-G. Tong, L.-X. Yue, P. Li, Y.-J. Ciren, and C.-G. Cao. 2010. Response of microbial characteristics to heavy metal pollution of mining soils in central Tibet, China. *Applied Soil Ecology* 45(3): 144–151.

Žibret, G., S. Adar, E. Ben-Dor, A. Bourguignon, C. Ehrler, E. Falck, C. Fischer, et al. 2013. *Indicators and Earth Observation Products for the Assessment of the Extractive Industry Environmental and Societal Impacts. Material and Information for the EO-Miners workshop at the Sokolovská uhelná demonstration site.* EO-MINERS Project, March. DOI: 10.5474/eo-miners.2013.01. Accessed December 10, 2014.

CHAPTER EIGHT

8 Appendix

8.1 Specific land requirements: list of mines, metals extracted and period (n=106)

#	Mine name	Current Status	DSO or NDSO, CP or NCP?	Type	Metals extracted /Average ore grade	Period considered for ore and area calculations	Number of satellite images used for area measurement
1	Awaso	Operating	NCP	OP	Al	1986-2002	2
2	Boddington Worsley	Operating	NCP	OP	Al	1984-2011	1
3	Boke Sangarédi	Operating	NCP	OP	Al	1973-2012	1
4	Discovery Bay	Operating	NCP	OP	Al	1985-2010	2
5	Friguia	Closed	NCP	OP	Al	1986-2010	2
6	Gove	Operating	NCP	OP	Al	1970-2011	1
7	Juruti	Operating	NCP	OP	Al	2009-2012	1
8	Kindia	Operating	NCP	OP	Al	1974-2010	1
9	Krasno Oktyabrsk	Operating	NCP	OP	Al	1995-2010	2
10	Los Pijiguaos	Operating	NCP	OP	Al	1987-2013	1
11	Moengo Coermotibo	Operating	NCP	OP	Al	1987-2009	2
12	Panchpatmali	Operating	NCP	OP	Al	1985-2012	1
13	Trombetas	Operating	NCP	OP	Al	1979-2011	1
14	Area C	Operating	DSO	OP	Fe (62%)	2003-2011	1

#	Mine name	Current Status	DSO or NDSO, CP or NCP?	Type	Metals extracted /Average ore grade	Period considered for ore and area calculations	Number of satellite images used for area measurement
15	Bailadila 10	Operating	DSO	OP	Fe (65.4%)	2002-2011	1
16	Bailadila 14 and 11 C	Operating	DSO	OP	Fe (65.4%)	1976-2011	1
17	Bailadila 5	Operating	DSO	OP	Fe (65.8%)	1980-2011	1
18	Capitão Do Mato	Operating	NDSO	OP	Fe (62%)	1971-2011	1
19	Carajás/Serra Norte	Operating	DSO	OP	Fe (66%)	1986-2011	1
20	Chadormalou	Operating	NDSO	OP	Fe (68%)	1998-2011	1
21	Channar	Operating	DSO	OP	Fe (63%)	1990-2010	1
22	Chitradurga	Operating	DSO	OP	Fe (63.7%)	2002-2010	1
23	Eastern Range	Operating	DSO	OP	Fe (63%)	2004-2010	1
24	El Gedida (el Bahariya)	Operating	DSO	OP	Fe (54.5%)	1973-2012	1
25	Frances Creek	Operating	NDSO	OP	Fe (56%)	1967-1974, 2007-2012	1
26	Gole Gohar	Operating	NDSO	OP	Fe (57%)	1994-2011	1
27	Hope Downs	Operating	DSO	OP	Fe (61%)	2007-2011	1
28	Jack Hills	Suspended	DSO	OP	Fe (62%)	2008-2010	1
29	Jimblebar	Operating	DSO	OP	Fe (61%)	1989-2008	1
30	Koolan Island	Operating	DSO	OP	Fe (67%)	1959-1993	1
31	Kudremukh	Closed	NDSO	OP	Fe (67.5%)	1976-2002	1
32	Marcona	Operating	NDSO	OP	Fe (57%)	1953-2012	1
33	Mont Wright	Operating	NDSO	OP	Fe (28%)	1975-2012	1

#	Mine name	Current Status	DSO or NDSO, CP or NCP?	Type	Metals extracted /Average ore grade	Period considered for ore and area calculations	Number of satellite images used for area measurement
34	Pardoo	Operating	DSO	OP	Fe (57%)	2008-2012	1
35	Savage River	Operating	NDSO	OP	Fe (35.3%)	1968-2010	1
36	Sydvaranger	Operating	NDSO	OP	Fe (65%)	1910-1994	1
37	Tallering Peak	Operating	DSO	OP	Fe (61%)	2004-2012	1
38	Tamanduá	Operating	NDSO	OP	Fe (61%)	1971-2011	1
39	Thabazimbi	Operating	NDSO	OP	Fe (60%)	1984-2012	2
40	Yandi	Operating	DSO	OP	Fe (57%)	1992-2012	1
41	Aitik Copper mine	Operating	CP	OP	Cu,Au,Ag	1986-2012	2
42	Alamo Dorado Silver mine	Operating	CP	OP	Ag,Au,Cu	2007-2013	1
43	Alumbrera Gold/Copper mine	Operating	CP	OP	Cu,Au,Ag	1997-2010	1
44	Amantaytau Oxides Gold mine	Operating	NCP	OP	Au	2004-2008	1
45	Antapite Gold mine	Closed	CP	UG	Au,Ag	2001-2010	1
46	Ares Gold mine	Operating	CP	UG	Au,Ag	1998-2011	1
47	Batu Hijau Copper/Gold mine	Operating	CP	OP	Cu,Au	2000-2011	1
48	Berezitovy Gold mine	Operating	NCP	OP	Au	2007-2013	1
49	Boroo Gold mine	Operating	NCP	OP	Au	2004-2013	1
50	Burnstone Gold mine	Suspended	NCP	UG	Au	2010-2012	1
51	Cerro Corona Copper/Gold mine	Operating	CP	OP	Cu,Au	2008-2011	1
52	Chapada Copper/Gold mine	Operating	CP	OP	Cu,Au	2006-2011	1

#	Mine name	Current Status	DSO or NDSO, CP or NCP?	Type	Metals extracted /Average ore grade	Period considered for ore and area calculations	Number of satellite images used for area measurement
53	Chatree Gold mine	Operating	CP	OP	Au,Ag	2001-2013	1
54	Chelopech Gold/Copper mine	Operating	CP	UG	Cu,Au,Ag	1954-2013	1
55	Chuquicamata Copper Mine	Operating	CP	OP	Cu,Au,Mo,Ag	1987-2013	2
56	Collahuasi Copper Mine	Operating	CP	OP	Cu,Mo	1998-2013	1
57	Corihuarmi Gold mine	Operating	NCP	OP	Au	2008-2013	1
58	Cracow Gold mine	Operating	CP	UG	Au,Ag	1988-2013	1
59	Denton-Rawhide Gold mine	Closed	CP	OP	Au,Ag	1990-2010	1
60	Dolores Gold mine	Operating	CP	OP	Au,Ag	2009-2013	2
61	El Sauzal Gold mine	Operating	NCP	OP	Au	2004-2011	1
62	Eloise Copper/Gold mine	Operating	CP	UG	Cu,Au,Ag	1996-2008	1
63	Escondida-Zaldivar Copper Mine	Operating	CP	OP	Cu,Au,Ag	1990-2011	1
64	Essakane Gold mine	Operating	NCP	OP	Au	2010-2012	1
65	Geita Gold mine	Operating	NCP	OP	Au	2000-2012	1
66	Gualcamayo Gold Mine	Operating	NCP	OP	Au	2009-2013	1
67	Guelb Mogrhein Copper/Gold mine	Operating	CP	OP	Cu,Au	2006-2011	1
68	Henty Gold mine	Operating	NCP	UG	Au	1997-2010	1
69	Holt-Holloway Gold mine	Operating	NCP	UG	Au	1988-2012	1
70	Hycroft (Crofoot/Lewis) Gold mine	Operating	CP	OP	Au,Ag	1987-2010	1
71	Joe Mann Gold mine	Suspended	CP	UG	Au,Cu,Ag	1987-2007	1

#	Mine name	Current Status	DSO or NDSO, CP or NCP?	Type	Metals extracted /Average ore grade	Period considered for ore and area calculations	Number of satellite images used for area measurement
72	Kiniero (Jean-Gobele) Gold mine	Suspended	NCP	OP	Au	2002-2012	1
73	Kisladag Gold mine	Operating	NCP	OP	Au	2006-2012	1
74	La Coipa Silver/Gold mine	Suspended	CP	OP	Ag,Au	1989-2011	1
75	La Herradura Gold mine	Operating	CP	OP	Au,Ag	1998-2012	1
76	Mahd ad´Dahab Gold mine	Operating	CP	UG	Au,Ag,Cu,Zn	1990-2012	1
77	Minera Florida/Alhue Gold mine	Operating	CP	UG	Au,Ag,Zn	2003-2012	2
78	Mineral Hill (Australia) Gold/Copper mine	Operating	CP	UG	Au,Cu	1989-2005	1
79	Morila Gold mine	Operating	NCP	OP	Au	2000-2011	1
80	Mount Polley Copper/Gold mine	Suspended	CP	OP	Au,Cu,Ag	1997-2012	1
81	Mount Rawdon Gold mine	Operating	CP	OP	Au,Ag	2001-2012	1
82	Mupane Gold mine	Operating	NCP	OP	Au	2004-2012	1
83	Musselwhite Gold mine	Operating	NCP	UG	Au	1997-2011	1
84	Neves Corvo Copper Mine	Operating	CP	UG	Cu,Zn,Ag,Sn	1988-2013	1
85	Ok Tedi Copper/Gold Mine	Operating	CP	OP	Cu,Au,Ag	1989-2013	2
86	Osborne (Trough Tank) Copper/Gold Mine	Operating	CP	UG	Cu,Au	1996-2010	1
87	Palito Gold mine	Operating	CP	UG	Au,Cu	2005-2010	1
88	Peak Gold mine	Operating	CP	UG	Au,Cu	1993-2011	1
89	Poracota Gold mine	Suspended	CP	UG	Au,Ag	2007-2013	1

#	Mine name	Current Status	DSO or NDSO, CP or NCP?	Type	Metals extracted /Average ore grade	Period considered for ore and area calculations	Number of satellite images used for area measurement
90	Robinson Copper/Gold mine	Operating	CP	OP	Cu,Au,Ag,Mo	1996-2012	2
91	Rochester Silver Mine	Operating	CP	OP	Ag,Au	1986-2013	1
92	Round Mountain Gold Mine	Operating	CP	OP	Au,Ag	1988-2013	2
93	Sadiola Gold Mine	Operating	NCP	OP	Au	1997-2011	1
94	Seabee Gold mine	Operating	NCP	UG	Au	1991-2011	1
95	Siguiri Gold mine	Operating	NCP	OP	Au	1998-2012	1
96	Sossego Copper mine	Operating	CP	OP	Cu,Au,Ag	2004-2011	1
97	Super Pit Gold Mine	Operating	NCP	OP	Au	1989-2013	1
98	Syama Gold mine	Operating	NCP	OP	Au	1990-2011	1
99	Tintaya Copper mine	Closed	CP	OP	Cu,Au,Ag	1985-2011	1
100	Tritton Copper mine	Operating	CP	UG	Cu,Au,Ag	2005-2011	1
101	Troilus Copper/Gold mine	Closed	CP	OP	Au,Cu,Ag	1997-2010	1
102	Troy Copper/Silver mine	Suspended	CP	UG	Cu,Ag	1981-2011	1
103	Varvarinskoye Gold/Copper mine	Operating	CP	OP	Au,Cu	2008-2013	1
104	Veladero Gold mine	Operating	CP	OP	Au,Ag	2006-2013	1
105	Yanacocha Gold mines	Operating	CP	OP	Au,Ag	1994-2012	1
106	Yatela Gold mine	Operating	NCP	OP	Au	2001-2011	1

8.2 Further examples of cumulative net area disturbed calculations

Figure 107: Boddington bauxite mine. Unclassified (left) and classified image (right).

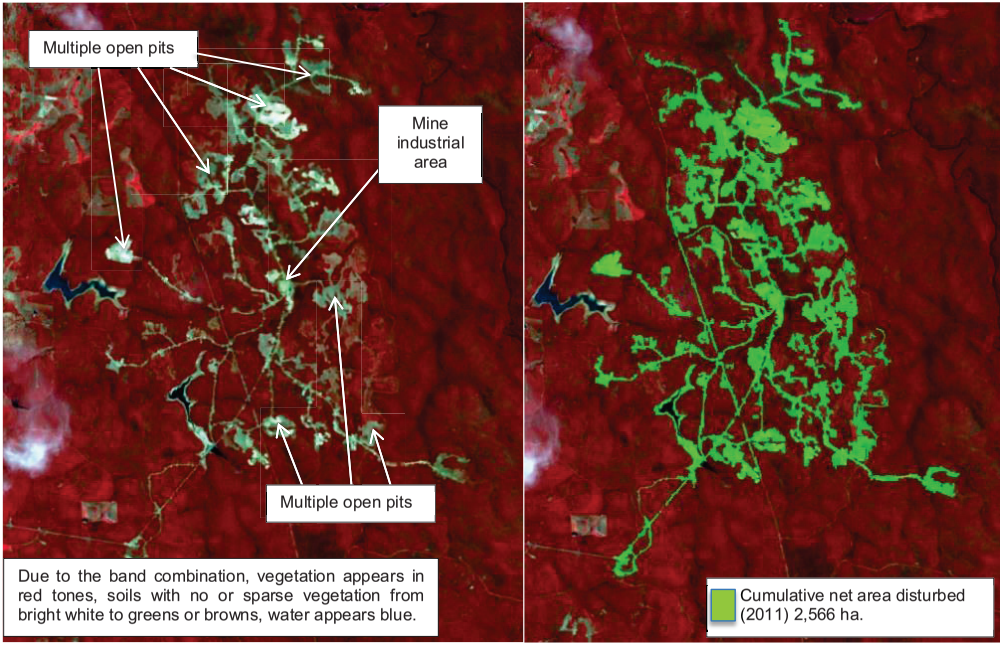

Source: self-elaboration based on a L7 image, acquisition date: 28/12/2011, Band combination (RGB): 432.

Figure 108: Yandi OP iron ore mine. Unclassified Landsat image. 2013.

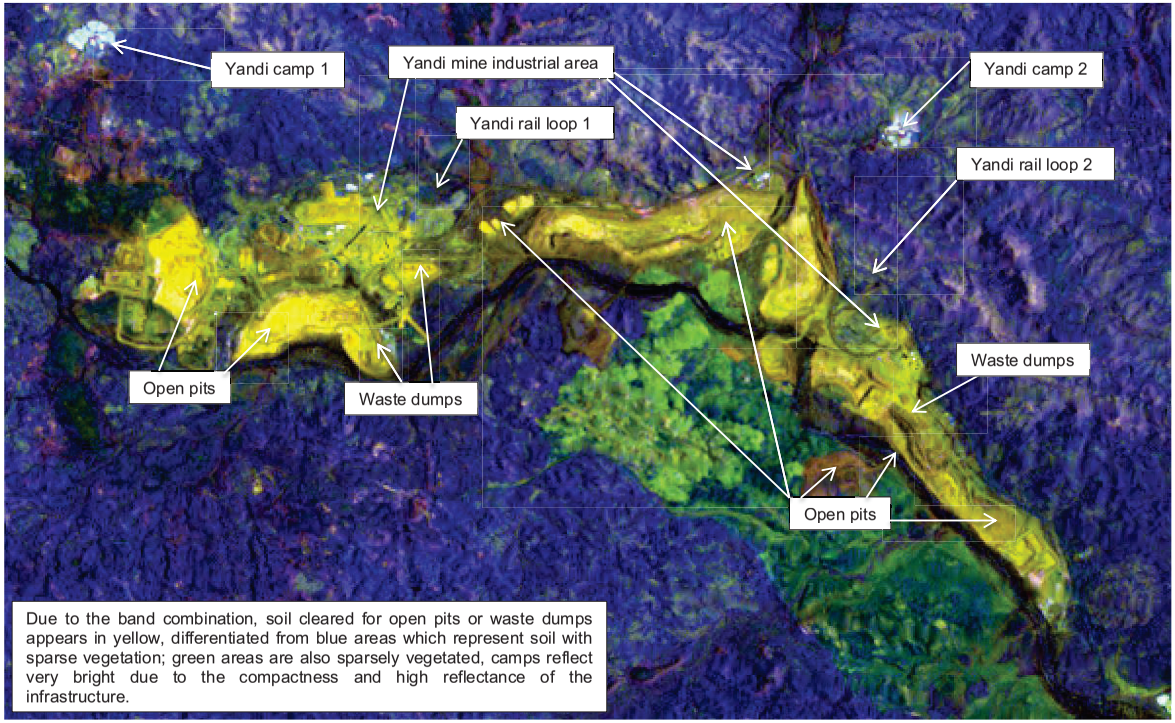

Source: self-elaboration based on a L5 image, acquisition date: 15/01/2013, Band combination (RGB): 571.

Figure 109: Yandi OP iron ore mine. Classified Landsat image (2013).

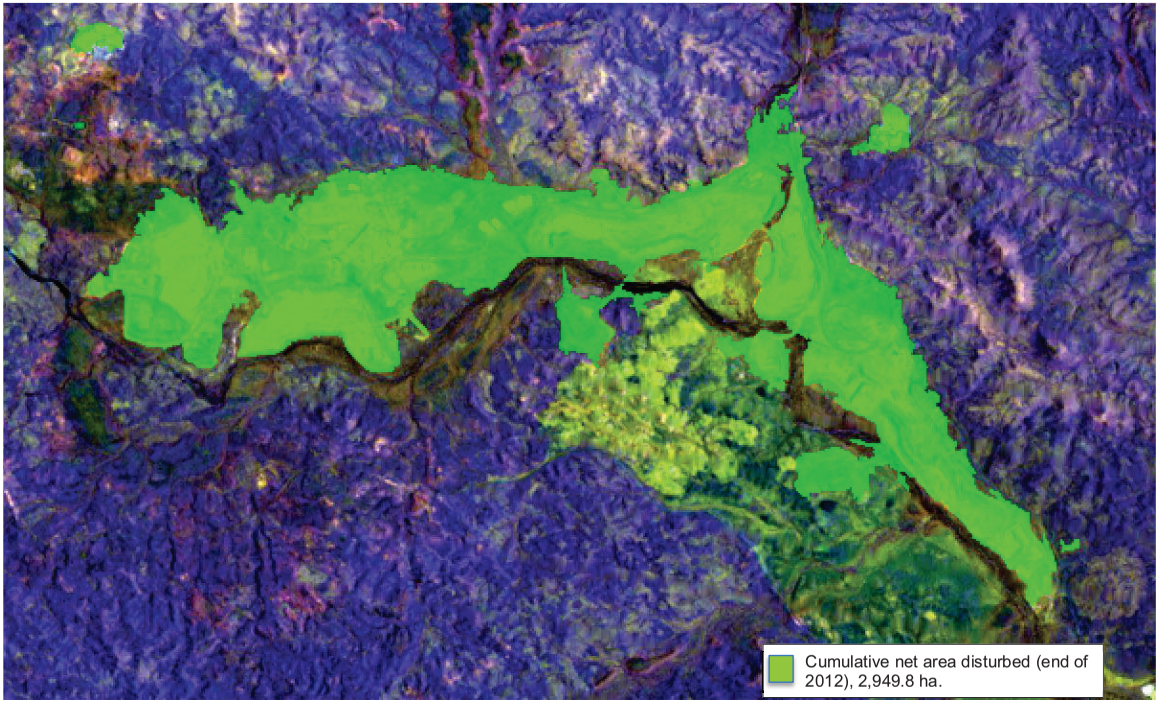

Source: self-elaboration based on an L5 image, acquisition date: 15/01/2013, Band combination (RGB): 571.

Figure 110: Burnstone NCP UG gold mine. Google Earth image.

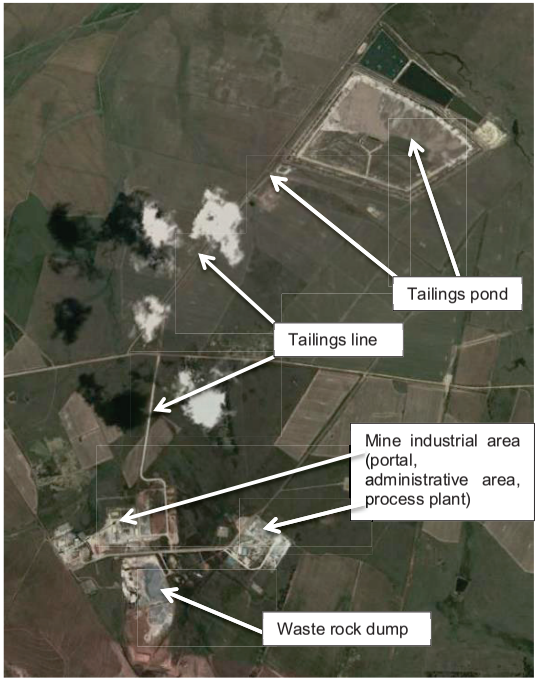

Source: Google Earth. Capture date: 14/09/2014.

Figure 111: Burnstone UG gold mine. Unclassified (left) and classified image (right).

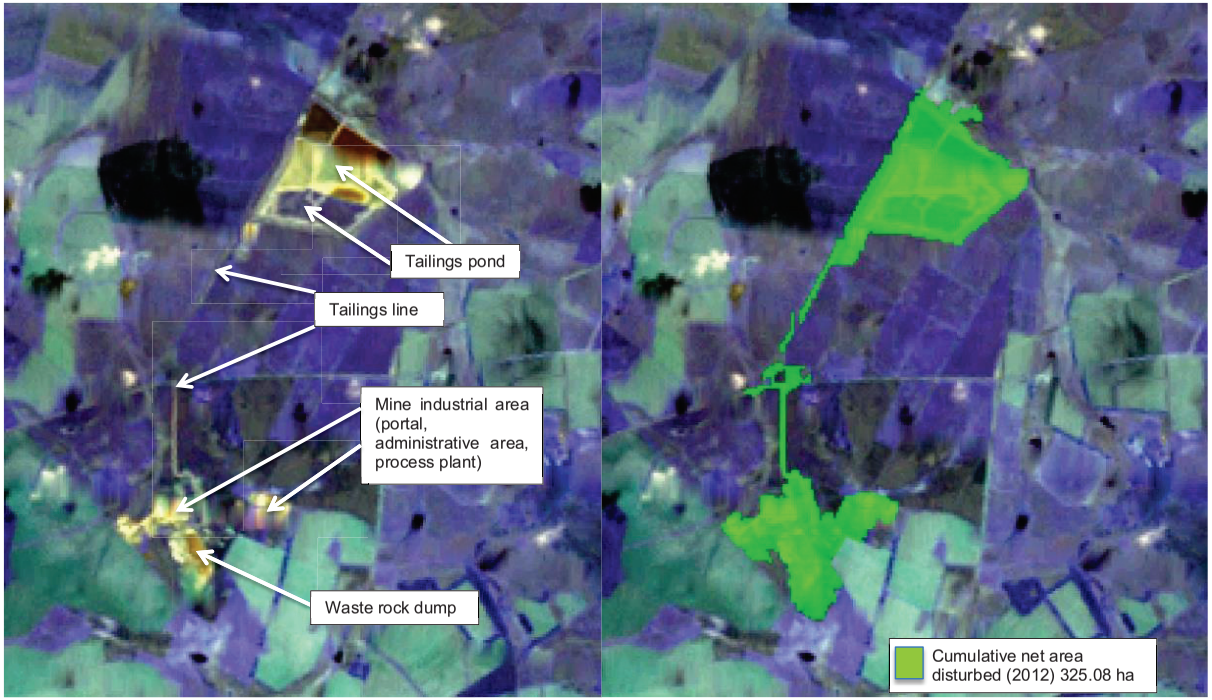

Source: self-elaboration based on gap-filled L7 image, acquisition date: 17/10/2012, Band combination (RGB): 234

Figure 112: Super pit NCP OP gold mine. Google Earth image. 2012.

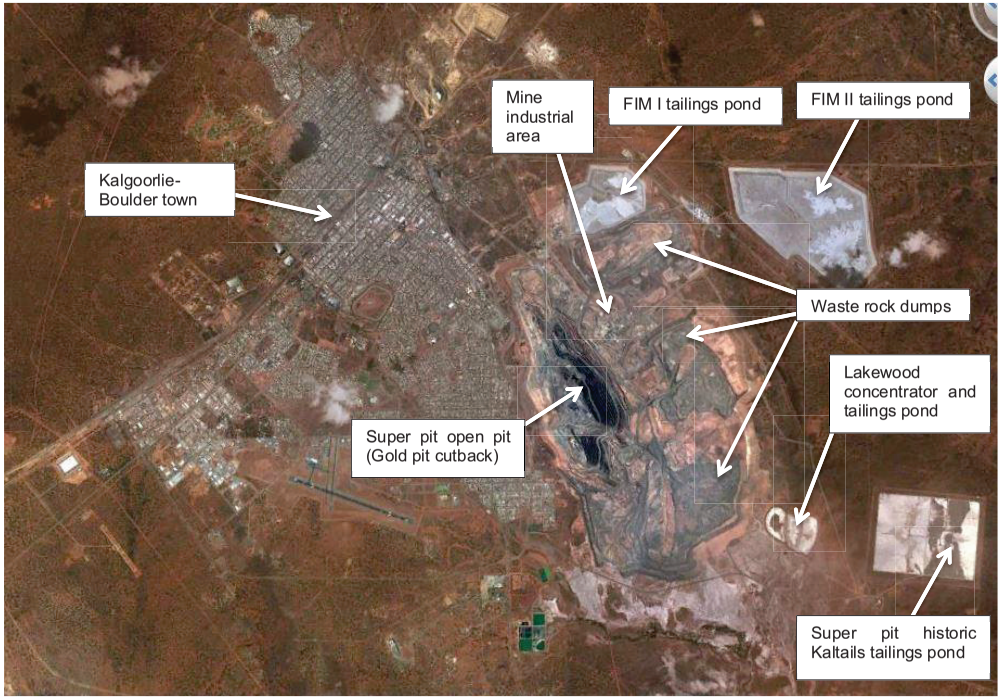

Source: Google Earth. Capture date: 14/09/2014.

Figure 113: Super pit NCP OP gold mine. Plan view of the proposed project (2007).

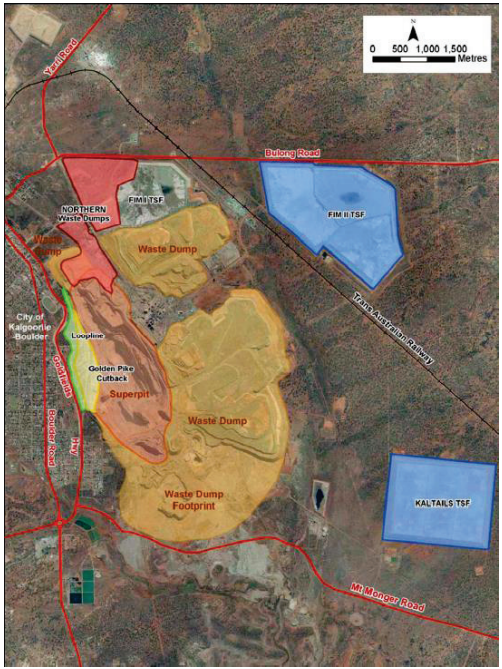

Source: Kalgoorlie Consolidated Gold Mines Pty Ltd, Fimiston Gold Mine Operations Extension (Stage 3) and Mine Closure Planning, December 2007.

Figure 114: Super pit NCP OP gold mine. Unclassified Landsat image (2013).

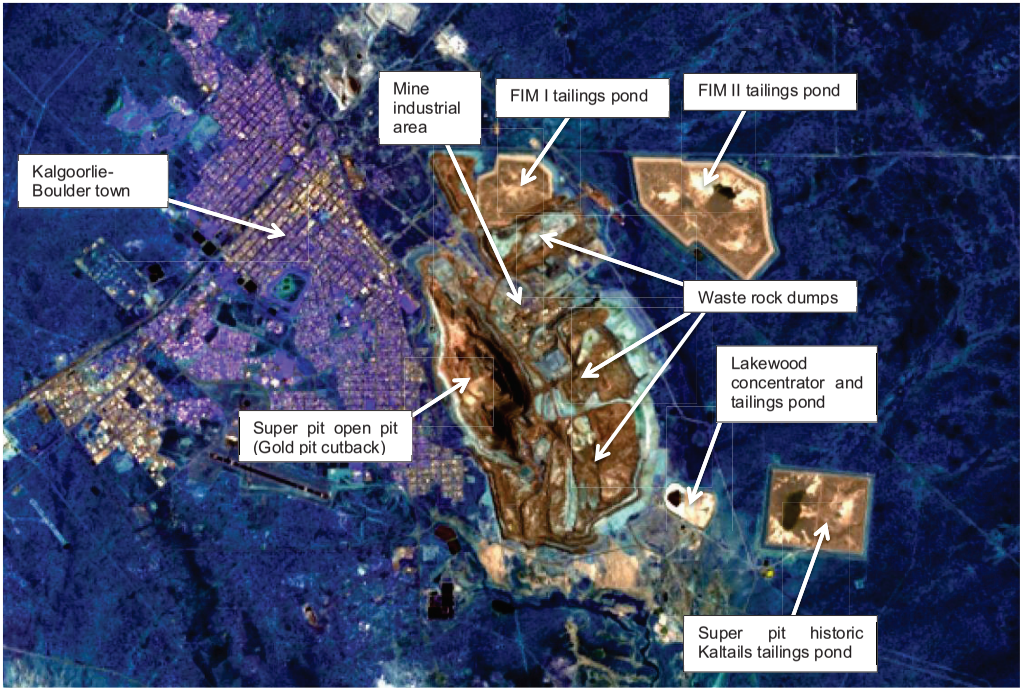

Source: self-elaboration on a L8 image (Acquisition date: 05/01/2014). Band combination (RGB): 234.

Figure 115: Super pit NCP OP gold mine. Classified Landsat image (2013).

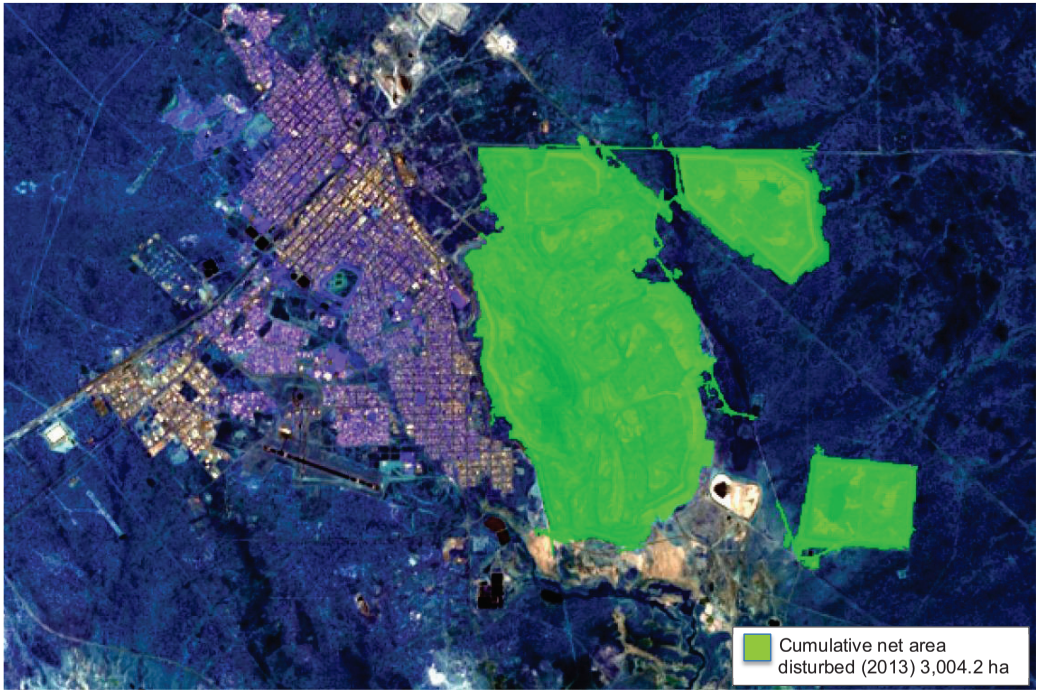

Source: self-elaboration on a L8 image (Acquisition date: 05/01/2014). Band combination (RGB): 234.

8.3 List of satellite images per mine and unallocated area disturbances

8.3.1 For specific land requirement calculations (n=119)

Bauxite (all NCP, OP mines)

#	Mine Name	Ope-ning year	Image acquisi-tion date (year-month-day)	Year it co-vers	Se n-sor	WRS2 Path_ Row	Band combin ation	SL [53]	Cumulative net area disturbed [ha]	Observation / Detail on mine elements included in the net area disturbed measurement
1	Awaso	1941	19860118	1985	L5	195_56	345	2	186.84	Open pit, mine industrial area (MIA) (including hospital area), tailings pond. No refinery plant at site, tailings result from washing. Atronsu and Awaso towns and Kanayerebo compound are not included.
2	Awaso	1941	20021224	2002	L7	195_56	345	2	221.85	Open pit, MIA (including hospital area), tailings pond. No refinery plant at site, tailings result from washing. Atronsu and Awaso towns and Kanayerebo compound are not included.
3	Boddington Worsley	1984	20111228	2011	L7	112_83	345	3	2,566.26	MIA and multiple open pits spread around the Saddleback mining operations area as shown in the plan of premises boundary (Department of Environment and Conservation 2012). Worsley alumina refinery not included.
4	Boke-Sangaredi	1973	20130512	2012	L8	203_52	345	6	3,060	MIA (incl. rail loading area) and multiple open pits. No tailings pond or dam visible or measured. Adjacent town not included.

[53] SL refers to the segmentation level used during the classification.

#	Mine Name	Ope-ning year	Image acquisi-tion date (year-month-day)	Year it co-vers	Se n-sor	WRS2 Path_ Row	Band combin ation	SL [53]	Cumulative net area disturbed [ha]	Observation / Detail on mine elements included in the net area disturbed measurement
5	Discovery Bay	1953	19850129	1985	L5	12_47	234	8	1,457.1	Multiple open pits, and MIA at Port Roades, incl. tailings pond. Based on the principal bauxite region in St Ann by Patterson et al. (1986)
6	Discovery Bay	1953	20110121	2010	L5	12_47	345	5	3,461.49	Multiple open pits, and MIA at Port Roades, including tailings pond.Based on the principal bauxite region in St Ann by Patterson et al. (1986)
7	Friguia	1960	19860103	1986	L5	202_53	234	5	597.51	Multiple open pits and MIA. No washing at mine site. Friguia alumina refinery plant located at the mine site is not considered in the calculation.
8	Friguia	1960	20110108	2010	L5	202_53	123	3	780.75	Multiple open pits and MIA. No washing at mine site. Friguia alumina refinery plant located at the mine site is not considered in the calculation.
9	Gove	1970	20111011	2011	L5	102_68	123	5	2,741.76	Open pits area, MIA, airstrip and the Nhulunbuy town. No washing at mine site (only crushing/screening). An alumina refinery located close to the mining area is not included.
10	Juruti	2009	20121023	2012	L7	228_62	457	5	1,484.46	Pits and MIA. A beneficiation washing plant with a tailings pond is present at mine site; they are both accounted for. The road between mine site and port facilities is also included in the calculation.
11	Kindia	1974	20110108	2010	L5	202_53	234	4	975.24	Multiple open pits, MIA, rail loading area. No washing facilities at mine site.
12	Krasno Oktyabrsk	1950	19950724	1995	L5	161_24	345	5	557.64	Open pits and MIA.

#	Mine Name	Ope-ning year	Image acquisi-tion date (year-month-day)	Year it co-vers	Se n-sor	WRS2 Path_ Row	Band combin ation	SL [53]	Cumulative net area disturbed [ha]	Observation / Detail on mine elements included in the net area disturbed measurement
13	Krasno Oktyabrsk	1950	20101021	2010	L5	161_24	345	5	1,609.83	Open pits and MIA.
14	Los Pijiguaos	1987	20131010	2013	L8	003_56	345	7	1,169.64	Open pits, MIA and the town with airstrip in which miners live and the road connecting the mine site with it
15	Moengo Coermotibo	1922	19870723	1987	L5	228_56	234	6	2,389.05	Open pits, MIA and the Moengo town.
16	Moengo Coermotibo	1922	20090804	2009	L5	228_56	234	6	3,307.41	Open pits, MIA and the Moengo town.
17	Panchpat-mali (Damanjodi)	1985	20121225	2012	L7	141_47	234	6	674.73	Open pit, MIA, includes part of the road connecting the mine site with the processing plant and the rail load area next to the refinery (refinery and its tailings pond are not included)
18	Trombetas	1979	20111029	2011	L5	228_61	234	6	5,863.77	Pits, MIA and tailings pond at mine site: in Trombetas there is no alumina refinery plant, but there is beneficiation and tailings are included as residues of beneficiation. Also includes the road between the Trombetas port and the mine area, the airstrip and town at the port.

Iron ore mines (all NCP, OP mines)

DSO mines

#	Mine Name	Ope-ning year	Image acquisi-tion date (year-month-day)	Year it co-vers	Se nsor	WRS2 Path_ Row	Band combin ation	SL	Cumulative net area disturbed [ha]	Observation / Clarification on mine elements included in the net area disturbed measurement
19	Area C	2003	20111228	2011	L7	112_76	571	3	2,486.61	Open pits, waste dumps, MIA, the camp on the Northwest and Mulla Mulla village and airport. Does not include the road connection between Mulla Mulla and the mine site. Based on BHP Billiton (2002); Environmental Protection Authority (1998)
20	Bailadila 10	2002	20111104	2011	L5	142_47	712	0	361.89	Bailadila 10 pit, MIA, rail loading area at Bacheli, pipelines and tailings pond at Bacheli. Based on Fig. 2 in Behre Dolbear (2010)
21	Bailadila 14 and 11 C	1976	20111104	2011	L5	142_47	345	0	637.74	Includes crushing and screening plant in Kurundil area, plus rail loading area and tunnels and Kadampal tailings pond
22	Bailadila 5	1980	20111104	2011	L5	142_47	234	0	526.5	Bacheli 5 pit area, MIA, rail loading area, and tailings pond in Bacheli complex. Based on Fig. 2 in Behre Dolbear (2010)
23	Carajás/ Serra Norte	1986	20110729	2011	L5	224_64	234	1	5,374.71	Includes only Serra Norte. MIA, EFC railway loading loop, waste dumps, the "núcleo habitacional" (6,000 inhabitants village) constructed by Vale and the Carajás/Parauapebas airport, PA-275 road connecting the mine with the village and the airport. Includes pits on deposits N3, N4 (N4WC, N4WN, N4E), N5 (N5W, N5E, N5E-N). Classification based on Cristiane and Fabrina

#	Mine Name	Ope-ning year	Image acquisi-tion date (year-month-day)	Year it co-vers	Se nsor	WRS2 Path_ Row	Band combin ation	SL	Cumulative net area disturbed [ha]	Observation / Clarification on mine elements included in the net area disturbed measurement
										(2013; Figuereido e Silva et al. (2011); Hilário et al. (2008); Sampaio et al. (2002)
24	Channar	1990	20101208	2010	L5	113_76	345	2	1,088.55	Open pits, waste dumps and MIA. Based on Pilbara Iron (2011)
25	Chitradurga	2000	20110117	2010	L7	145_50	712	2	441.81	Open pits, waste dumps and MIA.
26	Eastern Range	2004	20101208	2010	L5	113_76	712	4	662.49	Open pits, waste dumps and MIA.
27	El Gedida (el Bahariya)	1973	20121221	2012	L7	177_40	712	4	941.67	Open pits, waste dumps and MIA.
28	Hope Downs	2007	20111228	2011	L7	112_76	234	3	2,119.23	Open pits (Hope North, Hope South), waste dumps and MIA (incl. rail loading area and loop). Based on the general site layout (Fig. 2) in Environmental Protection Authority (2001)
29	Jack Hills	2007	20110118	2010	L5	112_78	571	4	141.93	Open pits, waste dumps and MIA. Based on Environmental Protection Authority (2011)
30	Jimblebar	1989	20090105	2008	L5	111_76	234	3	729.72	Open pits, waste dumps, MIA, 2009 and 2010 were years of no production. Based on Environmental Protection Authority (2010, 1995)
31	Koolan Island	1959	19931102	1993	L5	110_71	345	3	562.41	Open pits (Main pit, Mullet-Acacia, Acacia East), waste dumps and MIA. (incl. ship loader, airstrip, camp). Based on Ecologia Environment (2005); and Mount Gibson Iron Limited (2013)
32	Pardoo	2008	20130115	2012	L7	112_74	234	1	486	Open pits, waste dumps and MIA. Based on Environmental Protection Authority (2008)

#	Mine Name	Ope-ning year	Image acquisi-tion date (year-month-day)	Year it co-vers	Se nsor	WRS2 Path_ Row	Band combin ation	SL	Cumulative net area disturbed [ha]	Observation / Clarification on mine elements included in the net area disturbed measurement
33	Tallering Peak	2004	20121221	2012	L7	113_79	345	4	487.71	Open pits, waste dumps and MIA. Based on Mount Gibson Iron Limited (2006)
34	Yandi	1992	20130115	2012	L7	112_76	345	3	2,949.84	Open pits, waste dumps and MIA, including two rail loops and two camps. No access road accounted for between camp sites included. Based on Environmental Protection Authority (2005)

NDSO mines

#	Mine Name	Ope-ning year	Image acquisi-tion date (year-month-day)	Year it co-vers	Se nsor	WRS2 Path_ Row	Band combin ation	SL	Cumulative net area disturbed [ha]	Observation / Clarification on mine elements included in the net area disturbed measurement
35	Capitão Do Mato	1971	20110921	2011	L5	218_74	234	3	1,020.87	At Capitão includes the open pit, waste dumps and the MIA; the Morro de Chapéu village is not included. At the beneficiation complex Vargem Grande includes the MIA, the tailings pond and stockpiling and rail loading area.
36	Chadormalou	1998	20111024	2011	L5	161_38	123	3	1,240.47	Open pit, waste dumps, MIA, tailings facilities and rail loading area
37	Frances Creek	1967	20121127	2012	L7	105_69	234	5	506.43	Pits mined between 1967 and 1974 and from 2007; pits and adjacent waste dumps included are: Jasmine East and Thelma Rosemary, Ochre Hill, Helene 5, Helene 6/7, main dam and

#	Mine Name	Ope-ning year	Image acquisi-tion date (year-month-day)	Year it co-vers	Se nsor	WRS2 Path_ Row	Band combin ation	SL	Cumulativ e net area disturbed [ha]	Observation / Clarification on mine elements included in the net area disturbed measurement
										smaller dams, and the MIA. Road connecting the MIA with Ochre Hill is not included. Based on MBS Environmental (2006)
38	Gole Gohar	1994	20120104	2011	L7	161_40	712	4	2,095.38	Open pit, waste dumps, MIA and rail loading area
39	Kudremukh	1976	20030127	2002	L7	145_51	345	4	1,058.04	Open pit, MIA, waste dumps, Lakya tailings pond and township to the Northeast are included. Roads connecting the mine with nearby townships and to the port town of Mangalore are not accounted.
40	Marcona	1953	20130124	2012	L7	006_70	345	2	2,423.61	Includes the San Nicolas area and tailings pond
41	Mont Wright	1975	20120912	2012	L7	012_23	345	8	4991.94	Open pit, waste dumps, MIA, tailings facilities and rail loading area. Based on ArcelorMittal (2012)
42	Savage River	1968	20110404	2010	L5	091_89	234	4	1,255.77	Open pits (North, Centre and South), waste dumps, MIA, tailings pond, town site. Based on Mining Ore Consultants (2008).
43	Sydvaranger	1910	19940909	1994	L5	191_11	345	1	1080.9	It includes the open pits operating succesively since 1910 (bjornevatn, grundtjern, sostervann, tverndalen, fisketind, bjornefell, jerntoppen), concentrator and tailings in the water at Slambanken and Beddariand port located 8 km from Kirkenes. Submarine tailings in Bokfjorden are counted. Based on RSG Global Consulting Pty Ltd (2007)

#	Mine Name	Ope-ning year	Image acquisi-tion date (year-month-day)	Year it co-vers	Se nsor	WRS2 Path_ Row	Band combin ation	SL	Cumulativ e net area disturbed [ha]	Observation / Clarification on mine elements included in the net area disturbed measurement
44	Tamanduá	1971	20110921	2011	L5	218_74	345	3	780.84	At Tamanduá includes the open pit, waste dumps and the MIA; the Morro de Chapéu village is not included. At the beneficiation complex Vargem Grande includes the MIA, the tailings pond and stockpiling and rail loading area.
45	Thabazimbi	1934	19841019	1984	L5	171_77	234	3	878.58	Includes the MIA, pits and waste dumps visible in 1984, rail loading area and concentrator plant
46	Thabazimbi	1934	20130317	2012	L7	171_77	234	3	1,813.95	MIA, waste dumps and the pits: east pit, buffelshoek east, buffelshoek west, bobbejaanwater, kumba, donkerpoort new, donkerpoort west, kwaggashoek east and vanderbjil. The two underground mining areas (active until 1997) east mine and kwaggashoek east underground are not included. Based on Shangoni Management Services (2011)

Copper, Gold and Silver (unallocated measurements)

#	Mine Name	Type	Ope-ning year	Image acquisi-tion date (year-month-day)	Year it co-vers	Se nsor	WRS2 Path_ Row	Band combin ation	SL	Unalloca-ted cumulati-ve net area disturbed [ha]	Observation / Clarification on mine elements included in the net area disturbed measurement
47	Aitik Copper	OP	1968	19860715	1986	L5	193_13	234	7	1,767	Includes Aitik and Salmijärvi pits/deposits. Tailings pond

#	Mine Name	Type	Ope-ning year	Image acquisi-tion date (year-month-day)	Year it co-vers	Se nsor	WRS2 Path_ Row	Band combin ation	SL	Unalloca-ted cumulati-ve net area disturbed [ha]	Observation / Clarification on mine elements included in the net area disturbed measurement
	Mine										included.
48	Aitik Copper Mine	OP	1968	20120907	2012	L7	193_13	123	1	4,347	Includes Aitik and Salmijärvi pits/deposits. Liikavaara deposit not included as not exploited in 2011.Tailings pond included. Based on Boliden Mineral (2014)
49	Alamo Dorado Silver mine	OP	2007	20131231	2013	L8	33_42	156	1	205.11	Open pit, waste dumps, MIA, and dry stack tailings area.
50	Alumbrera Gold/Copper mine	OP	1997	20101202	2010	L5	231_79	156	1	2,413	MIA, open pit, waste dumps and tailings pond. Classification based on Hennessey et al. (2009)
51	Amantaytau Oxides Gold mine	OP	2004	20081128	2008	L7	157_31	456	1	622.53	Open pits, waste dumps, MIA, tailings ponds
52	Antapite Gold mine	UG	2001	20101124	2010	L5	006_70	126	2	266.67	MIA, Huinchulla tailings pond, Machucancha camp, other areas
53	Ares Gold mine	UG	1998	20110910	2011	L5	004_70	126	4	158.31	MIA, waste dump and tailings pond. Based on SVS Ingenieros (2012)
54	Batu Hijau Copper/Gold mine	OP	2000	20110827	2011	L7	115_66	345	8	2,186	Includes the open pit, waste dumps and the copper-gold concentrator. Buin Batu town, Benete port, tailings outfall pipeline and submarines tailings area is not included (bad image resolution). Based on Craig Vogt Inc (2012)

#	Mine Name	Type	Ope-ning year	Image acquisi-tion date (year-month-day)	Year it co-vers	Se nsor	WRS2 Path_ Row	Band combin ation	SL	Unalloca-ted cumulati-ve net area disturbed [ha]	Observation / Clarification on mine elements included in the net area disturbed measurement
55	Berezitovy Gold mine	OP	2007	20130926	2013	L8	122_22	234	6	505.17	Open pits, waste dumps, MIA, tailing ponds. Measurement according to Kenwright et al. (2013), Figure 17.1 (page 168)
56	Boroo Gold mine	OP	2004	20131011	2013	L8	131_26	234	4	906.84	Open pits (3,5,6), waste dumps, MIA, heap leach pad, alluvial mine area and Ikh Dashir tailings pond. Based on Raponi and Redmond (2009)
57	Burnstone Gold mine	UG	2010	20121017	2012	L7	170_78	234	3	325.08	MIA, waste dump and tailings pond. Based on Great Basin Gold Ltd (2011)
58	Cerro Corona Copper/Gold mine	OP	2008	20120207	2011	L7	9_65	234	6	554.76	Cerro Corona open pit, Chorro Blanco and Gordas, waste dumps, oxide stockpiles, MIA, Hierba, Aguilas and Gordas dam. Based on Gold Fields (2011)
59	Chapada Copper/Gold mine	OP	2006	20110917	2011	L5	222_70	234	3	1,760.85	Central open pit, south central, NE and SW waste dump, MIA and tailings pond. Based on Avila de Moura (2007)
60	Chatree Gold mine	OP	2001	20131130	2013	L8	129_49	234	5	763.2	Open pits (A + Q pits), waste dumps, MIA, tailings ponds (1 + 2). Based on Fig. 2 in GME (2013)
61	Chelopech Gold/Copper	UG	1954	20140111	2013	L8	183_30	345	2	167.04	Main North & South sites, MIA and the tailings pond. Kachulka dam and

#	Mine Name	Type	Ope-ning year	Image acquisi-tion date (year-month-day)	Year it co-vers	Se nsor	WRS2 Path_ Row	Band combin ation	SL	Unalloca-ted cumulati-ve net area disturbed [ha]	Observation / Clarification on mine elements included in the net area disturbed measurement
	mine										the adjacent Chelopech village are not included. Based on Chelopech Mining EAD (2010) and Dundee Precious Metals Inc. (2011)
62	Chuquicamata Copper Mine	OP	1915	19861103	1987	L5	1_75	571	1	6,075	Includes the main pit and workings in Chuquicamata North. Waste dumps, the mining town, the refinery, the beneficiation plant, the PTMP plant (opened Nov. 2005) and the tailings pond (Talabre) are included. In the North, the mine Radomiro Tomic, and in the South the South Mine (Exotica), mine Minister Hales and Chuquicamata Smelter are not included.
63	Chuquicamata Copper mine	OP	1915	20131129	2013	L8	1_75	123	10	11,681	Includes the main pit and workings in Chuquicamata North. Waste dumps, the mining town, the refinery, the beneficiation plant, the PTMP plant (opened Nov. 2005) and the tailings pond (Talabre) are included. In the North, the mine Radomiro Tomic, and in the South the South Mine (Exotica), mine Minister Hales and Chuquicamata Smelter are not included.
64	Collahuasi Copper mine	OP	1998	20140201	2013	L8	1_74	712	10	5,423	MIA, Rosario and Ujina open pits, road connecting them and

#	Mine Name	Type	Ope-ning year	Image acquisi-tion date (year-month-day)	Year it co-vers	Se nsor	WRS2 Path_ Row	Band combin ation	SL	Unalloca-ted cumulati-ve net area disturbed [ha]	Observation / Clarification on mine elements included in the net area disturbed measurement
											tailings.Based on (Mining Technology 2015a)
65	Corihuarmi Gold mine	OP	2008	20131218	2013	L8	06_69	345	8	467.01	Open pits, waste dumps, MIA, heap leach pad. Based on Coffey Mining Pty Ltd (2010)
66	Cracow Gold mine	UG	1988	20131221	2013	L8	91_78	234	6	217.35	MIA, waste dump and tailings pond. Based on Beadell Resources Ltd (2008)
67	Denton-Rawhide Gold mine	OP	1990	20100917	2010	L5	42_33	345	4	526.32	Open pit, waste dump, MIA, heap leach pad
68	Dolores Gold mine	OP	1860s	20091211	2009	L5	34_40	345	1	489	MIA, open pits, waste dumps and heap leach facilities.
69	Dolores Gold mine	OP	1860s	20140107	2013	L8	34_40	234	6	671	MIA, open pits, waste dumps and heap leach facilities.
70	El Sauzal Gold mine	OP	2004	20111108	2011	L5	33_41	345	4	371.97	Open pit, waste dumps, MIA, and dry stack tailings area.
71	Eloise Copper/Gold mine	UG	1996	20081225	2008	L5	98_74	234	2	185.22	MIA, waste dump and tailings pond.
72	Escondida-Zaldivar Copper mine	OP	1990	20111117	2011	L5	233_77	345	3	30,774	Includes area disturbances for Escondida, Escondida Norte and Zaldívar mine: pits, camps, tailings ponds and roads connecting the spatial continuum of the mines.

#	Mine Name	Type	Ope-ning year	Image acquisi-tion date (year-month-day)	Year it co-vers	Se nsor	WRS2 Path_ Row	Band combin ation	SL	Unalloca-ted cumulati-ve net area disturbed [ha]	Observation / Clarification on mine elements included in the net area disturbed measurement
											Opening year belongs to Escondida. Based on Golder Associates (2008). Well field in Punta Negra and Coloso port facilities not included.
73	Essakane Gold mine	OP	2010	20121228	2012	L7	194_50	234	4	1,708.02	Open pits, waste dumps, MIA, tailing ponds. Off channel storage not included. Based on Gignac et al. (2009)
74	Geita Gold mine	OP	2000	20130301	2012	L7	171_62	234	4	2,469.87	Area includes open pits, waste dumps, MIA, tailings pond, camp, airstrip and roads connecting open pits with MIA.
75	Gualcamayo Gold mine	OP	2001	20131201	2013	L8	129_49	234	5	667.35	Open pit, waste dump, MIA, heap leach pad
76	Guelb Mogrhein Copper/Gold mine	OP	2006	20110903	2011	L5	204_46	345	4	891.27	Open pit, waste dumps, MIA, and tailings ponds. Based on Scott Wilson Mining (2005)
77	Henty Gold mine	UG	1996	20110404	2010	L7	91_89	234	2	169.65	MIA, waste dump, areas at portals and tailings pond.
78	Holt-Holloway Gold mine	UG	1988	20121116	2012	L7	19_26	345	3	273.24	The ore from Holloway is processed at Holt facilities. Tailings pond is included.
79	Hycroft (Crofoot/Lewis) Gold mine	OP	1987	20100917	2010	L5	42_32	345	3	1,544.13	Mine closed from 2003 until 2009. Based on Scott E. Wilson Consulting Inc (2009)

#	Mine Name	Type	Ope-ning year	Image acquisi-tion date (year-month-day)	Year it co-vers	Se nsor	WRS2 Path_ Row	Band combin ation	SL	Unalloca-ted cumulati-ve net area disturbed [ha]	Observation / Clarification on mine elements included in the net area disturbed measurement
80	Joe Mann Gold mine	UG	1987	20071005	2007	L5	16_26	345	1	103.86	MIA, waste dump and tailings pond.
81	Kiniero (Jean-Gobele) Gold mine	OP	2002	20121222	2012	L7	200_53	123	2	524.43	Open pits (2), waste dumps, MIA, tailings ponds and the airstrip.
82	Kisladag Gold mine	OP	2006	20130205	2012	L7	179_33	234	7	804.42	Open pits, waste dumps, MIA, heap leach pad. Based on Hatch (2003)
83	La Coipa Silver/Gold mine	OP	1989	20111117	2011	L5	233_79	126	3	1,991	Includes the MIA, Ladera Farellon, Can Can, Coipa Norte, Brecha Norte pits and waste dumps, tailings pond. Includes Puren and Chimberos deposits and disturbances around them.Based on Belanger (2003).
84	La Herradura Gold mine	OP	1998	20121216	2012	L7	37_38	456	3	1,700	MIA, open pits, waste dumps and heap leach facility.
85	Mahd ad´Dahab Gold mine	UG	1990	20121229	2012	L7	169_44	345	2	168.66	MIA, camp and dry-tailings storage facilities. Based on SRK Consulting (2007)
86	Minera Florida/Alhue Gold mine	UG	1986	20031229	2003	L5	233_84	234	2	148.14	MIA, tailings pond, roads connecting the MIA and accesses to the mine (Marisol area). Based on MYMA (2012)
87	Minera Florida/Alhue	UG	1986	20121229	2012	L7	233_84	234	4	275.76	MIA, tailings pond, roads connecting the MIA and accesses to

#	Mine Name	Type	Ope-ning year	Image acquisi-tion date (year-month-day)	Year it co-vers	Se nsor	WRS2 Path_ Row	Band combin ation	SL	Unalloca-ted cumulati-ve net area disturbed [ha]	Observation / Clarification on mine elements included in the net area disturbed measurement
	Gold mine										the mine (Milennium and Marisol areas)
88	Mineral Hill (Australia) Gold/Copper mine	UG	1987	20051120	2005	L5	92_83	156	3	138.96	MIA, waste dumps, eastern pit and tailings and evaporations ponds.
89	Morila Gold mine	OP	2000	20111112	2011	L5	198_52	345	5	1,135.17	Open pit, waste dumps (active + inactive), MIA, heap leach pads (Lewis, Brimstone and Crofoot)
90	Mount Polley Copper/Gold mine	OP	1997	20121003	2012	L7	48_23	234	6	1,475.28	Open pits (Springer, Bell, Cariboo, Wight), waste dumps (East), MIA and tailings pond. Based on Gillstrom (2004)
91	Mount Rawdon Gold mine	OP	2001	20121203	2012	L7	90_78	156	4	577.8	Open pit, waste dump, MIA, tailings pond. Based on Boon (2013)
92	Mupane Gold mine	OP	2004	20130128	2012	L7	171_75	234	6	329.04	Open pits (Kwena, Tau and Tholo), waste dumps, MIA, tailing ponds. Based on Tomkinson and Putland (2006)
93	Musselwhite Gold mine	UG	1997	20110927	2011	L7	27_23	123	6	570.42	MIA, waste dump and tailings pond. Classification based on ERM (2013); Goldcorp (2007)
94	Neves Corvo Copper Mine	UG	1989	20140123	2013	L8	203_34	571	4	432.72	MIA, railway terminal and the Barragem Cerro do Lobo TMF, including the road between the mine

#	Mine Name	Type	Ope-ning year	Image acquisi-tion date (year-month-day)	Year it co-vers	Se nsor	WRS2 Path_ Row	Band combin ation	SL	Unalloca-ted cumulati-ve net area disturbed [ha]	Observation / Clarification on mine elements included in the net area disturbed measurement
											site and the TMF. Based on Lunding Mining (2012)
95	Ok Tedi Copper/Gold mine	OP	1985	19890423	1988	L5	100_64	345	1	1,062	Includes the mine pit area, gold process facility, mine access road, workshop and Tabubil town. No tailings pond exists, the ground rock tailings from the process are disposed of via the unconfined end of the pipe discharge to Harvey Creek, which drains to the Ok Mani, and then to the Ok Tedi and Fly rivers. Therefore the Ok Mani river until its confluence with the Ok Tedi river (in Tabubil town) and the Fly river until it intersects the Ok Tedi are considered part of the net area disturbed. Based on Hendry et al. (2005)
96	Ok Tedi Copper/Gold mine	OP	1985	20140428	2013	L8	100_64	234	2	2,034.8	Includes the mine pit area, gold process facility, mine access road, workshop and Tabubil town. No tailings pond exists, the ground rock tailings from the process are disposed of via the unconfined end of the pipe discharge to Harvey Creek, which drains to the Ok Mani, and then to the Ok Tedi and Fly rivers. Hence the Ok Mani river until its confluence with the Ok Tedi river

#	Mine Name	Type	Ope-ning year	Image acquisi-tion date (year-month-day)	Year it co-vers	Se nsor	WRS2 Path_ Row	Band combin ation	SL	Unalloca-ted cumulati-ve net area disturbed [ha]	Observation / Clarification on mine elements included in the net area disturbed measurement
											(in Tabubil town) and the Fly river until it intersects the Ok Tedi are included as net area disturbed. Based on Hendry et al. (2005)
97	Osborne (Trough Tank) Copper/Gold Mine	UG	1995	20101215	2010	L5	98_75	571	1	440.1	Includes the tailings pond, the camp site and the airstrip. Also includes the open pit (operated only one year during 1995) because the mine portal is located directly within the pit. Based on Ebbels et al. (2012)
98	Palito Gold mine	UG	2004	20101104	2010	L5	227_64	456	4	163.53	MIA, waste dump and tailings ponds Based on Guzmán and Mello (2012). Given the lack of other land uses in the nearby areas, it was assumed that some areas disturbed to the East and North of the general site also belong to the mine´s activities.
99	Peak Gold mine	UG	1992	20111011	2011	L5	93_82	234	2	294.3	Includes road in the perimeter of the mine. Classification based on Lloyd et al. (2009).
100	Poracota gold mine	UG	2007	20131220	2013	L8	004_70	345	6	55.08	MIA and waste dump. No tailings ponds at mine site because the ore is sent to Orcopampa´s concentrator for beneficiation.

#	Mine Name	Type	Ope-ning year	Image acquisi-tion date (year-month-day)	Year it co-vers	Se nsor	WRS2 Path_ Row	Band combin ation	SL	Unalloca-ted cumulati-ve net area disturbed [ha]	Observation / Clarification on mine elements included in the net area disturbed measurement
101	Robinson Copper/Gold mine	OP	1904	19961217	1996	L5	40_33	456	4	1,994.49	Open pits, waste dumps, MIA, tailings ponds
102	Robinson Copper/Gold mine	OP	1904	20121103	2012	L7	40_33	456	4	3,651.75	Open pits, waste dumps, MIA, tailings ponds
103	Rochester Silver mine	OP	1986	20140115	2013	L8	42_32	234	8	802.7	MIA, open pits (Rochester and Nevada Packard), waste dumps and heap leach pad in the north.
104	Round Moutain Gold mine	OP	1977	19880609	1987	L5	41_33	571	1	1,366	MIA, open pits, waste dumps, heap leach, tailings pond and the town west of the mine (Hadley town).
105	Round Moutain Gold mine	OP	1977	20140124	2013	L8	41_33	712	10	3,314	Includes the MIA, open pits, waste dumps, heap leach, tailings pond and the Hadley town. Includes the developments visible in 2014 at the North of the big mine. Based on Fig. 3-2 in Hanson (2006)
106	Sadiola Gold mine	OP	1997	20110921	2011	L5	202_50	234	1	2,019.51	Open pit (main pit and four satellite pits), waste dumps, MIA, tailings pond and water body next to it. The camp located north of the main pit is also included, also with the road connecting it. The City Sadiola is next to the mine and is not included. Based on Mining Technology

#	Mine Name	Type	Ope-ning year	Image acquisi-tion date (year-month-day)	Year it co-vers	Se nsor	WRS2 Path_ Row	Band combin ation	SL	Unalloca-ted cumulati-ve net area disturbed [ha]	Observation / Clarification on mine elements included in the net area disturbed measurement
											(2015b)
107	Seabee Gold mine	UG	1991	20110910	2011	L7	36_21	234	2	297.1	MIA (incl. airstrip), tailings ponds, and infrastructure at Porky West, Porky Main and Santoy 7 and 8. Roads connecting the access to the mine are included. Based on Fig. 2 in Longo and Skanderberg (2012)
108	Siguiri Gold mine	OP	1998	20121222	2012	L7	200_52	156	4	2,834.1	Open pits, waste dump, MIA, heap leach pad, solution ponds and tailings pond. Villages located adjacent to the mining area (Boukaria) are not included.
109	Sossego Copper mine	OP	2004	20110923	2011	L7	224_64	234	4	2,811.15	Open pits, waste dumps, MIA, tailings pond
110	Super Pit Gold mine	OP	1989	20140105	2013	L8	109_81	234	8	3,004.29	Includes the Superpit, waste dumps, including the waste dump footprint bordering southwards with the Mt Monger road. Tailings pond included in the footprint are Fim I and II and the historic Kaltails TSF. The Kalgoorlie-Boulder town and the Lakewood concentrator and its tailings pond are not included. Classification based on Kalgoorlie Consolidated Gold Mines Pty Ltd (2007); Gold Field Tourism (2015); Mining Technology (2015c)

#	Mine Name	Type	Ope-ning year	Image acquisi-tion date (year-month-day)	Year it co-vers	Se nsor	WRS2 Path_ Row	Band combin ation	SL	Unalloca-ted cumulati-ve net area disturbed [ha]	Observation / Clarification on mine elements included in the net area disturbed measurement
111	Syama Gold mine	OP	1990	20111112	2011	L7	198_52	234	4	768.42	Open pit, waste dumps, MIA, tailings ponds
112	Tintaya Copper mine	OP	1984	20111106	2011	L5	003_70	345	4	2,952.54	Open pits, waste dumps, MIA, tailings ponds (Huinipampa and Ccamacmayo). Based on Mesa de Diálogo Espinar (2013)
113	Tritton Copper mine	UG	2005	20111020	2011	L5	92_82	126	2	290.7	MIA, waste dump and tailings pond.
114	Troilus Copper/Gold mine	OP	1997	20110609	2010	L7	17_24	123	8	1,112.04	Z87 and J4 open pits, waste dumps, MIA, tailings pond. Nearby lakes not included. Based on Copper One (2014)
115	Troy Copper/Silver mine	UG	1981	20110803	2011	L5	42_26	156	4	351.63	MIA, old pit, waste dump and tailings pond to the north of the MIA. Based on Fig. 2. in SRK Consulting (2005)
116	Varvarinskoye Gold/Copper mine	OP	2008	20131114	2013	L8	161_23	345	5	947.7	Central open pit, waste dumps, MIA, heap leach pad area and tailings pond. Based on Bateman (1998)
117	Veladero Gold mine	OP	2006	20131122	2013	L8	233_80	571	6	1,763.01	Open pits (Filo Federico and Amable), waste dump, MIA (incl. Veladero camp), heap leach pad. The road connecting the mine site with the camp is not included. The Argenta pit is also not included.

#	Mine Name	Type	Ope-ning year	Image acquisi-tion date (year-month-day)	Year it co-vers	Se nsor	WRS2 Path_ Row	Band combin ation	SL	Unalloca-ted cumulati-ve net area disturbed [ha]	Observation / Clarification on mine elements included in the net area disturbed measurement
											Based on MAGSA (2009)
118	Yanacocha Gold mine	OP	1993	20120907	2012	L7	9_65	123	2	5,586	MIA, open pits (La Quinua, San Jose, Yanacocha, Cerro Negro, Carachugo, Chaquicocha, Maqui Maqui), waste dumps, heap leach facilities (pads and ponds), San Jose reservoir. Based on Briggs (2005) and Newmont (2013)
119	Yatela Gold mine	OP	2001	20110921	2011	L5	202_50	234	6	779.76	Open pits, waste dump, MIA, heap leach pad

8.3.2 For global status quo (2011) calculations (n=116)

Bauxite (all NCP, OP mines)

#	Mine Name	Ope-ning year	Image acquisi-tion date (year-month-day)	Year it co-vers	Se n-sor	WRS2 Path_ Row	Band combin ation	SL [54]	Cumulative net area disturbed [ha]	Observation / Detail on mine elements included in the net area disturbed measurement
1	Awaso	1941	20021224	2002	L7	195_56	345	2	221.85	Open pit, MIA (including hospital area), tailings pond. No refinery plant at site, tailings result from washing. Atronsu and Awaso towns and Kanayerebo compound are not included.
2	Boddington Worsley	1984	20111228	2011	L7	112_83	345	3	2,566.26	MIA and multiple open pits spread around the Saddleback mining operations area as shown in the plan of premises boundary (Department of Environment and Conservation 2012). Worsley alumina refinery not included.
3	Boke-Sangaredi	1973	20130512	2012	L8	203_52	345	6	3,060	MIA (incl. rail loading area) and multiple open pits. No tailings pond or dam visible or measured. Adjacent town not included.
4	Discovery Bay	1953	20110121	2010	L5	12_47	345	5	3,461.49	Multiple open pits, and MIA at Port Roades, including tailings pond.Based on the principal bauxite region in St Ann by Patterson et al. (1986)
5	Friguia	1960	20110108	2010	L5	202_53	123	3	780.75	Multiple open pits and MIA. No washing at mine site. Friguia alumina refinery plant located at the

[54] It refers to the segmentation level used during the classification.

#	Mine Name	Ope-ning year	Image acquisi-tion date (year-month-day)	Year it co-vers	Se n-sor	WRS2 Path_ Row	Band combin ation	SL 54	Cumulative net area disturbed [ha]	Observation / Detail on mine elements included in the net area disturbed measurement
										mine site is not considered in the calculation.
6	Gove	1970	20111011	2011	L5	102_68	123	5	2,741.76	Open pits area, MIA, airstrip and the Nhulunbuy town. No washing at mine site (only crushing/screening). An alumina refinery located close to the mining area is not included.
7	Juruti	2009	20121023	2012	L7	228_62	457	5	1,484.46	Pits and MIA. A beneficiation washing plant with a tailings pond is present at mine site; they are both accounted for. The road between mine site and port facilities is also included in the calculation.
8	Kindia	1974	20110108	2010	L5	202_53	234	4	975.24	Multiple open pits, MIA, rail loading area. No washing facilities at mine site.
9	Krasno Oktyabrsk	1950	20101021	2010	L5	161_24	345	5	1,609.83	Open pits and MIA.
10	Los Pijiguaos	1987	20131010	2013	L8	003_56	345	7	1,169.64	Open pits, MIA and the town with airstrip in which miners live and the road connecting the mine site with it.
11	Moengo Coermotibo	1922	20090804	2009	L5	228_56	234	6	3,307.41	Open pits, MIA and the Moengo town.
12	Panchpat-mali (Damanjodi)	1985	20121225	2012	L7	141_47	234	6	674.73	Open pit, MIA, includes part of the road connecting the mine site with the processing plant and the rail load area next to the refinery (refinery and its tailings pond are not included)
13	Trombetas	1979	20111029	2011	L5	228_61	234	6	5,863.77	Pits, MIA and tailings ponds at mine site: in Trombetas there is no alumina refinery plant, but there is beneficiation and tailings are included as

#	Mine Name	Ope-ning year	Image acquisi-tion date (year-month-day)	Year it co-vers	Se n-sor	WRS2 Path_ Row	Band combin ation	SL [54]	Cumulative net area disturbed [ha]	Observation / Detail on mine elements included in the net area disturbed measurement
										residues of beneficiation. Also includes the road between the Trombetas port and the mine area, the airstrip and town at the port.

Iron ore mines (all NCP, OP mines)

DSO mines

#	Mine Name	Ope-ning year	Image acquisi-tion date (year-month-day)	Year it co-vers	Se nsor	WRS2 Path_ Row	Band combin ation	SL	Cumulative net area disturbed [ha]	Observation / Clarification on mine elements included in the net area disturbed measurement
14	Area C	2003	20111228	2011	L7	112_76	571	3	2,486.61	Open pits, waste dumps, MIA, the camp on the Northwest and Mulla Mulla village and airport. Does not include the road connection between Mulla Mulla and the mine site. Based on BHP Billiton (2002); Environmental Protection Authority (1998)
15	Bailadila 10	2002	20111104	2011	L5	142_47	712	0	361.89	Bailadila 10 pit, MIA, rail loading area at Bacheli, pipelines and tailings pond at Bacheli. Based on Fig. 2 in Behre Dolbear (2010)
16	Bailadila 14 and 11 C	1976	20111104	2011	L5	142_47	345	0	637.74	Includes crushing and screening plant in Kurundil area, plus rail loading area and tunnels and Kadampal tailings pond

#	Mine Name	Ope-ning year	Image acquisi-tion date (year-month-day)	Year it co-vers	Se nsor	WRS2 Path_ Row	Band combin ation	SL	Cumulative net area disturbed [ha]	Observation / Clarification on mine elements included in the net area disturbed measurement
17	Bailadila 5	1980	20111104	2011	L5	142_47	234	0	526.5	Bacheli 5 pit area, MIA, rail loading area, and tailings pond in Bacheli complex. Based on Fig. 2 in Behre Dolbear (2010)
18	Carajás/ Serra Norte	1986	20110729	2011	L5	224_64	234	1	5,374.71	Includes only Serra Norte. MIA, EFC railway loading loop, waste dumps, the "núcleo habitacional" (6,000 inhabitants village) constructed by Vale and the Carajás/Parauapebas airport, PA-275 road connecting the mine with the village and the airport. Includes pits on deposits N3, N4 (N4WC, N4WN, N4E), N5 (N5W, N5E, N5E-N). Classification based on Cristiane and Fabrina (2013); Figuereido e Silva et al. (2011); Hilário et al. (2008); Sampaio et al. (2002)
19	Channar	1990	20101208	2010	L5	113_76	345	2	1,088.55	Open pits, waste dumps and MIA. Based on Pilbara Iron (2011)
20	Chitradurga	2000	20110117	2010	L7	145_50	712	2	441.81	Open pits, waste dumps and MIA.
21	Eastern Range	2004	20101208	2010	L5	113_76	712	4	662.49	Open pits, waste dumps and MIA.
22	El Gedida (el Bahariya)	1973	20121221	2012	L7	177_40	712	4	941.67	Open pits, waste dumps and MIA.
23	Hope Downs	2007	20111228	2011	L7	112_76	234	3	2,119.23	Open pits (Hope North, Hope South), waste dumps and MIA (incl. rail loading area and loop). Based on the general site layout (Fig. 2) in Environmental Protection Authority (2001)
24	Jack Hills	2007	20110118	2010	L5	112_78	571	4	141.93	Open pits, waste dumps and MIA. Based on

#	Mine Name	Ope-ning year	Image acquisi-tion date (year-month-day)	Year it co-vers	Se nsor	WRS2 Path_ Row	Band combin ation	SL	Cumulative net area disturbed [ha]	Observation / Clarification on mine elements included in the net area disturbed measurement
										Environmental Protection Authority (2011)
25	Jimblebar	1989	20090105	2008	L5	111_76	234	3	729.72	Open pits, waste dumps, MIA, 2009 and 2010 were years of no production. Based on Environmental Protection Authority (2010, 1995)
26	Koolan Island	1959	19931102	1993	L5	110_71	345	3	562.41	Open pits (Main pit, Mullet-Acacia, Acacia East), waste dumps and MIA (incl. ship loader, airstrip, camp). Based on Ecologia Environment (2005); and Mount Gibson Iron Limited (2013)
27	Pardoo	2008	20130115	2012	L7	112_74	234	1	486	Open pits, waste dumps and MIA. Based on Environmental Protection Authority (2008)
28	Tallering Peak	2004	20121221	2012	L7	113_79	345	4	487.71	Open pits, waste dumps and MIA. Based on Mount Gibson Iron Limited (2006)
29	Yandi	1992	20130115	2012	L7	112_76	345	3	2,949.84	Open pits, waste dumps and MIA, including two rail loops and two camps. No access road accounted for between camp sites included. Based on Environmental Protection Authority (2005)

NDSO mines

#	Mine Name	Ope-ning year	Image acquisi-tion date (year-month-day)	Year it co-vers	Se nsor	WRS2 Path_ Row	Band combin ation	SL	Cumulative net area disturbed [ha]	Observation / Clarification on mine elements included in the net area disturbed measurement
30	Capitão Do Mato	1971	20110921	2011	L5	218_74	234	3	1,020.87	At Capitão includes the open pit, waste dumps and the MIA; the Morro de Chapéu village is not included. At the beneficiation complex Vargem Grande includes the MIA, the tailings pond and stockpiling and rail loading area.
31	Chadormalou	1998	20111024	2011	L5	161_38	123	3	1,240.47	Open pit, waste dumps, MIA, tailings facilities and rail loading area
32	Frances Creek	1967	20121127	2012	L7	105_69	234	5	506.43	Pits mined between 1967-1974 and from 2007; pits and adjacent waste dumps included are: Jasmine East and Thelma Rosemary, Ochre Hill, Helene 5, Helene 6/7, main dam and smaller dams, and the MIA. Road connecting the MIA with Ochre Hill is not included. Based on MBS Environmental (2006)
33	Gole Gohar	1994	20120104	2011	L7	161_40	712	4	2,095.38	Open pit, waste dumps, MIA and rail loading area
34	Kudremukh	1976	20030127	2002	L7	145_51	345	4	1,058.04	Open pit, MIA, waste dumps, Lakya tailings pond and township to the Northeast are included. Roads connecting the mine with nearby townships and to the port town of Mangalore are not accounted.
35	Marcona	1953	20130124	2012	L7	006_70	345	2	2,423.61	Includes the San Nicolas area and tailings pond
36	Mont Wright	1975	20120912	2012	L7	012_23	345	8	4,991.94	Open pit, waste dumps, MIA, tailings facilities and rail loading area. Based on ArcelorMittal

#	Mine Name	Ope-ning year	Image acquisi-tion date (year-month-day)	Year it co-vers	Se nsor	WRS2 Path_ Row	Band combin ation	SL	Cumulative net area disturbed [ha]	Observation / Clarification on mine elements included in the net area disturbed measurement
										(2012)
37	Savage River	1968	20110404	2010	L5	091_89	234	4	1,255.77	Open pits (North, Centre and South), waste dumps, MIA, tailings pond, town site. Based on Mining Ore Consultants (2008).
38	Sydvaranger	1910	19940909	1994	L5	191_11	345	1	1,080.9	It includes the open pits operating succesively since 1910 (bjornevatn, grundtjern, sostervann, tverndalen, fisketind, bjornefell, jerntoppen), concentrator and tailings in the water at Slambanken and Beddariand port located 8 km from Kirkenes. Submarine tailings in Bokfjorden are counted. Based on RSG Global Consulting Pty Ltd (2007)
39	Tamanduá	1971	20110921	2011	L5	218_74	345	3	780.84	At Tamanduá includes the open pit, waste dumps and the MIA; the Morro de Chapéu village is not included. At the beneficiation complex Vargem Grande includes the MIA, the tailings pond and stockpiling and rail loading area.
40	Thabazimbi	1934	20130317	2012	L7	171_77	234	3	1,813.95	MIA, waste dumps and the pits: east pit, buffelshoek east, buffelshoek west, bobbejaanwater, kumba, donkerpoort new, donkerpoort west, kwaggashoek east and vanderbjil. The two underground mining areas (active until 1997) east mine and kwaggashoek east underground are not included. Based on Shangoni Management Services (2011)

Copper, Gold and Silver

#	Mine Name	Type	Ope-ning year	Image acquisi-tion date (year-month-day)	Year it co-vers	Se nsor	WRS2 Path_ Row	Band combin ation	SL	Unalloca-ted cumulati-ve net area disturbed [ha]	Observation / Clarification on mine elements included in the net area disturbed measurement
41	Aitik Copper mine	OP	1968	20120907	2012	L7	194_13	123	1	4,347	Includes Aitik and Salmijärvi pits/deposits. Liikavaara deposit not included as not exploited in 2011.Tailings pond included. Based on Boliden Mineral (2014)
42	Alamo Dorado Silver mine	OP	2007	20131231	2013	L8	33_42	156	1	205.11	Open pit, waste dumps, MIA, and dry stack tailings area.
43	Alumbrera Gold/Copper mine	OP	1997	20101202	2010	L5	231_79	156	1	2,413	MIA, open pit, waste dumps and tailings pond. Classification based on Hennessey et al. (2009)
44	Amantaytau Oxides Gold mine	OP	2004	20081128	2008	L7	157_31	456	1	622.53	Open pits, waste dumps, MIA, tailings ponds
45	Antapite Gold mine	UG	2001	20101124	2010	L5	006_70	126	2	266.67	MIA, Huinchulla tailings pond, Machucancha camp, other areas
46	Arcata Silver mine	UG	1961	20131220	2013	L8	4_70	612	4	120.6	MIA, waste dump and tailings pond.
47	Ares Gold mine	UG	1998	20110910	2011	L5	004_70	126	4	158.31	MIA, waste dump and tailings pond. Based on SVS Ingenieros (2012)
48	Batu Hijau Copper/Gold mine	OP	2000	20110827	2011	L7	115_66	345	8	2,186	Includes the open pit, waste dumps and the copper-gold concentrator. Buin Batu town, Benete port, tailings outfall pipeline and submarines tailings area is not included (bad

#	Mine Name	Type	Ope-ning year	Image acquisi-tion date (year-month-day)	Year it co-vers	Se nsor	WRS2 Path_ Row	Band combin ation	SL	Unalloca-ted cumulati-ve net area disturbed [ha]	Observation / Clarification on mine elements included in the net area disturbed measurement
											image resolution).Based on Craig Vogt Inc (2012)
49	Berezitovy Gold mine	OP	2007	20130926	2013	L8	122_22	234	6	505.17	Open pits, waste dumps, MIA, tailing ponds. Measurement based on Fig. 17.1 (page 168) in Kenwright et al. (2013)
50	Bingham Canyon Copper Mine	OP	1906	20140324	2013	L8	38_32	123	12	7,332	Main pit area, the beneficiation plant area (Copperton concentrator) and the tailings impoundments (1 and 2) next to the Magna town. The refinery and the Kennecot copper smelter are not included. The Lark tailings area (according to Rio Tinto completely reclaimed and nowadays the state motorcycle park) is also not included. Based on Rio Tinto (2006); U.S. EPA (2009)
51	Boroo Gold mine	OP	2004	20131011	2013	L8	131_26	234	4	906.84	Open pits (3,5,6), waste dumps, MIA, heap leach pad, alluvial mine area and Ikh Dashir tailings pond. Based on Raponi and Redmond (2009)
52	Burnstone Gold mine	UG	2010	20121017	2012	L7	170_78	234	3	325.08	MIA, waste dump and tailings pond. Based on Great Basin Gold Ltd (2011)
53	Cerro Corona Copper/Gold	OP	2008	20120207	2011	L7	9_65	234	6	554.76	Cerro Corona open pit, Chorro Blanco and Gordas, waste dumps,

#	Mine Name	Type	Ope-ning year	Image acquisi-tion date (year-month-day)	Year it co-vers	Se nsor	WRS2 Path_ Row	Band combin ation	SL	Unalloca-ted cumulati-ve net area disturbed [ha]	Observation / Clarification on mine elements included in the net area disturbed measurement
	mine										oxide stockpiles, MIA, Hierba, Aguilas and Gordas dam. Based on Gold Fields (2011)
54	Chapada Copper/Gold mine	OP	2006	20110917	2011	L5	222_70	234	3	1,760.85	Central open pit, south central, NE and SW waste dump, MIA and tailings pond. Based on Avila de Moura (2007)
55	Chatree Gold mine	OP	2001	20131130	2013	L8	129_49	234	5	763.2	Open pits (A + Q pits), waste dumps, MIA, tailings ponds (1 + 2). Based on Fig. 2 in GME (2013)
56	Chelopech Gold/Copper mine	UG	1954	20140111	2013	L8	183_30	345	2	167.04	Main North & South sites, MIA and the tailings pond. Kachulka dam and the adjacent Chelopech village are not included. Based on Chelopech Mining EAD (2010) and Dundee Precious Metals Inc. (2011)
57	Chuquicamata Copper mine	OP	1915	20131129	2013	L8	1_75	123	10	11,681	Includes the main pit and workings in Chuquicamata North. Waste dumps, the mining town, the refinery, the beneficiation plant, the PTMP plant (opened Nov. 2005) and the tailings pond (Talabre) are included. In the North, the mine Radomiro Tomic, and in the South the South Mine (Exotica), mine Minister Hales and Chuquicamata Smelter are not included.

#	Mine Name	Type	Ope-ning year	Image acquisi-tion date (year-month-day)	Year it co-vers	Se nsor	WRS2 Path_ Row	Band combin ation	SL	Unalloca-ted cumulati-ve net area disturbed [ha]	Observation / Clarification on mine elements included in the net area disturbed measurement
58	Collahuasi Copper mine	OP	1998	20140201	2013	L8	1_74	712	10	5,423	MIA, Rosario and Ujina open pits, road connecting them and tailings.Based on Mining Technology (2015a)
59	Corihuarmi Gold mine	OP	2008	20131218	2013	L8	06_69	345	8	467.01	Open pits, waste dumps, MIA, heap leach pad. Based on Coffey Mining Pty Ltd (2010)
60	Cracow Gold mine	UG	1988	20131221	2013	L8	91_78	234	6	217.35	MIA, waste dump and tailings pond. Based on Beadell Resources Ltd (2008)
61	Cuajone (SPCC) Copper Mine	OP	1976	20140114	2013	L8	3_72	345	10	2,931	MIA, pits and waste dumps, Includes Villa Botiflaca, does not include Villa Cuajone. Includes 50% of the Quebrada Honda tailings pond (shared with Toquepala mine since 1996, before both mines dumped tailings into the Locumba river). Does not include the pipeline or any connection from Cuajone to the tailings pod. Based on Walsh Peru SA (2011)
62	Denton - Rawhide Gold mine	OP	1990	20100917	2010	L5	42_33	345	4	526.32	Open pit, waste dump, MIA, heap leach pad
63	Dolores Gold mine	OP	1860s	20111030	2011	L5	34_40	345	1	559	MIA, open pits, waste dumps and heap leach facilities.

#	Mine Name	Type	Ope-ning year	Image acquisi-tion date (year-month-day)	Year it co-vers	Se nsor	WRS2 Path_ Row	Band combin ation	SL	Unalloca-ted cumulati-ve net area disturbed [ha]	Observation / Clarification on mine elements included in the net area disturbed measurement
64	El Sauzal Gold mine	OP	2004	20111108	2011	L5	33_41	345	4	371.97	Open pit, waste dumps, MIA, and dry stack tailings area.
65	Eloise Copper/Gold mine	UG	1996	20081225	2008	L5	98_74	234	2	185.22	MIA, waste dump and tailings pond.
66	Escondida-Zaldivar Copper mine	OP	1990	20111117	2011	L5	233_77	345	3	30,774	Includes area disturbances for Escondida, Escondida Norte and Zaldívar mine: pits, camps, tailings ponds and roads connecting the spatial continuum of the mines. Opening year belongs to Escondida. Based on Golder Associates (2008). Well field in Punta Negra and Coloso port facilities not included.
67	Essakane Gold mine	OP	2010	20121228	2012	L7	194_50	234	4	1,708.02	Open pits, waste dumps, MIA, tailing ponds. Off channel storage not included. Based on Gignac et al. (2009)
68	Fort Knox Gold mine	OP	1996	20120911	2012	L7	69_14	234	7	1,611	MIA, open pit, heap leach pad, waste dump. Does not include the water reservoir to the East of the tailings pond. Based on Quandt et al. (2008).
69	Geita Gold mine	OP	2000	20130301	2012	L7	171_62	234	4	2,469.87	Area includes open pits, waste dumps, MIA, tailings pond, camp, airstrip and roads connecting open

#	Mine Name	Type	Ope-ning year	Image acquisi-tion date (year-month-day)	Year it co-vers	Se nsor	WRS2 Path_ Row	Band combin ation	SL	Unalloca-ted cumulati-ve net area disturbed [ha]	Observation / Clarification on mine elements included in the net area disturbed measurement
											pits with MIA.
70	Greens Creek Polymetallic mine	UG	1989	20120829	2012	L7	58_19	234	2	149.3	Mill and mine portal area, waste rock site 23 and E, road "B" connecting mine facilities and tailings pond, and Hawk Inlet seaplane base. Based on Fig. 2 in Gilliam (2012)
71	Gualcamayo Gold mine	OP	2001	20131201	2013	L8	129_49	234	5	667.35	Open pit, waste dump, MIA, heap leach pad
72	Guanaceví Silver mine	UG	2004	20131224	2012	L8	32_42	234	3	115.7	Includes the concentrator and tailings area (old and new tailings pond), and the mine portal one. Includes the road connecting both spatially distanced areas.
73	Guelb Mogrhein Copper/Gold mine	OP	2006	20110903	2011	L5	204_46	345	4	891.27	Open pit, waste dumps, MIA, and tailings ponds. Based on Scott Wilson Mining (2005)
74	Henty Gold mine	UG	1996	20110404	2010	L7	91_89	234	2	169.65	MIA, waste dump, areas at portals and tailings pond.
75	Holt-Holloway Gold mine	UG	1988	20121116	2012	L7	19_26	345	3	273.24	The ore from Holloway is processed at Holt facilities. Tailings pond is included.
76	Hycroft (Crofoot/Lewis) Gold mine	OP	1987	20100917	2010	L5	42_32	345	3	1,544.13	Mine closed from 2003 until 2009. Based on Scott E. Wilson Consulting Inc (2009)

#	Mine Name	Type	Ope-ning year	Image acquisi-tion date (year-month-day)	Year it co-vers	Se nsor	WRS2 Path_ Row	Band combin ation	SL	Unalloca-ted cumulati-ve net area disturbed [ha]	Observation / Clarification on mine elements included in the net area disturbed measurement
77	Joe Mann Gold mine	UG	1987	20071005	2007	L5	16_26	345	1	103.86	MIA, waste dump and tailings pond.
78	Kiniero (Jean-Gobele) Gold mine	OP	2002	20121222	2012	L7	200_53	123	2	524.43	Open pits (2), waste dumps, MIA, tailings ponds and the airstrip.
79	Kisladag Gold mine	OP	2006	20130205	2012	L7	179_33	234	7	804.42	Open pits, waste dumps, MIA, heap leach pad. Based on Hatch (2003)
80	La Coipa Silver/Gold mine	OP	1989	20111117	2011	L5	233_79	126	3	1,991	Includes the MIA, Ladera Farellon, Can Can, Coipa Norte, Brecha Norte pits and waste dumps, tailings pond. Includes Puren and Chimberos deposits and disturbances around them.Based on Belanger (2003).
81	La Herradura Gold mine	OP	1998	20121216	2012	L7	37_38	456	3	1,700	MIA, open pits, waste dumps and heap leach facility.
82	Mahd ad´Dahab Gold mine	UG	1990	20121229	2012	L7	169_44	345	2	168.66	MIA, camp and dry-tailings storage facilities. Based on SRK Consulting (2007)
83	Minera Florida/Alhue Gold mine	UG	1986	20121229	2012	L7	233_84	234	4	275.76	MIA, tailings pond, roads connecting the MIA and accesses to the mine (Milennium and Marisol areas)
84	Mineral Hill (Australia)	UG	1987	20051120	2005	L5	92_83	156	3	138.96	MIA, waste dumps, eastern pit and tailings and evaporations ponds.

#	Mine Name	Type	Ope-ning year	Image acquisi-tion date (year-month-day)	Year it co-vers	Se nsor	WRS2 Path_ Row	Band combin ation	SL	Unalloca-ted cumulati-ve net area disturbed [ha]	Observation / Clarification on mine elements included in the net area disturbed measurement
	Gold/Copper mine										
85	Morila Gold mine	OP	2000	20111112	2011	L5	198_52	345	5	1,135.17	Open pit, waste dumps (active + inactive), MIA, heap leach pads (Lewis, Brimstone and Crofoot)
86	Mount Polley Copper/Gold mine	OP	1997	20121003	2012	L7	48_23	234	6	1,475.28	Open pits (Springer, Bell, Cariboo, Wight), waste dumps (East), MIA and tailings pond. Based on Gillstrom (2004)
87	Mount Rawdon Gold mine	OP	2001	20121203	2012	L7	90_78	156	4	577.8	Open pit, waste dump, MIA, tailings pond. Based on Boon (2013)
88	Mupane Gold mine	OP	2004	20130128	2012	L7	171_75	234	6	329.04	Open pits (Kwena, Tau and Tholo), waste dumps, MIA, tailing ponds. Based on Tomkinson and Putland (2006)
89	Muruntau Gold Mine	OP	1967	20131017	2013	L8	157_31	123	12	8,740	MIA, open pits, waste dumps and heap leach facility and tailings pond in the south-west.
90	Musselwhite Gold mine	UG	1997	20110927	2011	L7	27_23	123	6	570.42	MIA, waste dump and tailings pond. Classification based on ERM (2013); Goldcorp (2007)
91	Neves Corvo Copper Mine	UG	1989	20140123	2013	L8	203_34	571	4	432.72	MIA, railway terminal and the Barragem Cerro do Lobo TMF, including the road between the mine site and the TMF. Based on Lunding

#	Mine Name	Type	Ope-ning year	Image acquisi-tion date (year-month-day)	Year it co-vers	Se nsor	WRS2 Path_ Row	Band combin ation	SL	Unalloca-ted cumulati-ve net area disturbed [ha]	Observation / Clarification on mine elements included in the net area disturbed measurement
											Mining (2012)
92	Ok Tedi Copper/Gold mine	OP	1985	20140428	2013	L8	100_64	234	2	2,034.8	Includes the mine pit area, gold process facility, mine access road, workshop and Tabubil town. No tailings pond exists, the ground rock tailings from the process are disposed of via the unconfined end of the pipe discharge to Harvey Creek, which drains to the Ok Mani, and then to the Ok Tedi and Fly rivers. Hence the Ok Mani river until its confluence with the Ok Tedi river (in Tabubil town) and the Fly river until it intersects the Ok Tedi are included as net area disturbed. Based on Hendry et al. (2005)
93	Olimpiada Gold mine	OP	1997	20131107	2013	L8	144_18	457	12	3,842.7	MIA, open pits, waste dumps and tailings pond.
94	Osborne (Trough Tank) Copper/Gold Mine	UG	1995	20101215	2010	L5	98_75	571	1	440.1	Includes the tailings pond, the camp site and the airstrip. Also includes the open pit (operated only one year during 1995) because the mine portal is located directly within the pit. Based on Ebbels et al. (2012)
95	Palito Gold mine	UG	2004	20101104	2010	L5	227_64	456	4	163.53	MIA, waste dump and tailings ponds Based on Guzmán and Mello (2012). Given the lack of other land

#	Mine Name	Type	Ope-ning year	Image acquisi-tion date (year-month-day)	Year it co-vers	Se nsor	WRS2 Path_ Row	Band combin ation	SL	Unalloca-ted cumulati-ve net area disturbed [ha]	Observation / Clarification on mine elements included in the net area disturbed measurement
											uses in the nearby areas, it was assumed that some areas disturbed to the East and North of the general site also belong to the mine´s activities.
96	Peak Gold mine	UG	1992	20111011	2011	L5	93_82	234	2	294.3	Includes road in the perimeter of the mine. Classification based on Lloyd et al. (2009).
97	Poracota gold mine	UG	2007	20131220	2013	L8	004_70	345	6	55.08	MIA and waste dump. No tailings ponds at mine site because the ore is sent to Orcopampa´s concentrator for beneficiation.
98	Robinson Copper/Gold mine	OP	1904	20121103	2012	L7	40_33	456	4	3,651.75	Open pits, waste dumps, MIA, tailings ponds.
99	Rochester Silver mine	OP	1986	20140115	2013	L8	42_32	234	8	802.7	MIA, open pits (Rochester and Nevada Packard), waste dumps and heap leach pad in the north.
100	Round Mountain Gold mine	OP	1977	20140124	2013	L8	41_33	712	10	3,314	Includes the MIA, open pits, waste dumps, heap leach, tailings pond and the Hadley town. Includes the developments visible in 2014 at the North of the big mine. Based on Fig. 3-2 in Hanson (2006)
101	Sadiola Gold	OP	1997	20110921	2011	L5	202_50	234	1	2,019.51	Open pit (main pit and four satellite pits), waste dumps, MIA, tailings

#	Mine Name	Type	Ope-ning year	Image acquisi-tion date (year-month-day)	Year it co-vers	Se nsor	WRS2 Path_ Row	Band combin ation	SL	Unalloca-ted cumulati-ve net area disturbed [ha]	Observation / Clarification on mine elements included in the net area disturbed measurement
	mine										pond and water body next to it. The camp located north of the main pit is also included, also with the road connecting it. The City Sadiola is next to the mine and is not included. Based on Mining Technology (2015b)
102	San José (Arg.) Gold/Silver mine	UG	2007	20130125	2012	L7	230_92	126	4	250.8	MIA, waste dump, tailings pond. Based on Fig. 3-1 in SRK Consulting (2009)
103	Seabee Gold mine	UG	1991	20110910	2011	L7	36_21	234	2	297.1	MIA (incl. airstrip), tailings ponds, and infrastructure at Porky West, Porky Main and Santoy 7 and 8. Roads connecting the access to the mine are included. Based on Fig. 2 in Longo and Skanderberg (2012)
104	Sepon Copper/Gold mine	OP	2002	20121216	2012	L7	126_48	234	4	1,710.9	Open pits, waste dumps, MIA, tailings ponds
105	Siguiri Gold mine	OP	1998	20121222	2012	L7	200_52	156	4	2,834.1	Open pits, waste dump, MIA, heap leach pad, solution ponds and tailings pond. Villages located adjacent to the mining area (Boukaria) are not included.
106	Sossego Copper mine	OP	2004	20110923	2011	L7	224_64	234	4	2,811.15	Open pits, waste dumps, MIA, tailings ponds

#	Mine Name	Type	Ope-ning year	Image acquisi-tion date (year-month-day)	Year it co-vers	Se nsor	WRS2 Path_ Row	Band combin ation	SL	Unalloca-ted cumulati-ve net area disturbed [ha]	Observation / Clarification on mine elements included in the net area disturbed measurement
107	Super Pit Gold mine	OP	1989	20140105	2013	L8	109_81	234	8	3,004.29	Includes the Superpit, waste dumps, including the waste dump footprint bordering southwards with the Mt Monger road. Tailings pond included in the footprint are Fim I and II and the historic Kaltails TSF. The Kalgoorlie-Boulder town and the Lakewood concentrator and its tailings pond are not included. Classification based on Kalgoorlie Consolidated Gold Mines Pty Ltd (2007); Gold Field Tourism (2015); Mining Technology (2015c)
108	Syama Gold mine	OP	1990	20111112	2011	L7	198_52	234	4	768.42	Open pit, waste dumps, MIA, tailings ponds
109	Tintaya Copper mine	OP	1984	20111106	2011	L5	003_70	345	4	2,952.54	Open pits, waste dumps, MIA, tailings ponds (Huinipampa and Ccamacmayo). Based on Mesa de Diálogo Espinar (2013)
110	Tritton Copper mine	UG	2005	20111020	2011	L5	92_82	126	2	290.7	MIA, waste dump and tailings pond.
111	Troilus Copper/Gold mine	OP	1997	20110609	2010	L7	17_24	123	8	1,112.04	Z87 and J4 open pits, waste dumps, MIA, tailings pond. Nearby lakes not included. Based on Copper One (2014)
112	Troy Copper/Silver	UG	1981	20110803	2011	L5	42_26	156	4	351.63	MIA, old pit, waste dump and tailings pond to the north of the MIA.

#	Mine Name	Type	Ope-ning year	Image acquisi-tion date (year-month-day)	Year it co-vers	Se nsor	WRS2 Path_ Row	Band combin ation	SL	Unalloca-ted cumulati-ve net area disturbed [ha]	Observation / Clarification on mine elements included in the net area disturbed measurement
	mine										Based on Fig. 2. in SRK Consulting (2005)
113	Varvarinskoye Gold/Copper mine	OP	2008	20131114	2013	L8	161_23	345	5	947.7	Central open pit, waste dumps, MIA, heap leach pad area and tailings pond. Based on Bateman (1998)
114	Veladero Gold mine	OP	2006	20131122	2013	L8	233_80	571	6	1,763.01	Open pits (Filo Federico and Amable), waste dump, MIA (incl. Veladero camp), heap leach pad. The road connecting the mine site with the camp is not included. The Argenta pit is also not included. Based on MAGSA (2009)
115	Yanacocha Gold mine	OP	1993	20120907	2012	L7	9_65	123	2	5,586	MIA, open pits (La Quinua, San Jose, Yanacocha, Cerro Negro, Carachugo, Chaquicocha, Maqui Maqui), waste dumps, heap leach facilities (pads and ponds), San Jose reservoir. Based on Briggs (2005) and Newmont (2013)
116	Yatela Gold mine	OP	2001	20110921	2011	L5	202_50	234	6	779.76	Open pits, waste dump, MIA, heap leach pad

8.4 Specific land requirement calculations per (allocated) metal

8.4.1 Data used per mine for non-linear regressions (rounded numbers)

Iron

DSO mines (n=16)

Mine name	Opening year	ROM data in period available		Cumulative ROM produced in period available [Mt]	Cumulative net area disturbed (per measurement year) [ha]	Cumulative net area disturbed [ha]	Specific land requirement [m^2/t]
		From	To				
Area C	2003	2003	2011	235.53	2,487 (2011)	2,486.6	0.1056
Bailadila 5	1980	1980	2011	179.2	526.5 (2011)	526.5	0.0294
Bailadila 10	2002	2002	2011	12.5	361.89 (2011)	361.89	0.2895
Bailadila 14/11C	1976	1976	2011	220.1	637.74 (2011)	637.74	0.0290
Carajás/ Serra Norte	1986	1986	2011	1,463.3	5,374.7 (2011)	5,374.7	0.0367
Channar	1990	1990	2010	183.8	1,088.5 (2010)	1,088.55	0.0592
Chitradurga	2000	2002	2010	18.20	441.8 (2010)	441.8	0.2427
Eastern Range	2004	2004	2010	51.4	662.49 (2010)	662.49	0.1289
El Gedida (el Bahariya)	1973	1973	2012	86.4	941.67 (2012)	941.67	0.1090
Hope Downs	2007	2007	2011	95.1	2,119.23 (2011)	2,119.23	0.2228
Jack Hills	2007	2008	2010	5.34	141.93 (2010)	141.93	0.2658
Jimblebar	1989	1989	2008	88.4	729.72 (2008)	729.72	0.0825
Koolan Island	1959	1959	1993	70	562.41 (1993)	562.41	0.0803
Pardoo	2008	2008	2012	15.34	486.00 (2012)	486.00	0.3168
Tallering Peak	2004	2004	2012	21.33	487.71 (2012)	487.71	0.2286
Yandi	1992	1992	2012	650.9	2,949.84 (2012)	2,949.84	0.0453

Source: self-elaboration based on SNL Metals & Mining (update April 2014).

Iron NDSO mines (n=11)

Mine name	Opening year	ROM data in period available		Cumulative ROM produced in period available [Mt]	Cumulative net area disturbed (per measurement year) [ha]	Cumulative net area disturbed [ha]	Specific land requirement [m^2/t]
		From	To				
Capitão Do Mato	1971	1971	2011	160.7	1,020 (2011)	1,020.87	0.0635
Chadormalou	1998	1998	2011	110.4	1,240.4 (2011)	1,240.47	0.1124
Frances Creek	1967	1967-1974	2007-2012	22.6[55]	506.4 (2012)	506.43	0.2241
Gole Gohar	1994	1994	2011	163.3	2,095.3 (2012)	2,095.38	0.1283
Kudremukh	1976	1976	2002	160	1,058.0 (2002)	1,058.04	0.0661
Marcona	1953	1953	2012	298.4	2,423 (2012)	2,423.61	0.0812
Mont Wright	1975	1975	2012	1,093.5	4,991 (2012)	4,991.94	0.0457
Savage River	1968	1968	2010	123.9	1,255 (2010)	1,255.77	0.1014
Sydvaranger	1910	1910	1994	193.9[56]	1,080 (1994)	1,080.90	0.0557
Tamanduá	1971	1971	2011	162.1	780 (2011)	780.84	0.0482
Thabazimbi	1934	1984	2012	67.6	878.5 (1984) 1,813.9 (2012)	935.37	0.138

Source: self-elaboration based on SNL Metals & Mining (update April 2014).

Bauxite (n=13)

Mine name	Opening year	Ore period available		Cumulative ore produced in period available [Mt]	Cumulative net area disturbed (per measurement year) [ha]	Cumulative net area disturbed [ha]	Specific land requirement [m^2/t]
		From	To				
Awaso	1941	1986	2002	7.23	186.84 (1985) 221.85 (2002)	35.01	0.0484
Boddington Worsley	1984	1984	2011	170.14	2,566.2 (2011)	2,566.26	0.1508
Boke	1973	1973	2012	437.98	3,060 (2012)	3,060	0.699

[55] At Frances Creek ore was mined from 1967 until 1974, then production was stopped after Cyclone Tracy, and production was resumed in 2007 until nowadays.

[56] In Sydvaranger, mining started in 1910 and was interrupted during 13 years between 1939 and 1952. It then resumed activities in 1952 until ceasing operations in 1997; mining was resumed in 2009. Given the availability of a satellite image for 1994, the cumulative ore production ranges from 1910 until 1939 (30 years) and from 1952 until 1994 (43 years) totaling 73 years of cumulative production correlated with the cumulative net area disturbed measured in the 1994 image.

Sangarédi								
Discovery Bay	1953	1985	2010	97.53	1,457.1 (1985)	3,461.4 (2010)	2,004.3	0.2055
Friguia	1960	1986	2010	54.01	597.5 (1986)	780.7 (2010)	183.24	0.0339
Gove	1970	1970	2011	252.35	2,741.7 (2011)		2,741.76	0.1086
Juruti	2009	2009	2012	10.78	1,484.4 (2012)		1,484.46	1.3771
Kindia	1974	1974	2010	89.94	975.2 (2010)		975.24	0.1084
Krasno Oktyabrsk	1950	1995	2010	50.05	557.6 (1995)	1609.8 (2010)	1,052.19	0.2102
Los Pijiguaos	1987	1987	2013	96.61	1,169.6 (2013)		1,169.64	0.1211
Moengo Coermotibo	1922	1987	2009	31.17	2,389 (1987)	3,307.8 (2009)	918.36	0.2946
Panchpatmali (Damanjodi)	1985	1985	2012	86.23	674.7 (2012)		674.73	0.0782
Trombetas	1979	1979	2011	307.83	5,863.7 (2011)		5,863.77	0.1905

Source: self-elaboration based on SNL Metals & Mining (update April 2014).

Copper-producing mines (all coupled production mines)

Cu - Open pit – Cumulative ore and cumulative net area disturbed allocated (n=17)

Mine name	Ore data in period available		Cumulative Cu ore produced in period available [Mt]	Cumulative net area disturbed in period available [ha]	Cumulative net area disturbed by Cu ore extraction [ha]	Specific land requirement [m^2/t]
	From	To				
Aitik Copper Mine	1986	2012	418.9	2,580 (2012-1986)	2,213.84	0.0528
Alamo Dorado Silver mine	2007	2013	0.10	205.11 (2013)	1.98	0.1980
Alumbrera Gold/Copper mine	1997	2010	283.47	2,413 (2010)	1,663	0.0587
Batu Hijau Copper/Gold mine	2000	2011	393.3	2,186 (2011)	1,705	0.0434
Cerro Corona Copper/Gold mine	2008	2011	12.14	554.76 (2011)	369.57	0.3044
Chapada Copper/Gold mine	2006	2011	67.01	1,760.85 (2011)	1,355.94	0.2023
Chuquicamata Copper mine	1987	2013	1,506.39	5,605 (2013-1987)	4,733.3	0.0314

Collahuasi Copper mine	1998	2013	557.59	5,423 (2013)	5,238.9	0.0940
Escondida-Zaldivar Copper mine	1990	2011	1,445.11	30,774 (2011)	29,835.3	0.2065
Guelb Mogrhein Copper/Gold mine	2006	2011	9.48	891.27 (2011)	702.36	0.7409
Mount Polley Copper/Gold mine	1997	2012	55.13	1,475.28 (2012)	1,002.07	0.1818
Ok Tedi Copper/Gold mine	1989	2013	474.26	972 (2013-1988)	722.6	0.0152
Robinson Copper/Gold mine	1996	2012	136.54	1,994.4 (1996), 3,651.7 (2012)	1,390.98	0.1019
Sossego Copper mine	2004	2011	81.34	2,811.15 (2011)	2,569.19	0.3159
Tintaya Copper mine	1985	2011	117.11	2,952.54 (2011)	2,722.70	0.2325
Troilus Copper/Gold mine	1997	2010	15.63	1,112.04 (2010)	232.97	0.1491
Varvarinskoye Gold/Copper mine	2008	2013	5.44	947.7 (2013)	308.57	0.5672

Cu – Underground – Cumulative ore and cumulative net area disturbed allocated (n=11)

Mine name	Ore data in period available		Cumulative Cu ore produced in period available [Mt]	Cumulative net area disturbed (per measurement year) [ha]	Cumulative net area disturbed by Cu ore extraction [ha]	Specific land require-ment [m^2/t]
	From	To				
Chelopech Gold/Copper mine	1954	2013	12.29	167.04 (2013)	86.79	0.0706
Eloise Copper/Gold mine	1996	2008	4.48	185.22 (2008)	170.37	0.3803
Joe Mann Gold mine	1987	2007	0.29	103.86 (2007)	7.24	0.2497
Mahd ad´Dahab Gold mine	1990	2012	0.31	168.66 (2012)	9.2	0.2968
Mineral Hill (Australia) Gold/Copper mine	1989	2005	0.64	138.96 (2005)	42.16	0.6588
Neves Corvo Copper Mine	1988	2013	57.66	432.72 (2013)	394.22	0.0684
Osborne (Trough Tank)	1996	2010	21.48	440.1 (2010)	392.87	0.1829

Copper/Gold Mine						
Palito Gold mine	2005	2010	0.06	163.53 (2010)	18.84	3.1400
Peak Gold mine	1993	2011	2.17	294.3 (2011)	51.55	0.2376
Tritton Copper mine	2005	2011	5.98	290.7 (2011)	281.12	0.4701
Troy Copper/Silver	1981	2011	31.4	351.63 (2011)	230.07	0.0733

Gold

Au - Open pit – Cumulative ore and cumulative net area disturbed allocated (n=44)

Mine name	Ore data in period available		Cumulative Au ore produced in period available [Mt]	Cumulative net area disturbed (per measurement year) [ha]	Cumulative net area disturbed by Au ore extraction [ha]	Specific land requirement [m^2/t]
	From	To				
Aitik Copper mine	1986	2012	48.8	2,580 (2012-1986)	258.16	0.0529
Alamo Dorado Silver mine	2007	2013	1.82	205.11 (2013)	33.03	0.1815
Alumbrera Gold/Copper mine	1997	2010	123	2,413 (2010)	721.3	0.0586
Amantaytau Oxides Gold mine	2004	2008	4.18	622.53 (2008)	622.53	1.4893
Batu Hijau Copper/Gold mine	2000	2011	110.7	2,186 (2011)	480.34	0.0434
Berezitovy Gold mine	2007	2013	7.56	505.17 (2013)	505.17	0.6682
Boroo Gold mine	2004	2013	23.17	906.84 (2013)	906.84	0.3914
Cerro Corona Copper/Gold mine	2008	2011	6.08	554.76 (2011)	185.19	0.3046
Chapada Copper/Gold mine	2006	2011	20.01	1,760.85 (2011)	404.91	0.2024
Chatree Gold mine	2001	2013	28.61	763.2 (2013)	711.4	0.2487
Chuquicamata Copper mine	1987	2013	16.4	5,605 (2013-1987)	51.65	0.0315
Corihuarmi Gold mine	2008	2013	10.44	467.01 (2013)	467.01	0.4473
Denton-Rawhide Gold mine	1990	2010	63.1	526.32 (2010)	464.61	0.0736
Dolores Gold	2009	2013	17.08	181.7 (2013-2009)	109.7	0.0642

mine						
El Sauzal Gold mine	2004	2011	14.4	371.97 (2011)	371.97	0.2583
Escondida-Zaldivar Copper mine	1990	2011	30.4	30,774 (2011)	628.5	0.2067
Essakane Gold mine	2010	2012	21.71	1,708.02 (2012)	1,708.02	0.7867
Geita Gold mine	2000	2012	61.02	2,469.87 (2012)	2,469.87	0.4048
Gualcamayo Gold Mine	2009	2013	32.54	667.35 (2013)	667.35	0.2051
Guelb Mogrhein Copper/Gold mine	2006	2011	2.55	891.27 (2011)	188.91	0.7408
Hycroft (Crofoot/Lewis) Gold mine	1987	2010	51.38	1,544.13 (2010)	1,479.47	0.2879
Kiniero (Jean-Gobele) Gold mine	2002	2012	4.99	524.43 (2012)	524.43	1.0510
Kisladag Gold mine	2006	2012	63.41	804.42 (2012)	804.42	0.1269
La Coipa Silver/Gold mine	1989	2011	46.48	1,991.7 (2011)	1,003	0.2158
La Herradura Gold mine	1998	2012	164.47	1,700 (2012)	1,675	0.1018
Morila Gold mine	2000	2011	42.28	1,135.17 (2011)	1,135.17	0.2685
Mount Polley Copper/Gold mine	1997	2012	24.25	1,475.28 (2012)	440.72	0.1817
Mount Rawdon Gold mine	2001	2012	35.78	577.8 (2012)	575.81	0.1609
Mupane Gold mine	2004	2012	6.55	329.04 (2012)	329.04	0.5024
Ok Tedi Copper/Gold mine	1989	2013	158.3	972 (2013-1988)	241.31	0.0152
Robinson Copper/Gold mine	1996	2012	23.76	1,657 (2012-1996)	242.08	0.1019
Rochester Silver mine	1986	2013	71	802.7 (2013)	323.9	0.0456
Round Mountain Gold mine	1988	2013	1,087.7	1,948 (2013-1987)	1,915	0.0176
Sadiola Gold Mine	1997	2011	71.37	2,019.51 (2011)	2,019.51	0.2830
Siguiri Gold mine	1998	2012	133.48	2,834.10 (2012)	2,834.1	0.2123

Sossego Copper mine	2004	2011	7.54	2,811.15 (2011)	238.05	0.3157
Super Pit Gold Mine	1989	2013	251.16	3,004.29 (2013)	3,004.29	0.1196
Syama Gold mine	1990	2011	16.07	768.42 (2011)	768.42	0.4782
Tintaya Copper mine	1985	2011	6.8	2,952.54 (2011)	158.06	0.2324
Troilus Copper/Gold mine	1997	2010	57.88	1,112.04 (2010)	862.52	0.1490
Varvarinskoye Gold/Copper mine	2008	2013	11.27	947.7 (2013)	639.13	0.5671
Veladero Gold mine	2006	2013	195.21	1,763.01 (2013)	1,720	0.0881
Yanacocha Gold mines	1994	2012	1,391	5,586 (2012)	5,491	0.0395
Yatela Gold mine	2001	2011	30.06	779.76 (2011)	779.76	0.2594

Au – Underground – Cumulative ore and Cumulative net area disturbed allocated (n=19)

Mine name	Ore data in period available		Cumulative Au ore produced in period available [Mt]	Cumulative net area disturbed (per measurement year) [ha]	Cumulative net area disturbed by Au ore extraction [ha]	Specific land require-ment [m^2/t]
	From	To				
Antapite Gold mine	2001	2010	1.39	266.67 (2010)	262.39	1.8877
Ares Gold mine	1998	2011	3.29	158.31 (2011)	127.6	0.3878
Burnstone Gold mine	2010	2012	0.6	325.08 (2012)	325.08	5.4180
Chelopech Gold/Copper mine	1954	2013	10.99	167.04 (2013)	77.61	0.0706
Cracow Gold mine	1988	2013	4.26	217.35 (2013)	216.68	0.5086
Eloise Copper/Gold mine	1996	2008	0.27	185.22 (2008)	10.45	0.3870
Henty Gold mine	1997	2010	2.97	169.65 (2010)	169.65	0.5712
Holt-Holloway Gold mine	1988	2012	11.44	273.24 (2012)	273.24	0.2388
Joe Mann Gold mine	1987	2007	3.9	103.86 (2007)	96	0.2462
Mahd ad´Dahab Gold mine	1990	2012	4.86	168.66 (2012)	143	0.2942

Minera Florida/Alhue Gold mine	2003	2012	4.38	127.62 (2012)	97.66	0.2230
Mineral Hill (Australia) Gold/Copper mine	1989	2005	1.46	138.96 (2005)	96.8	0.6630
Musselwhite Gold mine	1997	2011	18.53	570.42 (2011)	570.42	0.3078
Osborne (Trough Tank) Copper/Gold Mine	1996	2010	2.58	440.1 (2010)	47.23	0.1831
Palito Gold mine	2005	2010	0.47	163.53 (2010)	144.69	3.0785
Peak Gold mine	1993	2011	10.2	294.3 (2011)	242.75	0.2380
Poracota Gold mine	2007	2013	1.02	55.08 (2013)	54.64	0.5357
Seabee Gold mine	1991	2011	4.36	297.18 (2011)	297.18	0.6816
Tritton Copper mine	2005	2011	0.12	290.7 (2011)	5.7	0.4750

Silver

Ag - Open pit – Cumulative ore and cumulative net area disturbed allocated (n=22)

Mine name	Ore data in period available		Cumulative Ag ore produced in period available [Mt]	Cumulative net area disturbed (per measurement year) [ha]	Cumulative net area disturbed by Ag ore extraction [ha]	Specific land require-ment [m^2/t]
	From	To				
Aitik Copper mine	1986	2012	20.5	2,580 (2012-1986)	108.6	0.0530
Alamo Dorado Silver mine	2007	2013	9.37	205.11 (2013)	170.1	0.1815
Alumbrera Gold/Copper mine	1997	2010	3.81	2,413 (2010)	22.3	0.0585
Chatree Gold mine	2001	2013	2.08	763.2 (2013)	51.8	0.2490
Chuquicamata Copper mine	1987	2013	35.5	5,605 (2013-1987)	111.6	0.0314
Denton-Rawhide Gold mine	1990	2010	8.38	526.32 (2010)	61.71	0.0736
Dolores Gold mine	2009	2013	11.2	181.7 (2013-2009)	72	0.0643
Escondida-Zaldivar Copper	1990	2011	15.1	30,774 (2011)	311.1	0.2060

mine						
Hycroft (Crofoot/Lewis) Gold mine	1987	2010	2.25	1,544.13 (2010)	64.66	0.2874
La Coipa Silver/Gold mine	1989	2011	45.8	1,991.7 (2011)	988.53	0.2158
La Herradura Gold mine	1998	2012	2.5	1,700 (2012)	25.2	0.1008
Mount Polley Copper/Gold mine	1997	2012	1.79	1,475.28 (2012)	32.49	0.1815
Mount Rawdon Gold mine	2001	2012	0.12	577.8 (2012)	1.99	0.1658
Ok Tedi Copper/Gold mine	1989	2013	5.6	972 (2013-1988)	8.5	0.0152
Robinson Copper/Gold mine	1996	2012	1.44	1,657 (2012-1996)	14.67	0.1019
Rochester Silver mine	1986	2013	104.9	802.7 (2013)	478.8	0.0456
Round Mountain Gold mine	1988	2013	18.62	1,948 (2013-1988)	32.78	0.0176
Sossego Copper mine	2004	2011	0.12	2,811.15 (2011)	3.91	0.3258
Tintaya Copper mine	1985	2011	3.09	2,952.54 (2011)	71.77	0.2323
Troilus Copper/Gold mine	1997	2010	1.11	1,112.04 (2010)	16.54	0.149
Veladero Gold mine	2006	2013	4.88	1,763.01 (2013)	43.01	0.0881
Yanacocha Gold mines	1994	2012	24.12	5,586 (2012)	95.2	0.0395

Ag – Underground - Ore and net area disturbed allocated (n=12)

Mine name	Ore data in period available		Cumulative Ag ore produced in period available [Mt]	Cumulative net area disturbed (per measurement year) [ha]	Cumulative net area disturbed by Ag ore extraction [ha]	Specific land require-ment [m^2/t]
	From	To				
Antapite Gold mine	2001	2010	0.02	266.67 (2010)	4.28	2.1400
Ares Gold mine	1998	2011	0.79	158.31 (2011)	30.71	0.3887
Chelopech Gold/Copper mine	1954	2013	0.37	167.04 (2013)	2.63	0.0711

Cracow Gold mine	1988	2013	0.01	217.35 (2013)	0.67	0.6700
Eloise Copper/Gold mine	1996	2008	0.12	185.22 (2008)	4.39	0.3658
Joe Mann Gold mine	1987	2007	0.03	103.86 (2007)	0.63	0.2100
Mahd ad´Dahab Gold mine	1990	2012	0.28	168.66 (2012)	8.14	0.2907
Minera Florida/Alhue Gold mine	2003	2012	0.43	127.62 (2012)	9.64	0.2242
Neves Corvo Copper Mine	1988	2013	1.13	432.72 (2013)	7.72	0.0683
Poracota Gold mine	2007	2013	0.01	55.08 (2013)	0.44	0.4400
Tritton Copper mine	2005	2011	0.08	290.7 (2011)	3.88	0.4850
Troy Copper/Silver	1981	2011	16.59	351.63 (2011)	121.56	0.0733

8.4.2 Calculating the weighted disturbance rates (2011)

Iron

The non-constant mine-specific slopes were calculated for each mine using the Eq. 4 (page 97) for each reference year as shown below in Table 21.

Table 21: Iron ore. Mine-specific slopes (n=27).

Mine name	Year of reference	Cumulative ROM produced in period available (until the year of reference) (Mt)	Mine-specific slope by Eq. 4 (ha/Mt_{rom})
Area C	2011	235.53	4.61
Bailadila 10	2011	12.49	12.89
Bailadila 14 and 11 C	2011	220.09	4.72
Bailadila 5	2011	179.18	5.07
Capitao Do Mato	2011	160.70	5.27
Carajás/Serra Norte	2011	1463.26	2.43
Chadormalou	2011	110.39	6.01
Channar	2010	183.75	5.03
Chitradurga	2010	18.20	11.30
Eastern Range	2010	51.39	7.86

El Gedida (el Bahariya)	2012	86.43	6.55
Frances Creek	2012	22.60	10.48
Gole Gohar	2011	163.28	5.24
Hope Downs	2011	95.06	6.34
Jack Hills	2010	5.35	17.34
Jimblebar	2008	88.36	6.50
Koolan Island	1993	69.98	7.05
Kudremukh	2002	159.99	5.28
Marcona	2012	298.39	4.25
Mont Wright	2012	1093.50	2.69
Pardoo	2012	15.34	12.00
Savage River	2010	123.90	5.77
Sydvaranger	1994	193.88	4.94
Tallering Peak	2012	21.33	10.69
Tamanduá	2011	162.09	5.26
Thabazimbi	2012	67.59	7.14
Yandi	2012	650.89	3.23

Based on the non-constant mine-specific slopes calculated in the Table 21, the following new net area disturbed per mine was computed multiplying the average in ROM extraction in the two years following the reference year by the mine-specific slope.

Table 22: Iron ore. Annual ore extraction and new area disturbed per mine (n=27).

Mine name	Year(s) considered for average ROM extracted	Annual ROM extracted (Mt/a) (average in two years following reference year)	New net area disturbed per year (ha/a) (A_i)	Observations
Area C	2012-2013	52.44	241.83	None
Bailadila 10	2012-2013	1.79	23.07	None
Bailadila 14 and 11 C	2012-2013	10.67	50.39	None
Bailadila 5	2012-2013	9.82	49.83	None
Capitao Do Mato	2012-2013	7.3	38.48	None

Carajás/Serra Norte	2012-2013	105.84	257.54	None
Chadormalou	2012-2013	12.75	76.66	None
Channar	2011-2012	10.985	55.26	None
Chitradurga	2011-2013	1.35	15.25	None
Eastern Range	2011-2012	9.345	73.43	None
El Gedida (el Bahariya)	2012-2013	3	19.65	None
Frances Creek	2012-2013	2	20.95	None
Gole Gohar	2012-2013	17.25	90.43	None
Hope Downs	2012-2013	32.29	204.57	None
Jack Hills	2011-2012	1.33	23.07	None
Jimblebar	2008-2013	5.185	33.70	None
Koolan Island	1994-1995	1.83	12.91	None
Kudremukh	2003-2004	12.785	67.50	None
Marcona	2012-2013	8.5	36.08	None
Mont Wright	2012-2013	52.75	142.13	None
Pardoo	2012-2013	3.58	42.94	None
Savage River	2011-2012	2.07	11.95	None
Sydvaranger	1995-1996	2.65	13.08	None
Tallering Peak	2012-2013	2.4995	26.72	None
Tamanduá	2012-2013	9.7	50.98	None
Thabazimbi	2012-2013	1.5	10.71	None
Yandi	2012-2013	66.816	215.88	None
All mines	-	448	1,905	-

Based on Eq. 5, the weighted disturbance rate was estimated at 4.25 ha/Mt ore.

Bauxite

The non-constant mine-specific slopes were calculated for each mine using the Eq. 4 (page 97) for each reference year as shown below in Table 23.

Table 23: Bauxite. Mine-specific slopes (n=12).

Mine name	Year of reference	Cumulative ore produced in period available (until the year of reference) (Mt)	Mine-specific slope by Eq. 4 (ha/Mt_{ore})
Awaso	2002	7.2	25.61

Boddington Worsley	2011	170.1	6.36
Boke Sangarédi	2012	438.0	4.19
Discovery Bay	2010	97.5	8.13
Friguia	2010	54.01	10.55
Gove	2011	252.3	5.34
Juruti	2012	10.78	21.47
Kindia	2010	89.9	8.42
Krasno Oktyabrsk	2010	50.1	10.91
Los Pijiguaos	2013	96.6	8.16
Moengo Coermotibo	2009	31.2	13.44
Panchpatmali	2012	86.2	8.58

Based on the non-constant mine-specific slopes calculated in the Table 23, the following new net area disturbed per mine was computed multiplying the average in ore extraction in the two years following the reference year by the mine-specific slope.

Table 24: Bauxite. Annual ore extraction and new area disturbed per mine (n=12).

Mine name	Year(s) considered for average ore extracted	Annual ore extracted (Mt/a) (average in two years following reference year)	New net area disturbed per year (ha/a)	Observations
Awaso	2002-2003	0.5	12.80	None
Boddington Worsley	2011-2012	8.25	52.47	None
Boke Sangarédi	2013	15.44	64.71	None
Discovery Bay	2011-2012	4.95	40.24	None
Friguia	2011-2012	1.205	12.71	None
Gove	2011-2012	7.985	42.68	None
Juruti	2012-2013	3.85	82.66	None
Kindia	2011-2012	3.165	26.66	None
Krasno Oktyabrsk	2011-2012	5.335	58.20	None
Los Pijiguaos	2013	2.5	20.41	None
Moengo Coermotibo	2010-2011	1.5	20.16	None

Panchpatmali	2013	5	42.91	None
All mines	-	59.68	476.61	-

Based on Eq. 5, the weighted disturbance rate was estimated at 7.98 ha/Mt ore.

Copper

The non-constant mine-specific slopes were calculated for each mine using the Eq. 4 (page 97) for each reference year as shown below in Table 25.

Table 25: Copper. Mine-specific slopes (n=27).

Mine name	Year of reference	Cumulative Cu ore (allocated) produced in period available (until the year of reference) (Mt)	Mine-specific slope by Eq. 4 (ha/$Mt_{Cu\ ore}$)
Aitik Copper mine	2012	418.89	2.94
Alamo Dorado Silver mine	2013	0.11	211.12
Alumbrera Gold/Copper mine	2011	283.48	3.59
Batu Hijau Copper/Gold mine	2011	393.33	3.03
Cerro Corona Copper/Gold mine	2011	12.14	18.32
Chapada Copper/Gold mine	2011	67.01	7.58
Chelopech Gold/Copper mine	2013	12.29	18.21
Chuquicamata Copper Mine	2013	1,506.39	1.52
Collahuasi Copper Mine	2013	557.60	2.53
Eloise Copper/Gold mine	2008	4.48	30.68
Guelb Mogrhein Copper/Gold mine	2011	9.48	20.82
Joe Mann Gold mine	2007	0.29	125.44
Mahd ad´Dahab Gold mine	2012	0.31	121.56
Mineral Hill (Australia) Gold/Copper mine	2005	0.64	84.09
Mount Polley Copper/Gold mine	2012	55.13	8.38

Neves Corvo Copper Mine	2013	57.66	8.19
Ok Tedi Copper/Gold Mine	2013	474.27	2.75
Osborne (Trough Tank) Copper/Gold Mine	2010	21.48	13.64
Palito Gold mine	2010	0.06	287.11
Peak Gold mine	2011	2.17	44.67
Robinson Copper/Gold mine	2012	136.54	5.24
Sossego Copper mine	2011	81.34	6.85
Tintaya Copper mine	2011	117.11	5.68
Tritton Copper mine	2011	5.98	26.42
Troilus Copper/Gold mine	2010	15.63	16.08
Troy Copper/Silver mine	2011	31.40	11.21
Varvarinskoye Gold/Copper mine	2013	5.44	27.75

Based on the mine-specific slopes the following new net area disturbed per mine was computed using the average in Cu ore extraction in the two years following the reference year. Three mines were excluded as they had suspended or closed status.

Table 26: Copper. Annual ore extraction and new area disturbed per mine (n=27).

Mine name	Year(s) considered for average ore extracted	Annual Cu ore extracted (Mt/a) (average in two years following reference year)	New net area disturbed per year (ha/a)	Observations
Aitik Copper mine	2013	32.11	94.29	None
Alamo Dorado Silver mine	2014	0.01	2.87	Ore production data from 2013 used to estimate 2014
Alumbrera Gold/Copper mine	2011-2012	28.06	100.84	None
Batu Hijau Copper/Gold mine	2012-2013	29.78	90.36	None

Cerro Corona Copper/Gold mine	2012-2013	4.02	73.73	None
Chapada Copper/Gold mine	2012-2013	17.25	130.69	None
Chelopech Gold/Copper mine	2014	0.71	12.93	Ore production data from 2013 used to estimate 2014
Chuquicamata Copper Mine	2014	33.08	50.13	Ore production data from 2013 used to estimate 2014
Collahuasi Copper Mine	2014	43.58	110.39	Ore production data from 2013 used to estimate 2014
Eloise Copper/Gold mine	2011-2012	0.05	1.42	Mine did not operate in 2009 and 2010
Guelb Mogrhein Copper/Gold mine	2012-2013	2.55	53.00	None
Joe Mann Gold mine	-	0.00	0.00	Excluded - suspended
Mahd ad´Dahab Gold mine	2013	0.02	2.48	No data on ore production for 2014
Mineral Hill (Australia) Gold/Copper mine	2012-2013	0.23	18.93	Mine suspended operations between 2006 and 2011
Mount Polley Copper/Gold mine	2013	5.79	48.51	No data on ore production for 2014
Neves Corvo Copper Mine	2014	2.32	18.97	Ore production data from 2013 used to estimate 2014
Ok Tedi Copper/Gold Mine	2014	13.95	38.41	Ore production data from 2013 used to estimate 2014
Osborne (Trough Tank) Copper/Gold	2010-2012	0.81	11.09	In 2011 the mine did not produce
Palito Gold mine	-	0.00	0.00	Excluded - suspended
Peak Gold mine	2012-2013	0.26	11.56	None
Robinson Copper/Gold mine	2013	13.17	69.03	No data on ore production for 2014
Sossego Copper mine	2012	10.09	69.14	No data on ore production for 2013
Tintaya Copper mine	2012	6.47	36.71	No data on ore production for 2013
Tritton Copper mine	2012-2013	1.22	32.20	None
Troilus	-	0.00	0.00	Excluded - mine is

Copper/Gold mine				closed
Troy Copper/Silver mine	2012	0.64	7.18	No data on ore production for 2013
Varvarinskoye Gold/Copper mine	2014	0.95	26.39	Ore production data from 2013 used to estimate 2014
All mines	-	247.12	1,111.25	-

Based on Eq. 5, the weighted disturbance rate was estimated at 4.5 ha/Mt ore.

Gold

The non-constant mine-specific slopes were calculated for each mine using the Eq. 4 (page 97) for each reference year as shown below in Table 27.

Table 27: Gold. Mine-specific slopes (n=63).

Mine name	Year of reference	Cumulative Au ore (allocated) produced in period available (until the year of reference) (Mt)	Mine-specific slope by Eq. 4 (ha/$Mt_{Au\ ore}$)
Aitik Copper mine	2012	48.85	8.35
Alamo Dorado Silver mine	2013	1.82	47.88
Alumbrera Gold/Copper mine	2010	122.97	5.11
Amantaytau Oxides Gold mine	2008	4.18	30.80
Antapite Gold mine	2010	1.39	55.28
Ares Gold mine	2011	3.29	34.96
Batu Hijau Copper/Gold mine	2011	110.76	5.40
Berezitovy Gold mine	2013	7.56	22.47
Boroo Gold mine	2013	23.17	12.40
Burnstone Gold mine	2012	0.60	86.01
Cerro Corona Copper/Gold mine	2011	6.08	25.23
Chapada Copper/Gold mine	2011	20.01	13.40
Chatree Gold mine	2013	28.61	11.09
Chelopech Gold/Copper mine	2013	10.99	18.43
Chuquicamata Copper	2013	16.44	14.88

Mine			
Corihuarmi Gold mine	2013	10.44	18.93
Cracow Gold mine	2013	4.26	30.48
Denton-Rawhide Gold mine	2010	63.10	7.28
Dolores Gold mine	2013	17.08	14.58
El Sauzal Gold mine	2011	14.40	15.97
Eloise Copper/Gold mine	2008	0.27	130.66
Escondida-Zaldivar Copper Mine	2011	30.44	10.73
Essakane Gold mine	2012	21.71	12.84
Geita Gold mine	2012	61.02	7.42
Gualcamayo Gold Mine	2013	32.54	10.35
Guelb Mogrhein Copper/Gold mine	2011	2.55	40.02
Henty Gold mine	2010	2.97	36.94
Holt-Holloway Gold mine	2012	11.44	18.04
Hycroft (Crofoot/Lewis) Gold mine	2010	51.38	8.12
Joe Mann Gold mine	2007	3.90	31.95
Kiniero (Jean-Gobele) Gold mine	2012	4.99	28.04
Kisladag Gold mine	2012	63.41	7.27
La Coipa Silver/Gold mine	2011	46.48	8.57
La Herradura Gold mine	2012	164.48	4.38
Mahd ad´Dahab Gold mine	2012	4.86	28.43
Minera Florida/Alhue Gold mine	2012	4.38	30.05
Mineral Hill (Australia) Gold/Copper mine	2005	1.46	53.77
Morila Gold mine	2011	42.28	9.01
Mount Polley Copper/Gold mine	2012	24.25	12.11
Mount Rawdon Gold	2012	35.78	9.85

mine			
Mupane Gold mine	2012	6.55	24.26
Musselwhite Gold mine	2011	18.53	13.96
Ok Tedi Copper/Gold Mine	2013	158.38	4.47
Osborne (Trough Tank) Copper/Gold Mine	2010	2.58	39.76
Palito Gold mine	2010	0.47	97.79
Peak Gold mine	2011	10.20	19.17
Poracota Gold mine	2013	1.02	65.22
Robinson Copper/Gold mine	2012	23.76	12.24
Rochester Silver Mine	2013	70.98	6.84
Round Mountain Gold Mine	2013	1087.74	1.61
Sadiola Gold Mine	2011	71.37	6.82
Seabee Gold mine	2011	4.36	30.11
Siguiri Gold mine	2012	133.48	4.89
Sossego Copper mine	2011	7.54	22.51
Super Pit Gold Mine	2013	251.16	3.50
Syama Gold mine	2011	16.07	15.06
Tintaya Copper mine	2011	6.80	23.78
Tritton Copper mine	2011	0.12	201.61
Troilus Copper/Gold mine	2010	57.88	7.63
Varvarinskoye Gold/Copper mine	2013	11.27	18.19
Veladero Gold mine	2013	195.21	4.00
Yanacocha Gold mines	2012	1391.92	1.41
Yatela Gold mine	2011	30.06	10.80

The new net area disturbed per mine was computed multiplying the average Au ore extraction in the two years following the reference year by the mine-specific slopes. Six mines were excluded as they had suspended or closed status.

Table 28: Gold. Annual ore extraction and new area disturbed per mine (n=63).

Mine name	Year(s) considered for average ore extracted	Annual Au ore extracted (Mt/a) (average in two years following reference year)	New net area disturbed per year (ha/a)	Observations
Aitik Copper mine	2013	3.3	27.63	None
Alamo Dorado Silver mine	2014	0.3	14.75	Ore production data from 2013 used to estimate 2014
Alumbrera Gold/Copper mine	2011-2012	10.3	52.66	None
Amantaytau Oxides Gold mine	-	0.0	0.00	Excluded - suspended
Antapite Gold mine	2011-2012	0.1	5.90	None
Ares Gold mine	2012-2013	0.2	8.31	None
Batu Hijau Copper/Gold mine	2012-2013	3.1	16.93	None
Berezitovy Gold mine	2014	1.7	39.12	Ore production data from 2013 used to estimate 2014
Boroo Gold mine	2014	2.4	29.69	Ore production data from 2013 used to estimate 2014
Burnstone Gold mine	2013	0.2	15.48	No data on ore production for 2014
Cerro Corona Copper/Gold mine	2012-2013	2.5	63.35	None
Chapada Copper/Gold mine	2012-2013	4.2	55.85	None
Chatree Gold mine	2014	5.6	61.64	Ore production data from 2013 used to estimate 2014
Chelopech Gold/Copper mine	2014	0.6	10.74	Ore production data from 2013 used to estimate 2014
Chuquicamata Copper Mine	2014	0.4	5.49	Ore production data from 2013 used to estimate 2014
Corihuarmi Gold mine	2014	2.4	44.99	Ore production data from 2013 used to estimate 2014
Cracow Gold mine	2014	0.5	15.77	Ore production data from 2013 used to

				estimate 2014
Denton-Rawhide Gold mine[57]	-	0.0	0.00	Excluded - Mine closed.
Dolores Gold mine	2014	2.8	41.47	Ore production data from 2013 used to estimate 2014
El Sauzal Gold mine	2012-2013	2.0	31.32	None
Eloise Copper/Gold mine	2011-2012	0.0	0.50	None
Escondida-Zaldivar Copper Mine	2012-2013	1.5	15.96	None
Essakane Gold mine	2013	10.6	136.23	No data on ore production for 2014
Geita Gold mine	2013	4.0	29.97	
Gualcamayo Gold Mine	2014	7.7	80.16	Ore production data from 2012 used to estimate 2014
Guelb Mogrhein Copper/Gold mine	2012-2013	0.5	20.58	None
Henty Gold mine	2011-2013	0.3	9.82	No data on ore production for 2012
Holt-Holloway Gold mine	2013	0.3	4.57	Ore production data from 2012 used to estimate 2013
Hycroft (Crofoot/Lewis) Gold mine	2012-2013	31.7	257.72	None
Joe Mann Gold mine	-	0.0	0.00	Excluded because it is suspended
Kiniero (Jean-Gobele) Gold mine	2013	0.2	6.39	No data on ore production for 2014
Kisladag Gold mine	2013	12.6	91.55	None
La Coipa Silver/Gold mine	2012-2013	3.3	28.27	None
La Herradura Gold mine	2013	14.1	61.77	None
Mahd ad´Dahab Gold mine	2013	0.2	4.64	No data on ore production for 2014

[57] The Denton Rawhide Mine was owned and operated by Kennecott Minerals Company from 1988 to 2010. Operations at the mine were suspended in May 2003 due to low gold prices but the mine continued to produce gold and silver from existing heap leach pads. Mine closed in 2010.

Minera Florida/Alhue Gold mine	2013	1.3	39.22	No data on ore production for 2014
Mineral Hill (Australia) Gold/Copper mine	2012-2013	0.0	1.07	None
Morila Gold mine	2012-2013	4.0	36.17	None
Mount Polley Copper/Gold mine	2013	2.2	27.04	No data on ore production for 2014
Mount Rawdon Gold mine	2013	3.4	33.31	Ore production data from 2012 used to estimate 2013
Mupane Gold mine	2013	1.0	24.26	Ore production data from 2012 used to estimate 2013
Musselwhite Gold mine	2012-2013	1.3	18.15	Ore production data from 2012 used to estimate 2013
Ok Tedi Copper/Gold Mine	2014	5.5	24.47	Ore production data from 2013 used to estimate 2014
Osborne (Trough Tank) Copper/Gold Mine	2010-2012	0.1	3.74	In 2011 the mine did not produce
Palito Gold mine	-	0.0	0.00	Excluded because it is suspended
Peak Gold mine	2012-2013	0.5	9.95	None
Poracota Gold mine	-	0.0	0.00	Excluded because it is suspended
Robinson Copper/Gold mine	2013	1.3	16.34	No data on ore production for 2014
Rochester Silver Mine	2014	3.9	26.70	Ore production data from 2013 used to estimate 2014
Round Mountain Gold Mine	2014	22.3	35.89	Ore production data from 2013 used to estimate 2014
Sadiola Gold Mine	2012-2013	6.1	41.67	None
Seabee Gold mine	2012-2013	0.3	8.05	None
Siguiri Gold mine	2013	11.9	58.43	None
Sossego Copper mine	2013	0.9	20.53	No data on ore production for 2013
Super Pit Gold Mine	2012	11.7	41.08	Ore production data from 2012 used to estimate 2014

Syama Gold mine	2014	1.7	25.15	None
Tintaya Copper mine	2012-2013	0.4	8.45	No data on ore production for 2013
Tritton Copper mine	2012	0.0	4.71	None
Troilus Copper/Gold mine	-	0.0	0.00	Excluded - mine is closed
Varvarinskoye Gold/Copper mine	2014	2.7	49.55	Ore production data from 2013 used to estimate 2014
Veladero Gold mine	2014	28.3	113.03	Ore production data from 2013 used to estimate 2014
Yanacocha Gold mines	2013	66.8	94.16	None
Yatela Gold mine	2012-2013	2.4	26.03	None
All mines	-	309.6	2,076.37	-

Based on Eq. 5, the weighted disturbance rate was estimated at 6.70 ha/Mt Au ore.

Silver

The non-constant mine-specific slopes were calculated for each mine using the Eq. 4 (page 97) for each reference year as shown below in Table 29.

Table 29: Silver. Mine-specific slopes (n=33).

Mine name	Year of reference	Cumulative Ag ore (allocated) produced in period available (until the year of reference) (Mt)	Mine-specific slope by Eq. 4 (ha/$Mt_{Ag\ ore}$)
Aitik Copper mine	2012	20.56	2.70
Alamo Dorado Silver mine	2013	9.22	4.12
Alumbrera Gold/Copper mine	2010	3.81	6.58
Antapite Gold mine	2010	0.02	98.95
Ares Gold mine	2011	0.79	15.10
Chatree Gold mine	2013	2.08	9.05
Chelopech Gold/Copper mine	2013	0.37	22.49
Chuquicamata Copper	2013	35.53	2.02

Mine			
Cracow Gold mine	2013	0.01	131.75
Denton-Rawhide Gold mine	2010	8.38	4.33
Dolores Gold mine	2013	11.21	3.71
Eloise Copper/Gold mine	2008	0.12	41.80
Escondida-Zaldivar Copper Mine	2011	15.07	3.18
Hycroft (Crofoot/Lewis) Gold mine	2010	2.25	8.70
Joe Mann Gold mine	2007	0.03	93.07
La Herradura Gold mine	2012	2.48	8.26
Mahd ad´Dahab Gold mine	2012	0.28	26.35
Minera Florida/Alhue Gold mine	2012	0.43	20.80
Mount Polley Copper/Gold mine	2012	1.79	9.81
Mount Rawdon Gold mine	2012	0.12	40.30
Neves Corvo Copper Mine	2013	1.13	12.51
Ok Tedi Copper/Gold Mine	2013	5.60	5.36
Poracota Gold mine	2013	0.01	170.33
Robinson Copper/Gold mine	2012	1.44	11.00
Rochester Silver Mine	2013	18.62	2.84
Round Mountain Gold Mine	2013	0.12	40.28
Sossego Copper mine	2011	3.09	7.35
Tintaya Copper mine	2011	0.08	49.95
Tritton Copper mine	2011	1.11	12.63
Troilus Copper/Gold mine	2010	16.59	3.02
Troy Copper/Silver mine	2011	4.88	5.77
Veladero Gold mine	2013	24.12	2.48

Yanacocha Gold mine	2012	20.56	2.70

The new net area disturbed per mine was computed by multiplying the average Ag ore extracted in the two years following the reference year by the mine-specific slope.

Table 30: Silver. Annual ore extraction and new area disturbed per mine (n=34).

Mine name	Year(s) considered for average ore extracted	Annual Ag ore extracted (Mt/a) (average in two years following reference year)	New net area disturbed per year (ha/a)	Observations
Aitik Copper mine	2013	1.65	4.45	None
Alamo Dorado Silver mine	2014	1.47	6.05	Ore production data from 2013 used to estimate 2014
Alumbrera Gold/Copper mine	2011-2012	0.59	3.87	None
Antapite Gold mine	2011-2012	0.00	0.22	None
Ares Gold mine	2012-2013	0.09	1.43	None
Chatree Gold mine	2014	0.67	6.09	Ore production data from 2013 used to estimate 2014
Chelopech Gold/Copper mine	2014	0.02	0.36	Ore production data from 2013 used to estimate 2014
Chuquicamata Copper Mine	2014	0.91	1.84	Ore production data from 2013 used to estimate 2014
Cracow Gold mine	2014	0.01	0.76	Ore production data from 2013 used to estimate 2014
Denton-Rawhide Gold mine	-	0.00	0.00	Excluded - Mine closed.
Dolores Gold mine	2014	2.51	9.32	Ore production data from 2013 used to estimate 2014
Eloise Copper/Gold mine	2011-2012	0.0012	0.05	None
Escondida-Zaldivar Copper Mine	2012-2013	1.21	3.84	None
Hycroft	2012-2013	2.68	23.29	None

(Crofoot/Lewis) Gold mine				
Joe Mann Gold mine	-	0.00	0.00	Excluded because it is suspended
La Herradura Gold mine	2013	0.26	2.16	None
Mahd ad´Dahab Gold mine	2013	0.01	0.22	No data on ore production for 2014
Minera Florida/Alhue Gold mine	2013	0.18	3.68	No data on ore production for 2014
Mount Polley Copper/Gold mine	2013	0.10	0.98	No data on ore production for 2014
Mount Rawdon Gold mine	2013	0.05	2.04	Ore production data from 2012 used to estimate 2013
Neves Corvo Copper Mine	2014	0.11	1.42	Ore production data from 2013 used to estimate 2014
Ok Tedi Copper/Gold Mine	2014	0.18	0.97	Ore production data from 2013 used to estimate 2014
Poracota Gold mine	-	0.00	0.00	Excluded because it is suspended
Robinson Copper/Gold mine	2013	0.13	1.41	No data on ore production for 2014
Rochester Silver Mine	2014	0.72	2.04	Ore production data from 2013 used to estimate 2014
Round Mountain Gold Mine	2014	0.00	0.00	Ore production data from 2013 used to estimate 2014
Sossego Copper mine	2012	0.16	1.1939	No data on ore production for 2013
Tintaya Copper mine	2012	0.02	0.93	No data on ore production for 2013
Tritton Copper mine	2012-2013	0.00	0.00	None
Troilus Copper/Gold mine	-	0.44	1.34	Excluded - mine is closed
Troy Copper/Silver mine	2012	0.82	4.70	No data on ore production for 2013
Veladero Gold mine	2014	0.59	1.47	Ore production data from 2013 used to estimate 2014
Yanacocha Gold	2013	1.65	4.45	None

mines				
All mines	-	15.57	86.12	-

Based on Eq. 5, the weighted disturbance rate was estimated at 5.53 ha/Mt ore.

8.5 Global status quo: proportion factors and allocated calculations

Iron ore

The Table 31 below shows the yearly evolution of the proportion factor between the world and the mines´ sample production. The 3-year average proportion factor was calculated at 6.999.

Table 31: Iron ore. Annual proportion factor calculation. 2010-2012.

Year	Sample production of run-of-mine [Mt] n=27	World production of iron ore (Mt) [USGS]	Proportion Factor (world production/sample ROM)	Sample proportion of world production (%)
2010	391.48	2,590	6.62	15.1
2011	404.02	2,940	7.28	13.74
2012	422.29	3,000	7.10	14.08

Source: self-elaboration based on SNL Metals & Mining database and Kelly and Matos (2013).

The Table 32 illustrates the adjusted measurements for each mine of the cumulative net area disturbed in 2011.

Table 32: Iron ore-producing mines. Status quo calculations for 2011.

Mine name (n=27)	Cumulative net area disturbed in 2011 [ha]
Area C	2,486.61
Carajás/Serra Norte	5,374.71
Channar	1,160
Chitradurga	482
Eastern Range	676.7
El Gedida (el Bahariya)	927.8
Hope Downs	2,119.23
Jack Hills	177.3
Jimblebar	766

Mine name (n=27)	Cumulative net area disturbed in 2011 [ha]
Koolan Island	703.08
Pardoo	488
Tallering Peak	433.5
Yandi	2,829
Bailadila 5	526.5
Bailadila 10	361.89
Bailadila 14 and 11 C	637.74
Chadormalou	1,240.4
Frances Creek	470.2
Gole Gohar	2,095.38
Kudremukh	949.2
Mont Wright	4,860
Savage River	1,255.77
Sydvaranger	1,200
Thabazimbi	1,791
Capitão do Mato	1,020.87
Tamanduá	780.84
Marcona	2,383
Total	38,197.5

Using the 3-year average proportion factor, we multiply it with the cumulative net area disturbed by mines in the sample for the year 2011 and we obtain: **7 * 38,197.5 ha = 267,344 ha.** The global cumulative net area disturbed by large-scale iron ore mining in 2011 was calculated to be 2,673 km^2.

Bauxite

According to the Table 33 below the 3-year average proportion factor was calculated at 3.43.

Table 33: Bauxite. Annual proportion factor calculation. 2010-2012.

Year	Sample production of bauxite – Ore mined [Mt] n=13	World production of bauxite ore (Mt) [USGS]	Proportion Factor (world production/sample)	Sample proportion of world production (%)
2010	72.27	238	3.29	30.4

2011	73.33	259	3.53	28.3
2012	74.25	258	3.47	28.8

Source: self-elaboration based on SNL Metals & Mining database and Kelly and Matos (2013).

The Table 34 below illustrates the adjusted measurements for each mine to calculate the cumulative net area disturbed in 2011.

Table 34: Bauxite ore-producing mines. Status quo calculations for 2011.

Mine name n=13	Cumulative net area disturbed in 2011 [ha]
Awaso	257
Boddington Worsley	2,566
Boke Sangaredi	2,984
Discovery Bay	3,521
Frigua	796
Gove	2,742
Juruti	1,440
Kindia	1,001
Krasno Oktyabrsk	1,636
Los Pijiguaos	1,083
Moengo Coermotibo	3,383
Panchpatmali	651
Trombetas	5,864
Total	27,924

Using the average proportion factor, we multiply it with the total cumulative net area disturbed by mines in the sample for the year 2011 and we obtain: **3.43 * 27,924 ha = 95,780 ha (or 958 km^2),** an area larger than the state of Berlin (890 km^2) or over three times the area the city of Munich (310 km^2)[58].

[58] The reclamation issue is important for the bauxite industry since according to the Aluminum Association, an average of 80% of the land mined for bauxite is returned to its native ecosystem. This is the result of a process of increasing awareness and social pressures, measured for instance in the growth of written rehabilitation procedures (International Aluminium Institute 2004:1).

Copper

The proportion factor fluctuates in the period 2010-2012 following fluctuations in the production within the sample, particularly decreases of production from 2007 until 2011 due to the decreasing Cu production of Escondida-Zaldivar, Alumbrera, Batu Hijau and Aitik mines. The 3-year average proportion factor was computed at 5.54.

Table 35: Copper. Annual proportion factor calculation. 2010-2012.

Year	Sample production of Cu [t] n= 31	World mine production of copper [t of Cu content]	Proportion Factor (world production/sample)	Sample proportion of world production (%)
2010	3,465,805	16,100,000	4.65	21.5
2011	2,826,034	16,200,000	5.73	17.4
2012	2,691,654	16,800,000	6.24	16.0

Source: Brown et al. (2014)

The Table 36 below shows the cumulative net area disturbed calculated for 2011, inclusive allocation by value relationships.

Table 36: Cu-producing mines. Status quo calculations for 2011.

Mine name n=31	(Allocated) cumulative net area disturbed in 2011 [ha]
Aitik Copper mine	3,646.8
Alamo Dorado Silver mine	1.4
Alumbrera Gold/Copper mine	1,663
Batu Hijau Copper/Gold mine	1,705.8
Bingham Canyon Copper Mine	4,992.7
Cerro Corona Copper/Gold mine	185.2
Chapada Copper/Gold mine	1,355.9
Chelopech Gold/Copper mine	85.3
Chuquicamata Copper Mine	9,863.5
Collahuasi Copper Mine	4,647.2
Cuajone (SPCC) Copper Mine	2,472.5
Eloise Copper/Gold mine	170.4

Mine name n=31	(Allocated) cumulative net area disturbed in 2011 [ha]
Escondida-Zaldivar Copper Mine	29,835
Guelb Mogrhein Copper/Gold mine	702.4
Joe Mann Gold mine	7.2
Mahd ad´Dahab Gold mine	8.8
Mineral Hill (Australia) Gold/Copper mine	42.2
Mount Polley Copper/Gold mine	939.4
Neves Corvo Copper Mine	363.9
Ok Tedi Copper/Gold Mine	1391
Osborne (Trough Tank) Copper/Gold mine	392.9
Palito Gold mine	18.8
Peak Gold mine	51.5
Robinson Copper/Gold mine	2,983.2
Sepon Copper/Gold mine	1,186
Sossego Copper mine	2,569.2
Tintaya Copper mine	2723
Tritton Copper mine	281.1
Troilus Copper/Gold mine	233
Troy Copper/Silver mine	230.1
Varvarinskoye Gold/Copper mine	205.7
Total	74,954.2

Using this 3-year average proportion factor (5.54), we multiply it with the cumulative net area disturbed by mines in the sample for the year 2011 and we obtain: **5.54 * 74,954.2 ha = 415,245 ha.** The global cumulative net area disturbed by large-scale copper-producing mines in 2011 was calculated to be 4,152 km^2.

Gold

The three-year average proportion factor was computed at 6.39.

Table 37: Gold. Annual proportion factor calculation. 2010-2012.

Year	Sample production of gold [t] n=73	World mine production of gold [t]	Proportion Factor (world production/sample)	Sample proportion of world

				production (%)
2010	438.06	2,620	5.98	16.7
2011	408.96	2,630	6.43	15.5
2012	390.79	2,640	6.76	14.8

Source: Brown et al. (2014).

The Table 38 below shows the calculations of the (allocated and adjusted to 2011) cumulative net area disturbed per mine for 2011.

Table 38: Au-producing mines. Status quo calculations for 2011.

Mine name n=73	(Allocated) cumulative net area disturbed in 2011 [ha]
Aitik Copper mine	425
Alamo Dorado Silver mine	33
Alumbrera Gold/Copper mine	721
Amantaytau Oxides Gold mine	623
Antapite Gold mine	262
Arcata Silver mine	17
Ares Gold mine	128
Batu Hijau Copper/Gold mine	480
Berezitovy Gold mine	361
Bingham Canyon Copper Mine	1,079
Boroo Gold mine	702
Burnstone Gold mine	332
Cerro Corona Copper/Gold mine	185
Chapada Copper/Gold mine	405
Chatree Gold mine	602
Chelopech Gold/Copper mine	75
Chuquicamata Copper Mine	104
Corihuarmi Gold mine	311
Cracow Gold mine	201
Cuajone (SPCC) Copper Mine	10
Denton-Rawhide Gold mine	465
Dolores Gold mine	337

Mine name n=73	(Allocated) cumulative net area disturbed in 2011 [ha]
El Sauzal Gold mine	372
Eloise Copper/Gold mine	10
Escondida-Zaldivar Copper Mine	628
Essakane Gold mine	1,139
Fort Knox Gold mine	1,517
Geita Gold mine	2,280
Greens Creek Polymetallic mine	21
Gualcamayo Gold Mine	400
Guanaceví Silver mine	15
Guelb Mogrhein Copper/Gold mine	189
Henty Gold mine	170
Holt-Holloway Gold mine	262
Hycroft (Crofoot/Lewis) Gold mine	1,479
Joe Mann Gold mine	96
Kiniero (Jean-Gobele) Gold mine	477
Kisladag Gold mine	704
La Coipa Silver/Gold mine	1,003
La Herradura Gold mine	1,566
Mahd ad´Dahab Gold mine	124
Minera Florida/Alhue Gold mine	207
Mineral Hill (Australia) Gold/Copper mine	97
Morila Gold mine	1,135
Mount Polley Copper/Gold mine	432
Mount Rawdon Gold mine	450
Mupane Gold mine	292
Muruntau Gold Mine	8,369
Musselwhite Gold mine	570
Ok Tedi Copper/Gold Mine	486
Olimpiada Gold Mine	3,391
Osborne (Trough Tank) Copper/Gold Mine	47
Palito Gold mine	145

Mine name n=73	(Allocated) cumulative net area disturbed in 2011 [ha]
Peak Gold mine	243
Poracota Gold mine	39
Robinson Copper/Gold mine	529
Rochester Silver Mine	267
Round Mountain Gold Mine	3,112
Sadiola Gold Mine	2,020
San Jose (Arg) Gold/Silver mine	98
Seabee Gold mine	297
Sepon Copper/Gold mine	392
Siguiri Gold mine	2,645
Sossego Copper mine	238
Super Pit Gold Mine	2,764
Syama Gold mine	768
Tintaya Copper mine	158
Tritton Copper mine	6
Troilus Copper/Gold mine	863
Varvarinskoye Gold/Copper mine	505
Veladero Gold mine	1,330
Yanacocha Gold mines	5,202
Yatela Gold mine	780
Total	58,187

Using this 3-year average proportion factor (6.39), we multiply it with the cumulative net area disturbed by mines in the sample for the year 2011 and we obtain: **6.39 * 58,187 ha = 371,815 ha.** The global cumulative net area disturbed by large-scale gold-producing mining in 2011 was calculated to be 3,718 km^2.

Silver

The three-year average proportion factor was computed at 11.69.

Table 39: Silver. Annual proportion factor calculation. 2010-2012.

Year	Sample production of silver [t]	World mine production of silver [t]	Proportion Factor (world	Sample proportion of world

	n=41		production/sample)	production (%)
2010	2,227	23,417	10.52	9.5
2011	2,047	23,422	11.44	8.7
2012	1,921	25,161	13.10	7.6

Source: Brown et al. (2014).

Table 40 shows the calculations of cumulative net area disturbed for 2011 per mine.

Table 40: Ag-producing mines. Status quo calculations for 2011.

Mine name n=41	(Allocated) cumulative net area disturbed in 2011 [ha]
Aitik Copper mine	183.1
Alamo Dorado Silver mine	170.1
Alumbrera Gold/Copper mine	22.3
Antapite Gold mine	4.3
Arcata Silver mine	87.7
Ares Gold mine	30.7
Bingham Canyon Copper Mine	154.7
Chatree Gold mine	43.8
Chelopech Gold/Copper mine	2.5
Chuquicamata Copper Mine	224.3
Cracow Gold mine	0.6
Cuajone (SPCC) Copper Mine	63.9
Denton-Rawhide Gold mine	61.7
Dolores Gold mine	221.6
Eloise Copper/Gold mine	4.4
Escondida-Zaldivar Copper Mine	311.1
Greens Creek Polymetallic mine	45.2
Guanaceví Silver mine	80.5
Hycroft (Crofoot/Lewis) Gold mine	64.7
Joe Mann Gold mine	0.6
La Coipa Silver/Gold mine	988.5
La Herradura Gold mine	23.5

Mine name n=41	(Allocated) cumulative net area disturbed in 2011 [ha]
Mahd ad´Dahab Gold mine	7.8
Minera Florida/Alhue Gold mine	20.1
Mount Polley Copper/Gold mine	30.5
Mount Rawdon Gold mine	1.6
Neves Corvo Copper Mine	7.1
Ok Tedi Copper/Gold Mine	17.2
Poracota Gold mine	0.31
Robinson Copper/Gold mine	31.5
Rochester Silver Mine	444.6
Round Mountain Gold Mine	53.3
San Jose (Arg) Gold/Silver mine	121.3
Sepon Copper/Gold mine	4.3
Sossego Copper mine	3.9
Tintaya Copper mine	71.8
Tritton Copper mine	3.9
Troilus Copper/Gold mine	16.5
Troy Copper/Silver mine	121.6
Veladero Gold mine	42.7
Yanacocha Gold mines	90.4
Total	3,880

Using this 3-year average proportion factor (11.69), we multiply it with the cumulative net area disturbed by mines in the sample for the year 2011 and we obtain: **11.69 * 3,880 ha = 45,357 ha.** The global cumulative net area disturbed by large-scale silver-producing mining in 2011 was calculated to be 453 km^2.

8.6 Frequency distribution of mines and deposits per DZ

8.6.1 Data preparation

Data preparation of mines and geological deposits in the SNL Metals & Mining database

Global location of mines was based on the dataset provided by the SNL Metals & Mining database (update April 2014). The inventories used were exported from the

SNL Metals & Mining database (update April 2014), from the Mines&Projs entry, selecting (filtering) one mineral for each “main metal”. Out of the full records of mines operating, closed, abandoned, suspended or under construction provided by the SNL Metals & Mining, records belonging to entities other than mines (categorized as “active”/”non-active” or for which no status was given) were excluded, as well as mine records for which no geographic coordinates were available. For mines, no differentiation was done regarding their type (OP or UG), they were all included.

Global location of deposits was also sourced from the SNL Metals & Mining dataset. From the Mines & Projects entry, they were identified as deposits under the Status: “Project/no spec, conceptual, pre-feasibility, feasibility”. Entities with a status of “abandoned” or “abandoned project” was considered a geological deposit. Latitude and longitude were not corrected given the lack of other sources. No distinction was done per Type of deposit.

Iron

The inventory to be used was exported from the SNL Metals & Mining database (update April 2014), from the Mines&Projs entry covering 1,104 entries. A first filter was applied per status leaving only records belonging to mines (status equals construction, operating, suspended or closed) and those belonging to deposits (status equals project, no spec, conceptual, feasibility, pre-feasibility, abandoned or project abandoned). 20 Records with status empty were filtered out. The 1,084 remaining records were split into 615 mines and 469 geological deposits. Of the 615 mines, only 495 had coordinates available whilst for deposits 328 had coordinates.

The next step involved visually scanning the mines and deposits sample to detect double entries, namely, a mine site for which two or more observations appeared; this happened in some cases because the same operating mine had two different extraction methods at the mine site or because two time periods were covered. In both cases entries were deleted in order to certify each mine site had only one point location in the shapefile. The deleted entries for mines totaled 16 cases: Codli Iron ore mines (1 entry deleted), Djebel Derissa (2 entries deleted), Gongchangling (2 entries deleted), Karara/Mungada Iron Ore mine (1 entry

deleted), Koira OMC (1 entry deleted), Korshunovsky Iron ore Mine (1 entry deleted), Sokolovsky (1 entry deleted), Vale Southeastern System (1 entry deleted), Vysokogorsky Iron ore mine (1 entry deleted); the 5 entries N4E, N4W, N5, N5E-N and N5-W are all deposits which belong to the Carajás mine (Serra Norte) and were also deleted since Carajás (Serra Norte) is already considered under the entry named "Vale Northern System (Carajas) Iron Ore Mines". In the case of deposits, the following 6 were fixed (1 entry deleted per each): Blue Hills Iron ore deposit, Cape Lambert iron ore deposit, Mount Oscar iron ore deposit, Trans Tasman Souther Iron ore Deposit, Wadi Shatti, Weld range. The final mines dataset comprised 479 and the deposits entailed 322 records.

Second, the next data preparation step comprised manually re-location some data points falling outside of any of the diversity zones; this was the case in some deposits located on islands not included within the DZ (e.g. Irvin Island iron ore deposit).

Bauxite

The inventories to be used were exported from the SNL Metals & Mining database (update April 2014), from the Mines&Projs entry. The total amount of entries totals 186, out of which 6 do not have information on status and thus are excluded. Out of the remaining 180, 143 belong to mines (according to status equaling construction, operating, suspended or closed) and 37 to deposits (status equals "project, no spec"). Of the 143 mine records, only 90 had coordinates available and were used.

Of the 37 deposits only 16 had coordinates in the SNL Metals & Mining database. Many of them are not strictly deposits but mining districts where many deposits are located, e.g. Lang Son province in Vietnam where 36 deposits can be found (ICSOBA 2011). The location of the deposits was revised and missing coordinates could be found and verified for 11 deposits, totaling 27 records usable; they are distributed among the countries with the biggest reserves (Australia, Brazil, Guinea, Guyana, India, Vietnam and a few others). 10 sites, particularly Russian sites (e.g. Tatarsk Bauxite Deposit, Timansk Kryazh Bauxite Deposit, Treugolnoye Bauxite Deposit), could not be located.

Once the shapefiles were created, the list of mines and deposits were visually inspected to remove double entries; no duplications were found. Second, the next data preparation step comprised manually re-location some data points falling outside of any of the diversity zones; this was the case in some deposits (e.g. North Onega Bauxite Deposit) and in some mines (e.g. Kirkvine Alpart Manchester plateau Bauxite mine). The criterion used was the shortest linear distance to a diversity zone (nearest zone). Then calculations were performed using the QGIS Vector analysis tool points in polygon. Final deposits dataset comprised 27.

Copper

The mines and deposits inventory was obtained from the Mines & Projects entry of the SNL Metals & Mining database (update April 2014) with the option "including all mines" ticked. Filtering by copper as "Main metal" the total amount of entries equaled 1,186. Of those, only 18 had no information on status (empty) and hence were excluded. The remaining 1,168 records were divided into mines and deposits according to their status. Records with status of construction, operating, suspended or closed were considered mines whilst those with status equals project, no spec, conceptual, feasibility, pre-feasibility, abandoned or project abandoned were considered deposits. This resulted in 650 mines and 518 deposits. Out of the 650 mines and 518 deposits, coordinates were available for 597 mines and 384 deposits.

The 597 mines were checked to remove double entries, especially numerous references to solvent extraction and electro winning plants (SX-EW) at mine sites; the following 58 records were deleted in order to leave one record (one point location) per mine: Buenavista del Cobre, Chambishi Copper Mine, Chibuluma South Copper Mine, Chuquicamata SX-EW Mine, Codelco Norte SXEW Copper Mine, Collahuasi Copper (SX-EW) Mine, Continental (NM) (SXEW) Copper Mine, Cuajone (SPCC) Copper (SX-EW) Mine, Dalmacia Copper Mine, El Soldado Copper (SX-EW) Mine, El Teniente Copper (SX-EW) Mine, Erdenet Copper (SX-EW) Mine, Escondida Copper (SX-EW) mine, Gaisky Copper/zink Mines, Gibraltar (McLeese Lake) Dump Leach Copper Mine, Grasberg UG Copper/Gold Mine, Grasberg Expansion Copper/Gold Mine, Jaguarari (Caraiba) UG Copper Mine, Kamoto Copper/Cobalt UG Mine, Kansanshi Copper (SXEW) Mine, Kolwezi

Copper Tailings Mine, La Caridad Copper (SX-EW) Mine, La Cascada (Tailings) Copper Mine, Leichhardt Area Copper Mines, Los Bronces Copper (SX-EW) Mine, Los Pelambres UG Copper Mine, Malanjkhand Copper Tailings, Mantos Blancos Copper (SX-EW) Mine, Michilla (EL Lince) Copper (SX-EW) Mine, Morenci Copper (SX-EW) Mine, Mount Isa Copper (SX-EW) Mine, Musoshi Copper Mine, Mutoshi Stage I, Nchanga UG Copper/Cobalt Mine, Nchanga OP Copper/Cobalt Mine, Nchanga Copper (Tailings Leach) Mine, Nifty Copper Concentrate Mine, Nikoliq 2 Copper Mine, Olympic Dam Copper (SX-EW) Mine, Palabora UG Copper Mine, Pinto Valley Miami Copper (SX-EW) Mine, Punta del Cobre (SX-EW) Mine, Ray Copper (SX-EW) Mine, Rehova Copper Mines, Rubik Copper Mines, San Manuel (SX-EW) Mine, Salvador Copper (SX-EW) Mine, Sar Cheshmeh Copper (SX-EW) Mine, Sepon (Khanong) copper (SX-EW) Mine, Sierrita Copper (SX-EW) Mine, Silver Bell Copper (SX-EW) Mine, Spaci Reps Copper Mines, Leichhardt Area Copper Mines, Tintaya Copper (SX-EW) Mines, Toquepala (SPCC) Copper (SX-EW) mine, Tyrone Copper (SX-EW) Mine, Uchalinsky UG Copper Mine, Zaldivar Copper Conc Mine. A total of 539 mines remained for the analysis.

As for the deposits, the 384 were also checked for double entries. No double entries were found.

The next data preparation step comprised checking that all point locations of mines and deposits fell under the polygon of a DZ by Barthlott et al. Some points were manually re-located to the closest DZ (Raul Copper Mine, Condestable Copper Mine, Toquepala (SPCC) Copper Mine, Santo Domingo Copper Mine, Ivan Zar, Michilla Copper Mine, Caleta el Cobre, Montecristo), (e.g. Catface Copper Deposit, Mina Justa (Marcona) Copper Deposit, Pan de Azucar Copper Deposit). In the case of San Antonio and Tapian Copper mines they were located in a non-represented island; they were re-located to the two closest DZ, one to each. In the case of the Sangihe deposit, it was placed in the DZ 7 since it was closer to this than to the DZ 8.

Gold

Data were obtained from the SNL Metals & Mining database (update April 2014), from the Mines & Projs entry button (including all mines) by setting in the filter “Gold” as the “main metal”. Retrieved records totaled 3,614, out of which 82 were

excluded since no status was given (status empty). The remaining 3,532 records were then divided by filtering their status the same as with other minerals into 1,904 mines and 1,628 deposits. Out of the 1,904 mines and 1,628 deposits, only 1,658 mines and 1,225 deposits had geographic coordinates available.

The 1,658 mines entries were checked to remove double entries. The following 44 entries were deleted: Aurora (CNG) Gold Mine, Bachelor Lake Gold Mines Inc, Ballarat East (Goldminco) Gold Mine, Barberton Mines, Blyvooruitzicht UG Gold Mine & Gold Tailings, Bousquet No 1 & Bousquet No 2 Gold Mine, Buffelsfontein (Harties) Tailings Gold Mine, Buffelsfontein (Harties) Gold Mine, Buffelsfontein (MWS) Gold Tailings, Carlin Trend Gold Mines, Carlin UG Gold Mines, Comstock Gold Mine, Cooke 4 (Ezulwini) Underground Gold Mine, Cosmo Deeps Gold Mine, Durban Deep (Roodepoort) Gold Mine, Durban Roodepoort Deep OP Gold Mine, Durban Roodepoort Deep UG Gold Mine, Evander OP Gold Mines, Fimiston Underground Gold Mines, Georgetown Alluvial Gold Mine, Harmony 2 Shaft Gold Mine, Hoyle Gold Mine, Kalgoorlie Tailings Gold Mine, KDC Gold Mine, Kettle River-Buckhorn Gold Mine, King of the Hills Gold Mine, Kusasalethu UG Gold Mine, Lady Bountiful Extended Gold Mine, Laverton (Crescent) Gold Mines, Manhattan Consolidated Gold Mine, Norseman (AGM) Gold Mine, Northparkes OP Copper/Gold Mine, Obuasi (Tailings) Gold Mine, Obuasi (Underground) Gold Mine, Ocampo UG Gold/Silver Mine, Pajingo Gold Mine, Raub Gold Tailings Mine, Red Lake (Old) Gold Mine, Teberebie North Gold Mine, Xiangxi(GZ) Gold Mine.

As a result, the gold mines universe comprises 1,614 mines. The 1,225 deposits were also checked for double entries. The following 2 were deleted: Diangounte West Gold Deposit, Lake Cowan (CNGC) Gold Deposit. 1,223 deposit remained as the final sample.

The next data preparation step comprised checking that all point locations of mines and deposits fell under the polygon of a DZ by Barthlott et al. Some points were manually re-located to the closest DZ, important to mention are 3 mines and 3 gold deposits in Fiji, excluded in the DZ map.

Silver

The data were obtained from the SNL Metals & Mining database (update April 2014) also from the Mines & Projs entry button (including all mines) and filtering

the full records by “silver” as the “main metal”. 314 records were retrieved out of which 6 were excluded due to a lack of information in the status. The remaining 308 records were divided, following the same criterion as other minerals, into 179 mines and 129 deposits. Of the former, only 141 had geographic coordinates available, and of the latter only 100.

The next step involved scanning the mines´ lists to remove double entries; the following 3 entries were removed from the mines´ list: Guanajuato (Bolanitos) Unit Silver Mines, Gümüsköy Silver Mine, Morococha (Pan Am) Group Silver Mines. For deposits, the following entry was removed: San Miguel Tailings Silver Deposit. The final dataset is then comprised 138 mines and 99 deposits.

8.6.2 Results of numerical frequency distributions per DZ and metal

Iron

Table 41: Numerical frequency distribution of Fe mines and deposits per DZ.

Barthlott Diversity Zone	World terrestrial surface area (excl. Antarctica) (km^2)	Number of iron ore mines[59]	Number of iron ore deposits	% of world terrestrial surface area	% of iron ore mines	% of iron ore deposits
1	3,216,586.24	0	1	2.42	0.00	0.31
2	9,910,294.50	2	8	7.47	0.42	2.48
3	27,962,149.74	57	67	21.07	11.90	20.81
4	32,935,379.70	130	110	24.82	27.14	34.16
5	20,326,144.55	88	45	15.32	18.37	13.98
6	15,735,289.27	57	36	11.86	11.90	11.18
7	12,312,992.81	52	30	9.28	10.86	9.32
8	7,775,535.49	55	20	5.86	11.48	6.21
9	2,176,082.24	38	5	1.64	7.93	1.55
10	334,366.25	0	0	0.25	0.00	0.00
Total	132,684,820.79[60]	479	322	100	100	100

Source: self-elaboration based on SNL Metals & Mining database (update Feb 2014 for deposits and April 2014 for mines) and Barthlott et al. (2007).

Bauxite

Table 42: Numerical frequency distribution of Al mines and deposits per DZ.

Barthlott Diversity Zone (DZ)	World terrestrial surface area (excl. Antarctica)	Number of bauxite ore mines[61]	Number of bauxite ore deposits	% of world terrestrial surface area	% of bauxite ore mines	% of bauxite deposits

[59] Includes mines in construction, operation, closed and suspended. Includes 3 iron sands mines in Indonesia. Based on the SNL Metals & Mining update April 2014, using the Mines&Projs entry (including all mines), filtering by main metal = iron ore. Entries are considered mines if: Status = construction, operating, operating,exp/plans, operating,exp/constr, operating,residual, suspended, suspended,rest/plans, closed (all forms) and Mines without status (but with ´mine´ in their name). Abandoned projects and abandoned iron sands deposits are not considered mines, but deposits. Deposits include entries in the raw crude export with Status = project, no spec, conceptual, pre-feasibility and feasibility, plus abandoned as mentioned.

[60] World terrestrial surface area (excl. Antarctica) differs with the global land mass (excl. Antarctica) usually considered in global studies (132,000,000.00 Km^2 if all continents except Antarctica are added according to Asner et al. 2004) by a total of 684,820 km^2 .

[61] Includes mines in construction, operation, closed and suspended.

	(km^2)					
1	3,216,586.24	0	0	2.42	0.00	0.00
2	9,910,294.50	1	0	7.47	1.11	0.00
3	27,962,149.74	1	2	21.07	1.11	7.41
4	32,935,379.70	8	2	24.82	8.89	7.41
5	20,326,144.55	13	7	15.32	14.44	25.93
6	15,735,289.27	21	4	11.86	23.33	14.81
7	12,312,992.81	19	5	9.28	21.11	18.52
8	7,775,535.49	25	7	5.86	27.78	25.93
9	2,176,082.24	2	0	1.64	2.22	0.00
10	334,366.25	0	0	0.25	0.00	0.00
Total	132,684,820.79	90	27	100	100	100

Source: self-elaboration based on SNL Metals & Mining and Barthlott et al. (2007)

Copper

Table 43: Numerical frequency distribution of Cu mines and deposits per DZ.

Barthlott Diversity Zone	World terrestrial surface area (km^2)	Number of mines	Number of deposits	% of world terrestrial surface area	% of mines	% of deposits
1	3,216,586.24	0	0	2.42	0.00	0.00
2	9,910,294.50	25	15	7.47	4.64	3.91
3	27,962,149.74	89	91	21.07	16.51	23.70
4	32,935,379.70	152	118	24.82	28.20	30.73
5	20,326,144.55	50	40	15.32	9.28	10.42
6	15,735,289.27	86	46	11.86	15.96	11.98
7	12,312,992.81	94	36	9.28	17.44	9.38
8	7,775,535.49	34	25	5.86	6.31	6.51
9	2,176,082.24	7	5	1.64	1.30	1.30
10	334,366.25	2	8	0.25	0.37	2.08
Total	132,684,820.8	539	384	100	100	100

Source: self-elaboration based on SNL Metals & Mining database (update Feb 2014 for deposits and April 2014 for mines) and Barthlott et al. (2007).

Gold

Table 44: Numerical frequency distribution of Au mines and deposits per DZ.

Barthlott Diversity Zone	World terrestrial surface area (km^2)	Number of mines	Number of deposits	% of world terrestrial surface area	% of mines	% of deposits
1	3,216,586.24	0	0	2.42	0.00	0.00
2	9,910,294.50	21	9	7.47	1.30	0.74
3	27,962,149.74	164	184	21.07	10.16	15.04
4	32,935,379.70	489	396	24.82	30.30	32.38
5	20,326,144.55	323	253	15.32	20.01	20.69
6	15,735,289.27	316	154	11.86	19.58	12.59
7	12,312,992.81	142	108	9.28	8.80	8.83
8	7,775,535.49	120	92	5.86	7.43	7.52
9	2,176,082.24	29	22	1.64	1.80	1.80
10	334,366.25	10	5	0.25	0.62	0.41
Total	132,684,820.8	1,614	1,223	100	100	100

Source: self-elaboration based on SNL Metals & Mining database (update Feb 2014 for deposits and April 2014 for mines) and Barthlott et al. (2007).

Silver

Table 45: Numerical frequency distribution of Ag mines and deposits per DZ.

Barthlott Diversity Zone	World terrestrial surface area (km^2)	Number of mines	Number of deposits	% of world terrestrial surface area	% of mines	% of deposits
1	3,216,586.24	0	0	2.42	0.00	0.00
2	9,910,294.50	1	1	7.47	0.72	1.01
3	27,962,149.74	15	12	21.07	10.87	12.12
4	32,935,379.70	35	23	24.82	25.36	23.23
5	20,326,144.55	19	9	15.32	13.77	9.09
6	15,735,289.27	26	18	11.86	18.84	18.18
7	12,312,992.81	23	16	9.28	16.67	16.16
8	7,775,535.49	18	20	5.86	13.04	20.20
9	2,176,082.24	1	0	1.64	0.72	0.00
10	334,366.25	0	0	0.25	0.00	0.00
Total	132,684,820.8	138	99	100	100	100

Source: self-elaboration based on SNL Metals & Mining database (update Feb 2014 for deposits and April 2014 for mines) and Barthlott et al. (2007).

9 Biography

Diego I. Murguía, born 20.12.1980 in Buenos Aires, is a Ph.D. candidate at the University of Kassel and a research fellow at the Wuppertal Institute for Climate, Environment and Energy since 2011. He previously received a M.Sc. in Sustainable Resource Management from the Technical University of Munich (TUM) (2008) and a Bachelor in Geography (Honors) from the University of Buenos Aires (2005). He has professional experience as consultant in the performance of Social and Environmental Impact Assessments of large-scale mining projects in Argentina and in research to raise shareholders´ awareness of socio-environmental impacts of large German companies. He has conducted research on assessing the role of sustainability reporting by the mining industry as a tool for conflict management summarized in a recent book entitled “Sustainability Reporting in the Mining Industry: Revealing or Hiding Conflicts? The case of Bajo de la Alumbrera in Argentina” (Murguía 2014) and a co-authored article titled “Sustainability reporting on large-scale mining conflicts: the case of Bajo de la Alumbrera, Argentina” (Murguía and Böhling 2013). The Ph.D. candidate has received a scholarship by the German Catholic Academic Exchange Service (KAAD), by the TUM to support his studies in Munich and by the association Friends of the Wuppertal Institute to support his travelling expenses to Bonn during his research time at the Center for Remote Sensing of Land Surfaces (ZFL) in 2013.

The rising global demand for metals in a context of declining ore grades is driving the opening of new mines and the expansion of existing ones, disturbing substantial land areas (especially by open pits). However, how much land is currently disturbed globally? How much land could be disturbed by metal mining in 2050? This study investigates the global area disturbed by mining of iron, bauxite, copper, gold, and silver for the first time. The first part consists of the calculation of the specific land requirements, i.e. the area newly disturbed caused by the ore extraction at the mine site. The second part addresses the global area disturbed in the year 2011 whereas the third presents scenarios of how such area might evolve until 2050. The last part addresses the current and future pressures on global biodiversity by metal mines and shows possibilities for the future opening of new mines in low biodiversity areas, alleviating pressures in high biodiversity ones. This study presents the findings of the author´s dissertation hoping they are used as a frame to develop policies and incentives to reduce the amount of area directly disturbed by mines and their pressures on biodiversity.

ZFL CESR Center for Environmental Systems Research UNIKASSEL VERSITÄT Wuppertal Institute for Climate, Environment and Energy

ISBN 978-3-7376-0040-8